Advances in Clinical and Experimental Medicine

MONTHLY ISSN 1899-5276 (PRINT) ISSN 2451-2680 (ONLINE) www.advances.umw.edu.pl

2022, Vol. 31, No. 4 (April)

Impact Factor (IF) – 1.727
Ministry of Science and Higher Education – 70 pts
Index Copernicus (ICV) – 166.39 pts

Wroclaw Medical University

Advances
in Clinical and Experimental
Medicine

Advances
in Clinical and Experimental Medicine

ISSN 1899-5276 (PRINT) ISSN 2451-2680 (ONLINE) www.advances.umw.edu.pl

MONTHLY 2022
Vol. 31, No. 4
(April)

Advances in Clinical and Experimental Medicine (*Adv Clin Exp Med*) publishes high-quality original articles, research-in-progress, research letters and systematic reviews and meta-analyses of recognized scientists that deal with all clinical and experimental medicine.

Editorial Office
ul. Marcinkowskiego 2–6
50-368 Wrocław, Poland
Tel.: +48 71 784 12 05
E-mail: redakcja@umw.edu.pl

Publisher
Wroclaw Medical University
Wybrzeże L. Pasteura 1
50-367 Wrocław, Poland

Online edition is the original version of the journal

Editorial Policy

Advances in Clinical and Experimental Medicine (Adv Clin Exp Med) is an independent multidisciplinary forum for exchange of scientific and clinical information, publishing original research and news encompassing all aspects of medicine, including molecular biology, biochemistry, genetics, biotechnology and other areas. During the review process, the Editorial Board conforms to the "Uniform Requirements for Manuscripts Submitted to Biomedical Journals: Writing and Editing for Biomedical Publication" approved by the International Committee of Medical Journal Editors (www.ICMJE.org/). The journal publishes (in English only) original papers and reviews. Short works considered original, novel and significant are given priority. Experimental studies must include a statement that the experimental protocol and informed consent procedure were in compliance with the Helsinki Convention and were approved by an ethics committee.

For all subscription-related queries please contact our Editorial Office:
redakcja@umw.edu.pl

For more information visit the journal's website:
www.advances.umw.edu.pl

Pursuant to the ordinance No. 134/XV R/2017 of the Rector of Wroclaw Medical University (as of December 28, 2017) from January 1, 2018 authors are required to pay a fee amounting to 700 euros for each manuscript accepted for publication in the journal Advances in Clinical and Experimental Medicine.

Indexed in: MEDLINE, Science Citation Index Expanded, Journal Citation Reports/Science Edition, Scopus, EMBASE/Excerpta Medica, Ulrich's™ International Periodicals Directory, Index Copernicus

Typographic design: Piotr Gil, Monika Kolęda
DTP: Wydawnictwo UMW
Cover: Monika Kolęda
Printing and binding: Drukarnia I-BiS Bierońscy Sp.k.

Advances
in Clinical and Experimental Medicine

MONTHLY 2022, Vol. 31, No. 4 (April)

ISSN 1899-5276 (PRINT)
ISSN 2451-2680 (ONLINE)
www.advances.umw.edu.pl

Contents

Recent advances in the study of the comorbidity of depressive and anxiety disorders

Chong Chen[A–F]

Division of Neuropsychiatry, Department of Neuroscience, Yamaguchi University Graduate School of Medicine, Japan

A – research concept and design; B – collection and/or assembly of data; C – data analysis and interpretation;
D – writing the article; E – critical revision of the article; F – final approval of the article

Advances in Clinical and Experimental Medicine, ISSN 1899–5276 (print), ISSN 2451–2680 (online) *Adv Clin Exp Med*. 2022;31(4):355–358

Address for correspondence
Chong Chen
E-mail: cchen@yamaguchi-u.ac.jp

Funding sources
None declared

Conflict of interest
None declared

Received on February 24, 2022
Accepted on March 17, 2022

Published online on April 8, 2022

Abstract

Depressive and anxiety disorders often comorbid, which causes more severe impairments. The high comorbidity and shared genetic and psychological factors between the 2 disorders have brought arguments about whether they represent a common construct, and whether the current classification is meaningful. In this editorial, a state-of-the-art overview of recent studies on the underlying mechanism of such comorbidity, and the association between and differentiation of the 2 disorders is provided. Recent studies employing data-driven approaches such as latent class analysis (LCA) and network analysis to investigate the symptomatology of depression and anxiety have indicated unique characteristics and bridging symptoms of their comorbidity. Whereas previous neurobiological and neuroendocrinological studies reported common alterations in prefrontal–limbic pathways, serotonergic projections and the hypothalamic–pituitary–adrenal (HPA) axis, recent research suggests that distinct neural circuits and heterogeneous changes in HPA activity may exist in depression when compared to anxiety. Lastly, both depression and anxiety have been long associated with decision-making deficits; however, emerging evidence from computational psychiatry demonstrate that there may be unique neurocognitive and computational alterations in each disorder. By investigating the common and unique symptomatic characteristics and underlying neurobiological and neurocomputational mechanisms of the 2 disorders as well as their comorbidity, it can be concluded that recent studies have greatly advanced our understanding of the etiology and neuropathophysiology of these disorders.

Keywords: depression, anxiety, comorbidity, data-driven, computational psychiatry

Cite as
Chen C. Recent advances in the study of the comorbidity of depressive and anxiety disorders. *Adv Clin Exp Med*. 2022;31(4):355–358. doi:10.17219/acem/147441

DOI
10.17219/acem/147441

Introduction

Depressive and anxiety disorders are 2 common mental disorders and affect 4.4% and 3.6% of the world population, respectively.[1] The 2 disorders, however, often comorbid.[2–7] For instance, it has been reported that 42% of people with 12-month major depressive disorder (MDD) also have 12-month anxiety disorders, and that 46% of people with lifetime MDD also have lifetime anxiety disorders.[5] Importantly, comorbid depression and anxiety causes more severe functional impairment, slower recovery and higher rate of suicidal ideation than each disorder alone.[2–7] Anxiety symptoms, even those not meeting the diagnostic criteria, often cause serious clinical concerns when they co-occur with depressive disorders: over half of patients with MDD have anxious depression, and these patients experience poorer treatment outcomes than those with non-anxious depression.[8] Given this high comorbidity and shared genetic and psychological risk factors (e.g., early life stress), it has been argued that the 2 disorders may represent a single, common construct of negative affect or psychological distress.[9] Therefore, a full understanding of the underlying mechanism of such comorbidity and the association between and differentiation of the 2 disorders is an urgent issue. In this editorial, an overview of recent studies focused on the symptomatology and neurobiological and neurocomputational mechanisms of the 2 disorders and their comorbidity is provided.

Symptomatology

Recent research has employed data-driven approaches such as latent class analysis (LCA) to investigate the typologies of depression and anxiety. Latent class analysis uses the full range of symptoms to classify individuals into homogeneous subtypes or the so-called latent classes, based on the patterns of symptom occurrence. So far, by employing LCA, a class of individuals with comorbid depression and anxiety has been consistently identified in samples from the general population at different ages and from different countries.[9–13] In several studies, the comorbidity occurs at multiple levels of symptom severity, for instance, low, moderate and high.[10,11] In some[9,12] but not other[10,11,13] studies, a depression or anxiety class only was also identified. Importantly, these studies have reported unique demographic and psychological characteristics of the comorbid class compared to other classes, for instance, being female, younger age, having fewer years of education, and experiencing more negative life events.

Another technique, the network approach, proposes that individual symptoms play a causal role in the psychopathology (by causing the onset of other symptoms) and seeks to clarify the connected network of symptoms which constitutes a disorder.[14] Network analysis of symptoms in patients with depressive and anxiety disorders has identified psychomotor agitation/retardation and irritability as the most important bridge symptoms connecting the 2 disorders and underlying the comorbidity.[15,16] Symptoms such as appetite change and suicidality are found to be unique to depression.[16]

Neurobiological mechanism

At the neurobiological level, the alterations in prefrontal-limbic pathways[17,18] and serotonergic projections arising from the raphe nuclei[19–21] have been proposed to underlie both depression and anxiety, which also explains why antidepressants such as selective serotonin reuptake inhibitors and serotonin noradrenaline reuptake inhibitors are effective for anxiety disorders. Nevertheless, a recent transcranial magnetic stimulation (TMS) was able to identify 2 distinct circuit targets for symptom clusters of depression (e.g., sadness) and anxiety (e.g., irritability). Specifically, TMS targeting the dorsomedial prefrontal cortex relieves anxiety symptoms, while TMS targeting the dorsolateral prefrontal cortex reduces depressive symptoms.[22]

From the neuroendocrinological point of view, dysfunctional hypothalamic–pituitary–adrenal (HPA) axis and elevated cortisol have been considered common to both depression and anxiety.[23,24] Nevertheless, comorbid depression and anxiety compared to each disorder alone[25] and anxious depression compared to non-anxious depression[26] may have more emphasized abnormalities in HPA axis and cortisol activity. It has to be noted that hypercortisolemia has also been reported in anxiety disorders,[27,28] which calls for a closer look at the potential heterogeneity of HPA abnormalities within the subtypes of anxiety disorders, as well as a reconsideration of the functional role of cortisol.[23]

Neurocomputational mechanism

Another recent trend is the neurocomputational approach known as computational psychiatry.[29–31] This approach builds mathematical models to simulate the neural and/or cognitive processes underlying behaviors including decision-making, which allows for the precise assay of fundamental neurocomputational constructs. Therefore, the parameters of these neural and cognitive processes may serve as useful biomarkers.[29–31]

Although both depression and anxiety have long been associated with decision-making deficits, emerging evidence from computational psychiatry suggest unique neurocomputational alterations in each disorder. Whereas depression is associated with reduced reward-seeking behaviors, including slower learning of reward contingencies and increased estimation of effort required to pursue rewards,[31–34] anxiety is associated with heightened sensitivity to threat and increased threat avoidance behaviors.[34]

For instance, 1 study reported that patients with generalized anxiety disorder have elevated risk aversion as indicated by a more concave utility function.[31] Furthermore, symptoms of anxiety are correlated with elevated risk aversion after controlling depression; however, symptoms of depression are not correlated with elevated risk aversion after controlling anxiety, suggesting a unique link between anxiety and risk aversion.[35] Somewhat contradictorily, a subsequent study with healthy adults employing 3 different methods to tease apart the comorbidity of depression and anxiety showed that neither depression nor anxiety is associated with risk aversion, while depression but not anxiety is associated with probability weighting of reward outcomes.[36] As the symptoms of depression increase, people's tendency to overweight small probabilities and underweight large probabilities is attenuated or even reversed. While these studies advance our understanding of the neurocomputational changes of the disorders, future research is required to address the inconsistencies and further clarify potential sex differences.[37]

By investigating the common and unique symptomatic characteristics and underlying neurobiological and neurocomputational mechanisms of the 2 disorders and their comorbidity, it can be concluded that recent studies have greatly advanced our understanding of the etiology and neuropathophysiology of these disorders. The insights provided by these studies also shed light on several treatment targets that may be of particular clinical interest, including bridge symptoms, distinct brain circuit targets and distinct neurocomputational alterations. We believe that future research will propel us towards a better, more refined understanding of depression, anxiety and their comorbidity, and bring us closer to personalized precision psychiatry.

ORCID iDs

Chong Chen https://orcid.org/0000-0002-3189-7397

References

1. World Health Organization. Depression and other common mental disorders: Global health estimates. World Health Organization. 2017. https://apps.who.int/iris/bitstream/handle/10665/254610/WHO-MSD-MER-2017.2-eng.pdf. Accessed February 22, 2022.
2. Mineka S, Vrshek-Schallhorn S. Comorbidity of unipolar depressive and anxiety disorders. In: Gotlib IH, Hammen CL, eds. *Handbook of Depression*. 3rd ed. New York, USA: Guilford Press; 2015:84–102.
3. Andrews G, Slade TIM, Issakidis C. Deconstructing current comorbidity: Data from the Australian National Survey of Mental Health and Well-Being. *Br J Psychiatry.* 2002;181(4):306–314. doi:10.1192/bjp.181.4.306
4. Hofmeijer-Sevink MK, Batelaan NM, van Megen HJ, et al. Clinical relevance of comorbidity in anxiety disorders: A report from the Netherlands Study of Depression and Anxiety (NESDA). *J Affect Disord.* 2012;137(1–3):106–112. doi:10.1016/j.jad.2011.12.008
5. Kessler RC, Sampson NA, Berglund P, et al. Anxious and non-anxious major depressive disorder in the World Health Organization World Mental Health Surveys. *Epidemiol Psychiatr Sci.* 2015;24(3):210–226. doi:10.1017/S2045796015000189
6. Melton TH, Croarkin PE, Strawn JR, McClintock SM. Comorbid anxiety and depressive symptoms in children and adolescents: A systematic review and analysis. *J Psychiatr Pract.* 2016;22(2):84. doi:10.1097/PRA.0000000000000132
7. Saris IMJ, Aghajani M, Van Der Werff SJA, Van Der Wee NJA, Penninx BWJH. Social functioning in patients with depressive and anxiety disorders. *Acta Psychiatr Scand.* 2017;136(4):352–361. doi:10.1111/acps.12774
8. Fava M, Rush AJ, Alpert JE, et al. Difference in treatment outcome in outpatients with anxious versus nonanxious depression: A STAR* D report. *Am J Psychiatry.* 2008;165(3):342–351. doi:10.1176/appi.ajp.2007.06111868
9. Lei H, Chen C, Hagiwara K, et al. Symptom patterns of the occurrence of depression and anxiety in a Japanese general adult population sample: A latent class analysis. *Front Psychiatry.* 2022;13:808918. doi:10.3389/fpsyt.2022.808918
10. Rhebergen D, van der Steenstraten IM, Sunderland M, et al. An examination of generalized anxiety disorder and dysthymic disorder by latent class analysis. *Psychol Med.* 2014;44(8):1701–1712. doi:10.1017/S0033291713002225
11. Hettema JM, Aggen SH, Kubarych TS, Neale MC, Kendler KS. Identification and validation of mixed anxiety-depression. *Psychol Med.* 2015;45(14):3075–3084. doi:10.1017/S0033291715001038
12. Curran E, Rosato M, Ferry F, Leavey G. Prevalence and factors associated with anxiety and depression in older adults: Gender differences in psychosocial indicators. *J Affect Disord.* 2020;267:114–122. doi:10.1016/j.jad.2020.02.018
13. Wang Y, Ge F, Zhang J, Zhang W. Heterogeneity in the co-occurrence of depression and anxiety symptoms among youth survivors: A longitudinal study using latent profile analysis. *Early Interv Psychiatry.* 2021;15(6):1612–1625. doi:10.1111/eip.13101
14. Robinaugh DJ, Hoekstra RH, Toner ER, Borsboom D. The network approach to psychopathology: A review of the literature 2008–2018 and an agenda for future research. *Psychol Med.* 2020;50(3):353–366. doi:10.1017/S0033291719003404
15. Beard C, Millner AJ, Forgeard MJ, et al. Network analysis of depression and anxiety symptom relationships in a psychiatric sample. *Psychol Med.* 2016;46(16):3359–3369. doi:10.1017/S0033291716002300
16. Kaiser T, Herzog P, Voderholzer U, Brakemeier EL. Unraveling the comorbidity of depression and anxiety in a large inpatient sample: Network analysis to examine bridge symptoms. *Depress Anxiety.* 2021;38(3):307–317. doi:10.1002/da.23136
17. Kovner R, Oler JA, Kalin NH. Cortico-limbic interactions mediate adaptive and maladaptive responses relevant to psychopathology. *Am J Psychiatry.* 2019;176(12):987–999. doi:10.1176/appi.ajp.2019.19101064
18. McTeague LM, Rosenberg BM, Lopez JW, et al. Identification of common neural circuit disruptions in emotional processing across psychiatric disorders. *Am J Psychiatry.* 2020;177(5):411–421. doi:10.1176/appi.ajp.2019.18111271
19. Deakin JF. Depression and 5HT. *Int Clin Psychopharmacol.* 1991;6(Suppl 3):23–31. doi:10.1097/00004850-199112003-00002
20. Maier SF, Seligman ME. Learned helplessness at fifty: Insights from neuroscience. *Psychol Rev.* 2016;123(4):349. doi:10.1037/rev0000033
21. An Y, Chen C, Inoue T, et al. Mirtazapine exerts an anxiolytic-like effect through activation of the median raphe nucleus-dorsal hippocampal 5-HT pathway in contextual fear conditioning in rats. *Prog Neuropsychopharmacol Biol Psychiatry.* 2016;70:17–23. doi:10.1016/j.pnpbp.2016.04.014
22. Siddiqi SH, Taylor SF, Cooke D, et al. Distinct symptom-specific treatment targets for circuit-based neuromodulation. *Am J Psychiatry.* 2020;177(5):435–446. doi:10.1176/appi.ajp.2019.19090915
23. Chen C, Nakagawa S, An Y, et al. The exercise-glucocorticoid paradox: How exercise is beneficial to cognition, mood, and the brain while increasing glucocorticoid levels. *Front Neuroendocrinol.* 2017;44:83–102. doi:10.1016/j.yfrne.2016.12.001
24. Tafet GE, Nemeroff CB. Pharmacological treatment of anxiety disorders: The role of the HPA axis. *Front Psychiatry.* 2020;11:443. doi:10.3389/fpsyt.2020.00443
25. Kircanski K, LeMoult J, Ordaz S, Gotlib IH. Investigating the nature of co-occurring depression and anxiety: Comparing diagnostic and dimensional research approaches. *J Affect Disord.* 2017;216:123–135. doi:10.1016/j.jad.2016.08.006
26. Ionescu DF, Niciu MJ, Mathews DC, Richards EM, Zarate Jr CA. Neurobiology of anxious depression: A review. *Depress Anxiety.* 2013;30(4):374–385. doi:10.1002/da.22095

27. Boyer P. Do anxiety and depression have a common pathophysiological mechanism? *Acta Psychiatr Scand*. 2000;102:24–29. doi:10.1111/j.0065-1591.2000.acp29-04.x
28. Faravelli C, Lo Sauro C, Lelli L, et al. The role of life events and HPA axis in anxiety disorders: A review. *Curr Pharm Des*. 2012;18(35):5663. doi:10.2174/138161212803530907
29. Chen C, Takahashi T. Reward processing in depression. In: Moustafa AA, ed. *Computational Models of Brain and Behavior.* Hoboken, USA: Wiley-Blackwell; 2018:55–71. ISBN: 978-1-119-15906-3.
30. Huys QJ, Browning M, Paulus MP, Frank MJ. Advances in the computational understanding of mental illness. *Neuropsychopharmacology*. 2021;46(1):3–19. doi:10.1038/s41386-020-0746-4
31. Chen C, Takahashi T, Nakagawa S, Inoue T, Kusumi I. Reinforcement learning in depression: A review of computational research. *Neurosci Biobehav Rev*. 2015;55:247–267. doi:10.1016/j.neubiorev.2015.05.005
32. Chen C, Takahashi T, Yang S. Remembrance of happy things past: Positive autobiographical memories are intrinsically rewarding and valuable, but not in depression. *Front Psychol*. 2015;6:222. doi:10.3389/fpsyg.2015.00222
33. Halahakoon DC, Kieslich K, O'Driscoll C, et al. Reward-processing behavior in depressed participants relative to healthy volunteers: A systematic review and meta-analysis. *JAMA Psychiatry*. 2020;77(12):1286–1295. doi:10.1001/jamapsychiatry.2020.2139
34. Bishop SJ, Gagne C. Anxiety, depression, and decision making: A computational perspective. *Annu Rev Neurosci*. 2018;41:371–388. doi:10.1146/annurev-neuro-080317-062007
35. Charpentier CJ, Aylward J, Roiser JP, Robinson OJ. Enhanced risk aversion, but not loss aversion, in unmedicated pathological anxiety. *Biol Psychiatry*. 2017;81(12):1014–1022. doi:10.1016/j.biopsych.2016.12.010
36. Hagiwara K, Mochizuki Y, Chen C, et al. Nonlinear probability weighting in depression and anxiety: Insights from healthy young adults. *Front Psychiatry*. 2022;13:810867. doi:10.3389/fpsyt.2022.810867
37. Lei H, Mochizuki Y, Chen C, et al. Sex difference in the weighting of expected uncertainty under chronic stress. *Sci Rep*. 2021;11(1):1–10. doi:10.1038/s41598-021-88155-1

Trephine-based foraminoplasty in PTED treatment of lumbar lateral recess stenosis

Xintao Wang[A–F], Leilei Wu[B–F], Kui Zhao[B–F], Dechun Chen[B,F], Bo Su[B,F], Yuanhang Kong[B,F], Jinmeng Li[B,F], Kunlong Kang[B,F], Daiwei Si[B,F]

Department of Orthopedics, The Second Affiliated Hospital of Harbin Medical University, China

A – research concept and design; B – collection and/or assembly of data; C – data analysis and interpretation; D – writing the article; E – critical revision of the article; F – final approval of the article

Advances in Clinical and Experimental Medicine, ISSN 1899–5276 (print), ISSN 2451–2680 (online) *Adv Clin Exp Med*. 2022;31(4):359–367

Address for correspondence
Xintao Wang
E-mail: xintaog6@163.com

Funding sources
None declared

Conflict of interest
None declared

Received on July 7, 2021
Reviewed on October 5, 2021
Accepted on December 7, 2021

Published online on January 24, 2022

Abstract

Background. During minimally invasive spine surgery, nerve root decompression is challenging due to the anatomical division and uncertainty in lumbar lateral recess (LLR).

Objectives. To evaluate the outcome and safety of foraminoplasty using percutaneous transforaminal endoscopic decompression (PTED) (performed with an aid of a trephine) in the treatment of lumbar lateral recess stenosis (LLRS).

Materials and methods. All operations were performed under local anesthesia and in prone position. The puncture point was 10–14 cm away from the midline of the spinous process. One hundred eight individuals with LLRS who underwent PTED from September 2016 to December 2020 in our hospital were enrolled in the study. Visual Analog Scale (VAS) and Oswestry Disability Index (ODI) scores were collected preoperatively after 1 day, 7 days, 1 month and at the final follow-up (June 2021). Low back pain and leg pain were measured using VAS score. Functional outcomes were assessed with ODI and modified Macnab criteria.

Results. After the surgery, the VAS score and ODI were statistically significant at all follow-up points compared with the pre-surgery (both $p < 0.05$). Based on the modified Macnab scores at the final follow-up, the satisfaction rate at postoperative 1 month was 96.3% and the satisfaction rate at postoperative 7 days was 70.38%. A significant difference was observed between the 2 groups ($p < 0.05$).

Conclusions. Foraminoplasty using PTED performed with a trephine is one of the safe and effective, minimally invasive methods to treat LLRS.

Key words: trephine, percutaneous transforaminal endoscopic decompression, lumbar lateral recess stenosis, foraminoplasty

Cite as
Wang X, Wu L, Zhao K, et al. Trephine-based foraminoplasty in PTED treatment of lumbar lateral recess stenosis. *Adv Clin Exp Med*. 2022;31(4):359–367. doi:10.17219/acem/144638

DOI
10.17219/acem/144638

Background

In 1954, Dutch neurosurgeon Henk Verbiest first defined lumbar spinal stenosis (LSS), bony canal stenosis and neurogenic claudication.[1] Lumbar lateral recess stenosis (LLRS) is a type of LSS. Based on the anatomical types, LLRS can occur in the retrodiscal space, upper part of bony lateral recess and lower part of bony lateral recess (Fig. 1).[2,3] Lumbar lateral recess stenosis indicates that the sagittal diameter of the bone canal is less than 3.0 mm and the diameter of the soft tissue tube is less than 1.0 mm, with varying degrees of lower limb pain, numbness and intermittent claudication.[4]

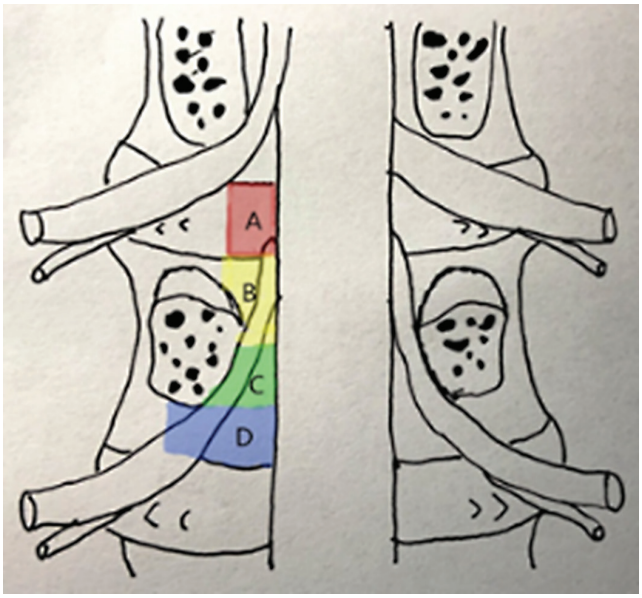

Fig. 1. Schematic diagram of A. retrodiscal space; B. upper part of bony lateral recess; C. lower part of bony lateral recess; D. intervertebral foramen

Several surgical options exist for the treatment of LLRS – foraminotomy, partial facetectomy, total laminectomy, posterior lumbar interbody fusion (PLIF), and transforaminal lumbar interbody fusion (TLIF).[5] However, these surgical approaches cause several complications such as muscle trauma, severe bleeding, high hospitalization costs, and fracture of internal fixator, which influence the stability of the spine.[6–9]

Schreiber et al. first applied endoscopic technology for percutaneous nucleus pulposus removal in 1989.[10] With the development of endoscopic theory and equipment, Hoogland designed Transforaminal Endoscopic Spine System (TESSYS), which positions the tip of the superior articular process (SAP) using multistage trephine to grind the tip of SAP (Fig. 2).[11] Yuan et al.[12] applied this technique to treat 48 cases of lumbar disc herniation (LDH) and obtained good results. However, for LLRS, the base of SAP blocked the working channel; LLR decompression was not complete. Therefore, the operation of foraminoplasty under the working channel is limited and the decompression takes

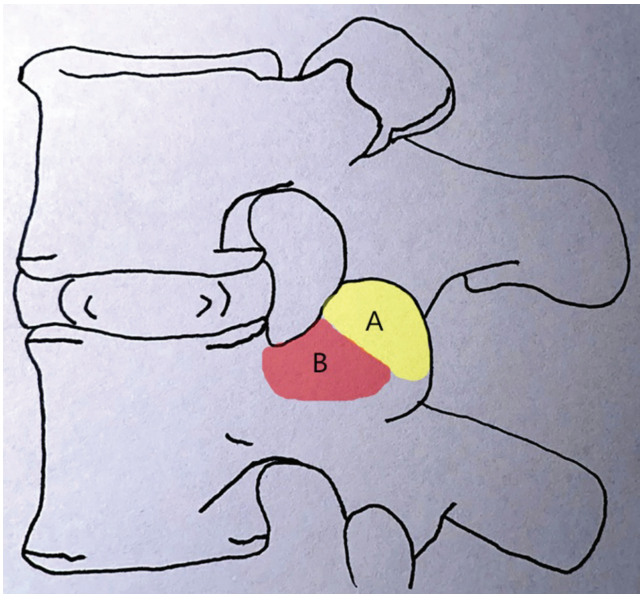

Fig. 2. Schematic diagram of A. the tip of the superior articular process (SAP); B. the bottom of the SAP

longer. The exiting root is easily injured by compression of working tube. The base of SAP is far away from exiting root, which is closer to the bony part of LLR. The 7.6 mm-diameter trephine rather than multistage trephine is easier to remove the base of SAP for foraminoplasty. This method is economical and effective, as well as it reduces the number of radiation leakage. In this study, percutaneous transforaminal endoscopic decompression (PTED) was applied with an aid of trephine to treat patients with LLRS, and the clinical outcomes were analyzed.

Objectives

The aim of this study was to evaluate the outcome and safety of foraminoplasty using percutaneous transforaminal endoscopic decompression (PTED) (performed with an aid of a trephine) to treat lumbar lateral recess stenosis.

Materials and methods

General information

This is a retrospective study. A total of 108 individuals with LLRS were assessed by 2 spine surgeons between September 2016 and December 2020. Those who were selected to undergo PTED with an aid of trephine for LLRS were invited to participate in the study. The inclusion criteria were as follows: (1) the imaging data were complete, consistent with clinical symptoms and signs, and the diagnosis of single-segment LLRS was clear; (2) some patients present with worse symptoms after receiving conservative treatment, which severely affects the quality of life; (3) patients

with coronary artery insufficiency, heart failure, diabetes, respiratory failure, etc. Exclusion criteria were as follows: (1) preoperative imaging data showed spinal instability such as spondylolisthesis and spondylolysis; (2) neurogenic diseases, such as cauda equina syndrome; (3) spinal deformity, spinal tumor or other diseases; (4) the iliac crest for L5-S1 segment was too high (the X-ray suggested that the theoretical puncture passage was blocked by ilium); (5) surgical contraindications (such as important organ dysfunction and bleeding tendency).

The present study followed the principles outlined in the Declaration of Helsinki, received an approval (No. KY2021-260) from our local hospital ethics committee (the Second Affliated Hospital of Harbin Medical University, China) and patients provided informed consent regarding the publication of their data.

Surgical technique

All operations were performed under local anesthesia and in prone position. Puncture point was 10–14 cm away from the midline of the spinous process. The vertical distance of the head side was 2–5 cm, and the puncture needle was inclined at approx. 25° to the horizontal. The average abduction angle of the puncture needle was 30–50°. Under anteroposterior and lateral fluoroscopy, the puncture needle reaches the base of SAP of the inferior vertebral body of the target intervertebral space.

Besides, the procedure was performed under local infiltration anesthesia induced with 0.7% lidocaine. The puncture needle was inserted and located at the bottom of SAP of the diseased segment, and the facet joint was anesthetized on the surface. Next, we removed the needle core, inserted the guidewire, made an 8.0 mm skin incision along with the needle entry point, and placed a four-stage dilatation catheter (Spinendos, Munich, Germany) step by step along the guidewire. These devices were placed at the inner edge of the pedicle under the anteroposteric X-ray, and at the anterior and lower edge of the superior articular process under the lateral X-ray. A 7.6 mm-diameter trephine (Spinendos) was introduced at the base of the SAP, so as to form the SAP.

The trephine was used to remove the partial base of SAP under fluoroscopic guidance. The space formed in this way can be more conducive for the subsequent work tube to access LLR. The procedure is performed in the working tube through the deformed SAP, and targeted decompression is conducted according to the LLRS type, including soft tissue and bony compression. If LLRS is biased to intervertebral foramen and retrodiscal space, the medial and ventral SAP are mainly removed; if the stenosis is partial to bony stenosis, the partial bottom of the SAP is largely removed. Therefore, the plastic scheme is in most cases designed in advance based on the preoperative magnetic resonance imaging (MRI) and computed tomography (CT) image data. Then, it is adjusted according to the specific conditions during the operation. A representative case treated with trephine foraminoplasty is illustrated in Fig. 3,4.

Evaluation of the curative effect

All patients were followed up (including outpatient and telephone follow-up), and the relevant indexes were recorded preoperatively, 1 day, 7 days, 1 month after the operation, and at the final follow-up. In this process, Visual Analogue Scale (VAS) was used to evaluate low back pain before and after the operation; Oswestry Disablity Index (ODI) was applied to evaluate the functional recovery of lumbar vertebrae before and after the operation; the modified Macnab standard was employed to evaluate the curative effect of the operation.

Statistical analyses

The data were processed using IMB SPSS v. 23.0 statistical software (IBM Corp., Armonk, USA), in which the measurement data such as VAS and ODI were presented with median (M), lower quartile (Q_L) and upper quartile (Q_U). All the data were analyzed with Shapiro–Wilk normality test and homogeneity of variance test. Comparisons of the continuous parameters were performed using the repeated measures analysis of variance (ANOVA) test when a normal distribution was present, and using the Kruskal–Wallis test when a normal distribution was absent. The numerical data were compared with the χ^2 test. The value of $p < 0.05$ reflects statistical significance. In this study, operation time, intraoperative bleeding volume, ODI, and VAS did not meet normal distribution.

Results

All operations were successfully completed and were followed up postoperatively after 1 day, 7 days, 1 month, and at the final follow-up 1 year after the operation, in June 2021. The operation time ranged from 60 min to 125 min, with an average of 88.74 min. The intraoperative bleeding volume ranged from 5 mL to 18 mL, with an average of 9.49 mL (Table 1). There were no related complications such as spinal instability, dural leakage or vascular or nerve injury. The VAS score and ODI of low back pain before the operation, on day 1, day 7, after 1 month, and at the final postoperative follow-up were compared. The postoperative scores were higher than those at the preoperative stage (Table 2, Fig. 5–7).

All the indexes improved, and the difference was statistically significant ($p < 0.05$). The symptom efficacy of the patients was evaluated with modified Macnab standard. Particularly, according to the Macnab standard, 1 month after the operation, 88 cases were excellent, 16 cases were good, and 4 cases were fair; the excellent and good rates

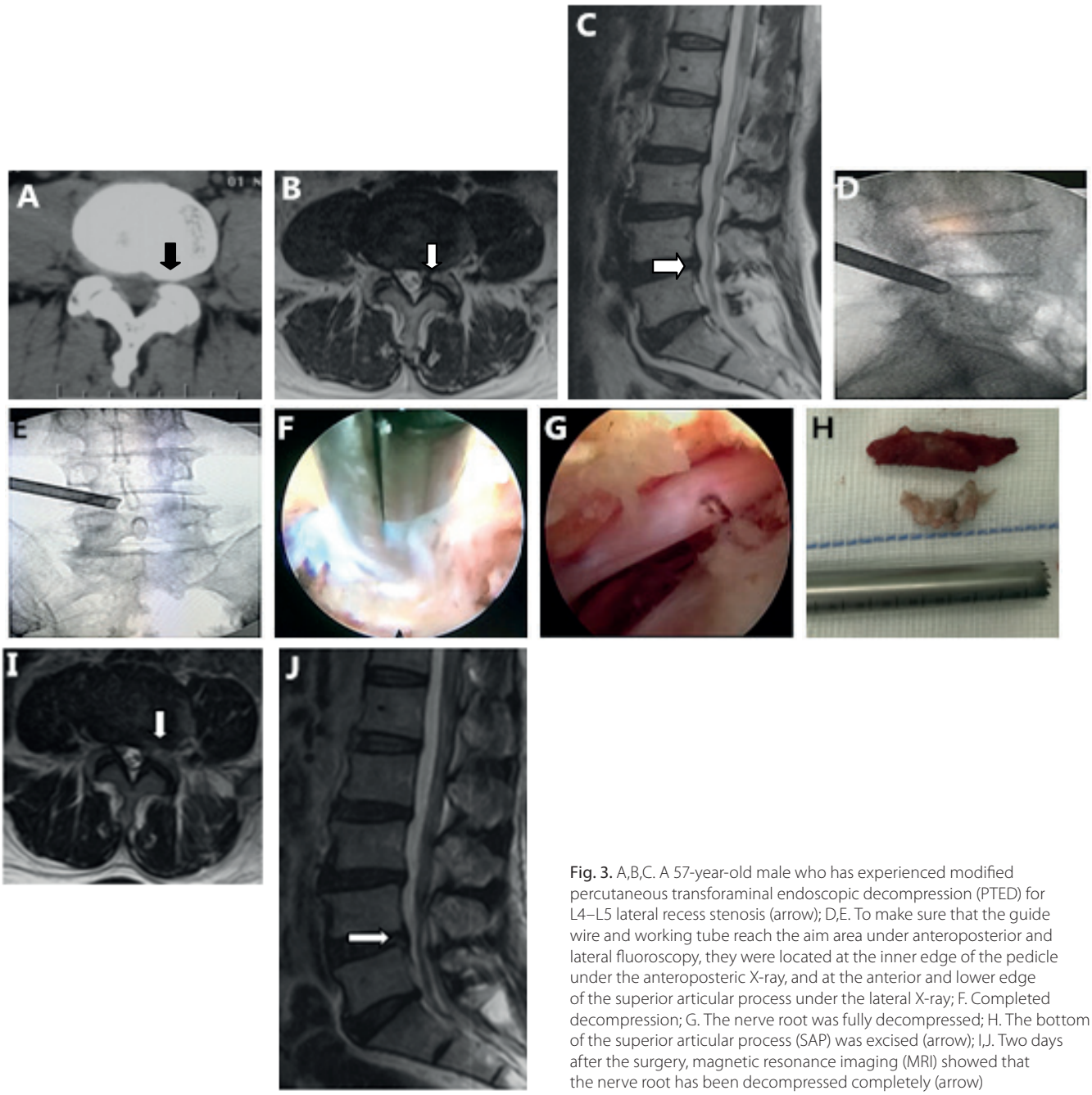

Fig. 3. A,B,C. A 57-year-old male who has experienced modified percutaneous transforaminal endoscopic decompression (PTED) for L4–L5 lateral recess stenosis (arrow); D,E. To make sure that the guide wire and working tube reach the aim area under anteroposterior and lateral fluoroscopy, they were located at the inner edge of the pedicle under the anteroposteric X-ray, and at the anterior and lower edge of the superior articular process under the lateral X-ray; F. Completed decompression; G. The nerve root was fully decompressed; H. The bottom of the superior articular process (SAP) was excised (arrow); I,J. Two days after the surgery, magnetic resonance imaging (MRI) showed that the nerve root has been decompressed completely (arrow)

were 96.30%. Seven days after the operation, 65 cases were excellent, 11 cases were good and 32 cases were fair; the excellent rate was 70.38%. The excellent and good rates at 1 month after the operation were significantly higher than at 7 days after the operation, and the difference was statistically significant ($p < 0.05$) (Table 3).

Discussion

Since Verbiest,[1] a Dutch neurosurgeon, first defined LSS in 1954, the international understanding of the definition and partition of the lateral region of the lumbar spinal canal has not been unified. Among them, experts such

Table 1. Baseline characteristics

Patient data	Modified PTED (n = 108)
Age	46.81 ±16.90
Gender male female	 58 50
Segment L2–L3 L3–L4 L4–L5 L5–S1	 1 7 67 33
Operation time [min]	90.000 (80.000, 95.000)
Intraoperative bleeding volume [mL]	9.000 (7.000, 12.000)

PTED – percutaneous transforaminal endoscopic decompression.

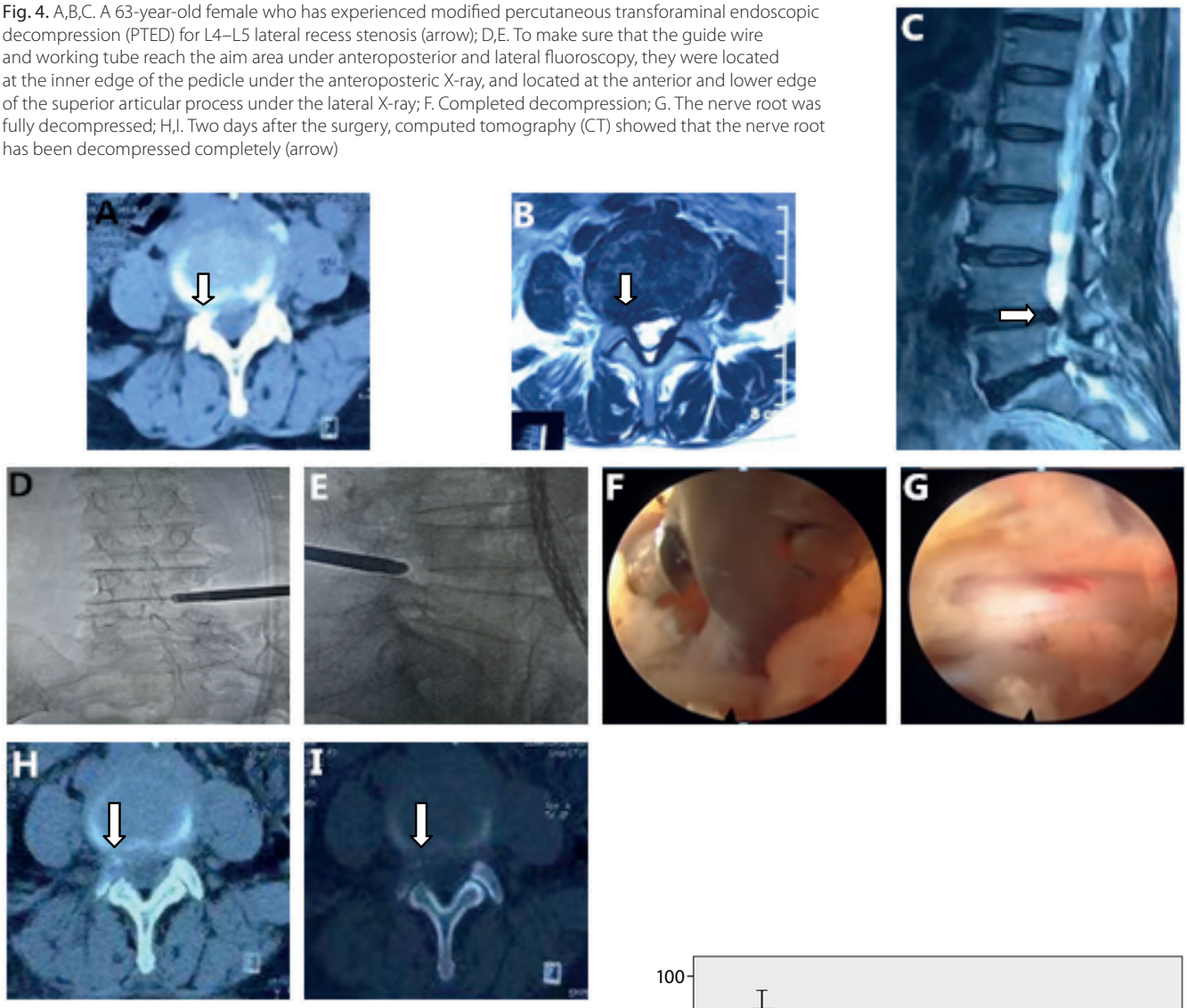

Fig. 4. A,B,C. A 63-year-old female who has experienced modified percutaneous transforaminal endoscopic decompression (PTED) for L4–L5 lateral recess stenosis (arrow); D,E. To make sure that the guide wire and working tube reach the aim area under anteroposterior and lateral fluoroscopy, they were located at the inner edge of the pedicle under the anteroposteric X-ray, and located at the anterior and lower edge of the superior articular process under the lateral X-ray; F. Completed decompression; G. The nerve root was fully decompressed; H,I. Two days after the surgery, computed tomography (CT) showed that the nerve root has been decompressed completely (arrow)

as Lee et al.[2] and Vital et al.[3] have proposed their views on the partition of lateral region of the lumbar spinal canal, and their concept became the most widely used partition basis: retrodiscal space, upper part of bony lateral recess, lower part of bony lateral recess, and intervertebral foramen. Regardless of the types, Mikhael et al.[4] defined LLRS as the sagittal diameter of the bony canal of LLR smaller than 3.0 mm or the diameter of soft tissue canal smaller than 1.0 mm.

The LLRS is often induced by sedentary work or fatigue, when the lumbar spine is overloaded, leading to the dehydration and denaturation of the intervertebral disc. This increases the stress of the tissue around the intervertebral disc, the range motion of the adjacent intervertebral joint, the hyperplasia and hypertrophy of ligament in lumbar spinal, and the formation of osteophyte. Finally, these pathological changes will eventually encroach LLR to reduce the diameter, resulting in nerve root compression and repeated friction by surrounding tissues, as well as nerve root ischemia and edema.[13] Therefore, patients with LLRS not only show varying

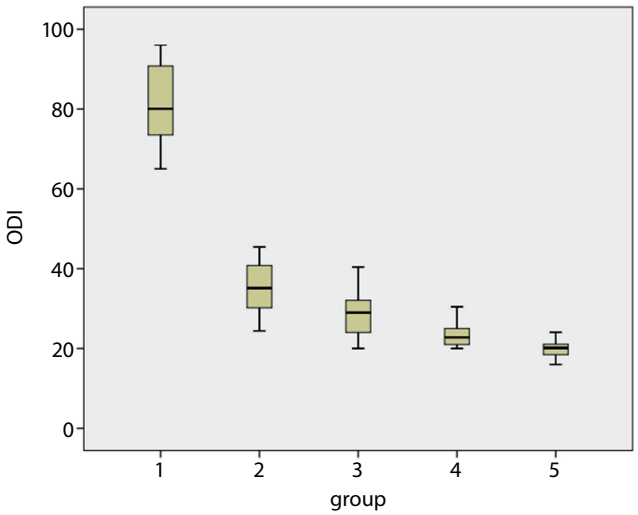

Fig. 5. Presentation of Oswestry Disability Index (ODI) value alteration before and after the operation (1 – before the operation; 2 – 1 day post operation; 3 – 7 days post operation; 4 – 1 month post operation; 5 – final follow-up). The M (Q_L, Q_U) of preoperative Oswestry Disability Index (ODI) score was 80.0700 (72.7500, 90.7800), while the values of this score 1 day after the operation, 7 days after the operation, 1 month after the operation, and at the final follow-up were 35.1300 (30.2100, 40.7800), 28.9950 (24.0400, 32.0600), 23.0200 (21.0000, 25.8525), and 20.1300 (18.4500, 21.0750), respectively

M – median; Q_L – lower quartile; Q_U – upper quartile.

Table 2. Comparison of back pain, leg pain, VAS and ODI before and after operation

Parameter	M (Q_L, Q_U)
ODI	
preoperative	80.070 (72.750, 90.780)
postoperative (1 day)	35.130 (30.210, 40.780)
postoperative (7 days)	28.995 (24.040, 32.060)
postoperative (1 month)	23.020 (21.000, 25.853)
postoperative (final follow-up)	20.130 (18.450, 21.075)
H	436.333
p-value	0.000*
VAS (back pain)	
preoperative	7.00 (6.00, 8.00)
postoperative (1 day)	3.00 (3.00, 4.00)
postoperative (7 days)	2.00 (2.00, 3.00)
postoperative (1 month)	2.00 (2.00, 3.00)
postoperative (final follow-up)	2.00 (2.00, 2.00)
H	351.958
p-value	0.000[&]
VAS (leg pain)	
preoperative	8.00 (7.00, 9.00)
postoperative (1 day)	3.00 (3.00, 4.00)
postoperative (7 days)	2.00 (2.00, 3.00)
postoperative (1 month)	2.00 (2.00, 2.00)
postoperative (final follow-up)	2.00 (2.00, 2.00)
H	370.405
p-value	0.000[#]

VAS – Visual Analog Scale; ODI – Oswestry Disability Index. * Kruskal–Wallis test results are as follows: H = 436.333, p < 0.001. According to the test standard α = 0.05, if H0 is rejected, ODI differences can be considered statistically significant before the surgery and after 1 day, 7 days, 1 month and at final follow-up (4 time nodes after the surgery). [&] Kruskal–Wallis test results are as follows: H = 351.958, p < 0.001. According to the test standard α = 0.05, if H0 is rejected, VAS (back pain) differences can be considered statistically significant before the surgery and after 1 day, 7 days, 1 month and at final follow-up (4 time nodes after the surgery). [#] Kruskal–Wallis test results are as follows: H = 370.405, p < 0.001. According to the test standard α = 0.05, if H0 is rejected, VAS (leg pain) differences can be considered statistically significant before the surgery and after 1 day, 7 days, 1 month and at final follow-up (4 time nodes after the surgery).

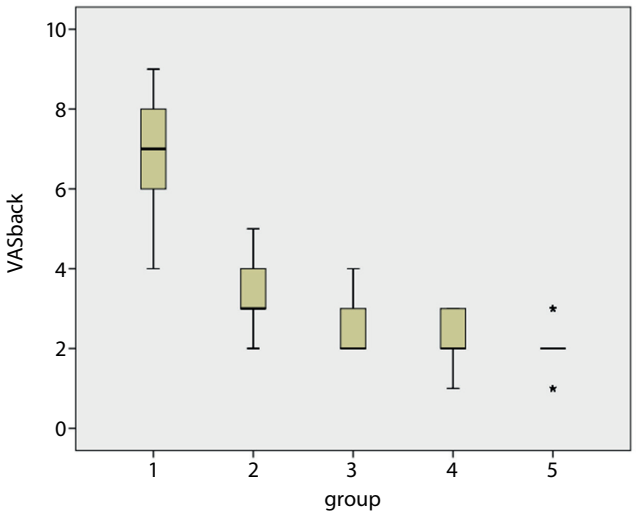

Fig. 6. Visual Analog Scale (VAS) for low back pain (VASback) value alteration before and after the operation (1 – before the operation; 2 – 1 day post operation; 3 – 7 days post operation; 4 – 1 month post operation; 5 – final follow-up). The M (Q_L, Q_U) of preoperative VASback was 7.00 (6.00, 8.00), while the values of this score 1 day after the operation, 7 days after the operation, 1 month after the operation, and at the final follow-up were 3.00 (3.00, 4.00), 2.00 (2.00, 3.00), 2.00 (2.00, 3.00), and 2.00 (2.00, 2.00), respectively

M – median; Q_L – lower quartile; Q_U – upper quartile.

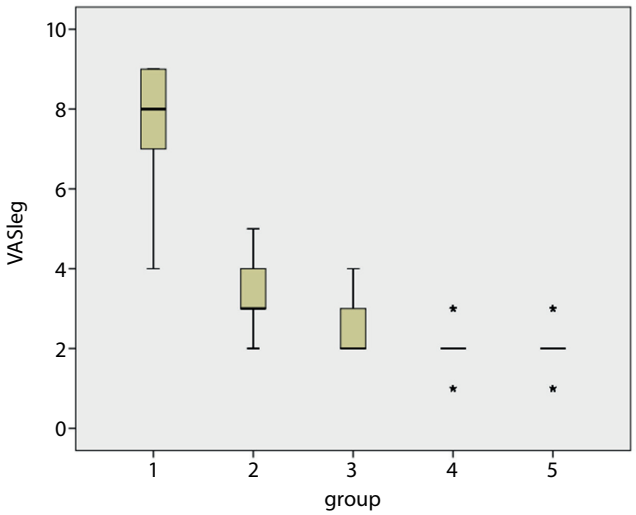

Fig. 7. Visual Analog Scale (VAS) for leg pain (VASleg) value alteration before and after operation (1 – before the operation; 2 – 1 day post operation; 3 – 7 days post operation; 4 – 1 month post operation; 5 – final follow-up). The M (Q_L, Q_U) of preoperative VASleg was 8.00 (7.00, 9.00), while the values of this score 1 day after the operation, 7 days after the operation, 1 month after the operation, and at the final follow-up were 3.00 (3.00, 4.00), 2.00 (2.00, 3.00), 2.00 (2.00, 2.00), and 2.00 (2.00, 2.00), respectively. In summary, it can be seen from the box plots of score that, except for the scores of individual research subjects which are quite different from those of others, the score values of almost all research subjects are getting closer and closer to each other, which can more intuitively express the effect of a surgical intervention

M – median; Q_L – lower quartile; Q_U – upper quartile.

degrees of low back pain but also show lower limb pain, numbness and intermittent claudication caused by LLRS.

For LLRS, nonoperative treatment is ineffective, and surgery is often needed. The traditional treatment of LLRS has always been PLIF, because it provides a way to directly contact the diseased vertebral body, relieving waist and leg pain and other discomforts, mainly through decompression and fusion. However, the operation is traumatic and destroys much tissue structure around the lumbar vertebrae. With time, the incidence of complications related to surgery is high, contributing to an increasing risk of the perioperative surgery. There is also a risk of the implanted internal fixator to fracture, loosen, and other complications to appear.[14] The trend of surgical treatment has turned to minimally invasive surgery, and many experts and scholars have presented new solutions.[14,15]

In 1989, Schreiber et al. first applied the endoscopic technique to percutaneous nucleus pulposus removal.[10] With the updating endoscopic theory and equipment, TESSYS technique has been one of the most reliable minimally invasive spinal surgery techniques and is widely used in the clinic. Due to SAP being an obstacle to the working channel and the anterolateral dura mater, foraminoplasty by removing part of SAP is the key to TESSYS.

Table 3. Comparison of efficacy 7 days and 1 month after the operation (n (%))

Variable	Excellent	Good	Fair	Poor	Excellent rate
Postoperative efficacy (7 days)	65 (60.19)	11 (10.19)	32 (29.62)	0 (0.00)	76 (70.38)
Postoperative efficacy (1 month)	88 (81.48)	16 (14.82)	4 (3.70)	0 (0.00)	104 (96.30)
χ^2 value	–	–	–	–	26.13
p-value	–	–	–	–	<0.05

For TESSYS, the failure rate of nonforaminal surgery is as high as 60%.[16] The traditional TESSYS technique involves removing the tip of SAP. The TESSYS technique uses a multistage trephine outside the guide rod. The surgeon gradually resects the tip of the superior articular process under X-ray fluoroscopy, enlarges the intervertebral foramen, and sends the endoscope into the spinal canal. First, the herniation in the spinal canal is removed. Then, the intervertebral disc is cleaned. The TESSYS technique significantly improves the curative effect of percutaneous endoscopic surgery by intervertebral foramen approach and expands the surgical indications. Nevertheless, the surgery site is at the tip of the superior articular process, the space is narrow, the range of surgery is limited, and the treatment of contralateral recess stenosis is still unsatisfactory.[17] In the past, Yang et al. have proposed that the base had more advantages than the tip.[18] At the same time, Li et al.[19] improved the existing foraminoplasty and changed the position of the foraminoplasty from the tip of SAP to the bottom of SAP. Since the site of foraminoplasty is far away from the exiting nerve root, theoretically, the incidence of dysfunction is low.

Our technique is improved based on the TESSYS technique. The 7.6 mm-diameter trephine is used to shape the base of the articular process under the protection of the casing of the trephine. Consequently, there is sufficient room for shaping, far away from the exit nerve root to avoid its injury.[20] The modified TESSYS technique can directly enlarge the lateral recess, remove the cohesive osseous structure of the articular process, the hypertrophic ligamentum flavum and the protruding nucleus pulposus, and complete more effective nerve root decompression.

It is essential for LLRS patients to enlarge the width of the intervertebral foramen during PTED treatment.[21] Spinal foraminoplasty can completely decompress the ventral and dorsal structures by cutting the SAP base part and removing the intervertebral foraminal ligament to expand the orifice, contributing to visually displaying the epidural space. The tools currently used for foraminoplasty include endoscopic burr, multistage trephine, and reamers.[22–24] Most of the SAP is removed under the working channel endoscope to ensure the safety of the operation. Nonetheless, it is limited by the working channel, the foramina efficiency is low and the expansion of the lateral recess is restricted. Besides, the microscopic drill will release heat while in use, damaging the nerve roots and causing temporary nerve stimulation, postoperative sensory disturbance and iatrogenic injury.[25]

Compared with reamer and laser, the 7.6 mm-diameter trephine is an economical and time-saving device for abrading part of the SAP base under fluoroscopy guidance to perform foraminoplasty. Nevertheless, there is also the risk of damaging the SAP covering ligaments. Additionally, the working channel has enough space after cutting a part of the SAP. When using a trephine, perspective must be used in order to ensure an acceptable instrument angle and depth, and confirm that the trephine has penetrated the inner edge of the SAP. However, part of the nerve root in lateral recess stenosis is compressed by the hyperplastic osteophyte of the bony channel, and the risk of damaging the nerve root during decompression is extremely high. Therefore, the extensive surgical experience is required to fully control the trephine depth during vertebroplasty.[26] Moreover, several fluoroscopic examinations are required, increasing the exposure of patients and medical staff to radiation.[27]

The technical advantage of the surgical method used in this study is that the intervertebral foramen is located at the bottom of the SAP rather than at the tip of it. During the operation, the direction and angle of decompression can be flexibly adjusted according to the specific location of the nerve root canal stenosis. If the stenosis of the LLRS is on the inner side of the intervertebral foramina and the yellow space of the intervertebral disc, the medial part of the SAP is mainly removed; if the stenosis is biased to the bony recess, the bottom of the SAP is mainly removed. Meanwhile, the hypertrophy that hinders the operation of the surgical field can be removed. The ligamentum flavum and the posterior longitudinal ligament can also remove the hyperplastic osteophytes, and the decompression can be maximized to the back of the intervertebral disc.

The 108 patients in our study population had good postoperative results without related complications such as spinal instability, dural leakage and vascular nerve damage. The indexes of this group of patients 3 months and 2 days after operation were significantly better than those 1 day before the operation, indicating the statistically significant difference ($p \leq 0.05$). However, there was no significant difference between the 2 groups in the average of the indicators on the 2nd day after the surgery due to incision pain and soft tissue spasm ($p > 0.05$). Most patients felt apparent relief after the surgery. Regarding some patients with residual nerve symptoms, such as numbness and pain in the lower limbs, it is believed that the edema and inflammation

caused by the disturbance of the nerve roots appeared during the operation. Satisfactory results were obtained after 2–3 weeks of treatment with dehydration, low-dose hormones and non-steroidal anti-inflammatory drugs. Although there was a certain complication rate reported in the past, a certain treatment was given in time, such as rehabilitation physiotherapy, hormone shock, and others, and the follow-up treatment effect was satisfactory.

Limitations

There are some limitations that need to be acknowledged and addressed regarding the present study. The first one concerns the small number of study group. Although our approach might not have been optimal, it enabled us to objectively evaluate the effectiveness of PTED in patients with LLRS. Because the results of the study were very consistent and showed a small standard deviation, this study might have scientific meaning despite the small number of participants. Second, due to the heterogeneity of the surgical techniques used and the experience of the surgeons, the findings could not have been simply generalized beyond the study group.

Conclusion

To sum up, PTED (performed with the aid of 7.6 mm-diameter trephine) has a satisfactory clinical effect in the treatment of LLRS. The use of a 7.6 mm trephine for foraminoplasty can improve the efficiency of foraminoplasty without reducing the stability of the lumbar spine. The PTED (performed with the aid of 7.6 mm trephine) is one of the safe and effective surgical methods in the treatment of LLRS.

ORCID iDs

Xintao Wang https://orcid.org/0000-0001-8844-8384
Leilei Wu https://orcid.org/0000-0001-9478-064X
Kui Zhao https://orcid.org/0000-0003-2979-3350
Dechun Chen https://orcid.org/0000-0003-0846-6078
Bo Su https://orcid.org/0000-0001-6288-1382
Yuanhang Kong https://orcid.org/0000-0001-9461-4617
Jinmeng Li https://orcid.org/0000-0001-5306-7805
Kunlong Kang https://orcid.org/0000-0002-6598-9660
Daiwei Si https://orcid.org/0000-0002-2971-6307

References

1. Verbiest H. A radicular syndrome from developmental narrowing of the lumbar vertebral canal. *J Bone Joint Surg Br*. 1954;36-B(2):230–237. doi:10.1302/0301-620X.36B2.230
2. Lee BC, Kazam E, Newman AD. Computed tomography of the spine and spinal cord. *Radiology*. 1978;128(1):95–102. doi:10.1148/128.1.95
3. Vital JM, Lavignolle B, Grenier N, Rouais F, Malgat R, Senegas J. Anatomy of the lumbar radicular canal. *Anat Clin*. 1983;5(3):141–151. doi:10.1007/BF01798999
4. Mikhael MA, Ciric I, Tarkington JA, Vick NA. Neuroradiological evaluation of lateral recess syndrome. *Radiology*. 1981;140(1):97–107. doi:10.1148/radiology.140.1.7244248
5. Lv Z, Jin L, Wang K, et al. Comparison of effects of PELD and fenestration in the treatment of geriatric lumbar lateral recess stenosis. *Clin Interv Aging*. 2019;14:2187–2194. doi:10.2147/CIA.S226295
6. Tang S, Jin S, Liao X, Huang K, Luo J, Zhu T. Transforaminal percutaneous endoscopic lumbar decompression by using rigid bendable burr for lumbar lateral recess stenosis: Technique and clinical outcome. *Biomed Res Int*. 2018;2018:2601232. doi:10.1155/2018/2601232
7. Ahn Y, Keum HJ, Lee SG, Lee SW. Transforaminal endoscopic decompression for lumbar lateral recess stenosis: An advanced surgical technique and clinical outcomes. *World Neurosurg*. 2019;125:e916–e924. doi:10.1016/j.wneu.2019.01.209
8. Yue B, Shen F, Ye ZF, Wang ZH, Yang HL, Jiang GQ. Accurate location and minimally invasive treatment of lumbar lateral recess stenosis with combined SNRB and PTED. *J Int Med Res*. 2020;48(3):300060519884817. doi:10.1177/0300060519884817
9. Xin Z, Huang P, Zheng G, Liao W, Zhang X, Wang Y. Using a percutaneous spinal endoscopy unilateral posterior interlaminar approach to perform bilateral decompression for patients with lumbar lateral recess stenosis. *Asian J Surg*. 2020;43(5):593–602. doi:10.1016/j.asjsur.2019.08.010
10. Schreiber A, Suezawa Y, Leu H. Does percutaneous nucleotomy with discoscopy replace conventional discectomy? Eight years of experience and results in treatment of herniated lumbar disc. *Clin Orthop Relat Res*. 1989;(238):35–42. PMID:2910617.
11. Hoogland T, Schubert M, Miklitz B, Ramirez A. Transforaminal posterolateral endoscopic discectomy with or without the combination of a low-dose chymopapain: A prospective randomized study in 280 consecutive cases. *Spine (Phila Pa 1976)*. 2006;31(24):E890–E897. doi:10.1097/01.brs.0000245955.22358.3a
12. Yuan C, Zhou Y, Pan Y, Wang J. Curative effect comparison of transforaminal endoscopic spine system and traditional open discectomy: A meta-analysis. *ANZ J Surg*. 2020;90(1–2):123–129. doi:10.1111/ans.15579
13. Li X, Liu T, Fan J, et al. Outcome of lumbar lateral recess stenosis with percutaneous endoscopic transforaminal decompression in patients 65 years of age or older and in younger patients. *Medicine (Baltimore)*. 2020;99(29):e21049. doi:10.1097/MD.0000000000021049
14. Chen X, Qin R, Hao J, et al. Percutaneous endoscopic decompression via transforaminal approach for lumbar lateral recess stenosis in geriatric patients. *Int Orthop*. 2019;43(5):1263–1269. doi:10.1007/s00264-018-4051-3
15. Kapetanakis S, Gkantsinikoudis N, Thomaidis T, Charitoudis G, Theodosiadis P. The role of percutaneous transforaminal endoscopic surgery in lateral recess stenosis in elderly patients. *Asian Spine J*. 2019;13(4):638–647. doi:10.31616/asj.2018.0179
16. Daniell JR, Osti OL. Failed back surgery syndrome: A review article. *Asian Spine J*. 2018;12(2):372–379. doi:10.4184/asj.2018.12.2.372
17. Benditz A, Grifka J. Lumbar spinal stenosis: From the diagnosis to the correct treatment [in German]. *Orthopade*. 2019;48(2):179–192. doi:10.1007/s00132-018-03685-3
18. Yang JS, Chu L, Chen CM, et al. Foraminoplasty at the tip or base of the superior articular process for lateral recess stenosis in percutaneous endoscopic lumbar discectomy: A multicenter, retrospective, controlled study with 2-year follow-up. *Biomed Res Int*. 2018;2018:7692794. doi:10.1155/2018/7692794
19. Li Y, Wang B, Wang S, Li P, Jiang B. Full-endoscopic decompression for lumbar lateral recess stenosis via an interlaminar approach versus a transforaminal approach. *World Neurosurg*. 2019;128:e632–e638. doi:10.1016/j.wneu.2019.04.221
20. Zhang L, Yang J, Hai Y, et al. Relationship of the exiting nerve root and superior articular process in Kambin's triangle: Assessment of lumbar anatomy using cadavers and computed tomography imaging. *World Neurosurg*. 2020;137:e336–e342. doi:10.1016/j.wneu.2020.01.195
21. Li X, Liu T, Fan J, et al. Outcome of lumbar lateral recess stenosis with percutaneous endoscopic transforaminal decompression in patients 65 years of age or older and in younger patients. *Medicine (Baltimore)*. 2020;99(29):e21049. doi:10.1097/MD.0000000000021049
22. Lin YP, Wang SL, Hu WX, et al. Percutaneous full-endoscopic lumbar foraminoplasty and decompression by using a visualization reamer for lumbar lateral recess and foraminal stenosis in elderly patients. *World Neurosurg*. 2020;136:e83–e89. doi:10.1016/j.wneu.2019.10.123
23. Hua W, Zhang Y, Wu X, et al. Full-endoscopic visualized foraminoplasty and discectomy under general anesthesia in the treatment of L4–L5 and L5–S1 disc herniation. *Spine (Phila Pa 1976)*. 2019;44(16):E984–E991. doi:10.1097/BRS.0000000000003014

24. He J, Tang J, Jiang X, et al. Efficacy and safety of foraminoplasty performed using an endoscopic drill to treat axillary disc herniation. *World Neurosurg*. 2020;138:e413–e419. doi:10.1016/j.wneu.2020.02.143
25. Lin YP, Wang SL, Hu WX, et al. Percutaneous full-endoscopic lumbar foraminoplasty and decompression by using a visualization reamer for lumbar lateral recess and foraminal stenosis in elderly patients. *World Neurosurg*. 2020;136:e83–e89. doi:10.1016/j.wneu.2019.10.123
26. Wu B, Zhan G, Tian X, et al. Comparison of transforaminal percutaneous endoscopic lumbar discectomy with and without foraminoplasty for lumbar disc herniation: A 2-year follow-up. *Pain Res Manag*. 2019;2019:6924941. doi:10.1155/2019/6924941
27. Ao S, Wu J, Zheng W, Zhou Y. A novel targeted foraminoplasty device improves the efficacy and safety of foraminoplasty in percutaneous endoscopic lumbar discectomy: Preliminary clinical application of 70 cases. *World Neurosurg*. 2018;115:e263–e271. doi:10.1016/j.wneu.2018.04.032

Prevalence of *CYLD* mutations in Vietnamese patients with polycythemia vera

Do Thi Trang[1,A–C], Nguyen Hoang Giang[1,A–C], Bui Kieu Trang[1,B,C], Nguyen Thy Ngoc[2,B,C,F], Nguyen Van Giang[4,C,E], Nguyen Xuan Canh[4,C,E], Nguyen Ba Vuong[5,E,F], Nguyen Thi Xuan[1,3,A,C–F]

[1] Institute of Genome Research, Vietnam Academy of Science and Technology, Hanoi, Vietnam
[2] Department of Life Sciences, University of Science and Technology of Hanoi, Vietnam Academy of Science and Technology, Vietnam
[3] Faculty of Biotechnology, Graduate University of Science and Technology, Vietnam Academy of Science and Technology, Hanoi, Vietnam
[4] Faculty of Biotechnology, Vietnam National University of Agriculture, Hanoi, Vietnam
[5] 103 Hospital, Vietnam Military Medical University, Hanoi, Vietnam

A – research concept and design; B – collection and/or assembly of data; C – data analysis and interpretation; D – writing the article; E – critical revision of the article; F – final approval of the article

Advances in Clinical and Experimental Medicine, ISSN 1899–5276 (print), ISSN 2451–2680 (online) *Adv Clin Exp Med*. 2022;31(4):369–380

Address for correspondence
Nguyen Thi Xuan
E-mail: xuannt@igr.ac.vn

Funding sources
This research was funded by the 562 program of the Ministry of Science and Technology for the field of Life Science under grant No. ĐTĐLCN.43/21.

Conflict of interest
None declared

Received on August 26, 2021
Reviewed on September 24, 2021
Accepted on November 17, 2021

Published online on January 13, 2022

Cite as
Trang DT, Giang NH, Trang BK, et al. Prevalence of CYLD mutations in Vietnamese patients with polycythemia vera. *Adv Clin Exp Med*. 2022;31(4):369–380. doi:10.17219/acem/144 027

DOI
10.17219/acem/144027

Abstract

Background. Polycythemia vera (PV) is characterized by increased proliferation and accumulation of erythroid and mature myeloid cells and megakaryocyte in the bone marrow and peripheral blood. The JAK2V617F mutation is present in most PV patients. Deubiquitinase (DUB) genes, including *TNFAIP3* (*A20*), *CYLD* and *Cezanne*, function as negative regulators of inflammatory reaction through nuclear factor kappa-light-chain-enhancer of activated B cells (NF-κB) signaling.

Objectives. To determine single nucleotide polymorphisms (SNPs) profiling and gene expression of the DUB genes as well as the immunophenotype of PV cells.

Material and methods. Seventy-seven patients with PV and 55 healthy individuals with well-characterized clinical profiles were enrolled. Gene expression profile was determined using quantitative real-time polymerase chain reaction (qRT-PCR), the immunophenotype with flow cytometry, secretion of cytokines using enzyme-linked immunosorbent assay (ELISA), and gene polymorphisms using direct DNA sequencing.

Results. Inactivation of *A20*, *CYLD* and *Cezanne*, and increases in interleukin 6 (IL-6) and tumor necrosis factor alpha (TNF-α) levels, as well as the enhanced number of $CD25^{+}CD4$ T, Th1 and regulatory T cells were observed in PV patients. The genetic analysis of the *CYLD* gene identified 11 SNPs, in which a novel W736G nsSNP in exon 15 and a SNP c.2483+6 T>G in intron 15 were observed in PV cases with the frequencies of 18.2% and 5.2%, respectively. The W736G non-synonymous SNP (nsSNP) was found to be most likely to exert deleterious effect and the intronic SNP c.2483+6 T>G was identified as aberrant splicing. Sequencing of *Cezanne* gene identified 7 SNPs in intron 10 and PV carriers of the SNPs had at least 2 SNPs in this gene. Importantly, PV carriers of the W736G nsSNP had multiple SNPs in *CYLD*, but not in *A20* or *Cezanne* gene.

Conclusions. Two identified SNPs, including the W736G nsSNP and the SNP c.2483+6 T>G, in *CYLD* gene might be associated with a risk of PV disease, in which the deleterious effect of the W736G nsSNP in *CYLD* gene could contribute to the pathogenesis of PV.

Key words: *JAK2*, *CYLD*, *A20*, *Cezanne*, polycythemia vera

Background

Polycythemia vera (PV) is one of the classic Philadelphia chromosome/BCR-ABL1 negative myeloproliferative neoplasms (MPNs) characterized by increased proliferation and accumulation of erythroid and mature myeloid cells and megakaryocyte in the bone marrow and peripheral blood, with subsequent increases in hematocrit and hemoglobin, and overproduction of red blood cells.[1,2] The most serious complication of PV are the symptoms of thrombosis and cardiovascular disease (CVD), which are major causes of the morbidity and mortality in these patients. The V617F activating mutation in exon 12 of the tyrosine kinase *JAK2* gene frequently occurs in PV patients[3] and constitutively induces persistent activation of Janus kinase and signal transducer and activator of transcription (JAK-STAT) pathway in hematopoietic cell precursors to promote multiple cellular processes, including survival, differentiation and proliferation.[4] In addition to the common *JAK2V617F* mutation, the *MPLW515L/K* and calreticulin (*CALR*) exon 9 indel mutations within the JAK/STAT signaling pathway were also shown to increase the risk of the disease.[5]

Deubiquitinases (DUB) genes, which include tumor necrosis factor alpha (TNF-α)-induced protein 3 (*TNFAIP3, A20*), tumor suppressor cylindromatosis (*CYLD*) and *Cezanne*, play important roles in deubiquitinating target proteins by cleaving their polyubiquitin chains to suppress activation of downstream signaling pathways. Lack of *A20* or *CYLD* in mouse immune cells results in constitutive activity of several pathways, including nuclear factor kappa-light-chain-enhancer of activated B cells (NF-κB) and signal transducer and activator of transcriptions (STATs).[6,7] In humans, inactivation of *A20* leads to the progression of lymphomas by inducing the proliferation of lymphoma cells.[8,9] Mutations in exon 3 of *A20* gene cause the risk of malignant T-cell acute lymphoblastic leukemia (T-ALL)[10] and chronic lymphocytic leukemia (CLL).[11] Genetic aberration and reduced expression of *CYLD* gene are related to solid cancers and lymphoblastic leukemia.[12–15] The presence of *CYLD* is known to promote cell death in ALL and CLL cells.[16,17] Patients having a 9 nucleotide deletion in exon 7 and a single nucleotide substitution in exon 10 of *CYLD* gene are at risk of B-cell acute lymphoblastic leukemia (B-ALL).[12] The *CYLD* expression is inhibited by miR-19 in T-ALL, while miR-19 is highly expressed in leukemia and several tumor cell lines.[18] Similar to *A20* and *CYLD, Cezanne* inhibits NF-κB signaling by deconjugating K63-polyubiquitin chain,[19] and *Cezanne* inactivation is associated with the progression and poor prognosis in hepatocellular carcinoma.[20] In contrast, *Cezanne* enhances tumor progression in lung squamous carcinoma and adenocarcinoma.[21]

Several investigations on immune features indicated that *A20* and *CYLD* participate in suppressing inflammatory reaction and accumulation of leukocytes in systemic organs,[6,7] which is associated with risk for the development of cancers.[22] The *A20*-deficient mice develop severe inflammation and cachexia by recruitment of activated lymphocytes, granulocytes and macrophages into liver and spleen.[23] The *CYLD*-knockout mice exhibit abnormalities in the activation and development of T cells and B cells.[24,25] In PV patients, regulatory T (Treg) cells are expanded to suppress function of immune effector cells, therefore contributing to the pathogenesis of PV.[26]

Objectives

In this study, single nucleotide polymorphisms (SNPs) profiling and gene expression of *A20*, *CYLD* and *Cezanne* genes in 77 patients with PV and 55 healthy individuals using direct DNA sequencing and quantitative real-time polymerase chain reaction (qRT-PCR) were performed to determine disease-associated SNPs in the DUB genes. Besides, immunophenotypic property of PV cells was also assessed with flow cytometry.

Materials and methods

Patients and control subjects

Total peripheral blood samples from 77 untreated PV patients with a median age of 58.7 (19–81) years and 55 normal healthy volunteers used as controls were taken at the 103 Hospital, Military Medical University, Hanoi, Vietnam. The diagnosis of PV was based on the 2016 WHO criteria.[2] The presence of JAK^{V617F} mutation in PV patients was determined according to Baxter et al.[27] No individuals in the control population took any medication or suffered from any known acute or chronic disease. All patients and volunteers gave a written consent to participate in the study. All care and experimental procedures were performed according to the Vietnamese law on the welfare of patients and were approved by the Ethical Committee of Institute of Genome Research, Vietnam Academy of Science and Technology, Hanoi, Vietnam. All experimental protocols on human subjects were in accordance with 1975 Declaration of Helsinki, as revised in 2008.

Isolation of PV cells and PBMCs

The PV cells from PV patients and peripheral blood mononuclear cells (PBMCs) from healthy donors were collected by venipuncture and transferred to sterile tubes containing ethylenediaminetetraacetic acid (EDTA) as an anticoagulant and isolated using density gradient centrifugation (Ficoll-Paque Plus; GE Healthcare Life Sciences, Chicago, USA). The cells were next counted in a Neubauer chamber, washed with phosphate-buffered saline (PBS) and analyzed for further experiments.

Cytokine quantification

Sera were isolated from the blood samples of PV patients and healthy subjects and stored at –20°C until being used for enzyme-linked immunosorbent assay (ELISA). The TNF-α, interleukin 6 (IL-6) and IL-1β concentrations were determined using ELISA kits (Thermo Fisher Scientific, Waltham, USA) according to the manufacturer's protocol.

RNA extraction and RT-PCR

Total mRNA was isolated using the QIAshredder and RNeasy Mini Kit from Qiagen (Hilden, Germany), according to the manufacturer's instructions. For cDNA first strand synthesis, 1 µg of total RNA in 12.5 µL of diethyl pyrocarbonate (DEPC)-H_2O was mixed with 1 µL of oligo-dT primer (500 µg/mL; Invitrogen, Waltham, USA) and heated for 2 min at 70°C. To determine transcript levels of *A20*, *Cezanne*, *CYLD*, *OTUB-1*, *OTUB-2*, and *GAPDH*, qRT-PCR with the LightCycler System (Roche, Basel, Switzerland) was applied. The following primers were used: *A20* primers: 5'-TCCTCAGGCTTTGTATTTGA-3' (forward) and 5'-TGTGTATCGGTGCATGGTTTT-3' (reverse); *OTUB-1* primers: 5'-ACAGAAGATCAAGGACCTCCA-3' (forward) and 5'-CAACTCCTTGCTGTCATCCA-3' (reverse); *OTUB-2* primers: 5'-CTCACGTCGGCCTTCATCA-3' (forward) and 5'-GCCATGGGCTCTACTTCGT-3' (reverse); *Cezanne* primers: 5'-ACAATGTCCGATTGGCCAGT-3' (forward) and 5'-ACAGTGGGATCCACTTCACATTC-3' (reverse); *CYLD* primers: 5'-TGCCTTCCAACTCTCGTCTTG-3' (forward) and 5'-AATCCGCTCTTCCCAGTAGG-3' (reverse), and *GAPDH* primers: 5'-GGAGCGAGATCCCTCCAAA-3' (forward) and 5'-GGCTGTTGTCATACTTCTCAT-3' (reverse). The qRT-PCR reactions were performed in a final volume of 20 µL containing 2 µL of cDNA, 2.4 µL of $MgCl_2$ (3 µM), 1 µL of primer mix (0.5 µM of both primers), 2 µL of cDNA SYBR Green I Master mix (Roche), and 12.6 µL of DEPC-treated water. The target DNA was amplified during 40 cycles of 95°C for 10 s, 62°C for 10 s and 72°C for 16 s, each with a temperature transition rate of 20°C/s, a secondary target temperature of 50°C and a step size of 0.5°C. Melting curve analysis was performed at 95°C (0 s), 60°C (10 s) and 95°C (0 s) to determine the melting temperature of primer dimers and the specific qRT-PCR products. The ratio between the respective gene and corresponding *GAPDH* was calculated per sample according to the ΔΔ cycle threshold method.[28]

DNA sequencing of *JAK2* and the DUB genes

Genomic DNA was isolated from peripheral blood samples using a DNeasy blood and tissue kit (Qiagen). To determine the polymorphisms of the *JAK2*, *A20*, *CYLD*, and *Cezanne* genes, qRT-PCR and DNA sequencing (3500 Genetic Analyzers; Thermo Fisher Scientific) were performed as previously described.[29] The GenBank accession numbers NM_004972.4, NM_00137874.1, NM_001270508.2 and NM_020205.4 were used for DNA sequence analysis of *JAK2, CYLD, A20* and *Cezanne*, respectively, by using primers: *JAK2-F*: 5'-TCCTCAGAACGTTGATGGCAG-3' and *JAK2-R*: 5'-ATTGCTTTCCTTTTTCACAAGAT-3'; *CYLD-F*: 5'-TAAGGTCTTGTGCCTGAGCA-3'; *CYLD-R*: 5'-TTCTTTGGCAGCAGAAATCC-3'; *A20-F*: 5'-TGAGCTAATGATGTAAAATCTTGTG-3' and *A20-R*: 5'-AGGAGGCCTCTGCTGTAGTC-3'; *Cezanne-F*: 5'-GCCTCCTGCATCAACTTCCT-3' and *Cezanne-R*: 5'-TCAGAGGACAGTGGGATCCA-3. The amplification product lengths of *JAK*2, *CYLD*, *A20*, and *Cezanne* were 453 bp, 546 bp, 731 bp, and 600 bp, respectively. All obtained PCR fragments were purified with a GeneJET PCR purification kit (Thermo Fisher Scientific). The PCR products were sequenced on both strands with the same primers as the ones used for the PCR.

Immunostaining and flow cytometry

Immunophenotypic features of PV cells and PBMCs were determined with flow cytometry (FACSAria Fusion; Becton Dickinson Biosciences, Franklin Lakes, USA), as previously described.[30] Cells (2×10^6) were incubated in 100 µL of flow cytometry staining (FACS) buffer (PBS plus 0.1% function control sequence (FCS)) containing fluorochrome-coupled antibodies to CD45, CD3, CD4, CD8α, CD11b, CD25, CD44, and FoxP3 (all from eBioscience; Thermo Fisher Scientific) at a concentration of 10 µg/mL. For intracellular cytokine staining of IL-4, IL-17 and interferon gamma (IFN-γ), cells were stimulated with phorbol 12-myristate 13-acetate (50 ng/mL; Sigma-Aldrich, St. Louis, USA) and ionomycin (500 ng/mL; Sigma-Aldrich) for 3 h, followed by addition of brefeldin A (10 µg/mL; Sigma-Aldrich) for another 4 h. The cells were then stained with anti-human IL-4, IL-17 and IFN-γ antibodies (Thermo Fisher Scientific). After incubating with the antibodies for 60 min at 4°C, the cells were washed twice and resuspended in FACS buffer for flow cytometry analysis.

Data analysis

Data related to the human *JAK2, A20, CYLD*, and *Cezanne* genes were collected from National Center for Biotechnology Information (NCBI; https://www.ncbi.nlm.nih.gov/). The information for SNP ID of these genes was retrieved from the NCBI SNP database (https://www.ncbi.nlm.nih.gov/snp/). BioEdit 7.2 software (https://bioedit.software.informer.com/7.2/) was used for the initial analysis of the sequences.

To analyze the functional consequence of deleterious SNPs of the DUB genes, the PolyPhen2 program (http://genetics.bwh.harvard.edu/pph2/index.shtml) was used. The PolyPhen-2 score varies from 0.0 (tolerated) to 1.0

(deleterious), in which the SNPs were designated "probably damaging", "potentially damaging", "benign", or "unknown". In addition, the possible impact of intronic SNPs on slicing was predicted using SD-Score (https://www.med.nagoya-u.ac.jp/neurogenetics/SD_Score/sd_score.html)[31] or MaxEntScan (http://hollywood.mit.edu/burgelab/maxent/Xmaxentscan_scoreseq.html)[32] predictor programs.

Statistical analyses

The IBM SPSS v. 20 software (IBM Corp., Armonk, USA) was used for statistical analysis. The χ^2 test was used to test whether allele distribution of each SNP follows the Hardy–Weinberg equilibrium (HWE). To examine the genotype association of control and PV groups, the Fisher's exact test was used for SNPs with expected sample sizes less than 20 and χ^2 test for those with larger expected sample sizes. Differences between control and PV groups or SNP relevance were tested for significance using Mann–Whitney U test or Kruskal–Wallis test (for many comparisons). All of the statistical tests were two-sided and represented the number of independent experiments. In all statistical analyses, the significance was determined at the level of $p < 0.05$.

Results

Analysis of gene expression and immunophenotypic profiles in PV patients

For expression of the DUB genes, we observed that mRNA levels of *A20, CYLD* and *Cezanne* were significantly downregulated in PV cells as compared to the control group; however, no difference in transcript expression of the other DUB genes, including *OTUB-1* and *OTUB-2*, between patient and control groups was detected (Fig. 1A). The inactivated expression of *A20, CYLD* and *Cezanne* is predicted to be caused by their genetic alterations in PV.

Inactivation of the DUBs may lead to constitutive activation and recruitment of immune cells into systemic organs[6,7]; therefore, changes in the number and activation of myeloid ($CD11b^+$) and CD4 T cells present in PV cells were examined. In our results, $CD45^+$ cells considered as leukocytes were gated in all experiments. Flow cytometry analysis showed that the percentage of $CD11b^+$ myeloid and $CD3^+$ T cells were increased in blood circulation of PV patients (Fig. 1B,E). However, the activation of $CD11b^+$ myeloid cells in PV cases was found to be similar to that in healthy individuals, as the number of $CD11b^+CD86^+$ and $CD11b^+CD40^+$ expressing cells remained unaltered in these patients (Fig. 1B,C). Unlike $CD11b^+$ myeloid cells, the activation of $CD3^+CD4^+$ T cells was partially enhanced, as the number of $CD3^+CD4^+CD25^+$ ($CD25^+$CD4 T cells), but not $CD3^+CD4^+CD44^+$ ($CD44^+$CD4 T cells) was significantly increased in PV cases (Fig. 1D,E).

Next, analysis of CD4 T cells subsets showed that the $CD3^+CD4^+CD25^+$ $FoxP3^+$ (Treg) and $CD3^+CD4^+IFN\text{-}\gamma^+$ (Th1) expressing cells were recruited into the circulation, whereas the number of $CD3^+CD4^+IL\text{-}4^+$ (Th2) and $CD3^+CD4^+IL\text{-}17^+$ (Th17) expressing cells was unaltered in PV cases (Fig. 1F,G). In agreement with a previous study, Treg cells are recruited to circulatory system to facilitate the development of PV,[26] suggesting that the inactivated expression of *A20, CYLD* and *Cezanne* genes in PV patients could be involved in the recruitment of $CD25^+$ CD4 T, T regulatory and Th1 cells into blood.

The *A20* and *CYLD* are also known as inhibitors of inflammatory reaction[7,33]; thus, cytokine production in sera of PV patients was examined. Similar to a recent study,[34] we also observed that levels of IL-6 and TNF-α in PV patients were found to be higher than in control individuals; however, these patients showed no change in the serum level of IL-1β (Fig. 1H).

Mutational analysis of *JAK2* and DUB genes in PV patients

Firstly, the p.V617F (c.1849 G>T) mutation of *JAK2* gene is well known to be pathogenic, has been identified in about 90% PV cases[3] and is used as an important diagnostic marker of PV. In this study, the results indicated that 51 out of 77 (66.23%) untreated PV cases were positive with the *JAK2V617F* (Fig. 2A and Table 1,2).

Sequencing of the *CYLD* gene identified 6 nucleotide changes in exon 15 (Fig. 2B), in which 5 out of the 6 SNPs, including p.A705P (c.2355 G>C), p.Q731H (c.2435 G>C), p.E735K (c.2445 G>A), p.W736G (c.2448 T>G), and p.E747K (c.2481 G>A), were non-synonymous SNPs (nsSNPs), causing changes in the amino acid residues, and the remaining SNP p.E723E (c.2411 G>A) was silent. Five intronic nucleotide changes, including 2 SNPs c.2351-118delA and c.2351-31 T>G in intron 14 and 3 SNPs c.2483+6 T>G, c. 2483+39 T>G and c. 2483+53 G>A in intron 15, were found (Fig. 2C). The genotype distribution of the observed SNPs, except for the 2 SNPs p.E747K and c.2483+53 G>A in CYLD gene, were in agreement with HWE. Importantly, we noted that the minor allele frequency (MAF) of the W736G nsSNP was significantly higher in PV group compared to control group ($p = 0.022$), and the difference in the MAFs for the 10 remaining SNPs between the 2 groups was not observed (Table 1).

For determination of susceptibility to PV by evaluating the deleterious effect of the nsSNPs in *CYLD* gene, the results indicated that among the 5 nsSNPs, only the W736G nsSNP was predicted to be probably damaging by PolyPhen-2 with a score of 0.9456 (score range: 0–1; sensitivity: 0.8; specificity: 0.95) (Fig. 2D). Accordingly, the W736G nsSNP might be one of the most deleterious nsSNPs in *CYLD* gene. Moreover, TG genotype of the W736G nsSNP showed higher frequency in PV patients (18.2%) compared to healthy individuals (1.81%; $p = 0.018$, Table 2),

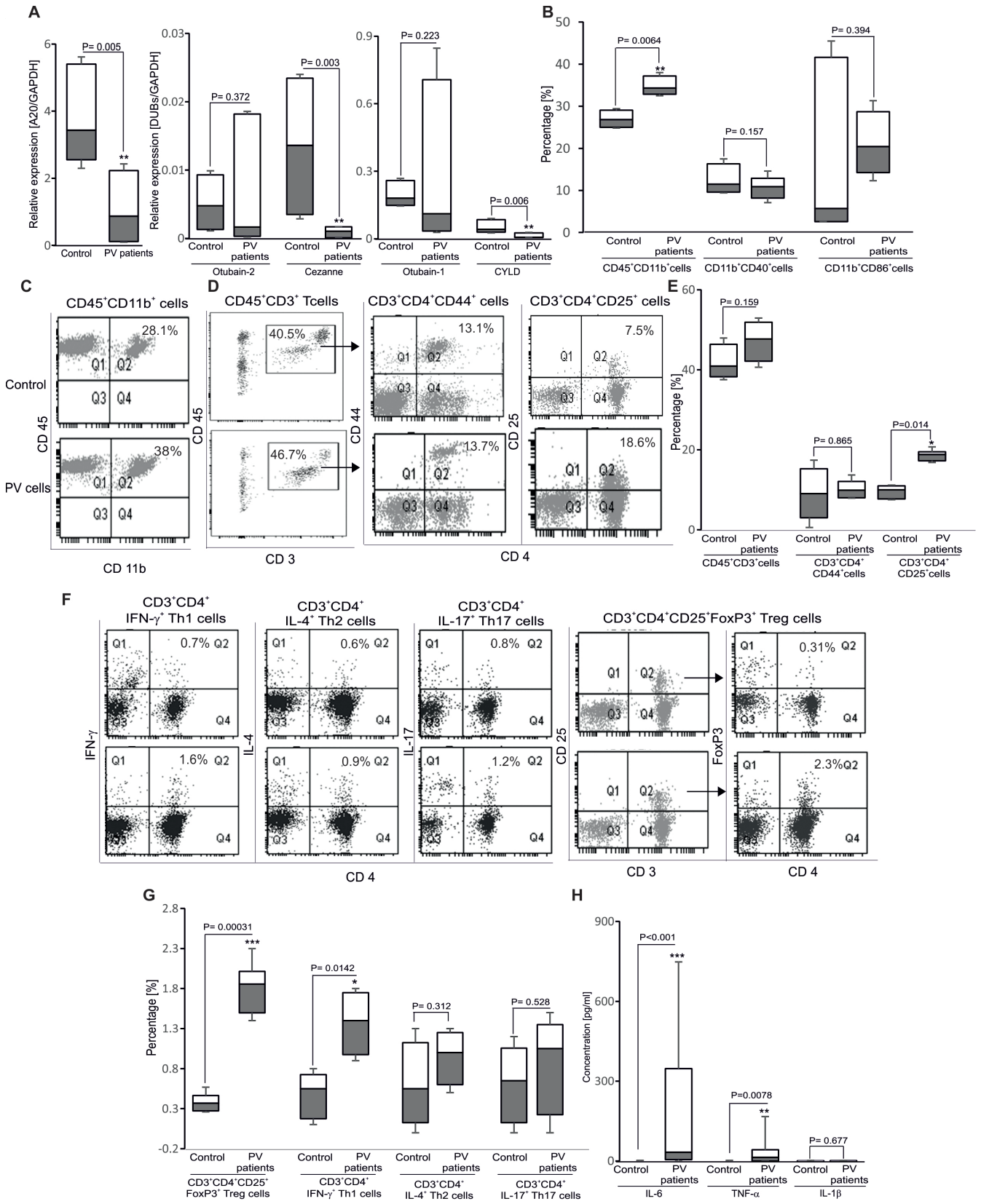

Fig. 1. Gene expression and immunophenotypic feature in polycythemia vera (PV) patients and controls. A. Box plot graphs of transcript levels of *A20, CYLD, OTUB1, OTUB2*, and *Cezanne* are shown for control and PV cells; ** ($p < 0.01$) indicates significant difference from healthy individuals (Mann–Whitney U test, n = 15). The box plots denote the median, interquartile range (IQR) and minimum and maximum values; B. Box plot graphs of percentages of $CD45^+CD11b^+$, $CD11b^+CD40^+$ and $CD11b^+CD86^+$ expressing cells are shown for control and PV cells; ** ($p < 0.01$) indicates significant difference from healthy individuals (Mann–Whitney U test, n = 5–7). The box plots denote the median, IQR and minimum and maximum values; C,D. Original dot plots of $CD45^+CD11b^+$ (C), $CD45^+CD3^+$, $CD3^+CD4^+CD44^+$ and $CD3^+CD4^+CD25^+$ (D) expressing cells are shown for control (upper panels) and PV cells (lower panels). All samples were gated with $CD45^+$ live cells; E. Box plot graphs of percentages of $CD45^+CD3^+$, $CD3^+CD4^+CD44^+$ and $CD3^+CD4^+CD25^+$ expressing cells are shown for control and PV cells; * ($p < 0.05$) indicates significant difference from healthy individuals (Mann–Whitney U test, n = 5–7). The box plots denote the median, IQR and minimum and maximum values; F. Original dot plots of $CD3^+CD4^+IFN\text{-}\gamma^+$ (Th1), $CD3^+CD4^+IL\text{-}4^+$ (Th2) and $CD3^+CD4^+IL\text{-}17^+$ (Th17) (gated with $CD45^+CD3^+$) and $CD3^+CD4^+CD25^+FoxP3^+$ (Treg) (gated with $CD45^+CD3^+CD25^+$) expressing cells are shown for control (upper panels) and PV cells (lower panels); G. Box plot graphs of percentages of $CD3^+CD4^+IFN\text{-}\gamma^+$ (Th1), $CD3^+CD4^+IL\text{-}4^+$ (Th2) and $CD3^+CD4^+IL\text{-}17^+$ (Th17) and $CD3^+$ $CD4^+CD25^+FoxP3^+$ (Treg) expressing cells are shown for control and PV cells; * ($p < 0.05$) and *** ($p < 0.001$) indicate significant differences from healthy individuals (Mann–Whitney U test, n = 5–7). The box plots denote the median, IQR and minimum and maximum values; H. Box plot graphs showing interleukin (IL)-6, tumor necrosis factor alpha (TNF-α) and IL-1β concentrations in sera of healthy donors and PV patients; ** ($p < 0.01$) and *** ($p < 0.001$) indicate significant differences from healthy donors (Mann–Whitney U test, n = 53–77). The box plots denote the median, IQR and minimum and maximum values.

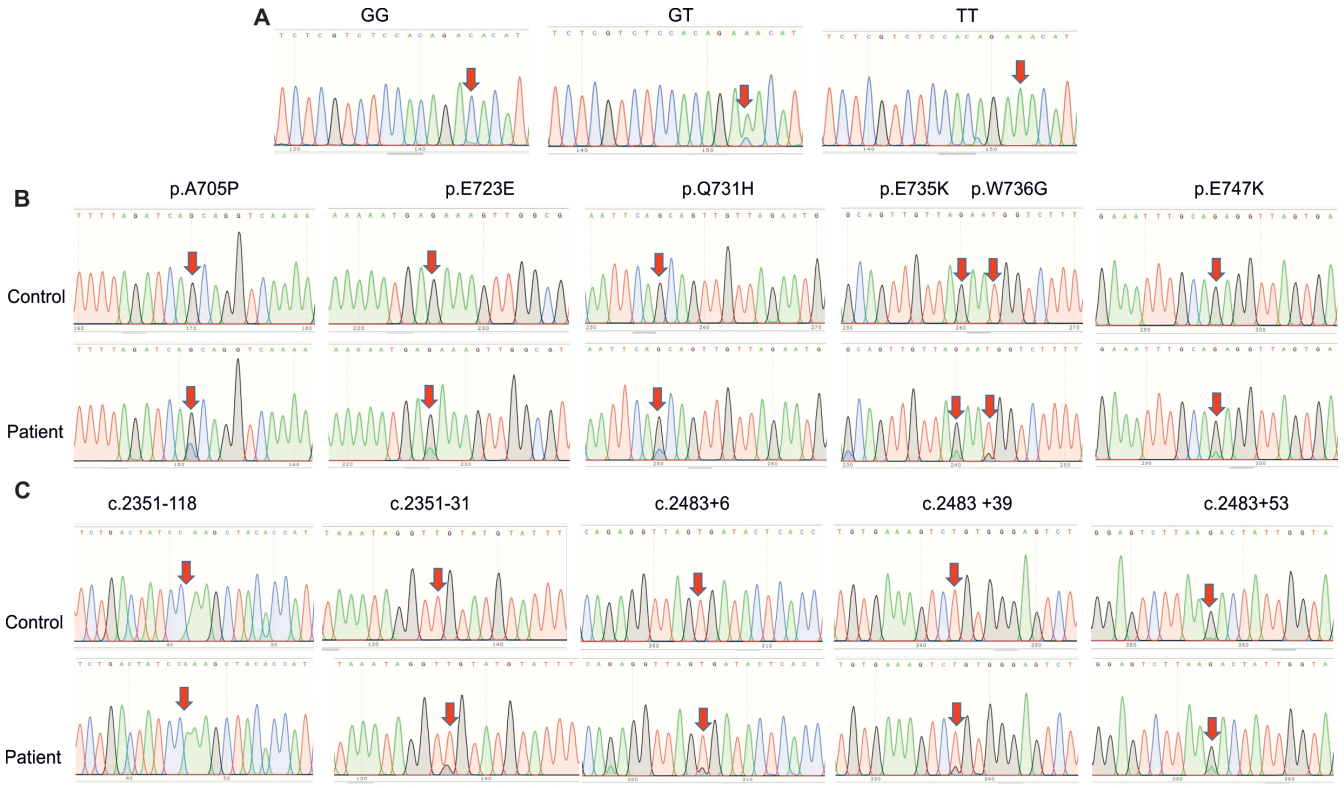

D

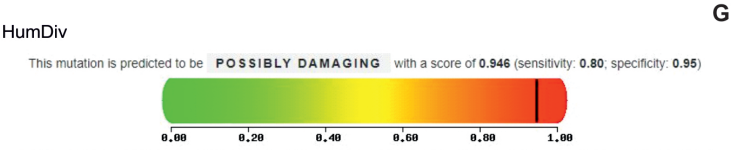

E

Wt.Seq				Mt.Seq				Difference				
pos	Wt.Seq (9bases)	SD-Score	Ri	CV	Mt.Seq (9bases)	SD-Score	Ri	CV	ΔSD-Score	ΔRi	ΔCV	Prediction
4	GAGGTTAGT	-3.08	7.568	0.87	GAGGTTAGG	-4.163	6.274	0.823	-1.087	-1.294	-0.049	Aberrant

F

Genotype	Sequence	MaxENT	MDD	MM	WMM
Wild type	gagGTTAGT	7.15	12.78	6.8	6.92
Mutant	gagGTTAGG	4.36	8.98	5.11	5.99

G

Species	p.W 736										
Homo sapiens (Human)	Q	L	L	E	**W**	S	F	I	N	S	N
Rattus norvegicus (Rat)	Q	L	L	E	**W**	S	F	I	N	S	N
Monodelphis domestica (Gray short-tailed opossum)	Q	L	L	E	**W**	S	F	I	N	S	N
Sarcophilus harrisii (Tasmanian devil)	Q	L	L	E	**W**	S	F	I	N	S	N
rnithorhynchus anatinus (Duckbill platypus)	Q	L	L	E	**W**	S	F	I	N	S	S
Myotis lucifugus (Little brown bat)	Q	L	L	E	**W**	S	F	I	N	S	N
Gallus gallus (Chicken)	Q	L	L	E	**W**	S	F	I	N	S	N
Meleagris gallopavo (Wild turkey)	Q	L	L	E	**W**	S	F	I	N	S	N
Xenopus tropicalis (Western clawed frog)	Q	L	L	E	**W**	S	F	I	N	S	S
Oreochromis niloticus (Nile tilapia)	Q	L	L	E	**W**	S	F	I	N	S	D
Danio rerio (Zebrafish)	Q	L	L	E	**W**	S	F	I	N	S	D
Gasterosteus aculeatus (Three-spined stickleback)	Q	L	L	E	**W**	S	F	I	N	S	D
Loxodonta africana (African elephant)	Q	L	L	E	**W**	S	F	I	N	S	N
Tetraodon nigroviridis (Spotted green pufferfish)	Q	L	L	E	**W**	S	F	I	N	S	D

Fig. 2. Polymorphisms of *JAK2* and *CYLD* genes in polycythemia vera (PV) patients and controls. A. Partial sequence chromatograms of *JAK2* gene from healthy individuals (left panel, GG genotype) and PV patients (middle and right panels, GT and TT genotypes) for the p.V617F (c.1849 G>T) mutation. Arrows indicate the location of the base changes; B. Partial sequence chromatograms of *CYLD* gene from healthy individuals (upper panels) and PV patients (lower panels), in which the p.A705P (c.2355 G>C), p.E723E (c.2411 G>A), p.Q731H (c.2435 G>C), p.E735K (c.2445 G>A), p.W736G (c.2448 T>G), and p.E747K (c.2481 G>A) polymorphisms are shown. Arrows indicate the location of the base changes; C. Partial sequence chromatograms of *CYLD* gene from healthy individuals (upper panels) and PV patients (lower panels), in which the c.2351-118delA, c.2351-31 T>G, c.2483+6 T>G, c.2483+39 T>G, and c.2483+53 G>A polymorphisms are shown. Arrows indicate the location of the base changes; D. Functional prediction of the p.W736G mutation using the PolyPhen-2 program; E,F. Splicing effect predictions of the intronic SNP c.2483+6 T>G using the SD-Score (E) or MaxEntScan (F) programs; G. Segments of multiple sequence alignments of CYLD protein from different species were shown using the PolyPhen-2 program. The position of the changed amino acid (p.W736) in CYLD protein is marked in a bold solid line box.

Pos – position; Wt.Seq – wild-type sequence; Mt.Seq – mutant sequence; SD-Score – a common logarithm of the frequency of a specific 5'splice site in human genes; Ri – information contents; CV – position weight matrix; MaxENT – Maximum Entropy Model; MDD – Maximum Dependence Decomposition Model; MM – Markov Model; WMM – Weight Matrix Model.

while the 10 other SNPs in *CYLD* gene were not significantly associated with PV phenotype. The evidence revealed the association of the W736G nsSNP in susceptibility to the progression of PV.

For the analysis of the possible impact of the 5 intronic SNPs in *CYLD* gene on splicing, only the SNP c. 2483+6 T>G was predicted as an aberrant splicing according to the SD-Score prediction program (Fig. 2E).[31] Besides, the MaxEntScan[32] splicing prediction through the score analysis of MaxENT (Maximum Entropy Model), MDD (Maximum Dependence Decomposition Model), MM (First-order Markov Model), and WMM

Table 1. General information on single nucleotide polymorphisms (SNPs) of *JAK2*, *CYLD*, *A20* and *Cezanne* genes in polycythemia vera (PV) patients and controls

Gene/SNP	Position	Type of variant	Allele	MAF in PV group	HWE in PV group (p)	MAF in control group	HWE in control group (p)	HWE in all population (p)
JAK2/rs77375493	9:5073770	missense	G>T	0.442	0.656	0	NaN	0.051
CYLD/c.2351-118	16:50791440	intron	Del A	0	0.993	0	0.913	0.938
CYLD/c.2351-31	16:50791527	intron	T>G	0.006	0.998	0	NaN	0.999
CYLD/c.2355 p.A705P	16:50791562	missense	G>C	0.020	0.985	0	NaN	0.991
CYLD/c.2411 p.E723E	16:50791618	synonymous	G>A	0.033	0.958	0.055	0.913	0.883
CYLD/c.2435 p.Q731H	16:50791642	missense	G>C	0.111	0.553	0.137	0.504	0.285
CYLD/c.2445 p.E735K	16:50791652	missense	G>A	0.130	0.424	0.173	0.302	0.138
CYLD/c.2448 p.W736G	16:50791655	missense	T>G	0.091	0.681	0.010	0.998	0.787
CYLD/c.2481 p.E747K	16:50791688	missense	G>A	0.169	0.204	0.219	0.118	0.027
CYLD/c.2483+6	16:50791696	splice-donor-site	T>G	0.026	0.973	0	NaN	0.985
CYLD/c.2483 +39	16:50791729	intron	T>G	0.039	0.939	0.010	0.998	0.952
CYLD/c.2483+53	16:50791743	intron	G>A	0.182	0.149	0.219	0.118	0.019
A20/rs776591390	6:137878495	missense	G>T	0.006	0.998	0	NaN	0.999
A20/rs141376366	6:137878670	synonymous	G>A	0	NaN	0.010	0.998	0.999
A20/rs745670694	6:137878786	synonymous	G>A	0	NaN	0.108	0.991	0.996
Cezanne/c.1584-287	1:149947622	intron	C>G	0.039	0.998	0	NaN	0.965
Cezanne/rs1168285629	1:149947587	intron	A>G	0.046	0.916	0.019	0.991	0.921
Cezanne/rs1394369937	1:149947537	intron	A>G	0.026	0.973	0	NaN	0.985
Cezanne/c.1584-167	1:149947502	intron	G>T	0.013	0.993	0	NaN	0.996
Cezanne/c.1584-122	1:149947457	intron	G>T	0.026	0.973	0.010	0.998	0.976
Cezanne/rs1158787149	1:149947449	intron	C>G	0.026	0.987	0	NaN	0.985
Cezanne/rs1553772411	1:149947450	intron	C>G	0.019	0.993	0	NaN	0.991

Position refers to the GRCh38.p10 assembly. MAF – minor allele frequency; HWE – Hardy–Weinberg equilibrium (checked using χ^2 test).

(Weight Matrix Model) indicated that the mutant scores of the SNP c.2483+6 T>G were lower than of the wild-type scores (Fig. 2F), suggesting that the SNP c.2483+6 T>G may be a splice-donor-site mutation.

Further analysis of an alignment of CYLD protein using the PolyPhen-2 software showed that the p.W736 residue is a highly conserved site among different species, including humans (*Homo sapiens*), rat (*Rattus norvegicus*), gray short-tailed opossum (*Monodelphis domestica*), Tasmanian devil (*Sarcophilus harrisii*), duckbill platypus (*Ornithorhynchus anatinus*), little brown bat (*Myotis lucifugus*), chicken (*Gallus gallus*), wild turkey (*Meleagris gallopavo*), western clawed frog (*Xenopus tropicalis*), nile tilapia (*Oreochromis niloticus*), zebrafish (*Danio rerio*), three-spined stickleback (*Gasterosteus aculeatus*), african elephant (*Loxodonta africana*), and spotted green pufferfish (*Tetraodon nigroviridis*) (Fig. 2G).

Next, the sequencing of *A20* gene identified 3 nucleotide changes, including rs776591390 G>T, rs141376366 G>A and rs745670694 G>A, in exon 7 (Fig. 3). The genotype distributions of the 3 SNPs in this gene were in accordance with HWE ($p > 0.05$) (Table 1). The MAF for the SNP rs776591390 was slightly higher, whereas the MAFs for the 2 remaining SNPs were lower in PV patients than in the control group. Among the 3 SNPs, the missense SNP rs776591390 of *A20* gene was identified in 1 out of 77 PV patients (1.81%) and the 2 remaining SNPs rs141376366 and rs745670694 were found only in control individuals with the carrier frequencies of 1.81% and 3.63%, respectively (Table 2).

Finally, the sequencing of *Cezanne* gene identified 7 nucleotide changes in intron 10, 3 out of the 7 intronic SNPs (c.1584-287 C>G, c.1584-167 G>T and c.1584-122 G>T) were unidentified SNPs and the 4 remaining intronic SNPs (rs1168285629 A>G, rs1394369937 A>G, rs1158787149 C>G, and rs1553772411 C>G) are reported in NCBI SNP database (Fig. 4). The genotype distributions of the 7 SNPs in *Cezanne* gene were in accordance with HWE ($p > 0.05$) (Table 1). The MAFs of the 7 intronic SNPs were slightly higher in the PV group than in healthy individuals. Among these SNPs, 5 out the 7 intronic SNPs (c.1584-287 C>G, rs1394369937 A>G, c.1584-167 G>T, rs1158787149 C>G and rs1553772411 C>G) appeared in PV patients, but not in the control group, with the carrier frequencies of 7.79%, 5.19%, 2.6%, 5.19%, and 3.89%, respectively (Table 2). Importantly, 7 out of 77 (9.09%) PV patients carried at least 2 SNPs in *Cezanne* gene.

Table 2. Comparison of genotype frequencies of *JAK2*, *CYLD*, *A20*, and *Cezanne* genes between polycythemia vera (PV) patients and controls

SNP	Gene	Test model	Controls (n = 55)	PV patients (n = 77)	p-value
rs77375493	*JAK2*	GG	55 (100%)	26 (33.76%)	**<0.001**[2]
		GT/TT	0 (0%)	51 (66.24%)	
c.2351-118	*CYLD*	AA	49 (89.09%)	75(97.4%)	0.052[1]
		DelA	6 (10.91%)	2 (2.6%)	
c.2351-31	*CYLD*	TT	55 (100%)	76 (98.7%)	1[1]
		TG	0	1 (1.3%)	
c.2355 p.A705P	*CYLD*	GG	55 (100%)	74 (96.1%)	0.121[1]
		GC	0 (0%)	3 (3.9%)	
c.2411 p.E723E	*CYLD*	GG	49 (89.09%)	72 (93.5%)	0.335[1]
		GA	6 (10.91%)	5 (6.5%)	
c.2435 p.Q731H	*CYLD*	GG	40 (72.73%)	60 (77.9%)	0.511[1]
		GC	15 (27.27%)	17 (22.1%)	
c.2445 p.E735K	*CYLD*	GG	36 (65.46%)	57 (44%)	0.055[1]
		GA	19 (34.54%)	20 (56%)	
c.2448 p.W736G	*CYLD*	TT	54 (98.19%)	63 (81.8%)	**<0.001**[1]
		TG	1 (1.81%)	14 (18.2%)	
c.2481 p.E747K	*CYLD*	GG	31 (56.36%)	51 (66.2%)	0.147[2]
		GA	24 (43.64%)	26 (33.8%)	
c.2483+6	*CYLD*	TT	55 (100%)	73 (94.8%)	0.059[1]
		TG	0 (0%)	4 (5.2%)	
c.2483+39	*CYLD*	TT	54 (98.19%)	71(92.2%)	0.101[1]
		TG	1 (1.81%)	6 (7.8%)	
c.2483+53	*CYLD*	GG	31 (56.37%)	49 (63.6%)	0.248[2]
		GA	24 (43.63%)	28 (36.4%)	
rs776591390	*A20*	GG	55 (100%)	76 (98.71%)	1[1]
		TG	0	1 (1.29%)	
rs141376366	*A20*	GG	54 (98.19%)	77 (100%)	0.497[1]
		GA	1 (1.81%)	0	
rs745670694	*A20*	GG	53 (96.37%)	77 (100%)	0.121[1]
		AG	2 (3.63%)	0 (0%)	
c.1584-287	*Cezanne*	CC	55 (100%)	71 (92.21%)	**0.007**[1]
		CG	0 (0%)	6 (7.79%)	
rs1168285629	*Cezanne*	AA	53 (96.36%)	70 (90.91%)	0.251[1]
		AG	2 (3.64%)	7 (9.09%)	
rs1394369937	*Cezanne*	AA	55 (100%)	73 (94.81%)	0.059[1]
		AG	0 (0%)	4 (5.19%)	
c.1584-167	*Cezanne*	GG	55 (100%)	75 (97.4%)	0.246[1]
		GT	0 (0%)	2 (2.60%)	
c.1584-122	*Cezanne*	GG	54 (98.18%)	73 (94.81%)	0.445[1]
		GT	1 (1.82%)	4 (5.19%)	
rs1158787149	*Cezanne*	CC	55 (100%)	73 (94.81%)	0.059[1]
		CG	0 (0%)	4 (5.19%)	
rs1553772411	*Cezanne*	CC	55 (100%)	74 (96.11%)	0.121[1]
		CG	0 (0%)	3 (3.89%)	

The p-values were calculated using either Fisher's exact test [1] or χ^2 test [2]; $p < 0.05$ (in bold) indicates statistical significance from genotype frequencies of healthy donors.

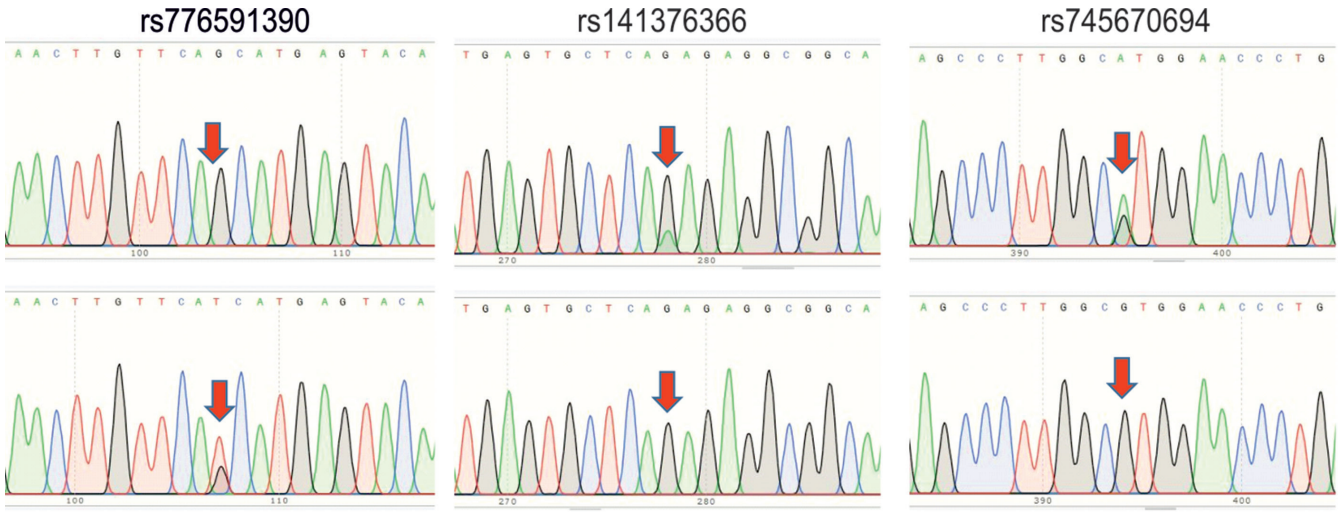

Fig. 3. Polymorphisms of *A20* gene in polycythemia vera (PV) patients and controls. Partial sequence chromatograms of *A20* gene from healthy individuals (upper panels) and PV patients (lower panels), in which the rs776591390, rs141376366 and rs745670694 polymorphisms are shown. Arrows indicate the location of the base changes

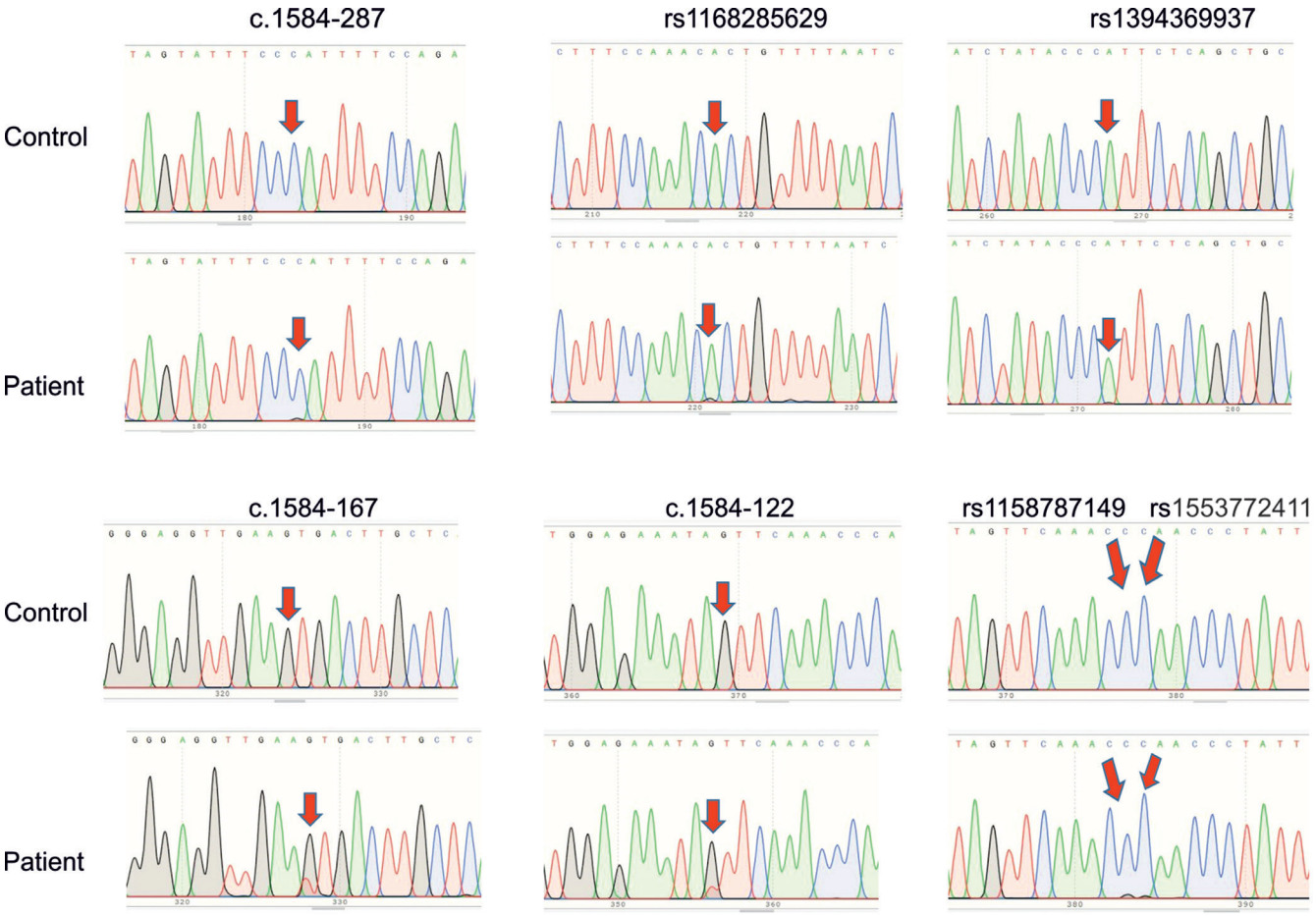

Fig. 4. Polymorphisms of *Cezanne* gene in polycythemia vera (PV) patients and controls. Partial sequence chromatograms of *Cezanne* gene from healthy individuals (upper panels) and PV patients (lower panels), in which the c.1584-287 C>G, rs1168285629 A>G, rs1394369937 A>G, c.1584-167 G>T, c.1584-122 G>T, rs1158787149 C>G, and rs1553772411 C>G polymorphisms are shown. Arrows indicate the location of the base changes

Association between the different SNPs in *JAK2* and the DUB genes in PV patients

For determination of the correlation among the SNPs in *JAK2* and the DUB genes, we observed that 10 out of 14 (71.4%) PV cases carrying the W736G nsSNP and 3 out of 3 (100%) carriers of the intronic SNP c. 2483+6 T>G in *CYLD* gene were positive for the $JAK2^{V617F}$ mutation (data not shown), whereas, the $JAK2^{V617F}$-positive rate of PV carriers of the other SNPs in the DUB genes were similar

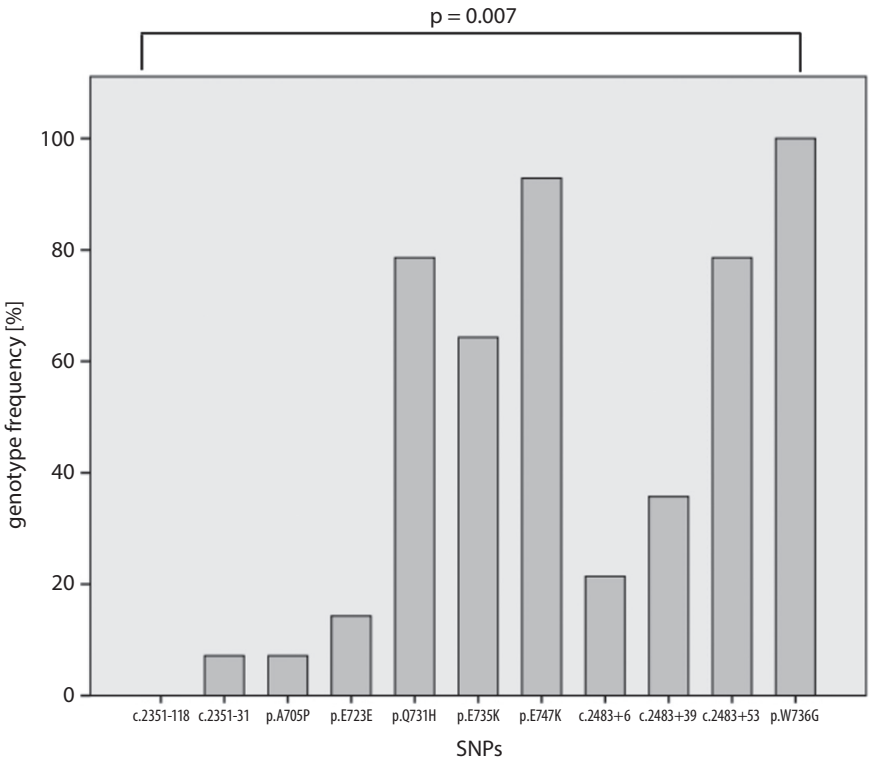

Fig. 5. The relevance of polycythemia vera (PV) carriers of the W736G nsSNP and the other 9 SNPs in *CYLD* gene. The p-value was calculated using Kruskal–Wallis test (K related samples); p = 0.007 indicates a significant relevance among the single nucleotide polymorphisms (SNPs) in *CYLD* gene

to healthy individuals (data not shown). The evidence indicated that there was a significant positive correlation between PV carriers of the W736G nsSNP or/and the intronic SNP c.2483+6 T>G and PV patients with $JAK2^{V617F}$ mutation.

Interestingly, out of the 14 patients carrying the W736G nsSNP in *CYLD* gene, 13 (92.8%) cases were found to carry the SNP p.E747K; 11 (78.6%) cases had both the SNP p.Q731H G>C and the SNP c.2483+53 G>A; 9 (64.3%) cases were found to carry the SNP p.E735K; and 3 (21.4%) carriers of the SNP c.2483+6 T>G and 5 (35.7%) cases infected with the SNP c.2483+39 T>G were observed (Fig. 5). According to the Kruskal–Wallis test results, significant relevance was observed among the SNPs in *CYLD* gene (χ^2=7.364, p = 0.007), suggesting that PV carriers of the W736G nsSNP had multiple SNPs in *CYLD* gene. Additionally, we observed that PV carriers of the W736G nsSNP and the intronic SNP c.2483+6 T>G in *CYLD* gene did not have SNP in *A20* or *Cezanne* gene (Fig. 5).

Discussion

In this study, inactivated expression of *A20, Cezanne* and *CYLD* in PV patients was revealed for the first time. Among the DUB genes, *A20* and *CYLD* but not *Cezanne* are known as inhibitors of immune reaction through JAK/STAT signaling, whose activation results in the development and pathogenesis of leukemia and lymphoma, including PV.[4,5] A recent study reported that the aberrant expression and mutations in *CYLD* gene are associated with the susceptibility to leukemia and lymphoma.[12,15] Among the 11 SNPs examined in *CYLD* genes, W736G nsSNP was found to be most likely to exert deleterious effect – it was observed using the PolyPhen-2 prediction tool and the intronic SNP c.2483+6 T>G was identified as an aberrant splicing by the SD-Score or MaxEntScan predictor program. Importantly, the 2 aberrant SNPs were not found in all samples from 90 patients with chronic myeloid leukemia (CML), 32 patients with acute myeloid leukemia (AML), 16 patients with acute lymphoblastic leukemia (ALL), and 21 patients with chronic lymphocytic leukemia (CLL) (unpublished data), suggesting that the two SNPs could be associated with significant risk of PV, but not leukemia.

Investigations on genetic alteration of *A20* gene indicated that carriers of SNPs in the *A20* gene at exons 5, 6 and 7 are at high risk for autoinflammatory disease and lymphocytic leukemia.[10,11,35,36] In this study, the SNP rs776591390 in *A20* gene was detected in PV patients with the frequency of 1.29%, pointing out that A20 polymorphisms associated with disease susceptibility are different.

Unlike the impact of *A20* and *CYLD*, the involvement of SNPs in *Cezanne* gene with the possible risk of leukemia is not fully documented, although *Cezanne* expression is linked to poor prognosis in hepatocellular carcinoma.[20] In this study, we also revealed for the first time that changes of 7 nucleotides at intron 10 in *Cezanne* gene were found in PV patients and in 7 out of 77 (9.09%) PV patients who carried at least the 2 SNPs in this gene. Similar to the 2 aberrant SNPs in *CYLD* gene, the 7 intronic SNPs in *Cezanne* gene were not carried by AML and CML patients (unpublished data). In addition, the MAFs of the 7 intronic SNPs had slightly higher frequencies in PV groups than in control groups, indicating that carriers of SNPs in *Cezanne* gene could tend to be at risk of the progression of PV.

In addition to the determination of DNA sequences of the DUB genes, the presence of the *JAK2V617F* mutation in PV patients was also conducted to determine the correlation between SNPs in the *JAK2* and the DUB genes. The *JAK2V617F* mutation was detected in 66.67% of PV patients in this study, whereas other study indicated the presence of this mutation is about 90% of PV cases.[3] The frequency of *JAK2V617F* allele burden is known to time-dependently increase in PV cases.[37] A recent study indicated that the absence of the *JAK2V617F* mutation in PV patients does not affect treatment effectiveness with JAK/STAT pathway inhibitors,[38] suggesting that the constitutive activation of the JAK-STAT pathway could be caused by not only *JAK2V617F* mutation. Besides the known mutations involved in the pathogenesis of PV, including *JAK2*, *MPL* and *CALR*, we additionally revealed that PV patients carrying the W736G nsSNP had multiple SNPs in the *CYLD*, but not in *A20* or *Cezanne* gene, suggesting that the effect of the W736G nsSNP in *CYLD* gene might be one of potential treatment targets for PV. The *CYLD* is known to suppress inflammatory reaction through the activation of several pathways, including JAK/STAT[7]; therefore, further studies would investigate the effects of the W736G nsSNP in regulating function of PV cells and underlying mechanisms.

In the analysis of involvement in SNPs and immunophenotype in PV patients, the *JAK2V617F* mutation is reported not to affect the function of T cells[3]; therefore, the recruitment of $CD25^+CD4$T, Th1 and Treg cells into the circulatory system in PV cases would be related to the activation of the 2 aberrant SNPs in *CYLD* gene. Importantly, the enhanced activation of Th1 cells in PV cells was also revealed for the first time in our study. As part of the immune response, Treg cells play an important role in suppressing tumor-specific immunity.[30] The aberrant expression of CD25 is associated with poor prognosis in AML[40] and CML.[41] A previous study indicated that factors related to thrombosis in PV include increased hematocrit, thrombocytosis, platelet activation, and leukocyte activation,[42] suggesting the regulatory effects of the 2 aberrant SNPs in *CYLD* gene on the development of thrombosis in PV. In addition, we did not find any significant association of the SNPs in *A20* and *CYLD* and *Cezanne* genes with increased levels of IL-6 and TNF-α in PV patients.

Limitations

There are some limitations to the current study. First, the sample size was not sufficient to verify a potential association between the SNPs in the DUB genes and risk of PV disease in the Vietnamese population. Second, further functional research is necessary for investigating the impacts of the W736G nsSNP and/or intronic SNP c.2483+6 T>G in *CYLD* gene on PV cell activation for the development of PV treatment. Finally, we only examined number and activation of myeloid ($CD11b^+$) and CD4 T cells present in PV cells, while other cell types, such as macrophages, inflammatory monocytes and B cells, might be also related to the activation of the 2 aberrant SNPs in *CYLD* gene.

Conclusions

The deleterious effect of the W736G nsSNP in *CYLD* gene could contribute to the pathogenesis of PV and be a good candidate for further study on its role in regulating functional activation of PV cells.

ORCID iDs

Do Thi Trang https://orcid.org/0000-0002-3168-1000
Nguyen Hoang Giang https://orcid.org/0000-0002-8298-3017
Bui Kieu Trang https://orcid.org/0000-0001-8285-1412
Nguyen Thy Ngoc https://orcid.org/0000-0002-3181-9209
Nguyen Thi Xuan https://orcid.org/0000-0003-3494-5136

References

1. Arber DA, Orazi A, Hasserjian R, et al. The 2016 revision to the World Health Organization classification of myeloid neoplasms and acute leukemia. *Blood*. 2016;127(20):2391–1405. doi:10.1182/blood-2016-03-643544
2. Barbui T, Thiele J, Gisslinger H, et al. The 2016 WHO classification and diagnostic criteria for myeloproliferative neoplasms: Document summary and in-depth discussion. *Blood Cancer J*. 2018;8(2):15. doi:10.1038/s41408-018-0054-y
3. James C, Ugo V, Le Couedic JP, et al. A unique clonal JAK2 mutation leading to constitutive signalling causes polycythaemia vera. *Nature*. 2005;434(7037):1144–1148. doi:10.1038/nature03546
4. Levine RL, Pardanani A, Tefferi A, Gilliland DG. Role of JAK2 in the pathogenesis and therapy of myeloproliferative disorders. *Nat Rev Cancer*. 2007;7(9):673–683. doi:10.1038/nrc2210
5. Tefferi A. Myeloproliferative neoplasms: A decade of discoveries and treatment advances. *Am J Hematol*. 2016;91(1):50–58. doi:10.1002/ajh.24221
6. Duy PN, Thuy NT, Trang BK, et al. Regulation of NF-kappaB- and STAT1-mediated plasmacytoid dendritic cell functions by A20. *PLoS One*. 2019;14(9):e0222697. doi:10.1371/journal.pone.0222697
7. Nishanth G, Deckert M, Wex K, et al. CYLD enhances severe listeriosis by impairing IL-6/STAT3-dependent fibrin production. *PLoS Pathog*. 2013;9(6):e1003455. doi:10.1371/journal.ppat.1003455
8. Compagno M, Lim WK, Grunn A, et al. Mutations of multiple genes cause deregulation of NF-kappaB in diffuse large B-cell lymphoma. *Nature*. 2009;459(7247):717–721. doi:10.1038/nature07968
9. Kato M, Sanada M, Kato I, et al. Frequent inactivation of A20 in B-cell lymphomas. *Nature*. 2009;459(7247):712–716. doi:10.1038/nature07969
10. Zhu L, Zhang F, Shen Q, et al. Characteristics of A20 gene polymorphisms in T-cell acute lymphocytic leukemia. *Hematology*. 2014;19(8):448–454. doi:10.1179/1607845414Y.0000000160
11. Philipp C, Edelmann J, Buhler A, et al. Mutation analysis of the TNFAIP3 (A20) tumor suppressor gene in CLL. *Int J Cancer*. 2011;128(7):1747–1750. doi:10.1002/ijc.25497
12. Arora M, Kaul D, Varma N. Functional nature of a novel mutant CYLD observed in pediatric lymphoblastic B-cell leukemia. *Pediatr Blood Cancer*. 2015;62(6):1066–1069. doi:10.1002/pbc.25387
13. Johari T, Maiti TK. Catalytic domain mutation in CYLD inactivates its enzyme function by structural perturbation and induces cell migration and proliferation. *Biochim Biophys Acta Gen Subj*. 2018;1862(9):2081–2089. doi:10.1016/j.bbagen.2018.05.016
14. Massoumi R. CYLD: A deubiquitination enzyme with multiple roles in cancer. *Future Oncol*. 2011;7(2):285–297. doi:10.2217/fon.10.187
15. Wu W, Zhu H, Fu Y, et al. Clinical significance of down-regulated cylindromatosis gene in chronic lymphocytic leukemia. *Leuk Lymphoma*. 2014;55(3):588–594. doi:10.3109/10428194.2013.809077

16. Liu P, Xu B, Shen W, et al. Dysregulation of TNFalpha-induced necroptotic signaling in chronic lymphocytic leukemia: Suppression of CYLD gene by LEF1. *Leukemia*. 2012;26(6):1293–1300. doi:10.1038/leu.2011.357
17. Xu X, Kalac M, Markson M, et al. Reversal of CYLD phosphorylation as a novel therapeutic approach for adult T-cell leukemia/lymphoma (ATLL). *Cell Death Dis*. 2020;11(2):94. doi:10.1038/s41419-020-2294-6
18. Ye H, Liu X, Lv M, et al. MicroRNA and transcription factor co-regulatory network analysis reveals miR-19 inhibits CYLD in T-cell acute lymphoblastic leukemia. *Nucleic Acids Res*. 2012;40(12):5201–5214. doi:10.1093/nar/gks175
19. Enesa K, Zakkar M, Chaudhury H, et al. NF-kappaB suppression by the deubiquitinating enzyme Cezanne: A novel negative feedback loop in pro-inflammatory signaling. *J Biol Chem*. 2008;283(11):7036–7045. doi:10.1074/jbc.M708690200
20. Wang JH, Wei W, Guo ZX, Shi M, Guo RP. Decreased Cezanne expression is associated with the progression and poor prognosis in hepatocellular carcinoma. *J Transl Med*. 2015;13:41. doi:10.1186/s12967-015-0396-1
21. Lin DD, Shen Y, Qiao S, et al. Upregulation of OTUD7B (Cezanne) promotes tumor progression via AKT/VEGF pathway in lung squamous carcinoma and adenocarcinoma. *Front Oncol*. 2019;9:862. doi:10.3389/fonc.2019.00862
22. Hasselbalch HC. Perspectives on chronic inflammation in essential thrombocythemia, polycythemia vera, and myelofibrosis: Is chronic inflammation a trigger and driver of clonal evolution and development of accelerated atherosclerosis and second cancer? *Blood*. 2012;119(14):3219–3225. doi:10.1182/blood-2011-11-394775
23. Lee EG, Boone DL, Chai S, et al. Failure to regulate TNF-induced NF-kappaB and cell death responses in A20-deficient mice. *Science*. 2000;289(5488):2350–2354. doi:10.1126/science.289.5488.2350
24. Jin W, Reiley WR, Lee AJ, et al. Deubiquitinating enzyme CYLD regulates the peripheral development and naive phenotype maintenance of B cells. *J Biol Chem*. 2007;282(21):15884–15893. doi:10.1074/jbc.M609952200
25. Reiley WW, Zhang M, Jin W, et al. Regulation of T cell development by the deubiquitinating enzyme CYLD. *Nat Immunol*. 2006;7(4):411–417. doi:10.1038/ni1315
26. Zhao WB, Li Y, Liu X, Zhang LY, Wang X. Involvement of $CD4^+CD25^+$ regulatory T cells in the pathogenesis of polycythaemia vera. *Chin Med J (Engl)*. 2008;121(18):1781–1786. PMID:19080357.
27. Baxter EJ, Scott LM, Campbell PJ, et al. Acquired mutation of the tyrosine kinase JAK2 in human myeloproliferative disorders. *Lancet*. 2005;365(9464):1054–1061. doi:10.1016/S0140-6736(05)71142-9
28. Livak KJ, Schmittgen TD. Analysis of relative gene expression data using real-time quantitative PCR and the 2(–delta delta C(T)) method. *Methods*. 2001;25(4):402–408. doi:10.1006/meth.2001.1262
29. Song LH, Toan NL, Xuan NT, et al. A promoter polymorphism in the *interferon alpha-2* gene is associated with the clinical presentation of hepatitis B. *Mutat Res*. 2006;601(1–2):137–143. doi:10.1016/j.mrfmmm.2006.06.011
30. Ohno K, Takeda JI, Masuda A. Rules and tools to predict the splicing effects of exonic and intronic mutations. *Wiley Interdiscip Rev RNA*. 2018;9(1). doi:10.1002/wrna.1451
31. Jian X, Boerwinkle E, Liu X. In silico tools for splicing defect prediction: A survey from the viewpoint of end users. *Genet Med*. 2014;16(7):497–503. doi:10.1038/gim.2013.176
32. Xuan NT, Wang X, Nishanth G, et al. A20 expression in dendritic cells protects mice from LPS-induced mortality. *Eur J Immunol*. 2015;45(3):818–828. doi:10.1002/eji.201444795
33. Pourcelot E, Trocme C, Mondet J, et al. Cytokine profiles in polycythemia vera and essential thrombocythemia patients: Clinical implications. *Exp Hematol*. 2014;42(5):360–368. doi:10.1016/j.exphem.2014.01.006
34. Canh NX, Giang NV, Nghia VX, et al. Regulation of cell activation by A20 through STAT signaling in acute lymphoblastic leukemia. *J Recept Signal Transduct Res*. 2021;41(4):331–338. doi:10.1080/10799893.2020.1808678
35. Birgen D, Ertem U, Duru F, et al. Serum Ca 125 levels in children with acute leukemia and lymphoma. *Leuk Lymphoma*. 2005;46(8):1177–1181. doi:10.1080/10428190500096690
36. Johansson P, Bergmann A, Rahmann S, et al. Recurrent alterations of TNFAIP3 (A20) in T-cell large granular lymphocytic leukemia. *Int J Cancer*. 2016;138(1):121–124. doi:10.1002/ijc.29697
37. Zhou Q, Wang H, Schwartz DM, et al. Loss-of-function mutations in TNFAIP3 leading to A20 haploinsufficiency cause an early-onset autoinflammatory disease. *Nat Genet*. 2016;48(1):67–73. doi:10.1038/ng.3459
38. Tefferi A, Strand JJ, Lasho TL, et al. Bone marrow JAK2V617F allele burden and clinical correlates in polycythemia vera. *Leukemia*. 2007;21(9):2074–2075. doi:10.1038/sj.leu.2404724
39. Tefferi A, Barbui T. Polycythemia vera and essential thrombocythemia: 2019 update on diagnosis, risk-stratification and management. *Am J Hematol*. 2019;94(1):133–143. doi:10.1002/ajh.25303
40. Schabowsky RH, Madireddi S, Sharma R, Yolcu ES, Shirwan H. Targeting $CD4^+CD25^+FoxP3^+$ regulatory T-cells for the augmentation of cancer immunotherapy. *Curr Opin Investig Drugs*. 2007;8(12):1002–1008. PMID:18058571.
41. Cerny J, Yu H, Ramanathan M, et al. Expression of CD25 independently predicts early treatment failure of acute myeloid leukaemia (AML). *Br J Haematol*. 2013;160(2):262–266. doi:10.1111/bjh.12109
42. Blatt K, Menzl I, Eisenwort G, et al. Phenotyping and target expression profiling of CD34(+)/CD38(–) and CD34(+)/CD38(+) stem and progenitor cells in acute lymphoblastic leukemia. *Neoplasia*. 2018;20(6):632–642. doi:10.1016/j.neo.2018.04.004
43. Kwaan HC, Wang J. Hyperviscosity in polycythemia vera and other red cell abnormalities. *Semin Thromb Hemost*. 2003;29(5):451–458. doi:10.1055/s-2003-44552

The influence of menstrual cycle on the efficiency of stretching

Piotr Michalik[1,A–D,F], Tomasz Michalski[1,A–C], Jarosław Witkowski[2,E,F], Wojciech Widuchowski[3,4,A,E,F]

[1] Department of Kinesitherapy and Special Methods, School of Health Sciences in Katowice, Medical University of Silesia, Katowice, Poland
[2] Department of Traumatology and Hand Surgery, Wroclaw Medical University, Poland
[3] District Hospital of Orthopedics and Trauma Surgery, Piekary Śląskie, Poland
[4] Physiotherapy School of Higher Education in Wrocław, Poland

A – research concept and design; B – collection and/or assembly of data; C – data analysis and interpretation;
D – writing the article; E – critical revision of the article; F – final approval of the article

Advances in Clinical and Experimental Medicine, ISSN 1899–5276 (print), ISSN 2451–2680 (online) *Adv Clin Exp Med*. 2022;31(4):381–387

Address for correspondence
Piotr Michalik
E-mail: pmichalik@sum.edu.pl

Funding sources
None declared

Conflict of interest
None declared

Received on February 10, 2021
Reviewed on June 25, 2021
Accepted on July 12, 2021

Published online on January 13, 2022

Abstract

Background. Muscle stretching has been practiced by people for thousands of years. Its effectiveness is well-proven, but the diversity of the obtained results should prompt a search for causative factors. One of the possible explanations can be hormonal fluctuations, which occur during the menstrual cycle.

Objectives. To assess the influence of menstrual cycle on the efficiency of static stretching of hamstrings with special reference to changes in their length.

Materials and methods. A total of 534 young women were recruited for the study, but after applying the inclusion criteria, only 48 of them have been accepted. The inclusion criteria for the study comprised a reduced length of the hamstring muscles and a regular menstrual cycle. The whole study included a twofold examination of hamstring length before and after the stretching (3×45 s), performed by a physiotherapist. All the measurements were carried out 3 times in individual phases of the menstrual cycle.

Results. Statistically significant influence of static stretching upon the length of hamstring muscle was revealed. A change in the passive knee extension (PKE) test was 13.34% (standard deviation (SD) = 10.97), and in active knee extension (AKE) test it was 8.46% (SD = 9.26). Hamstrings length demonstrated no differences in various phases of the menstrual cycle.

Conclusions. Static stretching is an effective tool for the improvement of the length of the hamstring muscle in young women. However, the effectiveness of stretching in healthy women is not influenced by the menstrual cycle phases.

Key words: elasticity, menstrual cycle, muscle stretching exercises, hamstring muscle

Cite as
Michalik P, Michalski T, Witkowski J, Widuchowski W. The influence of menstrual cycle on the efficiency of stretching. *Adv Clin Exp Med*. 2022;31(4):381–387. doi:10.17219/acem/140163

DOI
10.17219/acem/140163

Background

Stretching in its various manifestations has been a part of human motor behavior for centuries. It was first mentioned in India about 5000 years ago, and after that in China around 2600 BCE.[1]

In modern times, initially used ballistic exercises were replaced in the 1960s by static stretching (SS), introduced as part of the warm-up.[2,3]

Static stretching is an effective form of increasing the length of the muscle, and the hamstrings (HAMS) area is most often used one for the therapeutic intervention. The length of the muscle is a measure resulting from the distance between its attachments. The most common indicator for the evaluation of the elongating capacity of a given muscle is the point of discomfort (POD) felt during stretching.[1,4]

The HAMS flexibility is traditionally measured using the straight leg raise (SLR) test. Other popular HAMS flexibility tests are the active knee extension (AKE) test and the passive knee extension (PKE) test, which measure the knee joint extension excluding the movement of the pelvis, which helps to isolate the tested motion.[1,4–6] The effect of static stretching based on PKE was an increase in the range of motion (ROM) by 7.53° to 9.62°.[7–9] According to the systematic review from 2016, the obtained results confirmed the effectiveness of the SS, increasing the length of HAMS by 8.58° in the PKE test and by 8.35° in AKE test, respectively.[1,5]

The differences between the tests indicate higher values in tests performed passively compared to those performed actively.[1,4,5] Significant differences in HAMS flexibility were observed among athletes engaging in various sport disciplines; however, no differences were noted between the dominant and nondominant leg.[10,11]

The reasons for increasing the length of muscles after stretching are not fully understood.[12] A long-term exposure of muscles to elongation stimuli may lead to the structural changes consisting of the increased number of sarcomeres in the sequence and changes in muscle stiffness.[13,14] However, some researchers claim that the observed improvement in mobility after stretching is not caused by muscle remodeling, but by an increased tolerance to stretching, i.e., sensory adaptation.[12,15,16]

The improvements in flexibility occur regardless of the gender, although the results are significantly better in women than in men. In the SLR test, women showed 10% bigger elasticity than men.[11] On the other hand, the phenomenon of sensory adaptation to stretching occurred only in men who also showed higher passive stiffness and greater sensitivity to pain than women.[10] The discrepancies in the results obtained in the conducted researches lead to the question whether the changes in elasticity are the result of plastic changes within the muscle subjected to stretching or whether they are related to the adaptive changes within the nervous system.[17] It is worth noting that the level of pain perception may be also influenced by, among others, gender and the phase of the menstrual cycle.

Female reproductive hormones fluctuating during the menstrual cycle affect numerous parameters of the cardiovascular, respiratory, thermoregulatory and metabolic systems, which in turn can affect the physiology of the locomotor system. The presence of estrogen and progesterone receptors in bones, skeletal muscles, ligaments and the nervous system has been proven, and the fluctuations in their levels during the menstrual cycle may affect the physical properties of these structures.[18]

The studies showed that the differences in estrogen levels during the menstrual cycle were associated with a different amount of collagen-I and -III. In periovulatory phase, the amount of collagen-III rose whereas the amount of collagen-I decreased leading to higher tolerance to mechanical stretching.[19] The risk of anterior cruciate ligament (ACL) damage increases fourfold with a decrease in passive stability by 1.3 mm. There is a suspicion that one of the potential causes of this phenomenon may be hormonal changes occurring in menstruating women.[20–22] At ACL Research Retreat VIII, the study of hormonal changes during the menstrual cycle was considered a priority area for future research on reducing the risk of ACL injuries.[23,24]

The research on the influence of the menstrual cycle on muscle flexibility is scarce and the results are inconclusive. No significant effect was observed by Teixeira et al. when testing young women using the Sit And Reach global mobility test.[25] Sung and Kim showed complex changes in flexibility in the flexor and extensor muscles of the knee joint during the menstrual cycle. The vastus medialis (VM) and the semitendinosus (ST) increased their stiffness during ovulation, while the vastus lateralis (VL) and the biceps femoris (BF) remained unchanged.[26] In a study by Eiling et al., muscle stiffness showed significant variability depending on the phase of the menstrual cycle, with the lowest levels being reached during the ovulatory phase.[27] An inverse relationship has been found between estrogen levels and muscle stiffness.[28,29] The force necessary to perform passive knee flexion movement decreased during ovulation, indicating increased flexibility of these muscles in this phase.[30] The potential impact of the cycle phase on the effectiveness of stretching was assumed by Hoge et al., who therefore conducted the experiments during the first days of the menstrual cycle, when the levels of these hormones are low.[31]

Despite the widespread use of stretching and the awareness of the need for proper muscle flexibility, there is little research on the effects of hormonal changes occurring during the menstrual cycle on the stretching efficiency. Table 1 presents a summary of the publications in this area together with the assessment of their methodological quality, in accordance with the Physiotherapy Evidence Database (PEDro) scale guidelines. As most of the studies were observational, the obtained scores indicate rather low quality. On the other hand, the discrepancies in the obtained results indicate the need for further research in this area.

Table 1. Summary of the publications with an assessment of their methodological quality in accordance with the Physiotherapy Evidence Database (PEDro) scale guidelines

Criteria	Teixeira et al.[25]	Sung and Kim[26]	Eiling et al.[27]	O'Hora et al.[7]	Bell et al.[28]	Lee et al.[30]	Hoge et al.[31]	Miyamoto et al.[33]
1. Eligibility criteria were specified	yes	yes	yes	yes	yes	yes	yes	yes
2. Subjects were randomly allocated to groups	0	0	0	1	0	0	0	0
3. Allocation was concealed	1	0	0	0	0	0	0	0
4. The groups were similar at baseline regarding the most important prognostic indicators	1	0	0	1	0	0	0	0
5. There was blinding of all subjects	0	0	0	1	0	0	0	0
6. There was blinding of all therapists who administered the therapy	0	0	0	1	0	0	0	0
7. There was blinding of all assessors who measured at least one key outcome	0	0	0	0	0	0	0	0
8. Measures of at least one key outcome were obtained from more than 85% of the subjects initially allocated to groups	1	1	1	1	1	1	1	1
9. All subjects for whom outcome measures were available received the treatment or control condition as allocated	0	0	0	0	0	0	0	0
10. The results of between-group statistical comparisons are reported for at least one key outcome	1	0	0	1	0	0	0	0
11. The study provides both point measures and measures of variability for at least one key outcome	1	1	1	1	1	1	1	1
Total score	5	2	2	7	2	2	2	2

Objectives

The assessment of the influence of static stretching on the length of HAMS in various phases of the menstrual cycle.

Materials and methods

Forty-eight women aged 21–24 were selected out of 534 women randomly chosen for the study. The study group was homogenous in terms of parameters such as age, body weight, height, body mass index (BMI), and the length of the menstrual cycle. The average age was 21.4 years (standard deviation (SD) = 0.4). The average value of body weight was 60.34 kg (SD = 7.51), and the average BMI value in this group was 21.49 (SD = 1.93). The height of the studied women oscillated between 158 cm and 177 cm (mean 167.34 cm, SD = 6.14 cm). The duration of the menstrual cycle ranged from 26 to 32 days (mean 29.25 days, SD = 1.74).

The inclusion criteria were: the lack of any orthopedic disorders within the spine and lower limbs, shortening of HAMS above 20° measured using PKE test, BMI between 18.5 and 24.99, regular menstrual cycle for the last 6 months lasting 28 days (±5 days), and not using hormonal contraception.

The initial stage of qualification for the research was the assessment of flexibility of HAMS in the dominant leg. Only 180 out of 534 (33.7%) women met the assumed criterion of muscle shortening. In the next stage of the study, the respondents completed an original personal questionnaire. The obtained data excluded participants whose answers eliminated the possibility of precisely determining the phase of the menstrual cycle. Only 48 (26.6%) women were qualified for further measurements. The length of the menstrual cycle for each participant was determined by averaging the length of her last 6 menstrual cycles, which allowed to define the phases of the menstrual cycle:

1. follicular phase (FOL) – from 2nd to 5th day of the menstrual cycle;
2. ovulatory phase (OV) – from 12th to 15th day of the menstrual cycle;
3. luteal phase (LUT) – from 16th to the 28th day of the menstrual cycle.

The study involved a therapeutic intervention of 3 × 45 s static stretching and 2 measurements

of flexibility of HAMS of the dominant leg performed before and immediately after this intervention during each phase of the menstrual cycle. All the measurements were conducted by the same 2 researchers (A and B) who had many years of experience in physiotherapy, each of whom had specific tasks to perform, in accordance with the prepared test protocol. Researcher B was responsible for operating the inclinometers and entering data to the test report. Researcher A performed the tests but was not informed about the result obtained by researcher B.[32]

To evaluate the flexibility of HAMS muscles, the following tests were used:

Test No. 1. Passive extension of the knee joint to the POD (PKE test). Before the measurements, a line connecting 2 bone points: the greater trochanter and the lateral epicondyle of the femur was marked. The lower limb of the examined subject was bent to the position of 90° at the knee and hip joints. The subject was informed that her knee will be passively extended until POD in the back of the limb. The test was performed 3 times.

Test No. 2. Active knee extension (AKE test). The subject's position and inclinometers placement were as in the previously described test. The participant was instructed to actively extend the knee joint avoiding hip rotation and pelvic lifting. The test was repeated 3 times, and the participant's task was to perform them with a similar force and speed during all repetitions of the active movement.

The study of mobility ranges in the knee joint in the tests was carried out by means of 2 Saunders electronic inclinometers (The Saunders Group, Inc., Chaska, USA) attached to the front of tibia and lateral side of femur in all measurements performed in this project. The BMI was assessed on Tanita Corporation scales.

Therapeutic intervention consisted of static stretching. The position was identical to the one used in the measurement phase for the PKE test. The researcher performed passive extension of the lower limb in the knee joint, while maintaining the unchanged position in the hip joint until the patient feels POD. This position is held for 45 s for 3 consecutive repetitions with a 15 s interval between the repetitions.[15]

Statistical analysis was performed using IBM SPSS v. 23 software (IBM Corp., Armonk, USA) with a significance level of $\alpha = 0.05$.

Basic descriptive statistics were analyzed together with two-factor analyses of variance (ANOVAs) in the within-group schema, one-factor ANOVAs in the within-group schema, Student's t-tests, and correlation analyses with Pearson correlation coefficient (r).

The project of the study was approved by Bioethical Committee of Medical University of Silesia, Katowice, Poland (approval No. KNW/0022/KB1/26/17). All subjects gave their informed consent to participate in the study. The study was carried out in accordance with the Declaration of Helsinki.

Results

PKE level depending on the phase of the cycle and intervention

Static stretching was performed in particular phases of the menstrual cycle, and the observed difference in flexibility after SS were 8.5° in FOL, 8.5° in OV and 6.6° in LUT (Fig. 1).

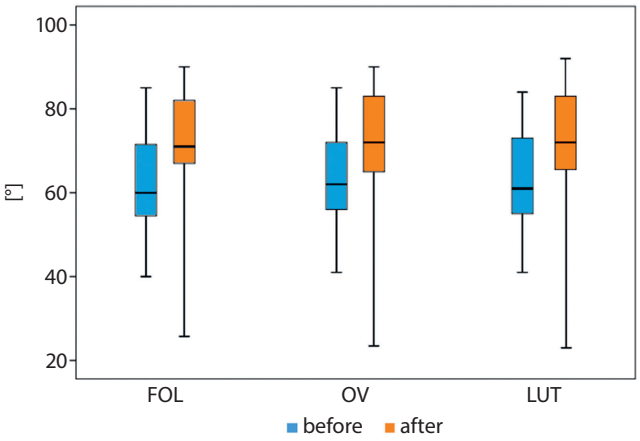

Fig. 1. Passive knee extension (PKE) level in all 6 measurements

FOL – follicular phase; OV – ovulatory phase; LUT – luteal phase.

There was no statistically significant or even nearly statistically significant effect of the main phase of the cycle on PKE ($F(2;92) = 0.26$; $p = 0.772$; $\eta^2 = 0.01$).

However, the main effect of the procedure was statistically significant ($F(1;46) = 230.63$; $p < 0.001$; $\eta^2 = 0.83$).

AKE level by cycle phase and intervention

Static stretching was performed in various phases of the menstrual cycle, and the results of the observed changes

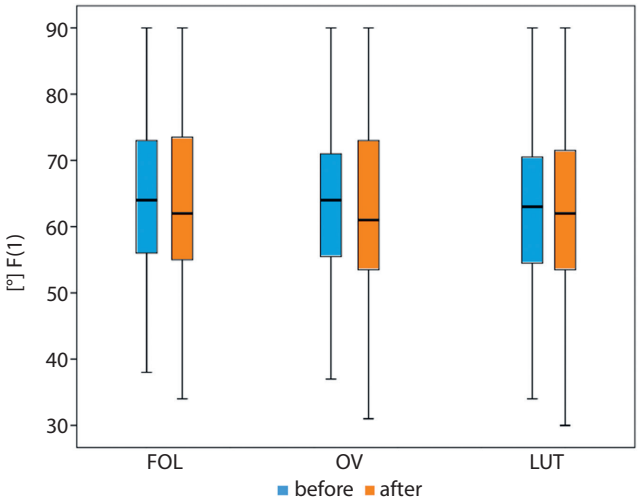

Fig. 2. Active knee extension (AKE) level in all 6 measurements

FOL – follicular phase; OV – ovulatory phase; LUT – luteal phase.

in flexibility after SS were 5.1° in the FOL, 5.7° in the OV and 4.1° in the LUT (Fig. 2).

The next step of the research aimed to verify whether the AKE level is different depending on the phase of the cycle and whether the measurement was carried out before or after the intervention.

There was no statistically significant or even nearly statistically significant effect of the main phase of the cycle on AKE ($F(2;92) = 0.03$; $p = 0.967$; $\eta^2 = 0$). However, the main effect of the intervention was statistically significant ($F(1;46) = 76.84$; $p < 0.001$; $\eta^2 = 0.63$). The strength of the observed effect was very high. As shown in Fig. 2, higher scores were recorded after the treatment. Additionally, there was no statistically significant interaction effect of the examined factors ($F(2;92) = 1.64$; $p = 0.200$; $\eta^2 = 0.03$).

For a better visualization of the changes taking place after the application of SS, the obtained results were expressed as a percentage, and the base value for all tested parameters was the state of the muscle before the intervention (100%). Then, the percentage values after stretching were compared to the values before stretching in 3 different phases of the cycle. One-factor ANOVAs were performed in the within-group schema. There were no statistically significant differences, as shown in Table 2.

Next, it was examined whether the percentage ratio of the results after stretching to the results before stretching is different in the case of AKE and PKE. Three paired samples t-tests were performed, separately in the FOL, OV and LUT. As shown in Table 3, all the observed differences turned out to be statistically significant. Higher values were recorded for the PKE. The strength of the observed effect in the case of the OV was moderately high, and in the case of the other 2 phases – low.

The correlations between the PKE and AKE indices were also examined. The correlation analyses with Pearson correlation coefficient (r) were performed. There were statistically significant positive relationships between these indices for the FOL ($r = 0.453$; $p = 0.001$), OV ($r = 0.606$; $p < 0.001$) and LUT ($r = 0.432$; $p = 0.002$). The strength of the relationship in the case of the OV was high, and moderately high in the other 2 phases.

Discussion

The effectiveness of stretching as well as flexibility depends on the gender and is definitely greater for women.[10] According to some researchers, including Hoge et al., it results from the occurrence of the so-called sensory adaptation through changes in sensory reactivity.[31,33] The strength of this phenomenon was significantly higher in men, but the reasons for these differences are still the subject of scientific research.[31]

This study is an attempt to assess whether the differences are due to variability associated with the phases of the menstrual cycle and whether this affects the effectiveness of SS. In the study, 2 tests were used to assess the length of the hamstring muscle: AKE and PKE. Both tests are based on the subjectively perceived end of movement associated with the feeling of discomfort. The results of both tests confirmed the effectiveness of the SS in improving HAMS flexibility. The observed change in the AKE test was 8.46% and it was lower than those obtained in the PKE test (13.34%), which is consistent with the results of other studies in this field.[1,4,5] The improvement of ROM assessed with the AKE test, examined immediately after the intervention, was comparable to the previous studies with similar methodology resulting in changes in ROM of 9.62° and 9.1°.[9] In the study by O'Hora et al., the SS effect based on the passive extension of the knee joint was an increase in ROM by 7.53° (PKE).[7]

When examining the correlations between the AKE and PKE tests, statistically significant positive relationships were noted in all phases: strong correlation in the OV and medium in the FOL and LUT. However, the results of both tests showed no significant influence of the phase of the menstrual cycle on HAMS length. There was also no

Table 2. The level of results after stretching as compared to the results before stretching depending on the phase

Test	Follicular phase		Ovulation phase		Luteal phase		F	df	p-value	η^2
	M	SD	M	SD	M	SD				
PKE	114.11	13.2	114.32	9.79	111.6	9.53	0.97	2.92	0.384	0.02
AKE	108.42	8.6	109.93	9.67	107.05	9.47	1.60	2.92	0.208	0.03

PKE – passive knee extension; AKE – active knee extension; M – mean; SD – standard deviation; df – degrees of freedom; η^2 – eta-squared.

Table 3. The percentage ratio of the post-procedure results to pre-procedure results for passive knee extension (PKE) and active knee extension (AKE) tests

Phase	PKE		AKE		t	df	p-value	d
	M	SD	M	SD				
Follicular	114.11	13.20	108.42	8.60	3.24	46	0.002	0.48
Ovulation	114.32	9.79	109.93	9.67	3.49	46	0.001	0.52
Luteal	111.60	9.53	107.05	9.47	3.08	46	0.003	0.46

M – mean; SD – standard deviation; df – degrees of freedom; t – Student's t-test result; d – Cohen's d.

significant influence of individual phases on the effectiveness of using SS within it.

The comparison of these results with the results of other studies is difficult due to the fact that the assessment of the efficiency of SS is an innovative project that has not yet been explored by other researchers. The flexibility changes occurring during the menstrual cycle are a possible reference. In a study by Teixeira et al., the whole myofascial superficial back line was assessed with a global test performed actively in 20 young women. In present study, no significant influence of the phase of the menstrual cycle on flexibility was shown. No differences were also observed in comparison to the results in the control group, to which 24 women using hormonal contraception were recruited.[25] Research on muscle elasticity assessed in various phases of the menstrual cycle conducted by Miyamoto et al. using shear wave elastography showed no significant reaction of this variable on muscle stiffness.[33] The study failed to prove any effect of the phases and the corresponding changes in muscles performed close to POD, similarly to the conditions applied in this study.

The research of Bell et al. brought contrary results. The HAMS length improved significantly in the OV (89.7–104.7°), as compared to the FOL (81.7–96.9°).[28] However, the study by Bell et al. remarkably differs from the present study. In the study by Bell et al., the assessments were performed only twice in the OV and FOL, thus omitting the LUT, which is studied in this project. It was assumed that the differences in the estrogen level are the highest when FOL and OV are compared, which would allow to determine their effect on HAMS. Furthermore, SLR test was applied instead of AKE and PKE tests used in our study. Also, the value of the SLR test obtained in the study by Bell et al. is 104.7°; therefore, it is much higher than normal values for this test, which confirms that patients without HAMS deficits were admitted for the tests. The effectiveness of SS in the group of subjects selected in that way can differ from the strict criteria of selection assumed in our study. However, the biggest difference results from the small size of the tested group (n = 8), which constitutes a high risk of random results.[28]

An important element for the interpretation of the obtained results, based on the moment of occurrence of POD, is the possible effect of the menstrual cycle phases on pain perception. As both tests assessing the length of HAMS were based on the subjective flexibility threshold related to POD, the changes in pain perception can influence the results. It is assumed that the fluctuations of sex hormone levels contribute to a higher, clinically and experimentally observed sensitivity to pain in women as compared to the men. These differences refer to both the higher sensitivity to nociceptive stimuli and pain sensation distribution, but the results of the research on the influence of hormonal changes occurring during the cycle on pain perception are ambiguous. Some researchers have indicated regular fluctuations of pain sensitivity depending on the cycle phases.[34] The research on potential estradiol regulation upon the functioning of neurotransmission of the endogenous opioids is a confirmation of such thinking. During the OV, a high activity level of this system, comparable to men's, was observed. However, during the FOL, when the estradiol level reaches its minimum, a reduction of the activity modulating the influence of opioids on pain perception occurred.

A result of the changes occurring during the menstrual cycle can be the reduction of tissue sensitivity to nociceptive stimuli during the OV, and the opposite reaction during the FOL. The influence of the menstrual cycle phase can also be observed in the differences in sensitivity to compression stimuli applied to muscles. Higher sensitivity occurred during the FOL than during the OV and LUT.[35] Veldhuijzen et al. studied the effect of the cycle upon the changes in the brain areas connected with pain, and presented similar conclusions.[36] In the systematic review of 2014, the majority of the studies indicated a possible effect of estrogen on pain sensitivity, with a clear tendency for the opposite relationship between these 2 parameters.[37] As the self-reporting of pain during the measurement can be influenced by hormonal changes during menstrual cycle, the objective methods of muscle extensibility assessment would be beneficial to exclude the possible changes of stretch tolerance on the efficiency of stretching.

Limitations

There are some limitations in this study. First, the assessment of menstrual cycle phase was based on expected hormonal peak levels, according to data obtained from a personal questionnaire. The ideal study would evaluate serum hormonal levels on a regular basis over a period longer than a single cycle in order to account for cycle differences, which occur even in women with regular cycle length. Second, the classical method used in this study to measure hamstrings flexibility (AKE and PKE tests) focuses on the maximum range of motion based on subjective pain response. More advanced methods, such as isokinetic dynamometry or muscle elastography, allow for the measurement of objective muscle length and passive stiffness. The tests used in this project cannot provide the arguments in the debate over the possible causes of changes in elasticity after SS related to either stretch tolerance or tissue remodeling.

Conclusions

The length of the hamstring muscles after SS increased significantly by 13.34% in the PKE test and by 8.46% in the AKE test. However, the effectiveness of stretching in healthy women is not influenced by the menstrual cycle phases.

ORCID iDs

Piotr Michalik https://orcid.org/0000-0002-6328-4106
Tomasz Michalski https://orcid.org/0000-0001-5505-256X
Jarosław Witkowski https://orcid.org/0000-0002-2754-1339
Wojciech Widuchowski https://orcid.org/0000-0002-3684-7823

References

1. Behm DG. *The Science and Physiology of Flexibility and Stretching*. London, UK: Routledge; 2018.
2. Dridi A, Chamari K, Wong DP, et al. Static stretching can impair explosive performance for at least 24 hours. *J Strength Cond Res*. 2014;28(1):140–146. doi:10.1519/jsc.0b013e3182964836
3. Judge LW, Petersen JC, Bellar DM, et al. An examination of preactivity and postactivity stretching practices of crosscountry and track and field distance coaches. *J Strength Cond Res*. 2013;27(9):2456–2464. doi:10.1519/JSC.0b013e318257703c
4. Gajdosik RL, Rieck MA, Sullivan DK, Wightman SE. Comparison of four clinical tests for assessing hamstring muscle length. *J Orthop Sports Phys Ther*. 1993;18(5):614–618. doi:10.2519/jospt.1993.18.5.614
5. Medeiros DM, Cini A, Sbruzzi G, Lima CS. Influence of static stretching on hamstring flexibility in healthy young adults: Systematic review and meta-analysis. *Physiother Theory Pract*. 2016;32(6):438–445. doi:10.1080/09593985.2016.1204401
6. Gnat R, Kuszewski M, Koczar R, Dziewońska A. Reliability of the passive knee flexion and extension tests in healthy subjects. *J Manipulative Physiol Ther*. 2010;33(9):659–665. doi:10.1016/j.jmpt.2010.09.001
7. O'Hora J, Cartwright A, Wade CD, Hough AD, Shum GL. Efficacy of static stretching and proprioceptive neuromuscular facilitation stretch on hamstrings length after a single session. *J Strength Cond Res*. 2011;25(6):1586–1591. doi:10.1519/JSC.0b013e3181df7f98
8. Lim KI, Nam HC, Jung KS. Effects on hamstring muscle extensibility, muscle activity, and balance of different stretching techniques. *J Phys Ther Sci*. 2014;26(2):209–213. doi:10.1589/jpts.26.209
9. Puentedura EJ, Huijbregts PA, Celeste S, et al. Immediate effects of quantified hamstring stretching: Hold-relax proprioceptive neuromuscular facilitation versus static stretching. *Phys Ther Sport*. 2011;12(3):122–126. doi:10.1016/j.ptsp.2011.02.006
10. Marshall PW, Siegler JC. Lower hamstring extensibility in men compared to women is explained by differences in stretch tolerance. *BMC Musculoskelet Disord*. 2014;15(1):223. doi:10.1186/1471-2474-15-223
11. Sierra-Silvestre E, Torres Lacomba M, de la Villa Polo P. Effect of leg dominance, gender and age on sensory responses to structural differentiation of straight leg raise test in asymptomatic subjects: A cross-sectional study. *J Man Manip Ther*. 2017;25(2):91–97. doi:10.1080/10669817.2016.1200216
12. Magnusson SP. Passive properties of human skeletal muscle during stretch maneuvers: A review. *Scand J Med Sci Sports*. 1998;8(2):65–77. doi:10.1111/j.1600-0838.1998.tb00171.x
13. Coutinho EL, Gomes ARS, França CN, Oishi J, Salvini TF. Effect of passive stretching on the immobilized soleus muscle fiber morphology. *Brazilian J Med Biol* Res. 2004;37(12):1853–1861. doi:10.1590/s0100-879x2004001200011
14. Kay AD, Blazevich AJ. Moderate-duration static stretch reduces active and passive plantar flexor moment but not Achilles tendon stiffness or active muscle length. *J Appl Physiol (1985)*. 2009;106(4):1249–1256. doi:10.1152/japplphysiol.91476.2008
15. Ben M, Harvey LA. Regular stretch does not increase muscle extensibility: A randomized controlled trial. *Scand J Med Sci Sports*. 2010;20(1):136–144. doi:10.1111/j.1600-0838.2009.00926.x
16. Ylinen J, Kankainen T, Kautiainen H, Rezasoltani A, Kuukkanen T, Häkkinen A. Effect of stretching on hamstring muscle compliance. *J Rehabil Med*. 2009;41(1):80–84. doi:10.2340/16501977-0283
17. Wiech K, Ploner M, Tracey I. Neurocognitive aspects of pain perception. *Trends Cogn Sci*. 2008;12(8):306–313. doi:10.1016/j.tics.2008.05.005
18. Barros RPA, Gustafsson JÅ. Estrogen receptors and the metabolic network. *Cell Metab*. 2011;14(3):289–299. doi:10.1016/j.cmet.2011.08.005
19. Fede C, Pirri C, Fan C, et al. Sensitivity of the fasciae to sex hormone levels: Modulation of collagen-I, collagen-III and fibrillin production. *PLoS One*. 2019;14(9):e0223195. doi:10.1371/journal.pone.0223195
20. Królikowska A, Sikorski Ł, Czamara A, Reichert P. Effects of postoperative physiotherapy supervision duration on clinical outcome, speed, and agility in males 8 months after anterior cruciate ligament reconstruction. *Med Sci Monit*. 2018;24:6823–6831. doi:10.12659/MSM.912162
21. Królikowska A, Sikorski Ł, Czamara A, Reichert P. Are the knee extensor and flexor muscles isokinetic parameters affected by the duration of postoperative physiotherapy supervision in patients eight months after ACL reconstruction with the use of semitendinosus and gracilis tendons autograft? *Acta Bioeng Biomech*. 2018;20(4):89–100. PMID:30520446.
22. Myer GD, Ford KR, Paterno MV, Nick TG, Hewett TE. The effects of generalized joint laxity on risk of anterior cruciate ligament injury in young female athletes. *Am J Sports Med*. 2008;36(6):1073–1080. doi:10.1177/0363546507313572
23. Shultz SJ, Schmitz RJ, Cameron KL, et al. Anterior cruciate ligament research retreat VIII summary statement: An update on injury risk identification and prevention across the anterior cruciate ligament injury continuum, March 14–16, 2019, Greensboro, NC. *J Athl Train*. 2019;54(9):970–984. doi:10.4085/1062-6050-54.084
24. Cieślik-Bielecka A, Bold T, Ziółkowski G, Pierchała M, Królikowska A, Reichert P. Antibacterial activity of leukocyte- and platelet-rich plasma: An in vitro study. *Biomed Res Int*. 2018;2018:9471723. doi:10.1155/2018/9471723
25. Teixeira AL da S, Fernandes W, Marques FAD, de Lacio ML, Dias MRC. Influence of different phases of menstrual cycle on flexibility of young women. *Rev Bras Med Esporte*. 2012;18(6):361–364. doi:10.1590/S1517-86922012000600002
26. Sung ES, Kim JH. The difference effect of estrogen on muscle tone of medial and lateral thigh muscle during ovulation. *J Exerc Rehabil*. 2018;14(3):419–423. doi:10.12965/jer.1836110.055
27. Eiling E, Bryant AL, Petersen W, Murphy A, Hohmann E. Effects of menstrual-cycle hormone fluctuations on musculotendinous stiffness and knee joint laxity. *Knee Surg Sports Traumatol Arthrosc*. 2007;15(2):126–132. doi:10.1007/s00167-006-0143-5
28. Bell DR, Blackburn JT, Norcorss MF, et al. Estrogen and muscle stiffness have a negative relationship in females. *Knee Surg Sports Traumatol Arthrosc*. 2012;20(2):361–367. doi:10.1007/s00167-011-1577-y
29. Schleip R, Jäger H, Klingler W. What is "fascia"? A review of different nomenclatures. *J Bodyw Mov Ther*. 2012;16(4):496–502. doi:10.1016/j.jbmt.2012.08.001
30. Lee H, Petrofsky JS, Daher N, Berk L, Laymon M, Khowailed IA. Anterior cruciate ligament elasticity and force for flexion during the menstrual cycle. *Med Sci Monit*. 2013;19:1080–1088. doi:10.12659/MSM.889393
31. Hoge KM, Ryan ED, Costa PB, et al. Gender differences in musculotendinous stiffness and range of motion after an acute bout of stretching. *J Strength Cond Res*. 2010;24(10):2618–2626. doi:10.1519/JSC.0b013e3181e73974
32. Gnat R, Kuszewski M, Koczar R, Dziewońska A. Reliability of the passive knee flexion and extension tests in healthy subjects. *J Manipulative Physiol Ther*. 2010;33:659–665. doi:10.1016/j.jmpt.2010.09.001
33. Miyamoto N, Hirata K, Miyamoto-Mikami E, Yasuda O, Kanehisa H. Associations of passive muscle stiffness, muscle stretch tolerance, and muscle slack angle with range of motion: Individual and sex differences. *Sci Rep*. 2018;8(1):8274. doi:10.1038/s41598-018-26574-3
34. Bartley EJ, Fillingim RB. Sex differences in pain: A brief review of clinical and experimental findings. *Br J Anaesth*. 2013;111(1):52–58. doi:10.1093/bja/aet127
35. Rezaii T, Hirschberg AL, Carlström K, Ernberg M. The influence of menstrual phases on pain modulation in healthy women. *J Pain*. 2012;13(7):646–655. doi:10.1016/j.jpain.2012.04.002
36. Veldhuijzen DS, Keaser ML, Traub DS, Zhuo J, Gullapalli RP, Greenspan JD. The role of circulating sex hormones in menstrual cycle-dependent modulation of pain-related brain activation. *Pain*. 2013;154(4):548–559. doi:10.1016/j.pain.2012.12.019
37. Hassan S, Muere A, Einstein G. Ovarian hormones and chronic pain: A comprehensive review. *Pain*. 2014;155(12):2448–2460. doi:10.1016/j.pain.2014.08.027

Impact of COVID-19 on pancreatic cancer surgery: A high-volume Polish center experience

Karolina Kędzierska-Kapuza[1,A–D], Grzegorz Witkowski[1,B], Katarzyna Baumgart-Gryn[1,E,F], Aleksandra Szylińska[2,C], Marek Durlik[1,E,F]

[1] Department of Gastroenterological Surgery and Transplantology, Center of Postgraduate Medical Education in Warsaw, Poland
[2] Department of Medical Rehabilitation and Clinical Physiotherapy, Pomeranian Medical University, Szczecin, Poland

A – research concept and design; B – collection and/or assembly of data; C – data analysis and interpretation; D – writing the article; E – critical revision of the article; F – final approval of the article

Advances in Clinical and Experimental Medicine, ISSN 1899–5276 (print), ISSN 2451–2680 (online) *Adv Clin Exp Med*. 2022;31(4):389–398

Address for correspondence
Karolina Kędzierska-Kapuza
E-mail: karolina.kedzierska@gmail.com

Funding sources
None declared

Conflict of interest
None declared

Received on July 29, 2021
Reviewed on November 3, 2021
Accepted on November 22, 2021

Published online on February 2, 2022

Abstract

Background. A total of 148 surgeries were performed in our center on patients with pancreatic cancer in 2020. In 2019, 263 such procedures were performed (77.7% more) in this facility.

Objectives. To analyze the impact of coronavirus disease 2019 (COVID-19) on pancreatic cancer surgery type, number and outcome in our center.

Materials and methods. Retrospective data analysis of medical documentation in a hospital database from January 2019 till December 2020.

Results. In 2020, we observed an increase of tumors localized in the tail of the pancreas (P) – 29 cases (19.9%) in 2020 compared to 26 cases (9.9%) in 2019 ($p = 0.005$). In 2020, our patients presented with much greater advancement of the disease illustrated by the increased tumor size (median 3.5 cm in 2020 compared to 3.0 cm in 2019), although it did not reach statistical significance ($p = 0.073$). In 2020, we performed more palliative procedures, e.g., bypassing anastomoses (17 (11.6%) in 2020 compared to 8 (3%) in 2019 ($p < 0.001$)), more open biopsies of P (21 (14.4%) in 2020 compared to 21 (7.9%) in 2019 ($p = 0.041$)), and more percutaneous biopsies of P (7 (4.8%) in 2020 and 0 in 2019 ($p = 0.001$)). We observed a significant decrease in the number of Whipple procedures (53 (36.3%) in 2020 and 125 (47.5%) in 2019 ($p = 0.037$)). The most common histopathological finding was adenocarcinoma of the P, accounting for 50% in 2020 and almost 52% of all tumor cases in 2019. In a group of 148 patients operated on due to a P tumor during the COVID-19 pandemic, only 6 patients died, which resulted in a mortality rate of 4.1% compared to 13.4% mortality rate in 2019 (34 deaths/263 patients; $p = 0.005$). We observed less leakage of gastrointestinal anastomosis (0/148 in 2020 and 10/263 in 2019 ($p = 0.038$)).

Conclusions. Particular attention should be paid to patients with an aggressive type of cancer who have completed neoadjuvant therapy, as they are unable to undergo other therapeutic options. Severe acute respiratory syndrome coronavirus 2 (SARS-CoV-2)-positive cancer patients should be postponed until recovery. Relatively few postoperative complications and low all-cause mortality are the result of a more careful selection of oncological patients before the admission to the surgical ward, as well as a ompliance with the principles of planning the procedure and organization of the operating theater during the COVID-19 pandemic.

Key words: adenocarcinoma, pancreatic cancer, COVID-19, adjuvant therapy, neoadjuvant therapy

Cite as
Kędzierska-Kapuza K, Witkowski G, Baumgart-Gryn K, Szylińska A, Durlik M. Impact of COVID-19 on pancreatic cancer surgery: A high-volume Polish center experience. *Adv Clin Exp Med*. 2022;31(4):389–398. doi:10.17219/acem/144134

DOI
10.17219/acem/144134

Background

From March 4, 2020 until November 9, 2021, the total number of coronavirus disease 2019 (COVID-19) cases in Poland reached 3,111,534. According to the Polish Ministry of Health, 77,760 infected patients died and most of them had been suffering from comorbidities.[1] Mortality rate from COVID-19 in Polish population is ~2.5%.

The severe acute respiratory syndrome coronavirus 2 (SARS-CoV-2) pandemic has caused a huge overload of the healthcare system worldwide.[2] From March 13, 2020, many hospitals in Poland were converted into infectious diseases hospitals, which resulted in unavailability of treatment for non-COVID-19 patients. In numerous hospitals, the scheduled operations were cancelled and the ambulatory care was suspended due to the medical staff shortages. In some cases, the delay of diagnosis or treatment might not significantly impact the prognosis; however, in oncological patients, timing is crucial. The decision on whether to postpone the operations of oncological patients should be carefully considered, especially for those who have completed neoadjuvant therapy and patients with biologically aggressive tumors, such as pancreatic cancer, or patients without therapeutic alternatives. Delaying the operation should not worsen the oncological prognosis. However, patients with pancreatic cancer should not undergo the surgery at the time of the COVID-19 infection and the operation should be postponed. The meetings of the oncological team play a significant role in the shared clinical decision-making process and in planning the best treatment available. Videoconferences are a preferred option for such meetings and telemedicine should be used for the time being, although this is not always possible due to technical and organizational reasons.

Pancreatic tumors are a heterogeneous group of rare neoplasms. However, epidemiological studies show a significant increase in the incidence of pancreatic cancer in Poland, as well as worldwide. It is foreseen that pancreatic cancer will be among the top 5 cancers with the highest mortality rates in 2030.[3,4]

According to the Polish National Cancer Registry, a total of 164,875 new cancer cases and 99,644 cancer-related deaths were recorded in 2017. The number of new cases of malignant pancreatic neoplasms in 2017 was 3508 (2.1% of all new cancer cases (n = 1738) in men and 2.18% (n = 1770) in women). In 2017, a total of 99,644 people died of cancer in Poland, out of which 4864 people died of pancreatic cancer (4.4% (n = 2409) men (6th place among all types of cancer in Poland) and 5.4% (n = 2455) women (5th place)).[3]

In Poland, in 2010, mortality due to pancreatic cancer was comparable to the average mortality level for EU countries (data from 2009) in both sexes: male around 8/105 and female around 5/105. [3]

Pancreatic cancer, among all cancers, is the 7th leading cause of cancer-related deaths worldwide.[4] The course of the disease is very rapid and the average survival time starting from the diagnosis is approx. 6 months. From the time of the pancreatic cancer diagnosis, the 5-year survival rate is <9%, and less than 50% of patients live 3 months or more.[4,5] In case of resectable lesions, the 5-year survival rate is approx. 20%, but only 10–20% of patients are primarily diagnosed at such stage.[5]

Most cases of malignant pancreatic neoplasms occur after the age of 50 (92% cases in men and 95% cases in women). It is more common in men (5.5 per 100,000) than in women (4.0 per 100,000).[4] Nearly 80% of pancreatic cancer patients are diagnosed between the age of 60 and 80.[4–6] Cases under the age of 40 are extremely rare.[1]

About 85–90% of malignant pancreatic neoplasms are cancers of the exocrine portion of the pancreas of the glandular type, i.e., adenocarcinomas.[4] Other, less common types of pancreatic cancer include follicular cell carcinoma, pancreatoblastoma (the cancer of embryonic origin found in children), solid pseudopapillary carcinoma, and anaplastic (undifferentiated) cancer. These tumors differ slightly in biology, prognosis and treatment management from the most common pancreatic adenocarcinoma.[7]

The diagnosis of pancreatic cancer, despite the recent progress in diagnostic methods, is still challenging and causes a delay of the final diagnosis by about 4–9 months, which has probably increased during the COVID-19 pandemic, yet it is difficult to make an exact estimation.

The surgical treatment of pancreatic cancer should be performed in high-volume centers with extensive experience in pancreatic surgery, that conduct clinical trials.[8] In Poland, in 2011, the Polish Pancreatic Club and the Working Group of the Polish National Consultant in Gastroenterology published recommendations of oncological surveillance and diagnostics as well as therapeutic recommendations regarding patients with chronic pancreatitis.[9] The Department of Gastroenterological Surgery and Transplantology of the Central Clinical Hospital of the Ministry of the Interior and Administration in Warsaw, Poland is a leading center in pancreatic oncology in Poland, where the largest number of pancreatic cancer surgeries are performed every year in our country. In 2019, a total of 251 surgeries were performed in our clinic due to pancreatic cancer, while the 2 leading centers in the Lower Silesia Province performed overall only 22 such procedures and the next 2 largest centers in the Lesser Poland Province performed 60 such procedures.[10]

Unfortunately, in Poland as well as worldwide, the COVID-19 pandemic impeded the access to the oncological treatment and in the worst period of the pandemic, the number of surgeries dropped by up to 40%.[11]

Based on the meta-analysis of 34 publications which included almost 1.2 million oncological patients, scientists from the UK and the USA found that every 3-month diagnosis and treatment delay worsens the 5-year survival by about 10%, and a 6-month delay worsens these results by up to 30%.[12] Hanna et al. calculated that in the case

of surgical treatment, the risk of death increased by 6–8% with every 4-week period of delay. This turned out to be even worse in case of chemotherapy and radiotherapy (the risk of death increased by 9–13% (for radiotherapy for head and neck cancer and chemotherapy for colorectal cancer)). In addition, the researchers calculated that the 8-week and 12-week delay increased the risk of death, i.e., an 8-week delay in cancer surgery increased the risk of death by 17%, and a 12-week delay by up to 26%.[12]

The authors calculated that delaying the surgery by 12 weeks per year for all breast cancer patients (for example during the COVID-19 pandemic) would lead to 1400 additional deaths in the UK, 6100 in the USA, 700 in Canada, and 500 in Australia.

Objectives

This study had 4 objectives: 1) to assess the advancement and localization of the pancreatic cancer in our study group; 2) to establish how COVID-19 pandemic impacted the types of surgical procedures performed; 3) to find if there was any change in histopathological findings in our study group; 4) to assess mortality and number of complications in a group of patients operated on for a pancreatic tumor during the COVID-19 pandemic.

Materials and methods

The retrospective data analysis of medical documentation in a hospital database was performed. The research covered a period from January 2019 until December 2020. This study was performed in compliance with the Declaration of Helsinki. Informed consent was not obtained since we have only analyzed retrospective data from hospital database and personal information was anonymized.

Study setting

In Poland, in accordance with the Law of March 2, 2020 on special solutions related to the prevention, counteraction and combating COVID-19, other infectious diseases and the emergencies caused by them, the model of infectious diseases hospitals was implemented.[13] Based on this Law, the selected multidisciplinary units have been completely transformed into infectious disease hospitals dedicated to the fight against COVID-19. It is a model unparalleled in other countries.

By the decision of the authorities of Masovian Voivodeship, on March 13, 2020, the Central Clinical Hospital of the Ministry of Interior and Administration was transformed into an infectious diseases hospital with the highest level of reference for patients with COVID-19. This caused a significant reduction in the number of beds in the Surgery Clinic (55 beds before the pandemic) – 15 beds were designated for surgical COVID-19 patients and 9 beds for patients without COVID-19, dedicated to oncological patients.

On May 9, 2020, the regulations on infectious diseases hospitals ceased to apply, but on November 9, 2020, due to the 2nd wave of COVID-19 pandemic, a decision to convert the Central Clinical Hospital of the Ministry of the Interior and Administration into a hospital of the highest level of reference for patients with COVID-19 was made again.

Preoperative management of oncological patients

The preparation of the patient and the operating room was based on the guidelines of the Polish Surgical Society and the guidelines of the European Society of Surgeons.[14,15]

All of the patients need to be consulted during multidisciplinary consultation meetings once a week. If the patient is qualified for the surgery, he or she is informed about the procedures before the hospital admission, including: home observation towards COVID-19 symptoms (fever, cough, shortness of breath, sore throat, but also myalgia, diarrhea, fatigue, runny nose or congestion, loss of smell, altered sense of taste); the reverse transcription polymerase chain reaction (RT-PCR) negative test (valid 72 h) and the blood donation made by family members (the lack of blood during the pandemic has been the rising problem because of the decreased number of the donors). If a test yielded a positive result for a given patient, the procedure would be postponed depending on symptoms and illness severity. On the admission day, after checking the RT-PCR test results, the patient is screened for their body temperature and COVID-19-related symptoms. If the screening result is negative, an antigen test is conducted and the patient is not transferred to the clean area until the negative result is obtained. In the clinic, there is no isolation ward; therefore, the observation of the patients qualified for surgery for 3–7 days, as has been suggested in some publications, could not be taken into consideration.[16] Despite this, none of the oncological patients developed SARS-CoV-2 symptoms or has been tested positive after the surgery.

Statistical analyses

The statistical analyses were performed with the use of the licensed program STATISTICA v. 13 (StatSoft Inc., Tulsa, USA). The data were presented with the use of descriptive statistics, mainly mean, standard deviation (SD) and medians, as well as numbers and percentages. The Shapiro–Wilk test was used to check the normality of the distribution of the examined variables (Table 1). Continuous variables divided into groups were analyzed using the t-test with Welch's correction. The χ^2 test was used to evaluate the qualitative data in the individual groups and if the subgroup was small, the Yates's correction was used. The correlation analysis was performed using the Spearman's rank correlation coefficient. The level of significance was set at $p \leq 0.05$.

Table 1. The distribution of normality of patients groups (2019 compared to 2020)

Variable	Total (n = 411)	2019 (n = 263)	2020 (n = 148)
	normality	normality	normality
Age	p < 0.001	p < 0.001	p < 0.001
Tumor size [cm]	p < 0.001	p < 0.001	p < 0.001
Surgery time [min]	p < 0.001	p < 0.001	p < 0.001
ICU hospitalization [days]	p < 0.001	p < 0.001	p < 0.001
Hospitalization from surgery [days]	p < 0.001	p < 0.001	p < 0.001

ICU – intensive care unit.

Results

Despite a significant reduction in the number of oncological beds in the 2020, a total of 148 surgeries were performed in the clinic in patients with pancreatic cancer. In 2019, 263 such procedures were performed (77.7% more). The characteristics of the 2019 group compared to the 2020 group are presented in Table 2.

The operated group in 2019 included 108 (41.22%) male (M) and 154 (58.78%) female (F), compared to 60 (40.82%) M and 87 (59.18%) F in 2020 (the correlation was not significant).

In 2020, when compared to 2019, our patients had much greater advancement of the disease defined by the increased tumor size (median 3.0 cm in 2019 and 3.5 cm in 2020), although this correlation did not reach statistical significance (p = 0.073). The duration of the intensive care unit (ICU) stay was longer in 2019 compared to 2020 (p < 0.001). Gender of patients, time of operation and hospitalization time after the surgery did not differ significantly between 2019 and 2020 (Table 2,3). The relatively short time of hospitalization in 2020 was caused by the limited number of beds in the clinic for COVID-19-negative patients and the necessity to quickly transfer patients in good condition to other hospitals in the area.

The most common location of the pancreatic tumor was the head of the pancreas – 97 cases (66.4%) in 2020 compared to 173 cases (66.3%) in 2019. In 2020, we observed an increase of tumors localized in the tail of the pancreas

Table 2. Characteristics of patient groups (2019 compared to 2020)

Variable	2019 (n = 263)					2020 (n = 148)					p-value
	mean	SD	Me	Q1	Q3	mean	SD	Me	Q1	Q3	
Age	62.49	11.46	64.0	57.0	70.0	61.15	11.29	63.0	55.0	69.0	0.259
Tumor size [cm]	3.41	1.86	3.0	2.0	4.2	3.81	2	3.5	2.5	5.0	0.073
Surgery time [min]	102.42	40.53	110.0	70.0	120.0	95.4	39.06	90.0	65.0	120.0	0.093
ICU hospitalization [days]	1.66	5.98	0.0	0.0	0.0	0.31	1.5	0.0	0.0	0.0	<0.001
Hospitalization from surgery [days]	12.74	11.92	9.0	7.0	13.0	12.42	15.79	9.0	7.0	13.0	0.835

ICU – intensive care unit; SD – standard deviation; Me – median; Q1– lower quartile; Q3 – upper quartile; t-test with Welch's correction was used.

Table 3. Gender of patients and localization of tumor of pancreas

Variable		2019 (n = 263)		2020 (n = 148)		p-value
		n	%	n	%	
Gender	male	108	41.22	60	40.82	0.936
	female	154	58.78	87	59.18	
Head of the pancreas	no	88	33.72	49	33.56	0.974
	yes	173	66.28	97	66.44	
Body of the pancreas	no	182	69.73	108	73.97	0.365
	yes	79	30.27	38	26.03	
Tail of the pancreas	no	235	90.04	117	80.14	0.005
	yes	26	9.96	29	19.86	
>1	no	243	93.10	137	93.84	0.939*
	yes	18	6.90	9	6.16	

The χ^2 test was used; * the Yates's correction was used.

– 29 cases (19.9%) in 2020 compared to 26 cases (9.9%) in 2019 (p = 0.005). The localization in body and multiple localization in pancreas did not differ significantly when compared with 2019 (Table 3). In 2020, patients with pancreatic cancer tended to be referred to our center with more advanced stage of the disease than in 2019. Due to that, in 2020 we performed more palliative procedures, e.g., bypassing anastomoses – 17 (11.6%) in 2020 compared to 8 (3%) in 2019 (p < 0.001); open biopsies of the pancreas – 21 (14.4%) in 2020 compared to 21 (7.9%) in 2019 (p = 0.041); and percutaneous biopsies of the pancreas – 7 (4.8%) in 2020 compared to 0 in 2019 (p = 0.001). Moreover, the number of Whipple procedures significantly dropped in 2020 to 53 (36.3%), compared to 125 (47.5%) in 2019 (p = 0.037). Statistical significance was also observed regarding the numer of operations titled as "other", performed in 2019 and 2020, which include operations such as central pancreatectomy, Frey's procedure, thoracoscopic transection of the visceral nerve, cholecystectomy, drainage of the peripancreatic abscess, and enucleation of a pancreatic tumor (Fig. 1).

The most common histopathological finding was adenocarcinoma of the pancreas, accounting for 50% of cases in 2020 and almost 52% of all tumor types in 2019. More pancreatic intraepithelial neoplasia cases were found in 2019 (51/263) than in 2020 (6/148) (p < 0.001), but in 2020, more chronic pancreatitis cases were diagnosed (p = 0.004, Fig. 2). In 2019, more "other" types of neoplasms were found, e.g., mixed types of tumor like adenocarcinoma/squamous cell carcinoma or anaplastic carcinoma (p = 0.016, Fig. 2).

In a group of 148 patients operated on for a pancreatic tumor during the COVID-19 pandemic, only 6 people died, which resulted in all-cause 30-day mortality rate of 4.1%, compared to 34 deaths/263 patients and all-cause mortality rate of 13.4% in 2019 (p = 0.005). We have observed less leakage of gastrointestinal anastomosis (0/148) in 2020 than in 2019 (10/263) (p = 0.038). Apart from that, we noted no difference in surgical and nonsurgical complications (Fig. 3).

In patients with advanced inoperable tumor who underwent percutaneous biopsies, open biopsies and/or bypass anastomoses, full staging according to TNM classification was impossible; therefore, the data presented in Table 4 concern only those patients who underwent a tumor resection and have a complete histopathological examination of the tumor (TNM). There were no differences between 2019 and 2020 in terms of TNM features or tumor resectability; however, much more frequent diagnoses of low-differentiated G3 and G4 anaplastic tumors were stated in 2020, and these tumors are characterized by a rapid growth (p = 0.037). A diagnosis of more advanced tumor influenced the decision to administer adjuvant chemotherapy. In 2020, the rate of qualification for adjuvant treatment significantly decreased – 51% of patients in 2020 received such treatment compared to 68% in 2019 (p < 0.001, Table 4). In our study, we have also

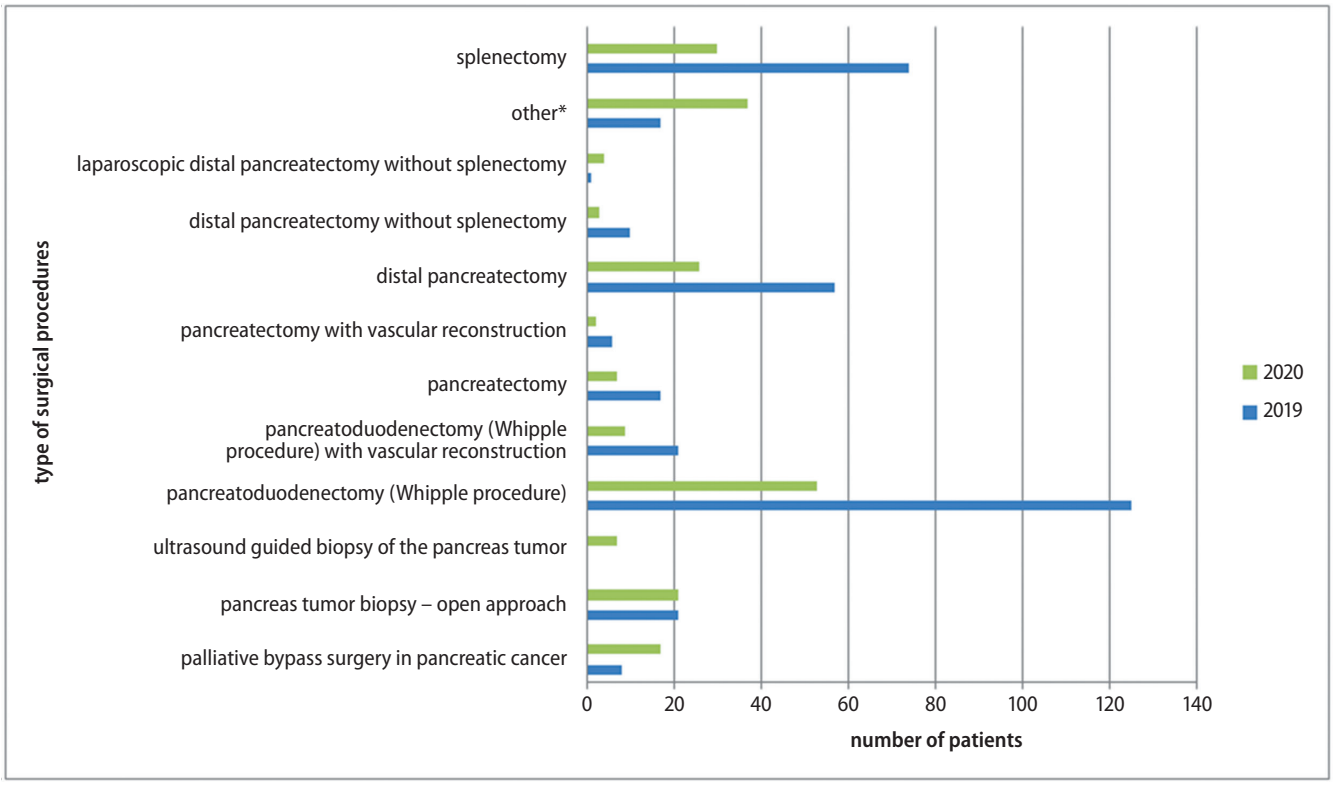

Fig. 1. Types of surgical procedures in 2019 compared to 2020

* other, e.g., central pancreatectomy, Frey's procedure, thoracoscopic transection of the visceral nerve, cholecystectomy, drainage of the peripancreatic abscess, enucleation of a pancreatic tumor.

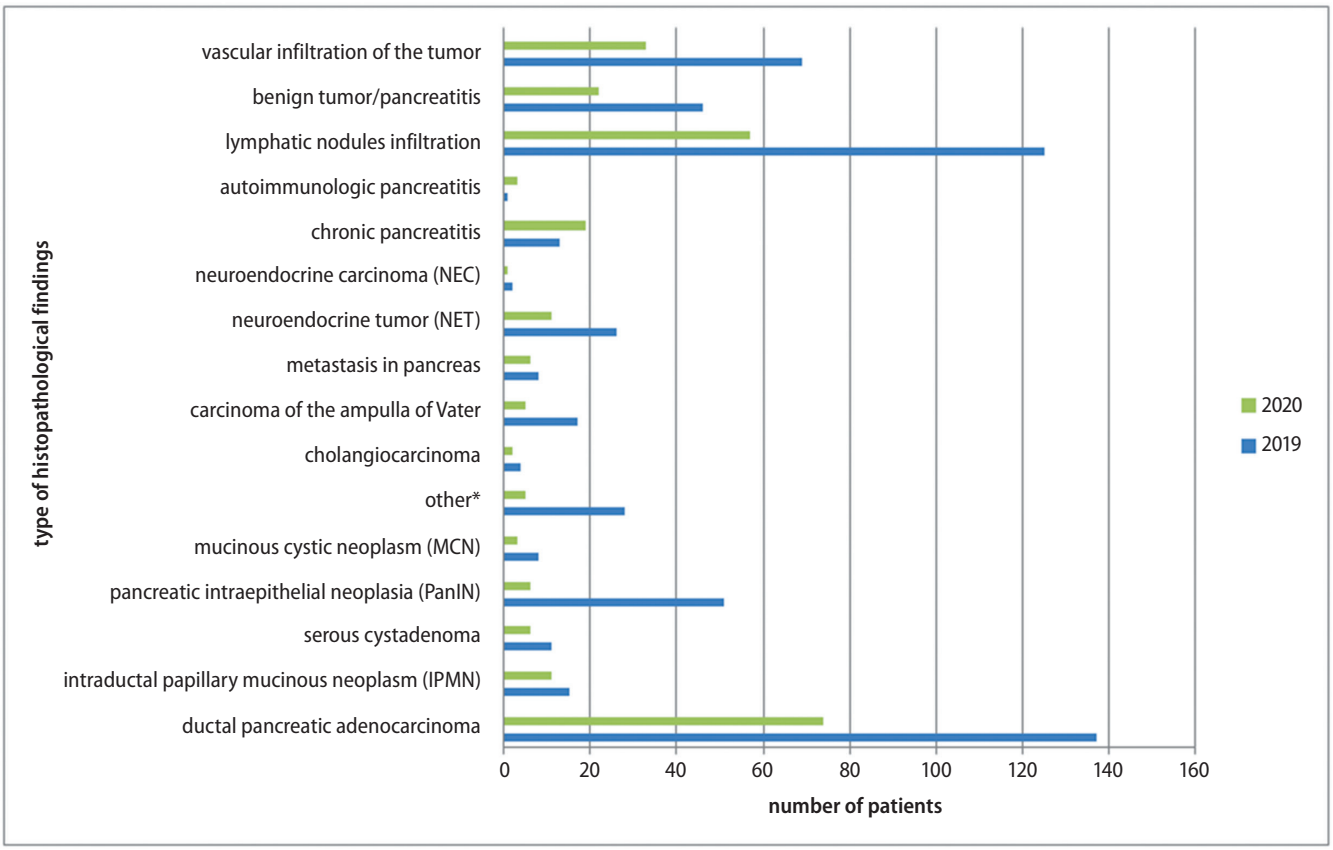

Fig. 2. Histopathological findings in 2019 and 2020

* other: mixed types of tumor like adenocarcinoma/squamous cell carcinoma, anaplastic carcinoma, lipomatous atrophy, serous cystadenoma, necrotic tissue, malignant neoplasm of epithelioid cells, sarcoma, additional spleen, mixed adenocarcinoma/sarcoma, yellow tufts, or B-cell lymphoma.

Table 4. Analysis of TNM tumor staging, tumor resection type and grading (patients after biopsies and palliative procedures were excluded) in 2019 compared to 2020

Variable		2019 (n = 263)		2020 (n = 148)		p-value
		n	%	n	%	
T1/T2/T3/T4	T1 T2 T3 T4	15 76 74 2	8.98 45.51 44.31 1.20	2 9 15 0	7.69 34.62 57.69 0.00	0.608
N0/N1/N2/N>3	N0 N1 N2 Nx	48 64 56 4	27.91 37.21 32.56 2.33	24 24 23 2	32.88 32.88 31.51 2.74	0.861
M/Mx	M1 Mx	17 6	73.91 26.09	18 4	81.82 18.18	0.780*
R0/R1/R2	R0 R1 R2	87 79 6	50.58 45.93 3.49	49 26 1	64.47 34.21 1.32	0.108
G1/G2/G3/G4	G1 G2 G3 G4	32 105 35 1	18.50 60.69 20.23 0.58	11 44 16 5	14.47 57.89 21.05 6.58	0.037
Neoadjuvant chemotherapy	no yes	225 19	92.21 7.79	129 18	87.76 12.24	0.145
Adjuvant chemotherapy	no yes	77 165	31.82 68.18	72 75	48.98 51.02	<0.001

The χ^2 test was used; * the Yates's correction was used.

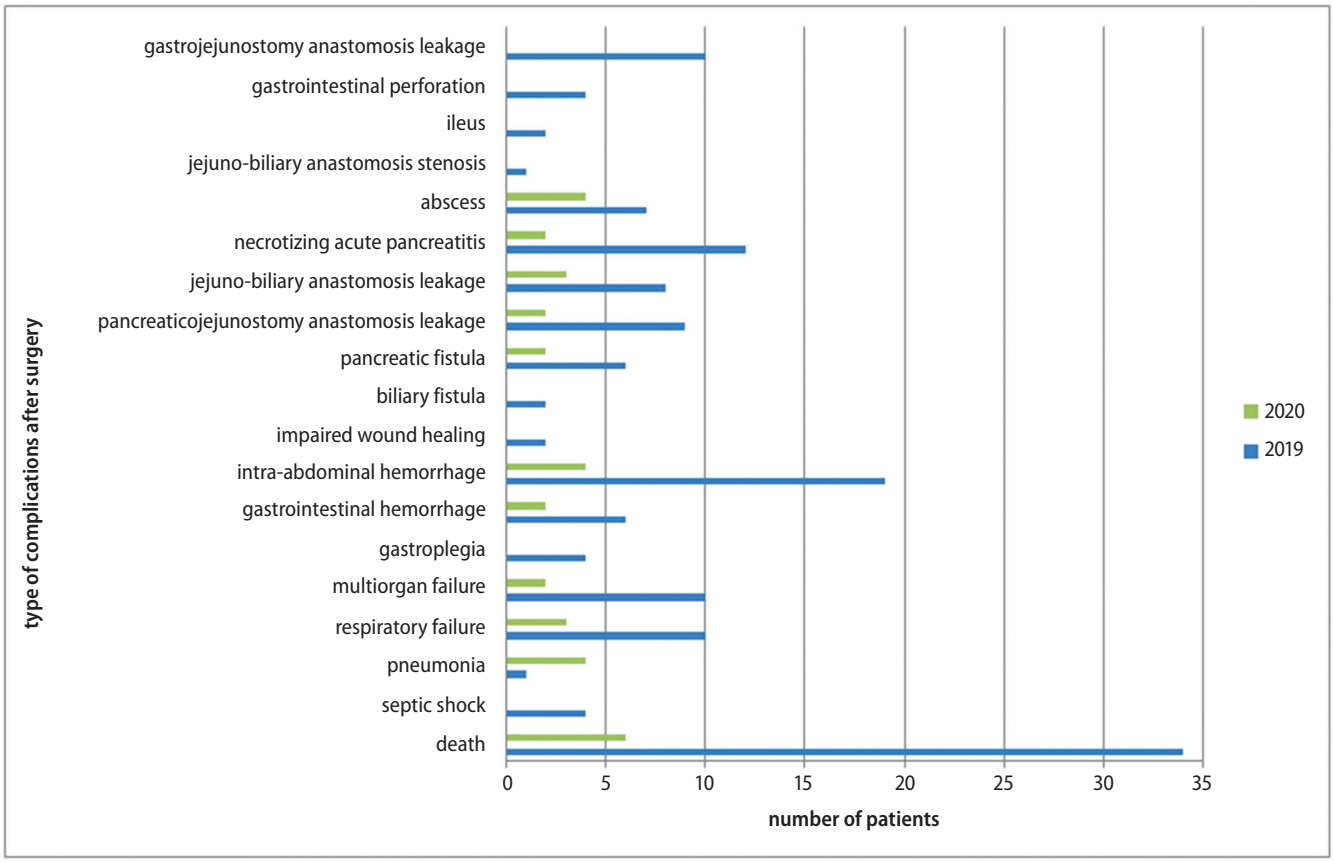

Fig. 3. All-cause mortality and complications after surgery according to type in 2019 compared to 2020. Other complications, not presented in this figure, include: mesenteric venous thrombosis, mesenteric artery thrombosis, pulmonary embolism, intraperitoneal hernia, acute gastritis, hydrothorax, transient ischemic attack, acute kidney failure, lymphocele, gastric ulcer, and atrial fibrillation.

observed that the larger the size of the primary tumor, the more frequently operations with venous reconstruction were performed (R = 0.129, p < 0.014). Moreover, the invasion of lymph nodes was diagnosed more often (R = 0.197, p < 0.001) and splenectomy was more often required (R = 0.146, p = 0.006).

The operative time was the shortest for open biopsy of a pancreatic tumor (R = –0.187, p < 0.001) and distal pancreatic resection with splenectomy (R = –0.225, p < 0.001), and the longest for Whipple procedure (R = 0.255, p < 0.001), Whipple procedure with venous reconstruction, and total pancreatic resection with venous reconstruction (R = 0.144, p < 0.004, and R = 0.149, p < 0.003, respectively).

The extended duration of the procedure was an important factor correlating with numerous parameters, including: the length of ICU stay (R = 0.119, p = 0.017), extended hospitalization time (R = 0.276, p < 0.001) and early mortality during the first hospitalization (R = 0.149, p = 0.003).

Shorter surgery time correlated with distal pancreatic resection with splenectomy (R = –0.225, p < 0.001).

Intensive care unit stay positively correlated with patients' older age (R = 0.109, p < 0.029), early mortality (R = 0.618; p < 0.001) and with the presence of complications such as sepsis (R = 0.141, p < 0.004), pneumonia (R = 0.173, p < 0.001), respiratory failure (R = 0.454, p < 0.001), multiple organ failure (R = 0.418, p < 0.001), and anastomotic leakage of pancreatic anastomosis (R = 0.303, p < 0.001). Moreover, similar correlations were observed when the hospitalization time was concerned. A negative correlation was stated between the length of the hospitalization and the type of surgery – distal pancreatectomy with splenectomy (R = –0.250, p < 0.001) (Table 5).

Discussion

In our clinic, we follow the actual National Comprehensive Cancer Network® (NCCN®) guidelines,[17] and we do not assess clinical TNM stage. According to those guidelines, a suspicion of pancreatic cancer or the evidence of dilated pancreatic and/or bile duct (stricture) are an indication for surgery, and the most important finding is the presence or absence of metastases. If there are no metastases in the diagnostic imaging, the next step is to check the vessel invasion. When metastases are present, this is an automatic contraindication to resection surgery and an indication for the biopsy and chemotherapy. In case of vessel invasion, depending on the kind of vessel and the experience of the high-volume center, a patient is qualified for resection surgery or neoadjuvant therapy.

Table 5. The list of most relevant correlations between obtained data

Correlated data	R	p-value
Primary tumor size & Whipple procedure + venous reconstructions	0.129	0.014
Primary tumor size & lymph node invasion	0.197	<0.001
Primary tumor size & splenectomy	0.146	0.006
Procedure time & open biopsy of the pancreatic tumor	–0.187	<0.001
Procedure time & Whipple procedure	0.255	<0.001
Procedure time & Whipple procedure + venous reconstruction	0.144	0.004
Procedure time & total pancreatic resection + reconstruction	0.149	0.003
Procedure time & distal with splenectomy	–0.225	<0.001
Procedure time & ICU stay	0.119	0.017
Procedure time & hospitalization time since surgery	0.276	<0.001
Procedure time & lymph node invasion	0.160	0.002
Procedure time & death	0.149	0.003
Procedure time & splenectomy	–0.146	0.003
ICU stay & age	0.109	0.029
ICU stay & total pancreatic resection + reconstruction	0.115	0.020
ICU stay & hospitalization time from surgery	0.242	<0.001
ICU stay & death	0.618	<0.001
ICU stay & 1 – sepsis	0.141	0.004
ICU stay & 2 – pneumonia	0.173	<0.001
ICU stay & 3 – respiratory failure	0.454	<0.001
ICU stay & 4 – organ failure (shock)	0.418	<0.001
ICU stay & 7 – hemorrhage into the peritoneal cavity	0.507	0.000
ICU stay & 12 – leakage of pancreatic anastomosis	0.303	<0.001
ICU stay & 13 – leakage of the biliary anastomosis	0.407	<0.001
Hospitalization time since surgery & distal with splenectomy	–0.250	<0.001

ICU – intensive care unit. Spearman's rank correlation was used.

It seems that the low number of postoperative complications and the low 30-day all-cause mortality rate in the group of oncological patients in 2020 is the result of a more precise selection of patients with pancreatic cancer before the admission, the observance of the newly developed procedures and the organization of the operating room during the COVID-19 pandemic. What's more, a decreased 30-day all-cause mortality in 2020 in our Center may be the result of a number of palliative surgeries (e.g., triple bypass anastomosis of intestines) in patients with advanced pancreatic cancer. In 2019, we performed much more extensive surgery procedures, e.g., Whipple pancreatectomy (125 (47.5%) in 2019 compared to 53 (36.3%) in 2020 ($p = 0.037$)). We have also noticed a much more frequent diagnosis of low-differentiated G3 and G4 anaplastic tumors in 2020, which tend to reach a larger size in a shorter time ($p = 0.037$). In 2020, our patients had much greater advancement of the disease, illustrated by the increased tumor size (median 3.0 cm in 2019 and 3.5 cm in 2020), although it did not reach statistical significance ($p = 0.073$). The diagnosis of a more advanced tumor influenced the decision of adjuvant chemotherapy administration. In 2020, the qualification rate for adjuvant treatment significantly decreased – 51% of patients in 2020 received such treatment compared to 2019, when as many as 68% of patients underwent adjuvant treatment ($p < 0.001$). It should be emphasized that in our center, there was not a single case of an oncological patient infected with the SARS-CoV-2 virus during the stay at the clinic.

Authors from Italy showed that the prolonged waiting time for surgery significantly increased mortality in cancer patients.[18] They emphasized that special attention should be paid to patients who have completed neoadjuvant therapy, patients with an aggressive type of cancer and those without any other therapeutic options. At the same time, the authors stated that COVID-19-positive oncological patients should have their surgery postponed until the recovery.

Solving the problem of a limited access to medical services in times of a pandemic is conditioned by local customs and in each country different solutions are found, e.g., in the abovementioned study by Cavaliere et al.,[18] the eligibility criteria for the surgical procedure are based on COVID-19 incidence in a particular area. If the coronavirus infection and hospitalization rate due to COVID-19 is high – >75% – then the surgeries are performed only due to life-saving, necessary and urgent

indications. If the coronavirus infection and hospitalization rate ranges between 25% and 50%, then surgeries are performed in oncological patients who cannot undergo neoadjuvant therapy and patients whose 3-month survival will be significantly affected by the lack of surgery. If hospitalization of COVID-19-infected patients does not exceed 5%, surgeries can be performed in the standard mode.

Based on the COVID-19 status of the region/hospital and the availability of healthcare resources, the American College of Surgeons (ACS) has proposed 3 different phases that a healthcare setup can encounter: phase 1 – semi-urgent settings (preparation phase) – the disease is not in the rapid escalation phase and institutions have adequate resources such as hospital and ICU beds, ventilators and manpower to provide the services; phase 2 – urgent settings – limited availability of resources due to an increased number of COVID-19 patients; phase 3 – hospitals are overburdened with COVID-19 patients and the nonavailability of healthcare facilities, such as operating rooms, beds, ICUs, and ventilators.[19]

The recommendations of the Society of Surgical Oncology (SSO) concerning hepato-pancreato-biliary (HPB) cancer[20] state that HPB malignancies are typically biologically aggressive and should not be planned as elective operations. The decision on performing an operation during the COVID-19 pandemic needs to be considered in the context of the hospital resources, multidisciplinary providers, presence and severity of symptoms, and the biology of the disease. The following factors should also be weighed in the decision-making process: hospital resources of personal protective equipment (PPE), bed/ICU/ventilator capacity and utilization, number of COVID-19 patients and the projected trajectory of COVID-19 patient influx.

Since the beginning of the pandemic, various protocols on qualifying oncological patients for surgery have been developed. The mortality rate is extremely high in COVID-19 infected patients, reaching up to 75% in patients after recent surgery due to cancer or patients after chemotherapy.[19] For this reason, oncological patients should not undergo scheduled surgery if they have an active infection, and all the procedures should be postponed until recovery.[20]

According to the extensive Chinese guidelines, cancer patients admitted to the hospital should have an antigen and PCR test, as well as computed tomography (CT) of the lungs. After excluding the COVID-19 infection, they should stay in the isolation ward for 3–7 days, and only if they have no suspicious symptoms they can be transferred to the surgical ward and have a surgery.[16]

Limitations

In patients with advanced inoperable tumor who underwent percutaneous biopsies, open biopsies and/or bypass anastomoses, full staging according to TNM was impossible, therefore the data presented in Table 4 concerns only patients who underwent a tumor resection and had a complete histopathological examination of the tumor (TNM).

In our clinic, we follow the actual National Comprehensive Cancer Network® (NCCN®) 2021 guidelines, and we do not assess cTNM.

Conclusions

The coronavirus epidemic in Poland as well as worldwide has made it difficult to access the oncological treatment. For many diseases, delayed treatment does not have a significant impact on the prognosis, but this does not apply to oncological patients, especially patients with pancreatic cancer, who require adjuvant or neoadjuvant chemotherapy. Particular attention should be paid to patients with an aggressive type of cancer who have completed neoadjuvant therapy, as there are no other therapeutic options for them. The treatment of SARS-CoV-2-positive cancer patients should be postponed until their recovery. In the presented material, relatively few postoperative complications and low all-causes mortality are the result of a more careful selection of oncological patients before the admission to the surgical ward, as well as the compliance with the principles of planning the procedure and organization of the operating theater during the COVID-19 pandemic.

The most common location of the pancreatic tumor was in the head of the pancreas. We observed a significant increase of tumors located in the tail of the pancreas in 2020. In the same year, palliative procedures were performed more often, which resulted in a decrease in number of Whipple procedures. The most common histopathological finding was adenocarcinoma of the pancreas, accounting for almost 52% of all tumor types in 2019 and 50% in 2020. In a group of 148 patients operated on for a pancreatic tumor during the COVID-19 pandemic, only 6 patients died, which resulted in an early all-cause mortality rate of 4.1%. None of the patients became infected with SARS-CoV-2 during hospitalization.

ORCID iDs

Karolina Kędzierska-Kapuza https://orcid.org/0000-0001-5853-2147
Grzegorz Witkowski https://orcid.org/0000-0003-3571-8701
Katarzyna Baumgart-Gryn https://orcid.org/0000-0001-8362-3171
Aleksandra Szylińska https://orcid.org/0000-0001-6105-5329
Marek Durlik https://orcid.org/0000-0002-1905-6114

References

1. Statista. Coronavirus (COVID-19) deaths worldwide per one million population as of January 18, 2022, by country. https://www.statista.com/statistics/1104709/coronavirus-deaths-worldwide-per-million-inhabitants/. Accessed November 9, 2021.
2. Haldane V, De Foo C, Abdalla SM, et al. Health systems resilience in managing the COVID-19 pandemic: Lessons from 28 countries. *Nat Med*. 2021;27(6):964–980. doi:10.1038/s41591-021-01381-y
3. Wojciechowska U, Didkowska J. Morbidity and mortality from malignant neoplasms in Poland. Polish National Cancer Registry. Maria Sklodowska-Curie National Research Institute of Oncology. http://onkologia.org.pl/nowotwory-trzustki. Accessed December 27, 2020.

4. Rawla P, Sunkara T, Gaduputi V. Epidemiology of pancreatic cancer: Global trends, etiology and risk factors. *World J Oncol*. 2019;10(1):10–27. doi:10.14740/wjon1166
5. Poruk KE, Firpo MA, Adler DG, Mulvihill SJ. Screening for pancreatic cancer: Why, how, and who? *Ann Surg*. 2013;257(1):17–26. doi:10.1097/SLA.0b013e31825ffbfb
6. Vujasinovic M, Dugic A, Maisonneuve P, et al. Risk of developing pancreatic cancer in patients with chronic pancreatitis. *J Clin Med*. 2020;9(11):3720. doi:10.3390/jcm9113720
7. Niger M, Prisciandaro M, Antista M, et al. One size does not fit all for pancreatic cancers: A review on rare histologies and therapeutic approaches. *World J Gastrointest Oncol*. 2020;12(8):833–849. doi:10.4251/wjgo.v12.i8.833
8. Canto MI, Harinck F, Hruban RH, et al; International Cancer of Pancreas Screening (CAPS) Consortium. International Cancer of the Pancreas Screening (CAPS) Consortium summit on the management of patients with increased risk for familial pancreatic cancer. *Gut*. 2013;62(3):339–347. doi:10.1136/gutjnl-2012-303108
9. Kadaj-Lipka R, Lipiński M, Adrych K, et al. Diagnostic and therapeutic recommendations for chronic pancreatitis: Recommendations of the Working Group of the Polish Society of Gastroenterology and the Polish Pancreas Club. *Prz Gastroenterol.* 2018;13(3):167–181. doi:10.5114/pg.2018.78067
10. https://ezdrowie.gov.pl/portal/home/zdrowe-dane. Accessed January 14, 2022.
11. Medycyna Praktyczna. Prezes PUO: więcej szkody z opóźnionej diagnozy niż z koronawirusa. https://www.mp.pl/pacjent/onkologia/aktualnosci/246414,prezes-puo-wiecej-szkody-z-opoznionej-diagnozy-niz-z-koronawirusa. Accessed May 15, 2021.
12. Hanna TP, King WD, Thibodeau S, et al. Mortality due to cancer treatment delay: Systematic review and meta-analysis. *BMJ*. 2020;371:m4087. doi:10.1136/bmj.m4087
13. Ustawa z dnia 2 marca 2020 r. o szczególnych rozwiązaniach związanych z zapobieganiem, przeciwdziałaniem i zwalczaniem COVID-19, innych chorób zakaźnych oraz wywołanych nimi sytuacji kryzysowych. https://dziennikustaw.gov.pl/D2020000037401.pdf. Accessed May 15, 2021.
14. Zhao H, Yan S, Zhang F, et al. Guidance for safely performing oncologic surgery during the COVID-19 pandemic. *Br J Surg*. 2020;107(10):e401–e402. doi:10.1002/bjs.11845
15. Towarzystwo Chirurgów Polskich. Wytyczne dla chirurgów podczas pandemii COVID-19. https://www.tchp.pl/376-wytyczne-dla-chirurgow-podczas-pandemii-covid-19. Accessed May 20, 2021.
16. Liang W, Guan W, Chen R, et al. Cancer patients in SARS-CoV-2 infection: A nationwide analysis in China. *Lancet Oncol*. 2020;21(3):335–337. doi:10.1016/S1470-2045(20)30096-6
17. National Comprehensive Cancer Network® (NCCN®). NCCN Guidelines. https://www.nccn.org/guidelines/guidelines-detail?category=1&id=1455. Accessed November 7, 2021.
18. Cavaliere D, Parini D, Marano L, et al; SICO (Italian Society of Surgical Oncology). Surgical management of oncologic patient during and after the COVID-19 outbreak: Practical recommendations from the Italian society of Surgical Oncology Updates in Surgery. *Updates Surg*. 2021;73(1):321–329. doi:10.1007/s13304-020-00921-4
19. American College of Surgeons. COVID-19 Guidelines for Triage of Cancer Surgery Patients. https://www.facs.org/covid-19/clinical-guidance/elective-case/cancer-surgery. Accessed May 20, 2021.
20. Society of Surgical Oncology (SSO). Resource for Management Options of GI and HPB Cancers During COVID-19. https://www.surgonc.org/wp-content/uploads/2020/03/GI-and-HPB-Resource-during-COVID-19-3.30.20.pdf. Accessed May 15, 2021.
21. Brücher BLDM, Nigri G, Tinelli A, et al; for the Pandemic Surgery Guidance Consortium (PSGC). COVID-19: Pandemic surgery guidance. *4open*. 2020;3:1. doi:10.1051/fopen/2020002

Rifaximin in gut microbiota modification in acute pancreatitis: 15 years of retrospective clinical study

Jacek Tatur[1,A–F], Michał Lipiński[1,A–F], Marta Sznurkowska[1,2,A–D,F], Ewa Józefik[1,B,D,F], Grażyna Rydzewska[1,2,A,C,E,F]

[1] Department of Gastroenterology, Central Clinical Hospital of The Ministry of Interior and Administration, Warsaw, Poland
[2] Collegium Medicum, Jan Kochanowski University of Kielce, Poland

A – research concept and design; B – collection and/or assembly of data; C – data analysis and interpretation;
D – writing the article; E – critical revision of the article; F – final approval of the article

Advances in Clinical and Experimental Medicine, ISSN 1899–5276 (print), ISSN 2451–2680 (online) *Adv Clin Exp Med*. 2022;31(4):399–405

Address for correspondence
Michał Lipiński
E-mail: michal7lipinski@yahoo.com

Funding sources
None declared

Conflict of interest
None declared

Received on July 8, 2021
Reviewed on November 15, 2021
Accepted on December 16, 2021

Published online on April 25, 2022

Abstract

Background. Gut decontamination could have some benefits in preventing infectious complications in acute pancreatitis (AP).

Objectives. To investigate whether the administration of rifaximin could have an impact on the outcomes of AP.

Materials and methods. We conducted a retrospective study on 373 patients with a median age of 50 years that were admitted to our Department of Gastroenterology in the years 2001–2016 with a diagnosis of AP. Patients were subclassified according to the revised Atlanta criteria: mild acute pancreatitis (MAP), moderately severe acute pancreatitis (MSAP) and severe acute pancreatitis (SAP). Thereafter, all the patients were divided into 2 groups: in the 1st group (R0) with MSAP and SAP, patients did not receive rifaximin, and in the 2nd group (R1), in the cases of MSAP and SAP, rifaximin was administered to patients at a dose of 3×400 mg (for at least 5 days and up to 7 days). There was no other difference in the treatment between the groups. The median duration of hospital stay, the number of infectious complications and the mortality rate were recorded for both groups.

Results. A significant difference was observed between median durations of hospitalization between the groups with (R1) and without (R0) rifaximin treatment (14 days compared to 24 days, $p = 0.001$) and in the number of patients infected with pancreatic necrosis (7 compared to 1, $p = 0.0487$). However, there was no statistically significant difference between the R1 and R0 group in terms of mortality rate.

Conclusions. The results indicate that rifaximin seems to be a promising novel therapeutic option in MSAP and SAP.

Key words: rifaximin treatment, selective digestive decontamination, gut decontamination, acute pancreatitis therapy

Cite as
Tatur J, Lipiński M, Sznurkowska M, Józefik E, Rydzewska G. Rifaximin in gut microbiota modification in acute pancreatitis: 15 years of retrospective clinical study. *Adv Clin Exp Med*. 2022;31(4):399–405. doi:10.17219/acem/144993

DOI
10.17219/acem/144993

Background

The knowledge and understanding of the pathogenesis of acute pancreatitis (AP) has improved in recent years. However, severe types of AP still remain difficult to treat, and, when followed by pancreatic infection, are associated with a high mortality rate, as well as a long duration of hospital stay.[1–3] The clinical course of necrotizing pancreatitis is widely acknowledged to present itself with 2 peaks, which are characterized by the highest risk of death. These originate from the subdivision of AP into 2 phases (early and late). The early phase refers to the first 7 days after the outset of AP, and is associated with systemic inflammatory response syndrome (SIRS) and multiple organ dysfunction syndrome (MODS), due to the release of inflammatory mediators.[4] The late phase occurs after a period of relative stability (usually a few weeks after the onset of AP), and is identified with a significantly higher mortality peak, as a consequence of the addition of septic complications, that being predominantly bacterial infections of pancreatic necrosis.[5,6]

It is reported that the gastrointestinal flora, contributing to the construction of the intestinal barrier, plays an important regulatory role in the progression of AP. The gut barrier and the intestinal flora affect each other in order to engage in the development of the disease.[7] It has been theorized that hypoperfusion of peripheral tissues (including the gut), microcirculatory injury in severe forms of AP and subsequent damage to the enteric mucosa with an increased permeability of the intestinal barrier are the causes of bacterial translocation from the intestine and further contamination of the pancreatic necrosis.[8–11] In consequence, as a response to the potential pathomechanism of infection of the pancreatic necrosis, selective digestive decontamination (SDD) being a method of eradication of enteric pathogens, may be considered an effective prophylaxis of septic complications in AP.[12,13]

In the present study, we attempted to settle whether the use of an oral antibiotic – rifaximin, used in gut microbiota modification treatment, can lead to the reduction of infectious complications, primarily related to the late phase of necrotizing pancreatitis.

Rifaximin is an oral nonabsorbable antibiotic with broad-spectrum antimicrobial activity. It was designed as a synthetic derivative of rifamycin, which irreversibly binds to the β-subunit of DNA-dependent RNA polymerase and consecutively inhibits the synthesis of bacterial RNA and proteins.[14] It is biologically active against a wide range of bacteria, including Gram-positive, Gram-negative, aerobic and anaerobic[15]; nonetheless, it has been shown that rifaximin induces no clinically important bacterial resistance.[16] It has been also demonstrated on animal models that rifaximin modulates the gut microbiota by promoting the growth of symbiotic cultures (*Lactobacillus, Bifidobacterium*), which differs from the mechanism of other antibiotics formerly used in selective digestive decontamination and which is why it can be preferably described as modification of gut microbiota.[15] Rifaximin, as a specific gastrointestinal ligand of the human pregnane X receptor (PXR), has a significant anti-inflammatory effect, reducing intestinal inflammation and restoring epithelial mucosal barrier.[16] Moreover, rifaximin is characterized by low gastrointestinal (GI) absorption (<0.4%),[15] while preserving high antibacterial effect, which attributes to the elimination of the risk of both systemic side effects and interactions with other drugs. All of the aforementioned features prove that rifaximin is a safe and very effective antibiotic in all patients, including the pediatric patients,[17] in the treatment of conditions of the GI tract that include small intestinal bacterial overgrowth (SIBO), irritable bowel syndrome (IBS)[18] and symptomatic uncomplicated diverticular disease (SUDD).[19] The indications for rifaximin treatment registered in Poland are shown in Table 1.

Despite the confirmed efficacy of rifaximin in such conditions, there are no studies assessing its effectiveness through modification of the gut microbiota in patients with AP. Therefore, it is needed to evaluate its use in the aspect of AP treatment.

Table 1. Indications for rifaximin treatment registered in Poland

Indications for rifaximin treatment registered in Poland
Hepatic encephalopathy in advanced liver disease
Traveler's diarrhea
Symptomatic uncomplicated diverticular disease (SUDD)
Diarrhea-predominant irritable bowel syndrome (IBS-D)

Objectives

The purpose of the present study was to analyze whether the modulation of gut microbiota with rifaximin could alter the outcome of patients treated with moderately severe acute pancreatitis (MSAP) and severe acute pancreatitis (SAP). The number of infected pancreatic necroses, mortality rate, as well as the time of patients' hospitalization were set as major endpoints of the research.

Materials and methods

A total of 373 patients with AP (242 men and 131 women, median age 50 years, age range 18–96 years) were included in this study. All patients were admitted to the Department of Gastroenterology in Central Clinical Hospital of The Ministry of Interior and Administration, Warsaw, Poland, between 2001 and 2016. The diagnosis and evaluation of the severity of AP were made according to the Revised Atlanta Classification for Acute Pancreatitis (2012).[20] On the basis of these criteria, patients were retrospectively recognized with mild acute pancreatitis (MAP), MSAP or SAP.

Mild acute pancreatitis was characterized by the absence of failure within the pancreas, with no local and systemic

complications. Moderately severe acute pancreatitis was described as transient organ failure, which resolves within 48 h, with local or systemic complications, while SAP indicates persistent organ failure lasting longer than 48 h, with single or multiple complications.[21] The organ failure was defined in accordance with the Modified Marshall Scoring System.[22]

Starting from the cut-off point of the year 2009, the patients admitted to the Gastroenterology Department who started to manifest features of MSAP or SAP received immediate rifaximin therapy through enteral feeding tube along with enteral nutrition. The treatment protocol of rifaximin therapy was arranged as follows; patients were administered rifaximin 3 times per day at a dose of 400 mg (for at least 5 days and up to 7 days), comparably to the maximal dosage of this drug in other registered indications in Poland.

This clinical intervention had received the approval of the hospital ethics committee (approval No. 14/2009 from August 4, 2009). The study complies with the 1975 Declaration of Helsinki. All patients who were treated for severe forms of AP and received rifaximin treatment had signed an informed consent form before participating in the study.

Subsequently, groups of patients that were admitted in different timeframes (2001–2008 compared to 2009–2016) were compared regarding their age, sex and AP severity (Table 2). It resulted in the fact that in the group of patients treated for AP in years 2009–2016, there was a larger number of cases of MAP, which proved to be statistically significant ($p = 0.0346$). Nonetheless, the 2 groups did not differ in both age ($p = 0.3789$) and sex ($p = 0.6776$) distribution.

Finally, 2 other cohorts were compared: patients diagnosed only with MSAP and SAP, admitted in the years 2001–2008, thus not receiving rifaximin (R0 group), and patients admitted in the years 2009–2016 who presented with MSAP and SAP and who were given rifaximin (R1 group) (Fig. 1). There was no other difference in treatment between those cohorts. Both groups (R0 and R1) were analyzed and characterized by their clinical features, including age, sex and severity of AP. There was no statistically significant difference between these groups in regard to age and sex distribution, as well as etiology and severity of AP. The characteristics for the 2 groups are listed in Table 3.

We determined the level of C-reactive protein (CRP) as a predictor for the disease severity. All individuals with CRP level above 150 mg/L and those with the most severe forms of AP on admission underwent a contrast-enhanced computed tomography (CE-CT) examination to confirm or exclude the presence of pancreatic necrosis. The CE-CT was performed not sooner than 4 days after the admission to the hospital. The necrosis of the pancreas was identified as areas of nonviable pancreatic components, commonly associated with necrosis of the peripancreatic adipose tissue in CE-CT findings.[23]

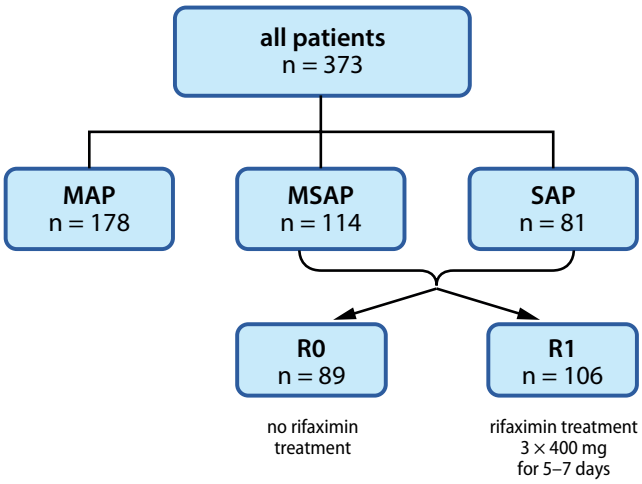

Fig. 1. Distribution of patients with acute pancreatitis (AP) included in the study

MAP – mild acute pancreatitis; MSAP –moderately severe acute pancreatitis; SAP – severe acute pancreatitis; R0 group – group of patients not receiving rifaximin in cases of MSAP or SAP; R1 group – group of patients with MSAP or SAP receiving rifaximin treatment.

Table 2. Profile of patients with AP included in the study

Category	Subgroup	Total	Patients admitted in 2001–2008	Patients admitted in 2009–2016	p-value (statistical method)
All patients, n (%)	–	373 (100.00)	147 (100.00)	226 (100.00)	–
Age [years], median (IQR)	–	50.00 (40.00, 64.00)	51.00 (42.00, 64.50)	50 (38.00, 63.00)	0.3789 (Mann–Whitney U test)
Sex, n (%)	male	242 (64.88)	93 (63.27)	149 (65.93)	0.6776 (χ^2 test with Yates' correction)
	female	131 (35.12)	54 (36.73)	77 (34.07)	
Severity of AP, n (%)	MAP	178 (47.72)	58 (39.46)	120 (53.10)	0.0346 (χ^2 test)
	MSAP	114 (30.56)	53 (36.05)	61 (26.99)	
	SAP	81 (21.72)	36 (24.49)	45 (19.91)	
	MSAP + SAP	195 (52.28)	89 (60.54) (R0 group)	106 (46.90) (R1 group)	–

IQR – interquartile range; AP – acute pancreatitis; MAP – mild acute pancreatitis; MSAP – moderately severe acute pancreatitis; SAP – severe acute pancreatitis; R0 group – group of patients not receiving rifaximin in cases of MSAP or SAP; R1 group – group of patients with MSAP or SAP receiving rifaximin treatment.

We investigated the relationship between administration of rifaximin and duration of hospital stay, as well as the number of infected pancreatic necroses, formerly recognized as pancreatic abscesses. Moreover, the mortality rate was recorded for both groups. The follow-up was continued until death or discharge from the hospital.

Statistical analyses

The Mann–Whitney U test was used in the comparison of the tendencies between groups with regard to continuous variables (age, duration of hospital stay). The χ^2 test with and without Yates' correction was applied when analyzing categorical variables in samples of an average size (sex distribution, age distribution, severity of AP, etiology of AP, number of pancreatic necroses in CE-CT examination), whilst Fisher's exact test was employed in the analysis of small samples (number of infected pancreatic necroses, mortality rate). A value of $p < 0.05$ was considered statistically significant.

Results

Distribution of patients with AP

Mild acute pancreatitis was recognized in 178 (47.7%) patients, MSAP in 114 (30.6%) patients and SAP in 81 (21.7%) patients, in accordance with the Revised Atlanta Classification (2012) described in methodology. From a total number of 195 cases of either MSAP or SAP, 89 patients (45.6%) did not receive rifaximin treatment, thus were further analyzed as R0 group, while 106 (54.4%) patients were given rifaximin and were assigned to the R1 group.

Hospital stay

A statistically significant difference was observed between the R0 and R1 groups in terms of the duration of hospital stay (Table 3). A median hospital stay for patients who did not receive rifaximin (R0) was 24 days, in comparison to the group treated with rifaximin (R1), in which median hospitalization time was 14 days ($p < 0.0001$).

Pancreatic necrosis and infected pancreatic necrosis

Necrosis of the pancreatic tissue was detected by means of computed tomography (CT) in a total number of 87 cases (23.3%), out of which it was present in 42 patients in R0 group (47.2%) and in 45 patients in R1 group (42.5%). No statistically significant difference was observed ($p = 0.5073$).

The overall incidence of infected pancreatic necroses during hospitalization in patients with AP was 7 out of 373 (1.9%). In the R0 group, 6 patients (6.7%) developed abscesses in pancreas, in contrast to only 1 patient (0.9%) in the R1 group. This difference was statistically significant ($p = 0.0487$) (Table 3).

Mortality

The overall mortality rate in patients with AP included in this study was 5.4% (20 out of 373). Seven patients (7.9%)

Table 3. The distribution of age, gender, etiology and severity of AP, duration of hospital stay, number of infected pancreatic necroses, and mortality rate, between R0 and R1 groups

Category	Subgroup	Total	R0 group	R1 group	p-value (statistical method)
All patients, n (%)	–	195 (100.00)	89 (100.00)	106 (100.00)	–
Age [years], median (IQR)	–	54.00 (40.00, 68.00)	52.00 (42.00, 65.00)	57.00 (39.25, 69.00)	0.2585 (Mann–Whitney U test)
Sex, n (%)	male female	135 (69.23) 60 (30.77)	60 (67.42) 29 (32.58)	74 (69.81) 32 (30.19)	0.8381 (χ^2 test with Yates' correction)
Etiology of AP, n (%)	biliary alcoholic	114 (58.46) 81 (41.54)	58 (65.17) 31 (34.83)	56 (52.83) 50 (47.17)	0.0816 (χ^2 test)
Severity of AP, n (%)	MSAP SAP	114 (58.46) 81 (41.54)	53 (59.55) 36 (40.45)	61 (57.55) 45 (42.45)	0.8911 (χ^2 test with Yates' correction)
Hospital stay [days], median (IQR)	–	18.00 (11.00, 27.00)	24.00 (17.00, 31.00)	14.00 (9.25, 22.50)	<0.0001 (Mann–Whitney U test)
Pancreatic necrosis, n (%)	–	87 (44.61)	42 (47.19)	45 (42.45)	0.5073 (χ^2 test)
Infected pancreatic necrosis, n (%)	–	7 (3.59)	6 (6.74)	1 (0.94)	0.0487 (Fisher's exact test)
Mortality, n (%)	–	20 (10.26)	7 (7.86)	13 (12.26)	0.3519 (Fisher's exact test)

IQR – interquartile range; AP – acute pancreatitis; MSAP – moderately severe acute pancreatitis; SAP – severe acute pancreatitis; R0 group – group of patients not receiving rifaximin in cases of MSAP or SAP; R1 group – group of patients with MSAP or SAP receiving rifaximin treatment.

in the R0 group died, in comparison to 13 patients (12.3%) in the R1 group. This difference was not statistically significant (p = 0.3519) (Table 3).

Discussion

Acute pancreatitis is one of the major gastroenterological causes of hospital admission. Seeing that the global incidence of AP varies between 5 and 80 persons per 100,000, the analysis of epidemiological studies puts Poland in the group characterized by the highest incidence rate of 72.1 persons per 100,000.[24] It is reported in literature that men have a higher risk of death in the course of AP than women.[25] However, our study compared 2 final groups of patients (R0 and R1) that did not differ statistically in sex, age, etiology of AP or disease severity distribution, which is why our research supports the hypothesis that it was rifaximin, not any other epidemiological factor, that could have altered the outcome of the disease in the group that underwent rifaximin treatment.

Acute pancreatitis is a condition characterized by an unpredictable clinical course, with a high mortality rate reaching 20% with an infection of pancreatic necrosis[26] and 60% with concomitant multiorgan dysfunction,[27,28] with the majority of deaths being a result of infection of the necrotic tissue, the most severe local complication of the disease.[29] In addition, the mortality level in patients with sterile pancreatic necrosis and organ failure is doubled in patients who develop additional infected pancreatic necrosis.[29] These infecting bacteria are most likely to be relocated from the digestive tract as an integrated effect of several possible pathomechanisms in necrotizing pancreatitis.

It has been illustrated in various reviews that patients with severe forms of AP develop splanchnic hypoperfusion, which is an outcome of fluid depletion in this disease.[30,31] As a result, microinjuries to the intestinal mucosa with subsequent reperfusion injuries induce a dysfunction of the enteric barrier. In a systematic review by Wu et al., 59% of patients with AP were found to have developed a gut barrier dysfunction.[32] This disruption can lead to the translocation of bacteria, mostly from the small bowel[33] to the peritoneal cavity, which may thereon be involved in the pathogenesis of local and systemic infectious complications in AP.[9] Furthermore, the dysmotility of the gut being another result of a decreased blood flow in the digestive tract in AP, as well as the consecutive bacterial overgrowth in the bowels could attribute to a facilitated process of translocation of visceral bacteria to the necrotic tissue in the pancreas. Yet, their role has been described mostly on murine models.[34] This theory of bacterial translocation is endorsed by the fact that the microorganisms isolated from infected pancreatic necroses are mainly Gram-negative aerobic bacteria consistent with the species found in the digestive tract (*Proteus, Escherichia coli, Pseudomonas*)[35]. As such, these bacteria become a subject of interest in studies investigating the possibility of reducing the number of infected pancreatic necroses and mortality rates in AP.

Routine systemic antimicrobial prophylaxis has been established in recent meta-analyses not to bring any benefit in the prevention of infection of pancreatic necrosis, thus it should not be considered as a method of treatment in necrotizing pancreatitis.[36] Guidelines advise against the antibiotic use due to their ineffectiveness, as well asthe higher risk of developing *Clostridium difficile* infection.[27,37–40] Nevertheless, a new effective method of treatment of panecreatic necrosis, with an impact restricted solely to the digestive tract with limited systemic side effects, could be of use and interest in the clinical surrounding.

Studies on animal models reveal that selective digestive decontamination (SDD) decreases the overall mortality rate and the number of infections of pancreatic necrosis in AP, albeit a handful of human studies have explored the effect of antimicrobial prophylaxis through the means of SDD in patients with AP. Luiten et al. reported that the treatment with colistin (200 mg/day), norfloxacin (50 mg/day) and amphotericin (500 mg/day) significantly reduced not only the incidence of infected necrosis and the risk of Gram-negative pancreatic sepsis, but also late mortality rate in patients with SAP, when compared with placebo.[35] Sawa et al. inspected the outcome of patients with SAP, which had been administered polymyxin B (1,500,000 units/day), L-glutamine (3 g/day) and lactulose (90 mL/day) through an enteral feeding tube. This study revealed that SDD reduced the incidence of organ dysfunction and the mortality rate, but the differences were not statistically significant.[12] The results from these major studies have not been well recognized due to the fact that the SDD regimen was repeatedly combined with parenteral antimicrobial treatment.[41]

To our knowledge, there have been no previous clinical studies assessing the purpose of rifaximin use in acute pancreatitis in humans. Preceding analyses demonstrated a possible effect of SDD in severe forms of AP with other antibiotics; however, our study concentrates on the application of rifaximin, which exhibits a peculiar antimicrobial activity and pharmacodynamics. By the eradication of pathogenic bacteria and concurrent promotion of symbiotic cultures, rifaximin shows its properties that are interpreted in literature as eubiotic and not antibiotic.[15] The addition of low GI absorption and the lack of increase of bacterial resistance, as well as the absence of risk of *Clostridium difficile* infections contribute to the wider clinical potential of this medication.

Limitations

Our study has several limitations. It is a retrospective study and the data came from 1 center with a limited number of patients. The 2 cohorts compared in the study (R0

and R1 groups) consisted of patients from different time frames (2001–2008 and 2009–2016). This limitation could have an impact on the immesurable organizational factors contributing to the decline of median length of hospital stay, that are not necessarily associated to the treatment protocol. Nevertheless, it is worth mentioning that the study took place at a tertiary referral center, to which patients from all over the country with the most severe types of AP are referred, hence the relatively high frequency of MSAP and SAP, which appears to be a strength of this research.

Conclusions

It has been found, for the first time, that rifaximin therapy reduced the incidence of infected pancreatic necroses and decreased the time of hospital stay of patients with severe forms of AP (by 86% and 42%, respectively), although it did not significantly affect the mortality ratio.

Our study indicates a possible correlation of rifaximin use with a decrease in the number of pancreatic necroses in AP patients, which is why this subject is currently being investigated in prospective studies in our clinic. Our results allow for a more reliable review of a complex area of gut microbiota modulation treatment with rifaximin in patients with MSAP and SAP. These outcomes indicate that rifaximin seems to be a promising therapeutic option in MSAP and SAP and should be further evaluated in a multicenter randomized prospective study.

ORCID iDs

Jacek Tatur https://orcid.org/0000-0001-8660-6422
Michał Lipiński https://orcid.org/0000-0002-9499-4178
Marta Sznurkowska https://orcid.org/0000-0001-8209-7827
Ewa Józefik https://orcid.org/0000-0003-2425-4008
Grażyna Rydzewska https://orcid.org/0000-0002-1267-7620

References

1. Isaji S, Mizuno S, Tabata M, Yamagiwa K, Yokoi H, Uemoto S. Bacterial analysis of infected pancreatic necrosis and its prevention (Symposium 8: Pancreatobiliary infection (IHPBA)). *J Hepatobiliary Pancreat Surg*. 2003;10(6):419–424. doi:10.1007/s00534-002-0811-x
2. Castineira J, Orpiano C, Hardigan P, Halleman C. Peripheral venous bicarbonate levels as a marker of predicting severity in acute pancreatitis: A retrospective study. *Prz Gastroenterol*. 2019;14(2):148–151. doi:10.5114/pg.2019.85899
3. Lipinski M, Rydzewska G. Immature granulocytes predict severe acute pancreatitis independently of systemic inflammatory response syndrome. *Prz Gastroenterol*. 2017;12(2):140–144. doi:10.5114/pg.2017.68116
4. Thoeni RF. Imaging of acute pancreatitis. *Radiol Clin North Am*. 2015; 53(6):1189–1208. doi:10.1016/j.rcl.2015.06.006
5. Sekimoto M, Takada T, Kawarada Y, et al. JPN Guidelines for the management of acute pancreatitis: Epidemiology, etiology, natural history, and outcome predictors in acute pancreatitis. *J Hepatobiliary Pancreat Surg*. 2006;13(1):10–24. doi:10.1007/s00534-005-1047-3
6. Beger HG, Rau B, Mayer J, Pralle U. Natural course of acute pancreatitis. *World J Surg*. 1997;21(2):130–135. doi:10.1007/s002689900204
7. Lu WW, Chen X, Ni JL, Zhu SL, Fei AH, Wang XS. The role of gut microbiota in the pathogenesis and treatment of acute pancreatitis: A narrative review. *Ann Palliat Med*. 2021;10(3):3445–3451. doi:10.21037/apm-21-429
8. Foitzik T, Hotz HG, Kinzig M, Sorgel F, Buhr HJ. Influence of changes in pancreatic tissue morphology and capillary blood flow on antibiotic tissue concentrations in the pancreas during progression of acute pancreatitis. *Gut*. 1997;40(4):526–530. doi:10.1136/gut.40.4.526
9. Schmid S, Uhl W, Friess H, Malfertheiner P, Buchler M. The role of infection in acute pancreatitis. *Gut*. 1999;45(2):311–316. doi:10.1136/gut.45.2.311
10. Akshintala VS, Talukdar R, Singh VK, Goggins M. The gut microbiome in pancreatic disease. *Clin Gastroenterol Hepatol*. 2019;17(2):290–295. doi:10.1016/j.cgh.2018.08.045
11. Fukui H. Endotoxin and other microbial translocation markers in the blood: A clue to understand leaky gut syndrome. *Cell Mol Med*. 2016;2:3. doi:10.21767/2573-5365.100023
12. Sawa H, Ueda T, Takeyama Y, et al. Treatment outcome of selective digestive decontamination and enteral nutrition in patients with severe acute pancreatitis. *J Hepatobiliary Pancreat Surg*. 2007;14(5): 503–508. doi:10.1007/s00534-007-1216-7
13. Marotta F, Geng TC, Wu CC, Barbi G. Bacterial translocation in the course of acute pancreatitis: Beneficial role of nonabsorbable antibiotics and lactitol enemas. *Digestion*. 1996;57(6):446–452. doi:10.1159/000201373
14. Tursi A, Scarpignato C, Brandimarte G, Di Mario F, Lanas A. Rifaximin for the management of colonic diverticular disease: Far beyond a simple antibiotic. *J Gastrointestin Liver Dis*. 2018;27(4):351–355. doi:10.15403/jgld.2014.1121.274.rif
15. Ponziani FR, Zocco MA, D'Aversa F, Pompil M, Gasbarrini A. Eubiotic properties of rifaximin: Disruption of the traditional concepts in gut microbiota modulation. *World J Gastroenterol*. 2017;23(25):4491–4499. doi:10.3748/wjg.v23.i25.4491
16. Cheng J, Shah YM, Ma X, et al. Therapeutic role of rifaximin in inflammatory bowel disease: Clinical implication of human pregnane X receptor activation. *J Pharmacol Exp Ther*. 2010;335(1):32–41. doi:10.1124/jpet.110.170225
17. Scarpignato C, Pelosini I. Rifaximin, a poorly absorbed antibiotic: Pharmacology and clinical potential. *Chemotherapy*. 2005;51(Suppl 1): 36–66. doi:10.1159/000081990
18. Li J, Zhu W, Liu W, Wu Y, Wu B. Rifaximin for irritable bowel syndrome: A meta-analysis of randomized placebo-controlled trials. *Medicine (Baltimore)*. 2016;95(4):e2534. doi:10.1097/MD.0000000000002534
19. Pietrzak AM, Dziki A, Banasiewicz T, Reguła J. Cyclic rifaximin therapy effectively prevents the recurrence of symptoms after exacerbation of symptomatic uncomplicated diverticular disease: A retrospective study. *Prz Gastroenterol*. 2019;14(1):69–78. doi:10.5114/pg.2019.83428
20. Foster BR, Jensen KK, Bakis G, Shaaban AM, Coakley FV. Revised Atlanta classification for acute pancreatitis: A pictorial essay. *Radiographics*. 2016;36(3):675–687. doi:10.1148/rg.2016150097
21. Dupuis CS, Baptista V, Whalen G, et al. Diagnosis and management of acute pancreatitis and its complications. *Gastrointest Interv*. 2013; 2(1):36–46. doi:10.1016/j.gii.2013.03.001
22. Banks PA, Bollen TL, Dervenis C, et al. Classification of acute pancreatitis – 2012: Revision of the Atlanta classification and definitions by international consensus. *Gut*. 2013;62(1):102–111. doi:10.1136/gutjnl-2012-302779
23. Bollen TL, van Santvoort HC, Besselink MG, et al. The Atlanta Classification of acute pancreatitis revisited. *Br J Surg*. 2008;95(1):6–21. doi:10.1002/bjs.6010
24. Koziel D, Gluszek S. Epidemiology of acute pancreatitis in Poland: Selected problems [in Polish]. *Stud Med*. 2016;32(1):1–3. doi:10.5114/ms.2016.58798
25. Drake M, Dodwad SJ, Davis J, Kao LS, Cao Y, Ko TC. Sex-related differences of acute and chronic pancreatitis in adults. *J Clin Med*. 2021; 10(2):300. doi:10.3390/jcm10020300
26. Banks PA. Epidemiology, natural history, and predictors of disease outcome in acute and chronic pancreatitis. *Gastrointest Endosc*. 2002;56(6 Suppl):S226–S230. doi:10.1067/mge.2002.129022
27. Rasslan R, Novo FDCF, Bitran A, Utiyama EM, Rasslan S. Management of infected pancreatic necrosis: State of the art. *Rev Col Bras Cir*. 2017;44(5):521–529. doi:10.1590/0100-69912017005015
28. Guo Q, Li A, Xia Q, et al. The role of organ failure and infection in necrotizing pancreatitis: A prospective study. *Ann Surg*. 2014;259(6): 1201–1207. doi:10.1097/SLA.0000000000000264
29. Werge M, Novovic S, Schmidt PN, Gluud LL. Infection increases mortality in necrotizing pancreatitis: A systematic review and meta-analysis. *Pancreatology*. 2016;16(5):698–707. doi:10.1016/j.pan.2016.07.004

30. Rahman SH, Ammori BJ, Holmfield J, Larvin M, McMahon MJ. Intestinal hypoperfusion contributes to gut barrier failure in severe acute pancreatitis. *J Gastrointest Surg*. 2003;7(1):26–36. doi:10.1016/S1091-255X(02)00090-2
31. Lipiński M, Rydzewski A, Rydzewska G. Early changes in serum creatinine level and estimated glomerular filtration rate predict pancreatic necrosis and mortality in acute pancreatitis: Creatinine and eGFR in acute pancreatitis. *Pancreatology*. 2013;13(3):207–211. doi:10.1016/j.pan.2013.02.002
32. Wu LM, Sankaran SJ, Plank LD, Windsor JA, Petrov MS. Meta-analysis of gut barrier dysfunction in patients with acute pancreatitis. *Br J Surg*. 2014;101(13):1644–1656. doi:10.1002/bjs.9665
33. Fritz S, Hackert T, Hartwig W, et al. Bacterial translocation and infected pancreatic necrosis in acute necrotizing pancreatitis derives from small bowel rather than from colon. *Am J Surg*. 2010;200(1):111–117. doi:10.1016/j.amjsurg.2009.08.019
34. Seerden TC, De Winter BY, Van Den Bossche RM, Herman AG, Pelckmans PA, De Man JG. Regional differences in gastrointestinal motility disturbances during acute necrotizing pancreatitis. *Neurogastroenterol Motil*. 2005;17(5):671–679. doi:10.1111/j.1365-2982.2005.00689.x
35. Luiten EJ, Hop WC, Lange JF, Bruining HA. Controlled clinical trial of selective decontamination for the treatment of severe acute pancreatitis. *Ann Surg*. 1995;222(1):57–65. doi:10.1097/00000658-199507000-00010
36. Working Group IAP/APA Acute Pancreatitis Guidelines. IAP/APA evidence-based guidelines for the management of acute pancreatitis. *Pancreatology*. 2013;13(4 Suppl 2):e1–e15. doi:10.1016/j.pan.2013.07.063
37. Cagle SD, Chopra A. Antibiotic prophylaxis for severe acute pancreatitis. *Am Fam Physician*. 2019;99(1):49. PMID:30600982.
38. Rosołowski M, Lipiński M, Dobosz M, et al. Management of acute pancreatitis (AP): Polish Pancreatic Club recommendations. *Prz Gastroenterol*. 2016;11(2):65–72. doi:10.5114/pg.2016.60251
39. Greenberg JA, Hsu J, Bawazeer M, et al. Clinical practice guideline: Management of acute pancreatitis. *Can J Surg*. 2016;59(2):128–140. doi:10.1503/cjs.015015
40. Trikudanathan G, Munigala S. Impact of *Clostridium difficile* infection in patients hospitalized with acute pancreatitis: A population based cohort study. *Pancreatology*. 2017;17(2):201–202. doi:10.1016/j.pan.2017.02.012
41. Tiong L, Jalleh R, Barreto SG. Selective digestive decontamination in severe acute pancreatitis. *Astrocyte*. 2014;1:93–94. doi:10.4103/2349-0977.137852

The involvement of ACO3 protein in diabetic retinopathy through the PI3k/Akt signaling pathway

*Yi Zhang[A,B,D,F], *Wenjun Wang[B,C,F], Anhuai Yang[A,E,F]

Eye Center, RenMin Hospital of Wuhan University, China

A – research concept and design; B – collection and/or assembly of data; C – data analysis and interpretation;
D – writing the article; E – critical revision of the article; F – final approval of the article

Advances in Clinical and Experimental Medicine, ISSN 1899–5276 (print), ISSN 2451–2680 (online) *Adv Clin Exp Med*. 2022;31(4):407–416

Address for correspondence
Anhuai Yang
E-mail: yah0525@126.com

Funding sources
None declared

Conflict of interest
None declared

* These two authors contributed equally to this work.

Received on February 19, 2020
Reviewed on March 4, 2020
Accepted on May 1, 2020

Published online on March 11, 2022

Abstract

Background. Diabetic retinopathy (DR) is one of the most common complications of diabetic microvascular disease and its pathogenesis is complicated. The PI3k/Akt signaling pathway plays an important role in the angiogenesis of DR.

Objectives. To explore the molecular mechanisms of the ACO3 protein and related proteins in DR, in order to provide a scientific theoretical basis for the clinical treatment of this disease.

Materials and methods. A DR rat model was used in this study. One group (anti-ACO3 group, n = 10) was injected with protein ACO3 antagonist; the 2nd study group (the DR group, n = 10) was injected with the same amount of normal saline; the control group (n = 10) did not undergo any procedures. We used hematoxylin and eosin (H&E) staining to observe the pathological features of the eye tissues. Immunohistochemistry was used to analyze the expression of ACO3 and AKT. Western blot was used to analyze the expression of ANGPT1, ANGPT4 and KDR; reverse transcription polymerase chain reaction (RT-PCR) was used to assess the mRNA expression of AKT, ACO3 and SMOX in the eye tissues of the rats.

Results. In the anti-ACO3 group, the results of H&E staining showed that there was a decrease in retinal edema and no obvious abnormality in the blood vessels. The immunohistochemistry analysis of proteins proved that ACO3 and AKT were strongly expressed in the DR group. The western blot analysis of ANGPT1, ANGPT4 and KDR expression showed that in the DR group, the expression of all 3 proteins was higher than in the anti-ACO3 group, and much higher than in the control group.

Conclusions. The mRNA expression of *AKT*, *ACO3* and *SMOX* was strong in the DR group, but decreased in the anti-ACO3 group.

Key words: diabetic retinopathy, mechanism, ACO3, PI3k/Akt signaling pathway

Cite as
Zhang Y, Wang W, Yang A. The involvement of ACO3 protein in diabetic retinopathy through the PI3k/Akt signaling pathway. *Adv Clin Exp Med*. 2022;31(4):407–416. doi:10.17219/acem/121930

DOI
10.17219/acem/121930

Background

Along with social and economic development, improved living standards and changes in eating habits, diabetes has become a common disease affecting people's health and life. Diabetic retinopathy (DR) is one of the most universal complications of diabetic microvascular disease, often causing serious visual impairment.[1] According to the research conducted by the World Health Organization (WHO), the number of diabetic patients in the world reached 366 million cases in 2011, and by 2025 this number will exceed 500 million.[2] It was recently reported that the global morbidity of DR was 34.6%, while in developed countries it was nearly 40.3%.[3] The number of patients with DR in China has been reported to be as high as 13.16 million.[4] The most common features of DR patients include decreased vision, microhemangioma, bleeding spots, hard exudate, retinal neovascularization, venous beading, and macular edema.[5,6] In some severe cases, vitreous hemorrhage, fibrogenesis and retinal angiogenesis have been noted, which might cause neovascular glaucoma or retinal detachment.[7] If effective treatment measures are not taken in time, retinal cell death and fibrosis are likely to occur, resulting in a permanent loss of vision. Therefore, an early and accurate diagnosis and treatment of DR is particularly important.[8]

The pathogenesis of DR is complicated. It is related to glucose metabolism, growth hormone and angiogenic growth factors. In terms of glucose metabolism, when blood glucose level is elevated, the osmotic pressure inside cells is higher than that of the outside cells due to the failure of glycolysis, leading to an imbalance of water electrolytes in eye cells.[9,10] Retinal microvascularization would interfere with the metabolism of inositol and accumulate advanced glycation end products (AGEs) under the stimulus of long-term high-sugar environment. At the same time, this process affects the activity of Na^+/K^+-ATPase in cells; increases the permeability of capillaries; thickens the basement membrane; narrows capillary lumens; increases retinal ischemia, hypoxia and the release of vascular proliferation factors; and promotes the formation of new blood vessels.[11]

As one of the important pathways involved in endothelial cell migration, proliferation and vascular dysfunction, the PI3k/Akt signaling pathway also plays an important role in the process of DR neovascularization.[12] Among proteins related to PI3k/Akt signaling pathway, the ACO3 protein is involved in regulating cell proliferation and inducing neovascularization.

Objectives

The aim of the study was to explore the molecular mechanisms of the ACO3 protein and related proteins in DR, in order to provide a scientific theoretical basis for the clinical treatment of this disease.

Materials and methods

The study used 30 Wistar rats (purchased from Harbin Medical University, China); streptozotocin (STZ; Sigma-Aldrich, St. Louis, USA); ACO3 antagonist (Thermo Fisher Scientific, Waltham, USA); hematoxylin (Invitrogen, Carlsbad, USA); phosphate-buffered saline (PBS) (0.1 m, pH 7.0); TRIzol RNA agent; 6-, 12- and 48-plate cell culture dishes (Thermo Fisher Scientific); 5 mL and 10 mL sterile pipettes (Corning, New York, USA); 10 µL, 20 µL, 200 µL, and 1000 µL transfer pipettes (Eppendorf, Enfield, USA); 10 mL and 50 mL centrifuge tubes (Thermo Fisher Scientific); a conventional polymerase chain reaction (PCR) instrument (Agilent Technologies Inc., Santa Clara, USA); western blotting instruments (Eppendorf AG, Hamburg, Germany); a confocal microscope (Olympus Corp., Tokyo, Japan); a LKB-V ultra-thin slicer (JEOL Ltd., Tokyo, Japan); and a Jem-2000EX fundus fluorescein angiograph (JEOL Ltd.).

Rat model of diabetic retinopathy

We divided 30 Wistar rats (8–9-week old) into 3 groups of 10 rats each. One was the control group, while the other 2 were used to establish the DR model. Twenty rats were randomly assigned to the 2 model diabetic groups. These rats were administered STZ (60 mg/kg) by intraperitoneal injection to induce diabetes. Their fasting glucose was monitored and glucose level ≥16.65 mmol/L was considered the standard model. After 1 month, the diabetic rats were injected with 0.05 µg of vascular endothelial growth factor (VEGF), 2 mm behind the temporal limbic cornea using a microinjector. It passed through the ciliary body and entered the vitreous cavity. The injection was done slowly to keep the needles in for 10 s, in order to create a model of ophthalmic lesions in proliferative diabetes mellitus. The fundus changes in the rats were examined to judge whether the DR model had been successfully constructed. One DR group (called anti-ACO3 group) was injected with 5 µL of ACO3 antagonist (10 µg/mL); the other DR group (called DR group) was injected with the same amount of saline in vitreous body.

Fundus fluorescein angiography

Fundus fluorescein angiography (FFA)[13] was carried out as follows: before the examination, 1 mL of 1% fluorescein sodium was injected intravenously for an allergy test, and was observed for 15 min to ensure that there was no abnormal reaction. Then, 5 mL of 10% fluorescein sodium was immediately injected into each rat and 1 eye was selected as the main eye. After 10–15 s of injection, the early image was shot continuously. After 1–10 min of injection, the middle image was shot. After 10 min, the late image was shot and stored for analysis.

H&E staining to examine the pathological features of the eye tissues

Eye tissues were taken from the 2 DR groups and the control group, and hematoxylin and eosin (H&E) staining was used to examine the pathological features of the tissues.[14] Four weeks after the administration of the ACO3 antagonist or saline to the diabetic rats, pentobarbital sodium was injected intraperitoneally for anesthesia and the retinal tissues of the rats were taken. The tissues were fixed with 4% paraformaldehyde and decalcified with 15% ethylenediamine tetraacetic acid (EDTA) at room temperature. After dehydration, the retinal tissues were embedded in paraffin and 4-μm tissue sections were prepared for pathological observation. The section samples of the 3 groups of rats were stained and dewaxed with xylene twice. Then, the samples were hydrated with gradient ethanol for 3 min and stained with hematoxylin for 5 min. The tissues were then rinsed with 1% hydrochloric acid-ethanol for 30 s, followed by reflux treatment in 0.2% ammonia for 2 min, stained with 0.5% eosin for 10 min, and washed with water once. Gradient ethanol was used for dehydration treatment, and finally, neutral gum was used for sealing. The image was analyzed using an optical microscope.

Immunohistochemistry analysis of ACO3 and AKT expression

Immunohistochemistry staining was used to detect the expression of ACO3 and AKT in the eye tissues.[15] The paraffin-embedded islet tissue of the rats was sectioned at a thickness of 4 μm. The two-step immunohistochemistry method was used for staining. The tissue sections were roasted at 65°C for 12 h, dewaxed and hydrated. Endogenous peroxidase was inactivated by 3% hydrogen peroxide, and the specimens were washed twice with PBS. Mouse anti-human primary antibody ACO3 and AKT were added and washed twice with PBS. Next, the streptomycin working solution (labeled with horseradish peroxidase (HRP)) was added and incubated at 37°C for 25 min. Then, it was washed with PBS, stained with hematoxylin and sealed with neutral chicle.

Western blot analysis of ANGPT1, ANGPT4 and KDR expression

Total proteins were extracted from the eye tissue and blood vessels of each group of rats, and 20-μg protein samples were prepared. We used 5% concentrated gel and 12% isolated gel to isolate proteins using sodium dodecyl sulphate–polyacrylamide gel electrophoresis (SDS-PAGE). Objective and internal proteins were transferred to nitrocellulose (NC) membranes, then sealed with 5% skimmed milk powder sealing fluid for 2 h at room temperature. Rat anti-human primary antibody ANGPT1 (1:500), rat anti-human primary antibody ANGPT4 (1:500), rat anti-human primary antibody KDR (1:500), and rat anti-human primary antibody β-actin (1:1000) were added and incubated overnight at 4°C. The specimens were washed 4 times in Tris-buffered saline with Tween (TBST), and HRP-labeled sheep anti-rat secondary antibody (1:5000) was added and incubated at 37°C for 1 h. The specimens were again washed 4 times in TBST. Color was developed with enhanced chemiluminescence (ECL) solution; protein bands were exposed using ECL blotting detection reagent (Beyotime, Shanghai, China); and the images were photographed and analyzed quantitatively. The experiment was repeated 3 times.

RT-PCR analysis of *AKT*, *ACO3* and *SMOX* mRNA expression

The analysis of *AKT*, *ACO3* and *SMOX* mRNA expression was conducted as described by Rouhani et al.[16]: total RNA was extracted with TRIzol reagent (Shanghai Pufei Biotech, Shanghai, China), according to the manufacturer's instructions. Nucleic acid-protein complexes were extracted with chloroform and precipitated in isopropanol. The complexes were cleaned using 75% ethanol and purified with RNase-free water. The expression level of *GAPDH* was selected as the internal reference. Primers for PCR detection were designed and synthesized according to the information of the target gene sequences, as shown in Table 1. The amplifications were performed in a 96-well plate at 95°C for 10 min, followed by 40 cycles of 95°C for 15 s and 60°C for 1 min. Each sample was run in triplicate. The relative miRNA-126 and mRNA expression was expressed using the $2^{-\Delta\Delta Ct}$ method.

Statistical analyses

One-way analysis of variance (ANOVA) followed by Tukey's post hoc test were used to analyze the data for comparison among 3 groups. The variance homogeneity was tested using Levene's variance homogeneity test. The distribution of the data was analyzed with Kolmogorov–Smirnov and Shapiro–Wilk method, and normally distributed data were expressed as mean ± standard deviation (SD). Statistical significance was defined

Table 1. Nucleic acid sequences of polymerase chain reaction (PCR) primers

Genes	Upstream primer 5′-3′	Downstream primers 5′-3′
AKT	GAGATCACAACAGTCCACAC	AAGGTGTCCTGCAAGCTGTC
ACO3	ACTTTGAGAATGTGGCACGG	TAACATGGCCAAAGTAGGCG
SMOX	TGAGGAGCCCGATCTAGAC	AAGGTCCCAGTACCCCCTC

as $p < 0.05$. All calculation was conducted using SPSS v. 18.0 software (SPSS Inc., Chicago, USA).

Results

Rat model of diabetic retinopathy

Rats with the blood glucose value ≥16.7 mmol/L were defined as diabetic rats. Then, the diabetic rats injected with vitreous cavity were subjected to fundus fluorescein examination to observe the obvious retinal hemorrhage or exudation, telangiectasia, arteriovenous abnormalities, and other conditions in the fundus of rats, indicating that the DR model of the rats was successfully established.

Fundus fluorescein angiography

The FFA results showed that there was no significant DR and no abnormal phenomena in the control group (Fig. 1A). However, background fluorescence enhancement, vascular tortuosity and dilatation, and fluorescence leakage from neovascularization, intraretinal hemorrhage and microhemangioma were observed in the DR group (Fig. 1B). The characteristics of the eye tissue of the DR rats in the anti-ACO3 group were significantly better than in the DR group, and the number of new microvessels was lower in the anti-ACO3 group (Fig. 1C). This indicates that the ACO3 protein is involved in regulating cell proliferation and inducing neovascularization.

H&E staining to examine pathological features of the eye tissues

The pathological histology of the retinas in all 3 groups was examined. It could be seen that the surface of the retina in the control group was smooth, and the cells in the inner and outer nuclear layer were arranged closely and orderly (Fig. 2A). In the DR group, there was obvious edema in the inner retina boundary; the cells in the inner and outer nuclear layers were not arranged neatly, and more synaptic membranes of vascular endothelial cells could be seen (Fig. 2B). However, in the anti-ACO3 group, there was a decrease in retinal edema, and loose arrangements of cells were observed only in the inner core layer (Fig. 2C).

Immunohistochemistry analysis of ACO3 and AKT expression

The expression levels of proteins ACO3 and AKT were the lowest in the control group, and were highly expressed in the DR group, as indicated by the red arrow in Fig. 3.

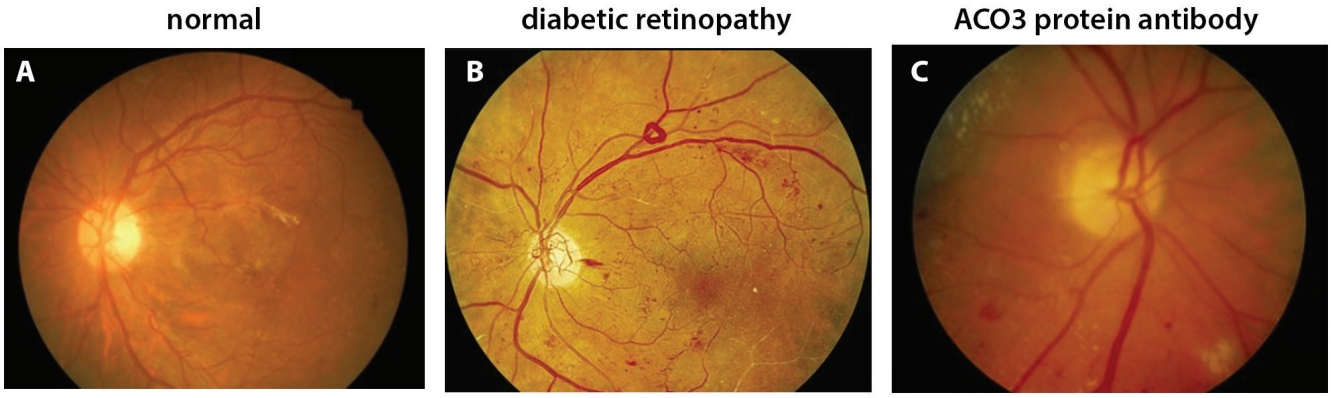

Fig. 1. Morphological characteristics of rat eye tissues observed by fundus fluorescein angiography (FFA) (×400) (n = 10). A. Control group; b. Diabetic retinopathy (DR) group; C. Anti-ACO3 group

Fig. 2. Histopathological examination of rat retinas using hematoxylin and eosin (H&E) staining (×400 magnification) (n = 10). A. Control group; B. Diabetic retinopathy (DR) group; C. Anti-ACO3 group

In the anti-ACO3 group, the expression levels of ACO3 and AKT were decreased.

Western blot analysis of ANGPT1, ANGPT4 and KDR expression

The expression levels of ANGPT1, ANGPT4 and KDR in the rat eye tissues are shown in Fig. 4. The expression of these proteins was higher in DR group than in the anti-ACO3 group (ANGPT1 $p < 0.001$, ANGPT4 $p < 0.001$, KDR $p < 0.001$, ANOVA followed by Tukey's post hoc test), and much higher than in the control group (ANGPT1 $p < 0.001$, ANGPT4 $p < 0.001$, KDR $p < 0.001$, ANOVA followed by Tukey's post hoc test). However, the expression levels of these proteins were high in anti-ACO3 group compared with the control group ($p < 0.05$). The original statistical data of western blot are shown in Table 2–5.

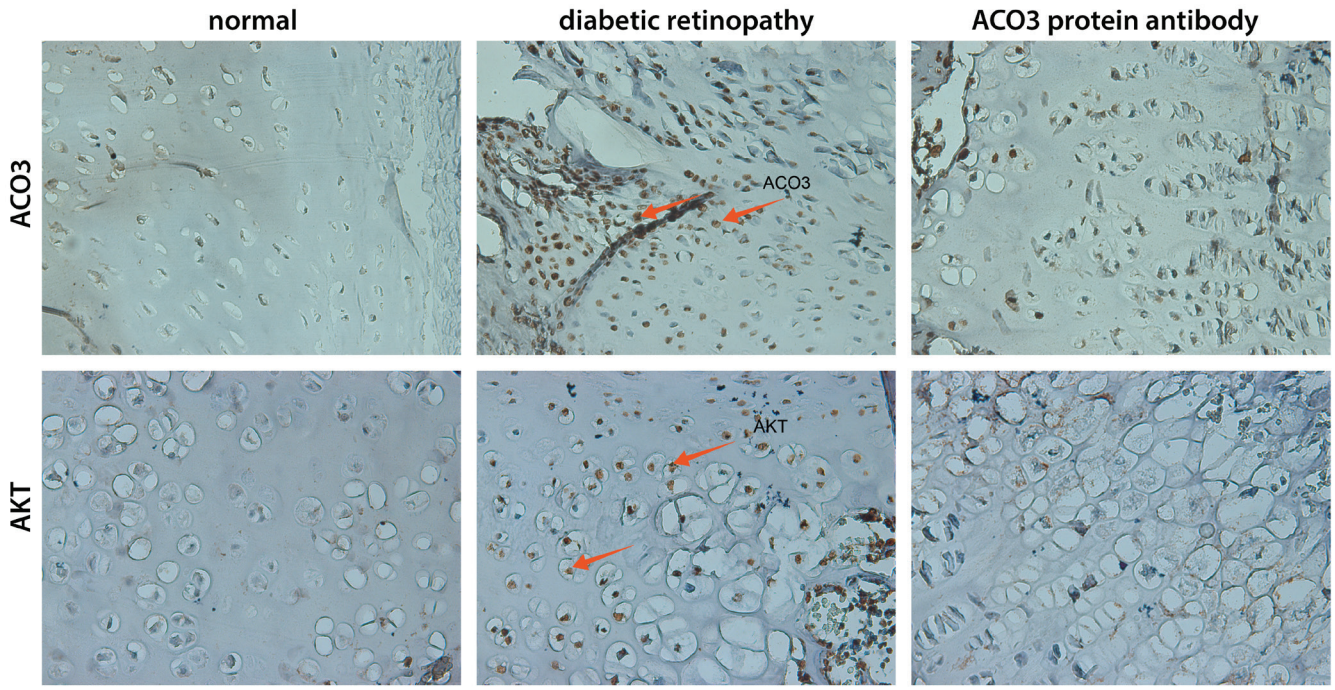

Fig. 3. Immunohistochemical analysis of the expression of proteins ACO3 and AKT in ocular tissues (×400 magnification) (n = 10). The arrows point to the positive cells

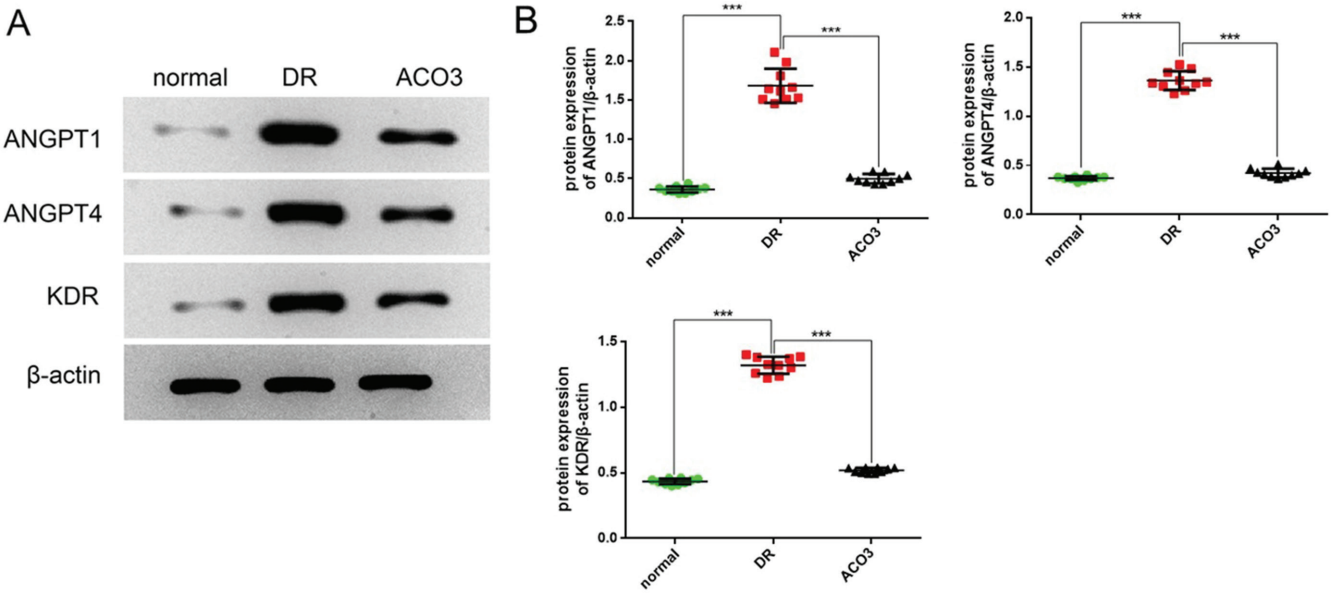

Fig. 4. Expression levels of proteins ANGPT1, ANGPT4 and KDR in different groups determined using western blot (mean ± standard deviation (SD), n = 10). A. Gray value; B. Statistical analysis; *** $p < 0.001$, compared with the diabetic retinopathy (DR) group. The statistical difference was analyzed using one-way analysis of variance (ANOVA) followed by Tukey's post hoc test

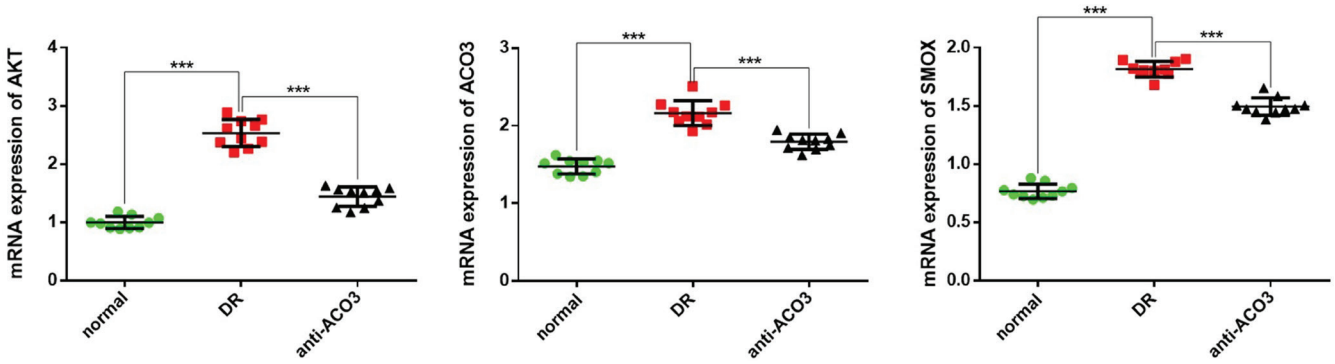

Fig. 5. The mRNA expression of *AKT, ACO3* and *SMOX* mRNA in eye tissues of diabetic rats (mean ± standard deviation (SD), n = 10). *** $p < 0.001$, compared with the diabetic retinopathy (DR) group. The statistical difference was analyzed using one-way analysis of variance (ANOVA) followed by Tukey's post hoc test

RT-PCR analysis of *AKT, ACO3* and *SMOX* mRNA expression

The mRNA expression levels of *AKT, ACO3* and *SMOX* in the DR rats with eye lesions were all increased, but were lower in the anti-ACO3 group compared with the DR group (*AKT* $p < 0.001$, *ACO3* $p < 0.001$, *SMOX* $p < 0.001$, ANOVA followed by Tukey's post hoc test) (Fig. 5). Cell proliferation in the DR group indicates that ACO3 is involved in regulating cell proliferation and inducing neovascularization. The ACO3 and SMOX have characteristics of mutual regulation, and synergistically participate in the regulation of amino acid metabolism and promotion of cell proliferation. The high expression levels of AKT indicate the the activation of the PI3K/Akt signaling pathway, which regulates the increase of NOS3, an enzyme related

Table 2. Description of the genes

Genes		n	Mean	Standard deviation	Standard error	95% CI		Minimum	Maximum
						lower limit	upper limit		
ANGPT1	1.0000	10	0.360867	0.0399287	0.0126266	0.332304	0.389430	0.3124	0.4382
	2.0000	10	1.681553	0.2184303	0.0690737	1.525297	1.837808	1.4524	2.1072
	3.0000	10	0.499627	0.0599933	0.0189716	0.456711	0.542544	0.4290	0.5946
	total	30	0.847349	0.6161856	0.1124996	0.617262	1.077436	0.3124	2.1072
ANGPT4	1.0000	10	0.370262	0.0206188	0.0065202	0.355513	0.385012	0.3295	0.4037
	2.0000	10	1.362208	0.0952097	0.0301079	1.294099	1.430317	1.2285	1.5247
	3.0000	10	0.422209	0.0448262	0.0141753	0.390142	0.454275	0.3648	0.5133
	total	30	0.718227	0.4674832	0.0853504	0.543665	0.892788	0.3295	1.5247
KDR	1.0000	10	0.434405	0.0210397	0.0066533	0.419354	0.449456	0.4012	0.4606
	2.0000	10	1.319921	0.0648779	0.0205162	1.273511	1.366332	1.2217	1.4007
	3.0000	10	0.519005	0.0192815	0.0060973	0.505212	0.532798	0.4947	0.5398
	total	30	0.757777	0.4077310	0.0744412	0.605528	0.910026	0.4012	1.4007
AKT	1.0000	10	0.998226	0.1035957	0.0327598	0.924118	1.072334	0.8884	1.1859
	2.0000	10	2.532469	0.2313107	0.0731469	2.367000	2.697939	2.2005	2.8856
	3.0000	10	1.441751	0.1663498	0.0526044	1.322751	1.560750	1.1740	1.6333
	total	30	1.657482	0.6770827	0.1236178	1.404655	1.910309	0.8884	2.8856
ACO3	1.0000	10	1.474441	0.0965224	0.0305231	1.405393	1.543489	1.3439	1.6208
	2.0000	10	2.161590	0.1599465	0.0505795	2.047171	2.276008	1.9295	2.5062
	3.0000	10	1.793600	0.0985943	0.0311783	1.723070	1.864131	1.6211	1.9456
	total	30	1.809877	0.3088590	0.0563897	1.694547	1.925207	1.3439	2.5062
SMOX	1.0000	10	0.767047	0.0611052	0.0193232	0.723335	0.810759	0.6958	0.8793
	2.0000	10	1.815675	0.0661369	0.0209143	1.768363	1.862986	1.6795	1.9028
	3.0000	10	1.493892	0.0755316	0.0238852	1.439860	1.547924	1.3850	1.6525
	total	30	1.358871	0.4508948	0.0823218	1.190504	1.527238	0.6958	1.9028

95% CI – 95% confidence interval.

Table 3. Multiple comparison genes

Tukey's HSD									
Dependent variable	(I) groups		(J) groups		Mean D (I–J)	SE	Sig	95% CI	
								lower limit	upper limit
ANGPT1	dimension2	1.0000	dimension3	2.0000	−1.3206857*	0.0593887	0.000	−1.467935	−1.173436
				3.0000	−0.1387606	0.0593887	0.068	−0.286010	0.008489
		2.0000	dimension3	1.0000	1.3206857*	0.0593887	0.000	1.173436	1.467935
				3.0000	1.1819251*	0.0593887	0.000	1.034676	1.329175
		3.0000	dimension3	1.0000	0.1387606	0.0593887	0.068	−0.008489	0.286010
				2.0000	−1.1819251*	0.0593887	0.000	−1.329175	−1.034676
ANGPT4	dimension2	1.0000	dimension3	2.0000	−0.9919460*	0.0276880	0.000	−1.060596	−0.923296
				3.0000	−0.0519463	0.0276880	0.165	−0.120597	0.016704
		2.0000	dimension3	1.0000	0.9919460*	0.0276880	0.000	0.923296	1.060596
				3.0000	0.9399997*	0.0276880	0.000	0.871349	1.008650
		3.0000	dimension3	1.0000	0.0519463	0.0276880	0.165	−0.016704	0.120597
				2.0000	−0.9399997*	0.0276880	0.000	−1.008650	−0.871349
KDR	dimension2	1.0000	dimension3	2.0000	−0.8855167*	0.0183004	0.000	−0.930891	−0.840142
				3.0000	−0.0846002*	0.0183004	0.000	−0.129975	−0.039226
		2.0000	dimension3	1.0000	0.8855167*	0.0183004	0.000	0.840142	0.930891
				3.0000	0.8009165*	0.0183004	0.000	0.755542	0.846291
		3.0000	dimension3	1.0000	0.0846002*	0.0183004	0.000	0.039226	0.129975
				2.0000	−0.8009165*	0.0183004	0.000	−0.846291	−0.755542
AKT	dimension2	1.0000	dimension3	2.0000	−1.5342430*	0.0782768	0.000	−1.728324	−1.340162
				3.0000	−0.4435245*	0.0782768	0.000	−0.637605	−0.249443
		2.0000	dimension3	1.0000	1.5342430*	0.0782768	0.000	1.340162	1.728324
				3.0000	1.0907186*	0.0782768	0.000	0.896638	1.284800
		3.0000	dimension3	1.0000	0.4435245*	0.0782768	0.000	0.249443	0.637605
				2.0000	−1.0907186*	0.0782768	0.000	−1.284800	−0.896638
ACO3	dimension2	1.0000	dimension3	2.0000	−0.6871487*	0.0545407	0.000	−0.822378	−0.551920
				3.0000	−0.3191597*	0.0545407	0.000	−0.454389	−0.183931
		2.0000	dimension3	1.0000	0.6871487*	0.0545407	0.000	0.551920	0.822378
				3.0000	0.3679890*	0.0545407	0.000	0.232760	0.503218
		3.0000	dimension3	1.0000	0.3191597*	0.0545407	0.000	0.183931	0.454389
				2.0000	−0.3679890*	0.0545407	0.000	−0.503218	−0.232760
SMOX	dimension2	1.0000	dimension3	2.0000	−1.0486278*	0.0303457	0.000	−1.123868	−0.973388
				3.0000	−0.7268455*	0.0303457	0.000	−0.802085	−0.651606
		2.0000	dimension3	1.0000	1.0486278*	0.0303457	0.000	0.973388	1.123868
				3.0000	0.3217822*	0.0303457	0.000	0.246542	0.397022
		3.0000	dimension3	1.0000	0.7268455*	0.0303457	0.000	0.651606	0.802085
				2.0000	−0.3217822*	0.0303457	0.000	−0.397022	−0.246542

* The significance level of mean difference was 0.05; SE – standard error; 95% CI – 95% confidence interval; HSD – honestly significant difference.

to vascular endothelial cells, and produces NO, which affects the permeability of blood vessels and increases damage to retinal cells. The original statistical data of PCR are shown in Table 2–5.

Discussion

The occurrence and development of DR is a complex pathological process, and a series of pathological changes of DR are caused by abnormal changes of cytokines, signal transduction metabolic enzymes, inflammation, ion channels, and related genes.[17,18] Neovascularization is a characteristic pathological marker of the entry of DR into the proliferative phase. Therefore, preventing and inhibiting the formation of DR neovascularization is a key target to delay the progression of DR. The PI3K/Akt signaling pathway is one of the signaling pathways that participate in the regulation of cell growth, proliferation and differentiation.[19,20] When the PI3K/Akt signaling pathway is activated, it can not only accelerate the survival cycle of endothelial cells, but also cooperate with VEGF in cell survival and migration, and finally induce the formation of new blood vessels.[21] The AKT regulates serine antiapoptotic signaling protein in endothelial cells from cell cycle G1 phase to S phase. Therefore, AKT regulates endothelial cell proliferation, migration and has a key role in inducing angiogenesis.[22,23] In this study, the ischemia and hypoxia

Table 4. Normality test

Genes	Groups		Kolmogorov–Smirnov[a]			Shapiro–Wilk		
			statistics	df	Sig.	statistics	df	Sig.
ANGPT1	dimension1	1.0000	0.162	10	0.200*	0.943	10	0.592
		2.0000	0.238	10	0.115	0.874	10	0.113
		3.0000	0.155	10	0.200*	0.920	10	0.358
ANGPT4	dimension1	1.0000	0.162	10	0.200*	0.967	10	0.858
		2.0000	0.200	10	0.200*	0.946	10	0.625
		3.0000	0.145	10	0.200*	0.950	10	0.665
KDR	dimension1	1.0000	0.180	10	0.200*	0.936	10	0.512
		2.0000	0.184	10	0.200*	0.920	10	0.355
		3.0000	0.209	10	0.200*	0.835	10	0.038
AKT	dimension1	1.0000	0.202	10	0.200*	0.892	10	0.179
		2.0000	0.149	10	0.200*	0.951	10	0.680
		3.0000	0.258	10	0.058	0.870	10	0.101
ACO3	dimension1	1.0000	0.257	10	0.060	0.894	10	0.186
		2.0000	0.170	10	0.200*	0.947	10	0.636
		3.0000	0.163	10	0.200*	0.981	10	0.972
SMOX	dimension1	1.0000	0.169	10	0.200*	0.909	10	0.275
		2.0000	0.182	10	0.200*	0.918	10	0.344
		3.0000	0.244	10	0.094	0.908	10	0.269

a – Lilliefors significant level correction; * The lower limit of the true significance level; df – degrees of freedom.

induced by high glucose level in the rat model activated and accelerated the expression of AKT in the PI3k/Akt signaling pathway, and increased its phosphorylation, thus accelerating the formation of neovascularization. The results of this experiment showed that the expression of AKT and related proteins in the DR group and anti-ACO3 group was significantly higher than in the control group, indicating that the expression of AKT was enhanced and the PI3k/Akt signaling pathway was activated during the formation of DR lesions.

Limitations of the study

This study is mainly based on the basic experiment of animal model. It explored the involvement of ACO3 protein in DR through the PI3k/Akt signaling pathway of rat model of DR. However, there are still great structural and pathological differences between animals and humans. Therefore, this study should also examine the differences and effects of various animal models, and further clinical studies should be performed.

Conclusions

As an important pathway involved in endothelial cell migration, proliferation and vascular dysfunction, the PI3K/Akt signaling pathway also plays an important role in the process of DR neovascularization. The ACO3 protein, also known as VAP1, is involved in regulating cell proliferation and inducing neovascularization.[24] Proteins ACO3 and SMOX have the characteristics of mutual regulation, and are synergistically involved in the regulation of amino acid metabolism.[25] The expression levels of ACO3, SMOX and AKT proteins were decreased in the anti-ACO3 group, which indicated that the PI3K/Akt signaling pathway was inhibited, and the formation of retinal neovascularization was inhibited to a certain extent. This delayed the progression of DR and played a certain therapeutic role in the proliferation phase.

ORCID iDs

Yi Zhang https://orcid.org/0000-0003-0536-9643
Wenjun Wang https://orcid.org/0000-0001-8725-6233
Anhuai Yang https://orcid.org/0000-0001-7429-277X

References

1. Hendrick AM, Gibson MV, Kulshreshtha A. Diabetic retinopathy. *Prim Care*. 2015;42(3):451–464. doi:10.1016/j.pop.2015.05.005
2. Ruta LM, Magliano DJ, Lemesurier R, Taylor HR, Zimmet PZ, Shaw JE. Prevalence of diabetic retinopathy in type 2 diabetes in developing and developed countries. *Diabet Med*. 2013;30(4):387–398. doi:10.1111/dme.12119
3. Thapa R, Bajimaya S, Sharma S, Rai BB, Paudyal G. Systemic association of newly diagnosed proliferative diabetic retinopathy among type 2 diabetes patients presented at a tertiary eye hospital of Nepal. *Nepal J Ophthalmol*. 2015;7(13):26–32. doi:10.3126/nepjoph.v7i1.13163
4. Song P, Yu J, Chan KY, Thodoratou E, Rudan I. Prevalence, risk factors and burden of diabetic retinopathy in China: A systematic review and meta-analysis. *J Glob Health*. 2018;8(1):010803. doi:10.7189/jogh.08.010803
5. Wang W, Lo ACY. Diabetic retinopathy: Pathophysiology and treatments. *Int J Mol Sci*. 2018;19(6):1816. doi:10.3390/ijms19061816

Table 5. All original data of Fig. 4 and Fig. 5 (normal group 1, diabetic retinopathy (DR) group 2, anti-ACO3 group 3)

Groups	ANGPT1	ANGPT4	KDR	AKT	ACO3	SMOX
1.0000	0.3751	0.3681	0.4012	1.1859	1.5135	0.8563
1.0000	0.3797	0.3630	0.4306	1.1366	1.5435	0.8793
1.0000	0.3442	0.3807	0.4442	1.0718	1.6208	0.7934
1.0000	0.3124	0.3815	0.4606	0.9978	1.5258	0.7756
1.0000	0.3361	0.3855	0.4583	0.9030	1.5464	0.7111
1.0000	0.3146	0.4037	0.4243	0.8884	1.5170	0.7290
1.0000	0.3368	0.3651	0.4156	0.9092	1.4031	0.7661
1.0000	0.3684	0.3295	0.4103	0.9118	1.3439	0.7236
1.0000	0.4032	0.3490	0.4461	0.9965	1.3493	0.7403
1.0000	0.4382	0.3766	0.4528	0.9812	1.3810	0.6958
2.0000	1.5104	1.3320	1.3188	2.6577	2.5062	1.8124
2.0000	1.4524	1.4466	1.2353	2.8856	2.2577	1.9028
2.0000	1.5086	1.5247	1.3260	2.7656	2.2703	1.8016
2.0000	1.6421	1.4825	1.3847	2.7385	2.0583	1.7821
2.0000	1.6139	1.3622	1.3804	2.6138	2.1176	1.7776
2.0000	1.5291	1.2285	1.3708	2.4437	1.9295	1.8797
2.0000	1.6609	1.2603	1.2588	2.3809	2.1160	1.8946
2.0000	1.8085	1.3353	1.3020	2.2655	2.0146	1.8209
2.0000	1.9824	1.3035	1.2217	2.3728	2.1738	1.6795
2.0000	2.1072	1.3465	1.4007	2.2005	2.1720	1.8055
3.0000	0.5871	0.5133	0.5087	1.5631	1.9046	1.5839
3.0000	0.5946	0.4715	0.4947	1.6333	1.8093	1.4745
3.0000	0.5418	0.4444	0.5353	1.5854	1.9456	1.4716
3.0000	0.5169	0.4306	0.5393	1.5326	1.8286	1.3850
3.0000	0.4756	0.3888	0.5091	1.5533	1.8504	1.4733
3.0000	0.4622	0.3648	0.5001	1.5094	1.7161	1.5046
3.0000	0.4294	0.3802	0.4947	1.3700	1.6973	1.4477
3.0000	0.4290	0.4171	0.5387	1.2463	1.8135	1.4429
3.0000	0.4578	0.4103	0.5398	1.2503	1.7495	1.5029
3.0000	0.5019	0.4010	0.5296	1.1740	1.6211	1.6525

6. Park HC, Lee YK, Cho A, et al. Diabetic retinopathy is a prognostic factor for progression of chronic kidney disease in the patients with type 2 diabetes mellitus. *PLoS One*. 2019;14(7):e0220506. doi:10.1371/journal.pone.0220506
7. Semeraro F, Morescalchi F, Cancarini A, Russo A, Rezzola S, Costagliola C. Diabetic retinopathy, a vascular and inflammatory disease: Therapeutic implications. *Diabetes Metab*. 2019;45(6):517–527. doi:10.1016/j.diabet.2019.04.002
8. Piao CL, Luo JL, Jin D, et al. Utilizing network pharmacology to explore the underlying mechanism of *Radix salviae* in diabetic retinopathy. *Chin Med*. 2019;14:58. doi:10.1186/s13020-019-0280-7
9. Xiao YL, Feng X. Mechanism of NLRP3/IL-1β pathway in the progression of diabetic retinopathy [in Chinese]. *Int Eye Sci*. 2019;19(9):1559–1562. http://www.ijo.cn/cn_publish/2019/9/201909026.pdf.
10. Solomon SD, Chew E, Duh EJ, et al. Diabetic retinopathy: A position statement by the American Diabetes Association. *Diabetes Care*. 2017;40(3):412–418. doi:10.2337/dc16-2641
11. He J, Qiu Y, Zhou X. A study of Na(+)-K(+)-ATPase activity in erythrocyte membrane from diabetic retinopathy patients [in Chinese]. *Zhonghua Yan Ke Za Zhi*. 1998;34(6):421–423. PMID:11877243.
12. Li H, Luo XX, Feng YP, Wang H. Effects of a traditional Chinese patent medicine for PI3K/Akt pro-survival signal channel in diabetic retinopathy rat. *Int Eye Sci*. 2016;16(12):2195–2199. doi:10.3980/j.issn.1672-5123.2016.12.06
13. Huali Z, Jing G, Zhe X, et al. A comparative study of fundus photography and fluorescein fundus angiography in the diagnosis of diabetic retinopathy in Tibetans [in Chinese]. *Sichuan Medical Journal*. 2019;7(40):726–728.
14. Guo D, Du N. Therapeutic effect and mechanism of paclitaxel on diabetic retinopathy model rats. *Int Eye Sci*. 2019;19(12):2026–2030. doi:10.3980/j.issn.1672-5123.2019.12.06
15. Zafirovic S, Sudar-Milovanovic E, Obradovic M, et al. Involvement of PI3K, Akt and RhoA in oestradiol regulation of cardiac iNOS expression. *Curr Vasc Pharmacol*. 2019;17(3):307–318. doi:10.2174/1570161116666180212142414
16. Rouhani F, Khodarahmi P, Naseh V. NGF, BDNF and Arc mRNA expression in the hippocampus of rats after administration of morphine. *Neurochem Res*. 2019;44(9):2139–2146. doi:10.1007/s11064-019-02851-z
17. Radha V, Rema M, Mohan V. Genes and diabetic retinopathy. *Indian J Ophthalmol*. 2002;50(1):1–5. PMID:12090088.
18. Fleissig E, Adhi M, Sigford DK, Barr CC. Foveal vasculature changes and nonperfusion in patients with diabetes types I and II with no evidence of diabetic retinopathy. *Graefes Arch Clin Exp Ophthalmol*. 2020;258(3):551–556. doi:10.1007/s00417-019-04588-5
19. Tao D. PI3K-AKT pathway and diabetic optic reticulum lesions [in Chinese]. *World Latest Medicine Information*. 2016;16(44):34–35.

20. Koga T, Suico MA, Shimasaki S, et al. Endoplasmic reticulum (ER) stress induces Sirtuin 1 (SIRT1) expression via the PI3K-Akt-GSK3β signaling pathway and promotes hepatocellular injury. *J Biol Chem*. 2015;290(51):30366–30374. doi:10.1074/jbc.M115.664169
21. Campo L, Turley H, Han C, et al. Angiogenin is up-regulated in the nucleus and cytoplasm in human primary breast carcinoma and is associated with markers of hypoxia but not survival. *J Patholog*. 2005;205(5):585–591. doi:10.1002/path.1740
22. Song Q, Han CC, Xiong XP, et al. PI3K-Akt-mTOR signal inhibition affects expression of genes related to endoplasmic reticulum stress. *Genet Mol Res*. 2016;15(3):1–8. doi:10.4238/gmr.15037868
23. Li S, Li Q, Yu W, Xiao Q. High glucose and/or high insulin affects HIF-1 signaling by regulating AIP1 in human umbilical vein endothelial cells. *Diabetes Res Clin Pract*. 2015;109(1):48–56. doi:10.1016/j.diabres.2015.05.005
24. Wang H, Clainche AL, Dall MTL, et al. Cloning and characterization of the peroxisomal acyl CoA oxidase *ACO3* gene from the alkane-utilizing yeast *Yarrowia lipolytica*. *Yeast*. 1998;14(15):1373–1386. doi:10.1002/(SICI)1097-0061(199811)14:15<1373::AID-YEA332>3.0.CO;2-1
25. Fan J, Chen M, Wang X, et al. Targeting Smox is neuroprotective and ameliorates brain inflammation in cerebral ischemia/reperfusion rats. *Toxicol Sci*. 2019;168(2):381–393. doi:10.1093/toxsci/kfy300

The effects of adalimumab on the rat autotransplantation endometriosis model: A placebo-controlled randomized study

Selçuk Kaplan[A–F], Pınar Kırıcı[C–E], Ahmet Türk[B,C]

Faculty of Medicine, Adıyaman University, Turkey

A – research concept and design; B – collection and/or assembly of data; C – data analysis and interpretation;
D – writing the article; E – critical revision of the article; F – final approval of the article

Advances in Clinical and Experimental Medicine, ISSN 1899–5276 (print), ISSN 2451–2680 (online) *Adv Clin Exp Med*. 2022;31(4):417–426

Address for correspondence
Selçuk Kaplan
E-mail: kaplan_2384@hotmail.com

Funding sources
None declared

Conflict of interest
None declared

Acknowledgements
The authors would like to thank Prof. Dr. Mehmet Şimşek from the Department of Obstetrics and Gynecology, Adiyaman University, Turkey, for his contribution.

Received on September 16, 2020
Reviewed on August 26, 2021
Accepted on November 30, 2021

Published online on January 18, 2022

Abstract

Background. Endometriosis is a chronic inflammatory pathology that can cause persistent pelvic pain and infertility by affecting women of reproductive age. It is defined as the placement of endometrial tissue outside the uterine cavity. Hormonal, genetic and immunological factors have an effect on the development of endometriotic implants. Adalimumab is a monoclonal antibody specific for tumor necrosis factor alpha (TNF-α), used in the treatment of autoimmune diseases.

Objectives. To investigate the effectiveness of adalimumab on histopathological and biochemical values in rats with experimental endometriosis.

Materials and methods. This study is a comparative, prospective, experimental rat study. Wistar albino female rats were divided into 4 groups. Group 1 was separated as the control group. Endometriotic implants were simultaneously induced in group 2 and group 3. After 4 weeks, developing endometriotic foci were measured. Adalimumab (5 mg/kg) was simultaneously intraperitoneally (ip.) administered to group 3 and group 4 for 4 weeks. At the end of the study, histopathological scoring and fibrillin-1 scoring were performed. Total antioxidant status (TAS), total oxidant status (TOS) and malondialdehyde (MDA) values were measured. Findings in all groups were compared.

Results. When group 1 and group 2 were compared, the histopathological score, as well as MDA and TOS levels increased, while TAS levels decreased in group 2 ($p < 0.001$). After adalimumab treatment, the average endometriotic implant size in group 3 (0.32 ±0.002 mm) decreased compared to group 2 (0.77 ±0.04 mm) ($p = 0.032$). While fibrillin-1 score increased in group 2 and group 3 compared to group 1, it decreased in group 3 compared to group 2 ($p < 0.001$). Histopathological score decreased, TAS levels increased and MDA levels decreased in group 3 compared to group 2 ($p < 0.001$).

Conclusions. Adalimumab may play a role in the regression of endometrial implants by showing antioxidant and anti-inflammatory effects on histopathological damage and fibrosis.

Key words: endometriosis, rat, adalimumab, antioxidant effect, fibrillin-1

Cite as
Kaplan S, Kırıcı P, Türk A. The effects of adalimumab on the rat autotransplantation endometriosis model: A placebo-controlled randomized study. *Adv Clin Exp Med*. 2022;31(4):417–426. doi:10.17219/acem/144369

DOI
10.17219/acem/144369

Background

Endometriosis is a common gynecological pathology affecting 5–10% of women in the reproductive age.[1] It causes symptoms such as chronic pelvic pain, dysmenorrhea, dyspareunia, and infertility.[2] It has negative effects on ovarian reserve, tubal anatomy, embryo quality, and implantation.[3] The pathophysiology of endometriosis is still not entirely clear and several theories have been proposed. It has been stated that proinflammatory cytokines play a role in the pathophysiology of endometriosis.[4–6] There are cytokines responsible for inflammatory reactions and tissue neovascularization. Interleukin (IL)-6 and tumor necrosis factor alpha (TNF-α) have been previously studied in the pathogenesis of endometriosis.[7] The estrogenic microenvironment activates peritoneal macrophages with secretion of TNF-α and IL-1, which are pro-inflammatory cytokines. The increase in the level of IL-6 and TNF-α in the peritoneal fluid of patients with abnormal immune cell activity shows the role of cytokines in the pathogenesis.[8–10]

Endometriosis is a pathology caused by the abnormal proliferation of endometrial tissue outside the uterine cavity.[1] Transforming growth factor beta (TGF-β) plays a key role in the pathological growth of many fibrotic tissues.[11] The TGF-β stimulates the expression of extracellular matrix proteins.[12,13] Its receptors have been detected in leiomyomas and myometrium, and it has been shown that estrogen and TGF-β expression are increased in endometriosis, and TGF-β activity mediates the effects of estrogen.[14] This interaction may play a role in the development of endometriosis. Fibrillin-1 is a protein that indicates the activation of TGF-β.[15]

Adalimumab is a fully human immunoglobulin G (IgG)1 neutralizing monoclonal antibody specific for TNF-α.[16,17] It is used in the treatment of many autoimmune diseases, such as rheumatoid arthritis, Crohn's disease and psoriatic arthritis.[16] In previous experimental studies in rats, agents such as etanercept and infliximab have been reported to decrease TNF-α levels in peritoneal fluid in rats with endometriosis.[18,19] As far as we know, there is no study reporting the relationship between histopathological and biochemical changes and adalimumab in endometriosis.

Objectives

The aim of this study is to determine whether adalimumab can be an effective medical treatment agent, by examining its histopathological and biochemical effects on endometriosis.

Materials and methods

The experiments in this study were carried out in accordance with the National Institutes of Health (NIH) animal research guidelines and were approved by Adıyaman Training and Research Hospital Ethics Commitee (approval No. 2019/062, December 26, 2019).

Animals and experimental protocol

Twenty-eight Wistar albino female rats, 10–12-week old, weighing 250–280 g, were divided into 4 groups with 7 animals in each group. No procedures were performed for 7 days to ensure the adaptation of animals. Rats were housed at 20 ±22°C room temperature during the adaptation and experimental period, in rooms with 12-hour light and 12-hour dark light cycle, with food and water ad libitum. The animals were classified into 4 groups (control group, endometriosis group, endometriosis + adalimumab group, and adalimumab group).

All rats were anesthetized by intramuscular administration of 60 mg/kg ketamine hydrochloric acid (Ketalar; Warner-Lambert, Istanbul, Turkey) and 7 mg/kg xylazine hydrochloric acid (Rompun; Bayer, Istanbul, Turkey).

In group 1 (control group, n = 7), the pelvic region was opened with laparotomy and the adnexa were localized as the right and left adnexa. After the adnexa was localized with the right and left uterine horn, the abdominal wall was closed with 4-0 nylon sutures. No action was taken until the end of the experiment.

In group 2 (endometriosis group, n = 7), the autotransplantation method was used for the induction of endometriosis. The reproductive cycles of the animals were controlled by vaginal smear and the rats in the estrus phase were selected. After general anesthesia, a vertical incision was made to expose the uterus. Both uterine horns were removed from the cervix to the point located about 1 cm from the ovaries. Electrocoagulation was used for hemostasis. The uterine horns were divided longitudinally, exposing the endometrium. Without removing the myometrium, endometrial segment (5 × 5 mm) was implanted into the peritoneal surface of the right abdominal wall, so that the endometrium came into contact with the peritoneal surface. Both ends of the implants were fixed to the interior with 6-0 nonabsorbable polypropylene suture.[20] All rats were allowed to recover for 4 weeks following surgical induction of endometriosis. At the end of the 4 weeks, the rats were operated to observe the growth of endometriotic implants. The equation: 6 × length × width × height of the implant was used to measure the surface areas of the implants and calculate the endometriotic volume. After the endometriotic lesions were photographed, the size of the lesion was recorded and the peritoneal cavity was closed. No procedure was performed on rats for 4 weeks after the development of endometriosis.

In group 3 (endometriosis + adalimumab group, n = 7), after the reproductive cycles of the animals were controlled by vaginal smear and the rats in the estrous phase were selected, the endometriosis induction was performed using autotransplantation method. At the end of the four-week

period, after calculating the endometriotic volume and photographing the lesions, 5 mg/kg adalimumab was administered intraperitoneally (ip.) for 4 weeks.[21]

In group 4 (adalimumab group, n = 7), after the adnexa was localized with the right and left uterine horn, the abdominal wall was closed with 4-0 nylon sutures and 5 mg/kg adalimumab was administered ip. every day for 4 weeks, to start at the same time as group 2.

Histopathological evaluation

The excised endometrial implants were fixed with 10% formalin solution upon histopathological examination. Sections approx. 5-µm thick were taken from a formalin-fixed endometriotic implant. Samples were stained with hematoxylin and eosin (H&E) and examined under light microscopy. Histopathological scoring was done[22] based on a following rating scale: +3: a well-preserved epithelial layer; +2: a moderately-preserved epithelial layer (leukocyte infiltrated epithelium); +1: a poorly-preserved epithelial layer (sparse epithelial cell); 0: no epithelial cells.

Immunohistochemical examination

For fibrillin-1 antigen retrieval, sections were rehydrated, then boiled in a microwave oven (750 W) 7 times for 5 min each in citrate buffer solution (pH 6). Sections were cooled at room temperature for 20 min, washed 3 times for 5 min each with phosphate-buffered saline (PBS; P4417; Sigma Chemical Co., St. Louis, USA), then incubated for 5 min with hydrogen peroxide block solution (TA-125-HP; Lab Vision Corp., San Francisco, USA) to block endogenous peroxidase activity. Then, the sections were washed 3 times for 5 min each with PBS. After applying Ultra V Block (TA-125-UB; Lab Vision Corp.) for 5 min, sections were incubated with primary antibodies for fibrillin-1 (rabbit polyclonal bs-1157R; Bioss Antibodies, Woburn, USA) and diluted 1:200 at room temperature for 60 min in a humid environment. After being washed with PBS 3 times for 5 min each, the sections were incubated at room temperature for 30 min in a humid environment with secondary antibody (biotinylated goat anti-mouse/rabbit IgG, TP-125-BN; Lab Vision Corp.). Sections were washed with PBS 3 times for 5 min each and incubated at room temperature for 30 min in a humid environment with streptavidin peroxidase (TS-125-HR; LabVision Corp.) and then placed in PBS. The 3-amino-9-ethylcarbazole (AEC) substrate + AEC chromogen (AEC substrate, TA-015 and HAS, AEC chromogen, TA-002-HAC; Lab Vision Corp.) solution was dripped on the sections. The sections were washed with PBS. Sections were counterstained with Mayer's hematoxylin, passed through PBS and distilled water and mounted with Large Volume Vision Mount (TA-125-UG; Lab Vision Corp.). Sections were evaluated and photographed using a digital microscope camera (Leica DFC295; Leica Camera AG, Wetzlar, Germany). The histoscore, which reflects the prevalence of immunoreactivity of fibrillin-1 on the tissue, was based on the rating scale: 0.1: < 25%; 0.4: 26–50%; 0.6: 51–75%; 0.9: 76–100%, and intensity of immunoreactivity: 0: unstained; 0.5: little staining; 1: some staining; 2: moderate staining; 3: strong staining. The histoscore was measured using the following equation:

histoscore = prevalence × intensity of immunoreactivity.

Determination of malondialdehyde (MDA) level

Determination of malondialdehyde level was performed by applying the Esterbauer method, which is a lipid peroxidation measurement method.[23] Malondialdehyde reacting with thiobarbituric acid at 90–95°C forms pink-colored chromogen. Fifteen minutes later, the absorbances of the rapidly cooled samples were read spectrophotometrically at 532 nm. The results are expressed in nmol/g.

Determination of total antioxidant status (TAS) and total oxidant status (TOS) levels

Total antioxidant status and total oxidant status were measured in serum samples using enzyme-linked immunoassay (ELISA) method. The TAS (Rat TAS Catalog No. YLA3889Ra; YL Biotechnology Co., Ltd, Shanghai, China) and TOS (Rat TOS Catalog No. YLA1892Ra; YL Biotechnology Co., Ltd) levels were measured in accordance with the procedures specified in the catalog of kits. The measurement range of the Rat TAS ELISA kit was: 1–300 pg/mL, intra-assay coefficient of variation (CV) <10%, inter-assay CV < 12%, sensitivity 0.54 pg/mL. The measurement range of the Rat TOS ELISA kit was 0.02–60 U/mL, intra-assay CV < 10%, inter-assay CV < 12%, sensitivity 0.013 U/mL. The automatic washer BioTek ELx50 (BioTek Instruments, Winooski, USA) was used for plate washing, while ChroMate Microplate Reader P4300 devices (Awareness Technology, Palm City, USA) were used for absorbance readings. The unit of test results is specified for serum samples in U/mL.

Statistical analyses

The IBM SPSS v. 22 software (IBM Corp., Armonk, USA) program was used to analyze the data. The Shapiro–Wilk test was used as a normal distribution test. The Shapiro–Wilk test results for MDA measurement were reported as p = 0.830 for group 1, p = 0.898 for group 2, p = 0.881 for group 3, and p = 0.716 for group 4. The Shapiro–Wilk test results for TAS measurement were 0.274 for group 1, 0.540 for group 2, 0.648 for group 3, and 0.355 for group 4. The Shapiro–Wilk test results for TOS measurement were reported as p = 0.707 for group 1, p = 0.598 for group 2, p = 0.700 for group 3, and p = 0.944 for group 4. The Shapiro–Wilk test results for fibrillin-1 measurement were

reported as p = 0.812 for group 1, p = 0.652 for group 2, p = 0.717 for group 3, and p = 0.941 for group 4. Levene's homogeneity test was performed, in which the data met the assumption of normal distribution for each group, and the results were p = 0.170 for MDA, p = 0.050 for TAS, p = 0.654 for TOS, and p = 0.191 for fibrillin-1 measurement. It was observed that the variances were homogeneous. One-way analysis of variance (ANOVA) test (post hoc Bonferroni test) was used in the analysis of the data conforming to the normal distribution. The score variable does not show a normal distribution. The p-value of the score variable is <0.001. Spearman's correlation test was used for the values where the score did not show normal distribution, and Pearson's correlation test was used for the others. The value of $p < 0.05$ was considered statistically significant.

Results

Histopathological scoring

The H&E staining and immunohistochemistry staining histopathological images were shown in Fig. 1 and Fig. 2. There was a statistically significant difference between the measurements in different groups. A statistical difference was observed between group 2 and group 3 ($p < 0.001$) (Table 1). When group 1 and group 2 were compared, the increase in histopathological damage in group 2 was statistically significant ($p < 0.001$). When group 3 and group 2 were compared, the histopathological damage score was significantly decreased in group 3 ($p < 0.001$).

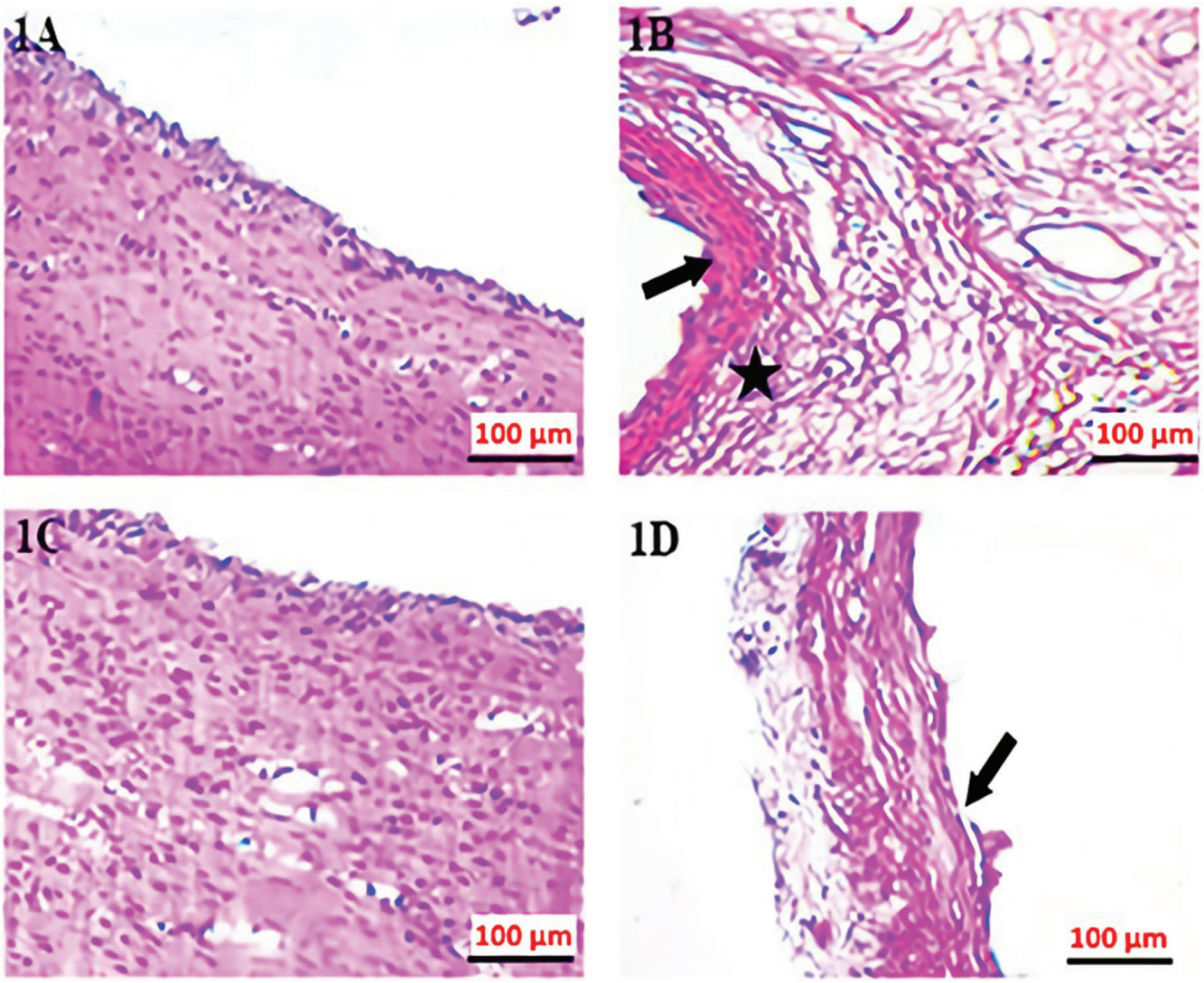

Fig. 1. Excised endometrial implants were stained with hematoxylin and eosin (H&E). Accordingly, group 1 (control) (1A) and group 4 (adalimumab) (1C) were of normal appearance. In group 2 (endometriosis) (1B), severe epithelial damage (black arrow) and leukocyte infiltration (black star) were observed. In group 3 (endometriosis + adalimumab) (1D), epithelial damage and leukocyte infiltration were observed to decrease

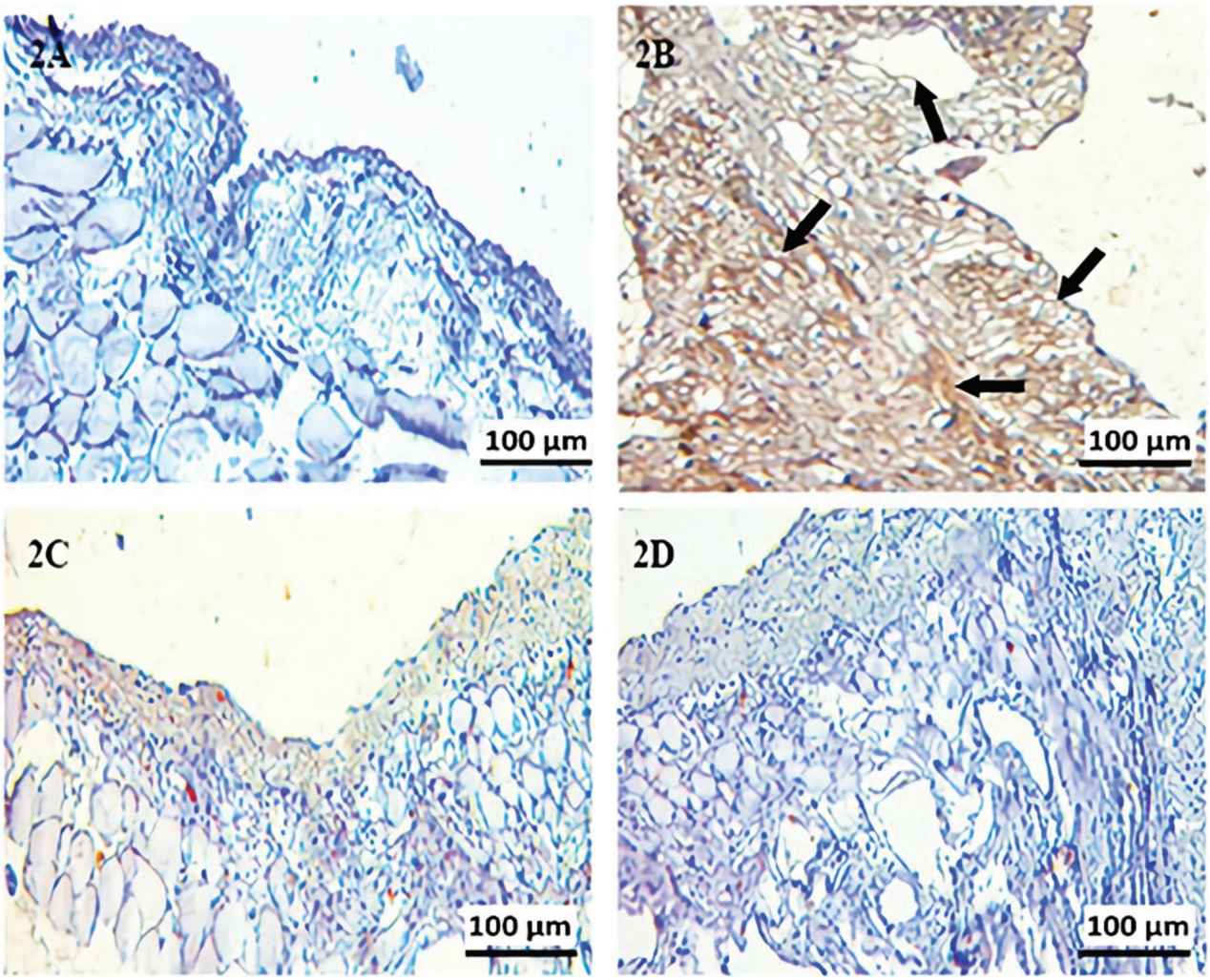

Fig. 2. Examination of immunohistochemical staining for fibrillin-1 immunoreactivity under light microscopy; fibrillin-1 immunoreactivity (black arrow) was observed; 2A. Group 1 (control); 2D. Group 3 (endometriosis + adalimumab); 2B. Group 2 (endometriosis); 2C. Group 4 (adalimumab)

Table 1. Comparison of biochemical measurements and fibrillin-1 scores by groups*

Group		Fibrillin-1	MDA	TAS	TOS
Group 1 (n = 7)	mean	2.31	17.92	1.18	12.98
	SD	0.77	0.99	0.04	1.06
	median	0.71	18.01	1.17	13.26
Group 2 (n = 7)	mean	5.51	25.02	0.43	19.75
	SD	2.61	1.61	0.20	1.48
	median	3.30	25.30	0.41	20.14
Group 3 (n = 7)	mean	3.64	19.86	0.81	17.68
	SD	1.47	1.77	0.14	1.81
	median	1.66	20.10	0.81	17.60
Group 4 (n = 7)	mean	0.93	16.88	1.29	15.55
	SD	0.14	0.94	0.12	1.26
	median	0.11	16.78	1.24	15.52
p-value	for each group	<0.001	<0.001	<0.001	<0.001
df (total)	for each group	27	27	27	27
f	for each group	12.741	48.104	53.812	28.671

SD – standard deviation; df – degrees of freedom; MDA – malondialdehyde; TAS – total antioxidant status; TOS – total oxidant status; ADA – adalimumab; group 1 – control; group 2 – endometriosis; group 3 – endometriosis + ADA; group 4 – ADA; *one-way analysis of variance (ANOVA) test.

Macroscopic examination

The mean size of rats endometriotic implants in group 2 was 0.77 ±0.04 mm^2. After adalimumab treatment, it measured 0.32 ±0.002 mm^2. This decrease was statistically significant ($p = 0.032$) (Fig. 3).

Biochemical analysis

Post hoc one-way ANOVA results for biochemical measurements are given in Table 2.

MDA level

The MDA levels significantly increased in group 2 compared with group 1 ($p < 0.001$). The MDA values were significantly decreased in group 3 compared with group 2 ($p < 0.001$). There was no statistically significant difference between group 1 and group 4 ($p > 0.05$) (Table 1, Table 2).

TAS level

The TAS levels were significantly decreased in group 2 compared with group 1 ($p < 0.001$). The TAS values increased in group 3 compared to group 2 ($p < 0.001$). There was no statistically significant difference in TAS values between group 1 and group 4 ($p > 0.05$) (Table 1, Table 2).

TOS level

The distribution of scores in respective groups is given in Table 3. The TOS levels were significantly increased in group 2 compared with group 1 ($p < 0.001$). The TOS values in group 2 were significantly decreased compared with group 4 ($p < 0.001$). However, there was no statistical difference in TOS values between group 2 and group 3 ($p > 0.05$). The TOS values were significantly increased in group 4 compared with group 1 ($p = 0.016$) (Table 1, Table 2).

When histopathological scores and biochemical values were compared, there was a strong negative correlation between MDA value and TOS value and a strong positive correlation between MDA value and TAS value ($p < 0.001$) (Table 3).

Immunohistochemistry examination score

In the immunohistochemistry examination, fibrillin-1 scores differed significantly for 4 groups. According to the post hoc one-way ANOVA analysis between groups, fibrillin-1 activity increased in groups 2 and 3 compared to group 1 ($p < 0.001$). Moreover, fibrillin-1 immune reactivity decreased in group 3 compared to group 2 ($p < 0.001$) (Table 3).

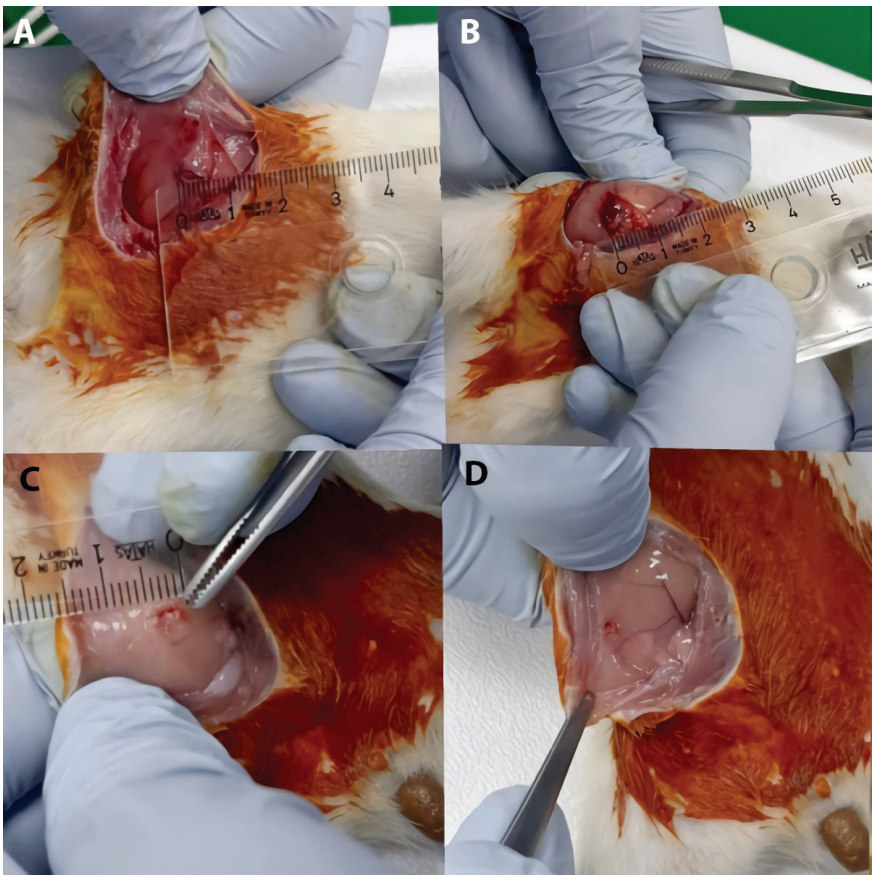

Fig. 3. A,B. Endometriotic foci developed as a result of autotransplantation; C,D. After adalimumab treatment, the size of the endometriotic foci decreased

Table 2. Post hoc one-way analysis of variance (ANOVA) of biochemical values and fibrillin-1 scores by groups

Dependent variable	Group (I)	Group (J)	Average difference (I–J)	p-value
MDA	group 1	group 2	**–7.10***	<0.001
		group 3	–1.94	0.087
		group 4	1.03	1.000
	group 2	group 1	**7.10***	<0.001
		group 3	**5.15***	<0.001
		group 4	**8.13***	<0.001
	group 3	group 1	1.94	0.087
		group 2	**–5.15***	<0.001
		group 4	**2.97***	0.003
	group 4	group 1	–1.03	1.000
		group 2	**–8.13***	<0.001
		group 3	**–2.97***	0.003
TAS	group 1	group 2	**0.74***	<0.001
		group 3	**0.36***	<0.001
		group 4	–0.11	0.907
	group 2	group 1	**–0.74***	<0.001
		group 3	**–0.38***	<0.001
		group 4	**–0.86***	<0.001
	group 3	group 1	**–0.36***	<0.001
		group 2	**0.38***	<0.001
		group 4	**–0.48***	<0.001
	group 4	group 1	0.11	0.907
		group 2	**0.86***	<0.001
		group 3	**0.48***	<0.001
TOS	group 1	group 2	**–6.77***	<0.001
		group 3	**–4.70***	<0.001
		group 4	**–2.56***	0.016
	group 2	group 1	**6.77***	<0.001
		group 3	2.07	0.075
		group 4	**4.20***	<0.001
	group 3	group 1	**4.70***	<0.001
		group 2	–2.07	0.075
		group 4	2.13	0.062
	group 4	group 1	**2.56***	0.016
		group 2	**–4.20***	<0.001
		group 3	–2.13	0.062
Fibrillin-1	group 1	group 2	**–1.28***	<0.001
		group 3	**–1.15***	<0.001
		group 4	0.37	0.083
	group 2	group 1	**1.28***	<0.001
		group 3	0.12	1.000
		group 4	**1.65***	<0.001
	group 3	group 1	**1.15***	<0.001
		group 2	–0.12	1.000
		group 4	**1.53***	<0.001
	group 4	group 1	–0.37	0.083
		group 2	**–1.65***	<0.001
		group 3	**–1.53***	<0.001

MDA – malondialdehyde; TAS – total antioxidant status; TOS – total oxidant status; ADA – adalimumab; group 1 – control; group 2 – endometriosis; group 3 – endometriosis + ADA; group 4 – ADA; I – group designated for comparison; J – other groups compared; * groups with statistically significant differences between them. Values in bold show statistically significant differences between groups.

Discussion

In this study, the effect of adalimumab on histopathological changes in endometriotic implants and its antioxidant effects were investigated. The size of endometriotic implants decreased after adalimumab treatment, as shown with macroscopic examination. Histopathological damage score increased in rats with experimental endometriosis and decreased with adalimumab administration. Fibrillin-1 score was increased in endometriotic implants, but fibrillin-1 score decreased in endometriotic implants treated with adalimumab. In addition, adalimumab decreased MDA levels and increased TAS levels in endometriotic implants. These findings show the histopathological

Table 3. Correlations between biochemical measurements*

Variables		Score	MDA	TAS	TOS
Score	r	1	–0.834	0.840	–0.680
	p-value	–	**<0.001**	**<0.001**	<0.001
MDA	r	–	1	–0.863	0.740
	p-value	–	–	**<0.001**	<0.001
TAS	r	–	–	1	–0.766
	p-value	–	–	–	<0.001
TOS	r	–	–	–	1
	p-value	–	–	–	–

MDA – malondialdehyde; TAS – total antioxidant status; TOS – total oxidant status; * Spearman's and Pearson's correlation test. Since the score did not show normal distribution, the values in bold were obtained with the Spearman's test, and the other results were obtained with the Pearson's correlation test.

improvement and antioxidant activity caused by adalimumab treatment in endometriotic implants.

Oxidative stress and inflammation play an important role in the pathogenesis of endometriosis.[24–26] Moreover, studies have shown that erythrocytes, apoptotic endometrial tissue, cell debris in the peritoneal cavity, and macrophages induce oxidative stress and inflammation, and cause endometriosis.[26] It is known that the balance between reactive oxygen species (ROS) and antioxidants is lost in the development of endometriosis.[27] The presence of ROS in the environment affects gene expression, causing protein dysfunction and cellular damage.[26–28] This oxidative stress can be both a cause and a consequence of endometriosis.[26] In addition, the role of mitophagy and autophagy in the pathophysiology of endometriosis supports the role of oxidative damage.[28] It has been hypothesized that eliminating oxidative stress may reduce the histopathological grade in endometrial implants and many studies have been conducted on this subject.[27,29,30]

Proinflammatory cytokines such as IL-1, IL-6, IL-8, and TNF-α have also been shown to play a role in the pathology of endometriosis.[31] It has been demonstrated that there is an increase in TNF-α levels in the peritoneal fluids of women with endometriosis.[32] It is thought that endometrial cell proliferation increases and endometriotic lesions develop by inducing IL-8 secretion with the increase of TNF-α.[33,34] In previous studies using etanercept, which has an anti-TNF-α activity, it was reported that endometriotic implants were reduced and histopathological scores decreased.[35] In another study, etanercept was reported to decrease MDA levels in endometriotic focus.[36] In our study, adalimumab treatment has decreased endometriotic implant dimensions, histopathological damage score and fibrillin-1 score, which is a fibrosis marker.

Fibrillin-1 has been associated with heart and liver fibrosis, and has been shown to cause the expression of extracellular matrix proteins in various studies in rats.[37,38] In addition, it has been previously observed that topical application of estrogen increases the activity of fibrillin-1 and other extracellular matrix proteins.[39] Moreover, it was demonstrated that fibrillin-1 activity increased in proportion to the size in leiomyomas.[40] In our study, the increase in fibrillin-1 score in endometriotic implants may be related to the role of the estrogenic microenvironment in endometrial implant development. Since estrogen levels were not measured in our study, large studies can be conducted to investigate this hypothesis.

Adalimumab is a drug that is effective both as monotherapy and in combination with disease-modifying antirheumatic drugs in the treatment of many chronic, inflammatory, immune-mediated diseases.[16] It has been reported that adalimumab decreases cell proliferation and increases the function of natural immune pathways by decreased IL-8 levels.[41] Considering the role of proinflammatory cytokines in the pathogenesis of endometriosis, it is not surprising that endometriotic implants and histopathological score decreased along with adalimumab treatment. Moreover, the immunomodulatory activity of adalimumab may demonstrate decreased fibrillin-1 activation in endometriotic implants.

Limitations

This study has some limitations. The fibrillin-1 score is established primarily with immunohistochemistry staining, but there were no polymerase chain reaction (PCR) tests measuring the fibrillin-1 protein expressions. Second, the study was experimentally performed in rats. In order to generalize the results to society, studies should be carried out primarily with large human populations.

Conclusions

Adalimumab, through its antioxidant and anti-inflammatory effects, plays an important role in the treatment of histopathological damage and fibrosis in endometriotic implants developed experimentally. It can be used as a nonhormonal agent in the treatment of endometriotic implants. However, experiments with different parameters are needed in large groups of animals and humans.

ORCID iDs

Selçuk Kaplan https://orcid.org/0000-0002-2887-6165
Pınar Kırıcı https://orcid.org/0000-0001-7616-4181
Ahmet Türk https://orcid.org/0000-0003-0903-3522

References

1. Liu Y, Zhang Z, Lu X, Meng J, Qin X, Jiang J. Anti-nociceptive and anti-inflammatory effects of sulforaphane on sciatic endometriosis in a rat model. *Neurosci Lett*. 2020;723:134858. doi:10.1016/j.neulet.2020.134858
2. Matarese G, De Placido G, Nikas Y, Alviggi C. Pathogenesis of endometriosis: Natural immunity dysfunction or autoimmune disease? *Trends Mol Med*. 2003;9(5):223–228. doi:10.1016/s1471-4914(03)00051-0
3. Gauché-Cazalis C, Koskas M, Cohen Scali S, Luton D, Yazbeck C. Endometriosis and implantation: Myths and facts. *Middle East Fertil Soc J*. 2012;17:79e81. doi:10.1016/j.mefs.2012.04.002
4. Calhaz-Jorge C, Costa AP, Barata M, Santos MC, Melo A, Palma-Carlos ML. Tumour necrosis factor alpha concentrations in the peritoneal fluid of infertile women with minimal or mild endometriosis are lower in patients with red lesions only than in patients without red lesions. *Hum Reprod*. 2000;15(6):1256–1260. doi:10.1093/humrep/15.6.1256
5. Gazvani R, Templeton A. Peritoneal environment, cytokines and angiogenesis in the pathophysiology of endometriosis. *Reproduction*. 2002;123(2):217–226. doi:10.1530/rep.0.1230217
6. Taskin MI, Gungor AC, Adali E, Yay A, Onder GO, Inceboz U. A humanized anti-interleukin 6 receptor monoclonal antibody, tocilizumab, for the treatment of endometriosis in a rat model. *Reprod Sci*. 2016;23(5):662–669. doi:10.1177/1933719115612134
7. Laganà AS, Vitale SG, Salmeri FM, et al. Unus pro omnibus, omnes pro uno: A novel, evidence-based, unifying theory for the pathogenesis of endometriosis. *Med Hypotheses*. 2017;103:10–20. doi:10.1016/j.mehy.2017.03.032
8. Kalu E, Sumar N, Giannopoulos T, et al. Cytokine profiles in serum and peritoneal fluid from infertile women with and without endometriosis. *J Obstet Gynaecol Res*. 2007;33(4):490–495. doi:10.1111/j.1447-0756.2007.00569.x
9. Mahnke JL, Dawood MY, Huang JC. Vascular endothelial growth factor and interleukin-6 in peritoneal fluid of women with endometriosis. *Fertil Steril*. 2000;73(1):166–170. doi:10.1016/s0015-0282(99)00466-5
10. Othman Eel-D, Hornung D, Salem HT, Khalifa EA, El-Metwally TH, Al-Hendy A. Serum cytokines as biomarkers for nonsurgical prediction of endometriosis. *Eur J Obstet Gynecol Reprod Biol*. 2008;137(2):240–246. doi:10.1016/j.ejogrb.2007.05.001
11. Branton MH, Kopp JB. TGF-beta and fibrosis. *Microbes Infect*. 1999;1(15):1349–1365. doi:10.1016/s1286-4579(99)00250-6
12. Sozen I, Arici A. Interactions of cytokines, growth factors, and the extracellular matrix in the cellular biology of uterine leiomyomata. *Fertil Steril*. 2002;78(1):1–12. doi:10.1016/s0015-0282(02)03154-0
13. Luo X, Ding L, Xu J, Chegini N. Gene expression profiling of leiomyoma and myometrial smooth muscle cells in response to transforming growth factor-beta. *Endocrinology*. 2005;146(3):1097–1118. doi:10.1210/en.2004-1377
14. Chegini N, Ma C, Tang XM, Williams RS. Effects of GnRH analogues, 'add-back' steroid therapy, antiestrogen and antiprogestins on leiomyoma and myometrial smooth muscle cell growth and transforming growth factor-beta expression. *Mol Hum Reprod*. 2002;8(12):1071–1078. doi:10.1093/molehr/8.12.1071
15. Kaartinen V, Warburton D. Fibrillin controls TGF-beta activation. *Nat Genet*. 2003;33(3):331–332. doi:10.1038/ng0303-331
16. Matsumoto T, Motoya S, Watanabe K, et al. Adalimumab monotherapy and a combination with azathioprine for Crohn's disease: A prospective, randomized trial. *J Crohns Colitis*. 2016;10(11):1259–1266. doi:10.1093/ecco-jcc/jjw152
17. Burmester GR, Landewé R, Genovese MC, et al. Adalimumab long-term safety: Infections, vaccination response and pregnancy outcomes in patients with rheumatoid arthritis. *Ann Rheum Dis*. 2017;76(2):414–417. doi:10.1136/annrheumdis-2016-209322
18. Barrier BF, Bates GW, Leland MM, Leach DA, Robinson RD, Propst AM. Efficacy of anti-tumor necrosis factor therapy in the treatment of spontaneous endometriosis in baboons. *Fertil Steril*. 2004;81(Suppl 1):775–779. doi:10.1016/j.fertnstert.2003.09.034
19. Falconer H, Mwenda JM, Chai DC, et al. Treatment with anti-TNF monoclonal antibody (c5N) reduces the extent of induced endometriosis in the baboon. *Hum Reprod*. 2006;21(7):1856–1862. doi:10.1093/humrep/del044
20. Pelch KE, Sharpe-Timms KL, Nagel SC. Mouse model of surgically-induced endometriosis by auto-transplantation of uterine tissue. *J Vis Exp*. 2012;59:e3396. doi:10.3791/3396
21. Yilmaz M, Tekekoglu S, Herek O, Ozmen O, Sahinduran Ş, Buyukoglu T. Ameliorative effect of adalimumab on experimentally induced acute pancreatitis in rats. *Pancreas*. 2010;39(8):1238–1242. doi:10.1097/MPA.0b013e3181dec1a6
22. Yavuz E, Oktem M, Esinler I, Toru SA, Zeyneloglu HB. Genistein causes regression of endometriotic implants in the rat model. *Fertil Steril*. 2007;88(4 Suppl):1129–1134. doi:10.1016/j.fertnstert.2007.01.010
23. Esterbauer H, Cheeseman KH. Determination of aldehydic lipid peroxidation products: Malonaldehyde and 4-hydroxynonenal. *Methods Enzymol*. 1990;186:407–421. doi:10.1016/0076-6879(90)86134-h
24. Yun BH, Chon SJ, Choi YS, Cho S, Lee BS, Seo SK. Pathophysiology of endometriosis: Role of high mobility group box-1 and toll-like receptor 4 developing inflammation in endometrium. *PLoS One*. 2016;11(2):e0148165. doi:10.1371/journal.pone.0148165
25. Santanam N, Kavtaradze N, Murphy A, Dominguez C, Parthasarathy S. Antioxidant supplementation reduces endometriosis-related pelvic pain in humans. *Transl Res*. 2013;161(3):189–195. doi:10.1016/j.trsl.2012.05.001
26. Donnez J, Binda MM, Donnez O, Dolmans MM. Oxidative stress in the pelvic cavity and its role in the pathogenesis of endometriosis. *Fertil Steril*. 2016;106(5):1011–1017. doi:10.1016/j.fertnstert.2016.07.1075
27. Harlev A, Gupta S, Agarwal A. Targeting oxidative stress to treat endometriosis. *Expert Opin Ther Targets*. 2015;19(11):1447–1464. doi:10.1517/14728222.2015.1077226
28. Siracusa R, D'Amico R, Impellizzeri D, et al. Autophagy and mitophagy promotion in a rat model of endometriosis. *Int J Mol Sci*. 2021;22(10):5074. doi:10.3390/ijms22105074
29. Cordaro M, Trovato Salinaro A, Siracusa R, et al. Hidrox® and endometriosis: Biochemical evaluation of oxidative stress and pain. *Antioxidants (Basel)*. 2021;10(5):720. doi:10.3390/antiox10050720
30. Siracusa R, D'Amico R, Cordaro M, et al. The methyl ester of 2-cyano-3,12-dioxooleana-1,9-dien-28-oic acid reduces endometrial lesions development by modulating the NFkB and Nrf2 pathways. *Int J Mol Sci*. 2021;22(8):3991. doi:10.3390/ijms22083991
31. Genovese T, Siracusa R, D'Amico R, et al. Regulation of inflammatory and proliferative pathways by fotemustine and dexamethasone in endometriosis. *Int J Mol Sci*. 2021;22(11):5998. doi:10.3390/ijms22115998
32. Dmowski PW, Braun DP. Immunology of endometriosis. *Best Pract Res Clin Obstet Gynaecol*. 2004;18(2):245–263. doi:10.1016/j.bpobgyn.2004.02.001
33. Kyama CM, Overbergh L, Debrock S, et al. Increased peritoneal and endometrial gene expression of biologically relevant cytokines and growth factors during the menstrual phase in women with endometriosis. *Fertil Steril*. 2006;85(6):1667–1675. doi:10.1016/j.fertnstert.2005.11.060
34. Arici A, Oral E, Attar E, Tazuke SI, Olive DL. Monocyte chemotactic protein-1 concentration in peritoneal fluid of women with endometriosis and its modulation of expression in mesothelial cells. *Fertil Steril*. 1997;67(6):1065–1072. doi:10.1016/s0015-0282(97)81440-9
35. Arici A. Local cytokines in endometrial tissue: The role of interleukin-8 in the pathogenesis of endometriosis. *Ann N Y Acad Sci*. 2002;955:101–406. doi:10.1111/j.1749-6632.2002.tb02770.x
36. Eraldemir FC, Keleş CD, Kum T, Vural B, Baydemir C. The effect of etanercept treatment on serum malonaldialdehyde levels in experimental endometriosis rat model. *KOU Sag Bil Derg*. 2015;1(1):26–29. doi:10.30934/kusbed.349539
37. Lorena D, Darby IA, Reinhardt DP, Sapin V, Rosenbaum J, Desmoulière A. Fibrillin-1 expression in normal and fibrotic rat liver and in cultured hepatic fibroblastic cells: Modulation by mechanical stress and role in cell adhesion. *Lab Invest*. 2004;84(2):203–212. doi:10.1038/labinvest.3700023
38. Bouzeghrane F, Reinhardt DP, Reudelhuber TL, Thibault G. Enhanced expression of fibrillin-1, a constituent of the myocardial extracellular matrix in fibrosis. *Am J Physiol Heart Circ Physiol*. 2005;289(3):H982–H991. doi:10.1152/ajpheart.00151.2005

39. Son ED, Lee JY, Lee S, et al. Topical application of 17beta-estradiol increases extracellular matrix protein synthesis by stimulating TGF-beta signaling in aged human skin in vivo. *J Invest Dermatol*. 2005; 124(6):1149–1161. doi:10.1111/j.0022-202X.2005.23736.x
40. Zhao Y, Wen Y, Polan ML, Qiao J, Chen BH. Increased expression of latent TGF-beta binding protein-1 and fibrillin-1 in human uterine leiomyomata. *Mol Hum Reprod*. 2007;13(5):343–349. doi:10.1093/molehr/gam007
41. Hendriks AG, van der Velden HM, Wolberink EA, et al. The effect of adalimumab on key drivers in the pathogenesis of psoriasis. *Br J Dermatol*. 2014;170(3):571–580. doi:10.1111/bjd.12705

The effects of taxifolin on neuropathy related with hyperglycemia and neuropathic pain in rats: A biochemical and histopathological evaluation

Murat Alay[1,A,B,D,F], Miyase Gulcin Sonmez[2,B,E,F], Aysegul Sakin[3,C,E,F], Murat Atmaca[4,C,E,F], Halis Suleyman[5,B,F], Gulce Naz Yazici[6,C,F], Abdulkadir Coban[7,C,F], Bahadir Suleyman[5,B,F], Seval Bulut[5,E,F], Durdu Altuner[5,A,D,F]

[1] Department of Endocrinology and Metabolism, Van Yuzuncu Yil University School of Medicine, Turkey
[2] Department of Internal Medicine, Van Yuzuncu Yil University School of Medicine, Turkey
[3] Department of Internal Medicine, Van Training and Research Hospital, University of Health Sciences, Turkey
[4] Department of Endocrinology and Metabolism, School of Medicine, Medipol University, Istanbul, Turkey
[5] Department of Pharmacology, School of Medicine, Erzincan Binali Yıldırım University, Turkey
[6] Department of Histology and Embryology, Faculty of Medicine, Erzincan Binali Yıldırım University, Turkey
[7] Department of Biochemistry, School of Medicine, Erzincan Binali Yıldırım University, Turkey

A – research concept and design; B – collection and/or assembly of data; C – data analysis and interpretation; D – writing the article; E – critical revision of the article; F – final approval of the article

Advances in Clinical and Experimental Medicine, ISSN 1899–5276 (print), ISSN 2451–2680 (online) *Adv Clin Exp Med*. 2022;31(4):427–435

Address for correspondence
Durdu Altuner
E-mail: durdualtuner@hotmail.com

Funding sources
None declared

Conflict of interest
None declared

Received on September 1, 2021
Reviewed on November 11, 2021
Accepted on November 16, 2021

Published online on February 17, 2022

Abstract

Background. Hyperglycemia can be considered a determining factor in the development of diabetic neuropathy as well as neuropathic pain. There is a relationship between the excessive production of reactive oxygen species (ROS) and the pathogenesis of diabetic neuropathic pain. Taxifolin, on the other hand, is a flavonoid that has been documented to inhibit ROS production.

Objectives. To investigate the effects of taxifolin, which has antioxidant and neuroprotective effects, on alloxan-induced hyperglycemia-induced neuropathy and neuropathic pain, biochemically and histopathologically.

Materials and methods. The albino Wistar male rats were divided into 3 groups: healthy group (HG), only alloxan group (AXG) and alloxan+taxifolin group (ATG). Hyperglycemia in animals was caused through intraperitoneal injection of alloxan at a dose of 120 mg/kg. Paw pain thresholds of animals were measured using Basile algesimeter. Sciatic nerve tissues were examined biochemically and histopathologically in order to evaluate neuropathy.

Results. Our experimental results revealed that taxifolin significantly prevented the increase of plasma glucose concentration level with alloxan administration, the decrease of the paw pain threshold related to hyperglycemia, the change of oxidant–antioxidant balance in the sciatic nerve tissue in favor of oxidants, and the deterioration of tissue morphology in animals.

Conclusions. Our experimental results indicate that taxifolin alleviates alloxan-induced hyperglycemia-related neuropathy and neuropathic pain.

Key words: hyperglycemia, rats, neuropathic pain, neuropathy, taxifolin

Cite as
Alay M, Sonmez MG, Sakin A, et al. The effects of taxifolin on neuropathy related with hyperglycemia and neuropathic pain in rats: A biochemical and histopathological evaluation. *Adv Clin Exp Med*. 2022;31(4):427–435. doi:10.17219/acem/144002

DOI
10.17219/acem/144002

Background

Peripheral nerve damage is usually caused by compression, various traumas, and ischemic and metabolic disorders.[1] Hyperglycemia, which is the main symptom of diabetes mellitus (DM), a metabolic disease, occurs due to the absence of insulin secreted by pancreatic cells, or the decrease in the sensitivity of target cells to insulin.[2] The risk of developing chronic peripheral neuropathy has been recorded as 30–50% in diabetic patients. Peripheral neuropathy is a significant complication of DM which can cause foot ulcers and lower extremity amputation.[3] Hyperglycemia is a determining factor in the development of diabetic neuropathy. In DM, it may lead to the deterioration of motor and sensory nerve conduction velocity.[4] Hyperglycemia has been reported to cause neuropathy also in individuals without DM.[5] It has also been described to have a role in the formation of neuropathic pain in both animal models and diabetic patients.[6] Nearly 30% of patients with DM develop chronic neuropathic pain.[2] Even though many scientific studies related to diabetic neuropathy exist, its pathogenesis is still not fully explained. Former studies have suggested that excessive mitochondrial glucose loading increases electron transfer to oxygen and the production of reactive oxygen species (ROS).[7,8] Reactive oxygen species facilitate the production of toxic products and lead to the oxidation of cell membrane lipids.[9] Lipid peroxidation (LPO) caused through increased ROS as a result of hyperglycemia, has been shown to be important in the development of DM complications.[10] Moustafa et al. reported that the amount of malondialdehyde (MDA), one of the LPO end products, increased significantly in the sciatic nerve tissue of rats with DM.[11] Galeshkalami et al. have shown that hyperglycemia, which causes diabetic neuropathy, leads to the generation of ROS in neurons and their subsequent death. In addition, they stated that increasing total antioxidant status (TAS) and glutathione (GSH) in neurons, and preventing the increase of ROS and LPO are associated with neuroprotection.[12] Solanki and Bhavsar revealed that the pain threshold decreased in diabetic rats having high oxidant levels and low antioxidant levels.[13] It has also been revealed that neuropathy developing in diabetic rats causes significant hyperalgesia.[14] The acquired information suggest that antioxidants may be useful in the treatment of diabetic neuropathy and neuropathic pain. In neuropathic pain, anti-inflammatory drug treatments are recommended to control neuroinflammation.[15] Today, opioids, tricyclic antidepressants and anticonvulsants, which have significant side effects, are used in the treatment of neuropathic pain. Therefore, research has focused on identifying alternative treatments with fewer side effects.[16]

Taxifolin (dihydroquercetin) is an antioxidant flavonoid which has been tested against diabetic neuropathy and neuropathic pain in this study.[17] Taxifolin has numerous pharmacological effects, including antioxidant, anti-inflammatory, antiviral, antibacterial, anticancer, as well as neuroprotective activities. Moreover, taxifolin was documented to inhibit the production of ROS, which suggests that taxifolin may be useful in the treatment of hyperglycemia-induced neuropathy and neuropathic pain.[18] In the literature, there is no information about the protective effect of taxifolin against hyperglycemia-related neuropathy and neuropathic pain.

Objectives

The aim of this study was to biochemically and histopathologically investigate the effect of taxifolin on alloxan-induced hyperglycemia-induced neuropathy and neuropathic pain in rats, as well as to examine the relationship of hyperglycemia-related neuropathy and neuropathic pain with oxidative stress, and to assess the benefits of the antioxidant therapy.

Materials and methods

Animals

A total of 18 albino Wistar male rats weighing from 235 g to 247 g were used for the experiment. The animals were obtained from Ataturk University Medical Experimental Application and Research Center (Erzurum, Turkey). Prior to the experiment, the animals were housed and fed for 1 week at normal room temperature (22°C) in the appropriate laboratory environment. The protocols and procedures were approved by the local Ataturk University Animal Experimentation Ethics Committee (meeting No. 2020/06, March 6, 2020).

Chemicals

Sodium thiopental (1 g solution for injection) utilized within the experiment was purchased from IE Ulagay (Istanbul, Turkey), while alloxan (Cat. No. A7413, 25 g, >98% purity) was provided by Sigma (St. Louis, USA). Taxifolin, each tablet containing 25 mg of dihydroquercetin, was obtained from Evalar (Biysk, Russia).

Experimental groups

The animals utilized in our study were divided into 3 groups (6 animals in each group): healthy group (HG), only alloxan group (AXG) and alloxan+taxifolin group (ATG).

Inducing diabetes

Alloxan dissolved in distilled water was injected intraperitoneally in rats at a dose of 120 mg/kg for 3 consecutive days in order to induce hyperglycemia. Fasting plasma glucose concentration was measured in blood samples taken from the tail veins of rats at the end of the 3rd month following alloxan

administration. A commercially available blood meter was employed for plasma glucose concentration measurement. Animals having plasma glucose concentration of 250 mg/dL and above were included in the study in line with our study. As it is commonly known, the animals having plasma glucose concentration above 250 mg/dL are considered diabetic.[19]

Experiment procedure

Taxifolin (50 mg/kg) was given orally to the ATG. The same volume of distilled water as a solvent was applied in the same way to the AXG and HG. The cited procedure was repeated once a day for 3 months. Paw pain thresholds of all animal groups were measured using the Basile algesimeter at the 1st, 2nd and 3rd h after the last dose of taxifolin was administered.[20] Immediately following the measurement at the 3rd h, the rats were sacrificed with high-dose thiopental anesthesia and their sciatic nerve tissues were removed. Malondialdehyde, total glutathione (tGSH), total oxidant status (TOS) and TAS capacity were measured in sciatic nerve tissue samples, which were removed later. Furthermore, tissues were examined histopathologically.

Biochemical analyzes

Determination of glucose concentration in plasma

Accu-Chek Performa Nano (Roche, Istanbul, Turkey) glucometer was used to determine the glucose concentration in the blood samples taken from the tail vein.

Preparation of samples

An amount of 0.2 g of nerve tissue was taken from rats thoroughly washed with NaCl (0.9%). Tissues were homogenized in ice cold with a high speed homogenizer. After the homeogenization process, 2 mL of 1.15% potassium chloride buffer solution (pH 7.4) was centrifuged at 10,000 × g at 4°C for 15 min. The obtained supernatants were used for biochemical analyzes, including MDA, tGSH, TOS, and TAS levels.

Measurements of tissue MDA and tGSH

Malondialdehyde measurements are based on the method utilized by Ohkawa et al., which includes spectrophotometric measurement of the absorbance of the pink-colored complex formed by thiobarbituric acid (TBA) and MDA.[21] Total glutathione measurement was performed, according to the method described by Sedlak and Lindsay.[22]

Measurements of tissue TOS and TAS

Tissue homogenate TOS and TAS levels were determined using a novel automated measurement method and commercially available kits (Rel Assay Diagnostics, Gaziantep, Turkey), both developed by Erel.[23,24] The TAS method is based on the bleaching of a characteristic color of a more stable ABTS (2,2'-azino-bis (3-ethylbenzothiazoline-6-sulfonic acid)) radical cation by antioxidants. The measurements are performed at 660 nm. The results are expressed as nmol H_2O_2 (hydrogen peroxide) equivalent/L. In the TOS method, the oxidants present in the sample oxidized the ferrous ion-o-dianisidine complex to ferric ion. The oxidation reaction was enhanced by glycerol molecules, which are abundantly present in the reaction medium. The ferric ion produced a colored complex with xylenol orange in an acidic medium. The color intensity, which could be measured spectrophotometrically at 530 nm, was related to the total amount of oxidant molecules present in the sample. The results are expressed as μmol Trolox equivalent/L. The percentage ratio of TOS to TAS was used as the oxidative stress index. Oxidative stress index was calculated as TOS divided by 100 × TAS.

Histopathological examination

All of the tissue samples were first identified in a 10% formaldehyde solution for light microscope assessment. Following the identification process, tissue samples were washed under tap water in cassettes for 24 h. Samples were then treated with conventional grade of alcohol (70%, 80%, 90%, and 100%) to remove the water within tissues, which were then passed through xylol and embedded in paraffin. Four-to-five micron sections were cut from the paraffin blocks and hematoxylin and eosin (H&E) staining was administered. Their photos were taken following the Olympus DP2-SAL firmware program (Olympus® Inc., Tokyo, Japan) assessment. Histopathological assessment was carried out by the pathologist blinded for the study groups.

Statistical analysis

The Shapiro–Wilk test was used to determine whether the data obtained from the groups were normally distributed. One-way analysis of variance (ANOVA) test was applied to normally distributed data. In the follow-up, Tukey's or Games–Howell test was performed, according to the results of Levene's test as post hoc test. The Kruskal–Wallis test was applied to the data that did not show normal distribution and Dunn's test was applied as post hoc test. Since the histopathological data were discrete variables, the evaluation was done with the Kruskal–Wallis test. The results from the experiments were expressed as mean value ± standard deviation (X ±SD) or median 1st quartile–3rd quartile (Q1–Q3). Paw pain threshold was evaluated using repeated measures ANOVA. Sphericity was confirmed using Mauchly's test of sphericity. When sphericity had been violated, the Greenhouse–Geisser correction was used. The effect of time and groups were shown as a line chart. All statistical operations were performed with the SPSS v. 22 software (IBM Corp., Armonk, USA), and a value of $p < 0.05$ was considered statistically significant.

Results

Analysis results of glucose concentration in plasma

Three months after alloxan administration, the mean fasting glucose concentration in plasma was 287.8 ±8.1 mg/dL in the AXG, while it was 144 ±4.6 mg/dL and 86.3 ±5 mg/dL in the ATG and HG, respectively. At the end of the 3rd month of taxifolin administration, a statistically significant decrease in the glucose concentration in plasma was achieved in the ATG compared to the AXG ($p < 0.001$) (Table 1, Supplementary Table 1).

Test results of paw pain threshold

As can be seen from Table 2 and Supplementary Table 2, taxifolin significantly prevented the reduction of the pain threshold in animal foot claws with hyperglycemia in the 1st, 2nd and 3rd h. When the AXG was compared to the HG, the pain threshold was statistically significantly decreased ($p < 0.001$). When the ATG was compared with the AXG, the pain threshold increased significantly ($p < 0.001$). Paw pain threshold was evaluated between groups using repeated measures ANOVA. According to the Mauchly's test of sphericity, sphericity had been violated ($\chi^2 = 10.203$, $p = 0.006$) and therefore, the Greenhouse–Geisser correction was used. There has been a significant effect of time on paw pain threshold, $F(1.318, 19.769) = 14.125$, $p = 0.001$. At the same time, the between-group effect was statistically significant ($p < 0.001$). While there was no statistically significant difference between the 1st and 2nd h paw pain threshold measurements of the animals, there was a statistical difference in terms of the 1st and 3rd h measurements and the values measured at the 2nd and 3rd h. Intra-group time-dependent comparisons of paw pain threshold measurements in the HG, AXG and ATG are presented in Table 3 and Supplementary Table 3. The levels of paw pain threshold are shown in Fig. 1. Taxifolin has decreased neuropathic pain in rats with hyperglycemia in the 1st, 2nd and 3rd h by 70.9%, 75.8% and 82%, respectively.

Biochemical findings

MDA and tGSH analysis results

As can be seen from Table 4 and Fig. 2, the development of hyperglycemia in the sciatic nerve tissue of animals, an increase in MDA and a decrease in tGSH created a statistically significant difference in the AXG when compared to the HG ($p < 0.001$). In the values obtained after

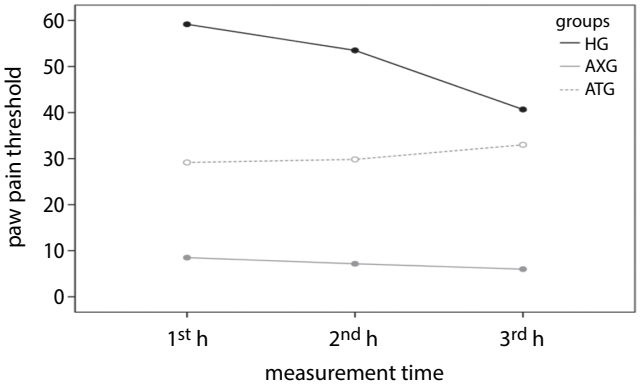

Fig. 1. Evaluation of time-dependent repeated paw pain threshold measures between groups using analysis of variance (ANOVA)

HG – healthy group; AXG – alloxan group; ATG – alloxan+taxifolin group.

Table 1. Analysis of variance (ANOVA) test results and post hoc p-values for group comparisons in plasma glucose concentration analysis

Plasma glucose concentration measurement times	Plasma glucose concentration (mg/dL) X ±SD			ANOVA results		Post hoc test p-values		
	HG	AXG	ATG	F (2,15)	p-value	HG vs AXG	HG vs ATG	AXG vs ATG
Before alloxan*	80.7 ±4.2	79.3 ±2.6	84.2 ±3.9	2.840	0.090	0.803	0.248	0.086
Third month after alloxan*	86.3 ±5.0	287.8 ±8.1	144.0 ±4.6	1742.708	0.001	0.001	0.001	0.001
The difference*	5.7 ±2.1	208.5 ±7.5	59.8 ±6.7	1867.067	0.001	0.001	0.001	0.001

HG – healthy group; AXG – alloxan group; ATG – alloxan+taxifolin group; X ±SD – mean value ± standard deviation. As the post hoc test, *Tukey's honestly significant difference (HSD) test was performed after ANOVA (F (2,15)).

Table 2. Analysis of variance (ANOVA) test results and post hoc p-values for group comparisons, and paw pain threshold and analgesic activity values of the groups

Measurement time	ANOVA results		Post hoc test p-values			Paw pain threshold [g] (X ±SD)			Analgesic effect (%)		
	F (2,15)	p-value	HG vs AXG	HG vs ATG	AXG vs ATG	HG	AXG	ATG	HG	AXG	ATG
1st h*	1141.63	0.001	0.001	0.001	0.001	59.2 ±2.1	8.5 ±1.0	29.2 ±2.1	85.7	–	70.9
2nd h**	137.57	0.001	0.001	0.001	0.001	53.5 ±7.5	7.2 ±0.8	29.8 ±3.7	87.0	–	75.8
3rd h**	254.35	0.001	0.001	0.008	0.001	40.7 ±2.9	6.0 ±0.9	33.0 ±3.7	85.3	–	82.0

HG – healthy group; AXG – alloxan group; ATG – alloxan+taxifolin group; X ±SD – mean value ± standard deviation. As the post hoc test, *Tukey's honestly significant difference (HSD) test or **Games–Howell test was performed after ANOVA (F (2,15)).

Table 3. The effect of time on the paw pain thresholds measured in the study groups

ANOVA results (repeated measures)						Paw pain threshold [g] (X ±SD)		
F (1.32,19.77)		p-value	p-value					
			1st h vs 2nd h	1st h vs 3rd h	2nd h vs 3rd h	1st h	2nd h	3rd h
All groups	14.13	0.001	0.350	0.001	0.037	32.28 ±0.4	30.17 ±1.1	26.56 ±0.7
HG	–	–	0.063	0.001	0.001	59.2 ±2.1	53.5 ±7.5	40.7 ±2.9
AXG	–	–	1.000	0.073	1.000	8.5 ±1.0	7.2 ±0.8	6.0 ±0.9
ATG	–	–	1.000	0.005	0.513	29.2 ±2.1	29.8 ±3.7	33.0 ±3.7

ANOVA – analysis of variance; HG – healthy group; AXG – alloxan group; ATG – alloxan+taxifolin group; X ±SD – mean value ± standard deviation. Since sphericity was violated according to the Mauchly's test of sphericity, the evaluation was made using the Greenhouse–Geisser correction.

taxifolin application, a decrease in MDA and an increase in tGSH were found in the ATG compared to the AXG ($p < 0.001$).

TOS and TAS analysis results

As can be seen from Table 4 and Fig. 3, taxifolin significantly prevented the increase in TOS and decrease in TAS associated with hyperglycemia in the sciatic nerve tissue. When the HG and AXG were compared for TOS and TAS values, a statistically significant difference was observed ($p < 0.01$). There was no significant difference between HG and ATG in terms of TOS values ($p = 0.324$). When the TAS values of the AXG and ATG were compared, a significant difference was observed ($p < 0.001$).

Histopathological findings

As described in Table 5, histological examination of the sciatic nerve of the HG revealed that the nerve structure was normal, axons were surrounded by myelin sheaths and were located centrally, and Schwann cell nuclei and blood capillaries were normal (Fig. 4A). In the AXG, myelinated nerve fibers were swollen, pale and with histopathological changes, while myelinated nerve fibers showed degenerative appearance. Also,

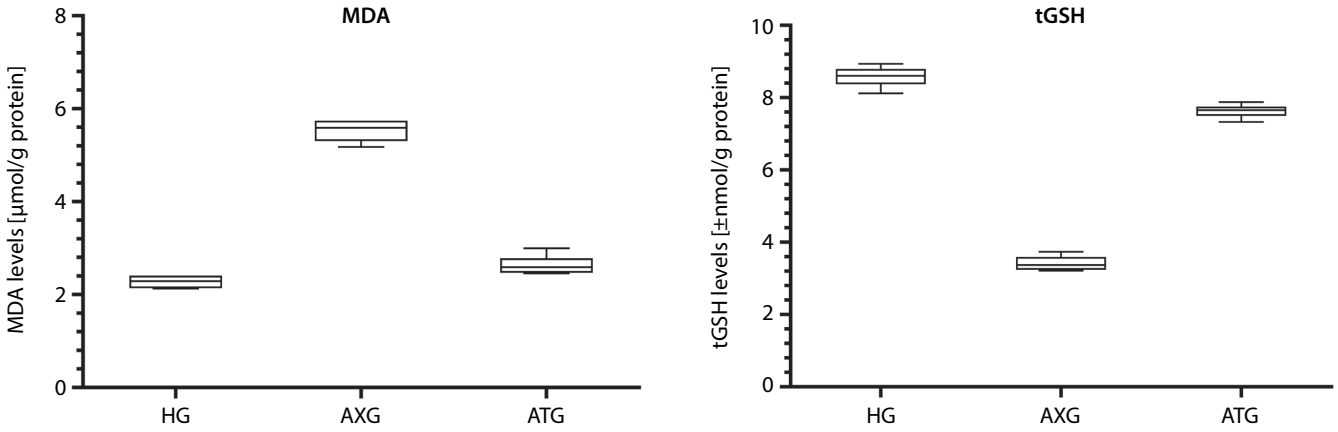

Fig. 2. MDA and tGSH levels in the sciatic nerve tissue of the study groups

Q – quartile; MDA – malondialdehyde; tGSH – total glutathione; HG – healthy group; AXG – alloxan group; ATG – alloxan+taxifolin group; horizontal line – median; bottom line of the box – Q1 (25th); topline of the box – Q3 (75th); whiskers – minimum and maximum observation.

Table 4. Analysis of variance (ANOVA) or Kruskal–Wallis test results and post hoc p-values of group comparisons for MDA, tGSH, TOS, and TAS values

Biochemical parameters	Mean value ± standard deviation or median (Q_1–Q_3)			ANOVA or KW		Post hoc test p-values		
	HG	AXG	ATG	F (2,15) or KW	p-value	HG vs AXG	HG vs ATG	AXG vs ATG
MDA*	2.28 ±0.13	5.53 ±0.23	2.64 ±0.20	517.270	0.001	0.001	0.014	0.001
tGSH*	8.58 ±0.28	3.41 ±0.21	7.63 ±0.18	898.772	0.002	0.001	0.001	0.001
TOS**	15.5 (14.8–17.8)	37.5 (35.3–39.3)	19.0 (16.0–25.3)	11.996	0.001	0.002	0.324	0.192
TAS*	22.83 ±2.48	10.95 ±1.32	19.83 ±1.60	65.663	0.001	0.001	0.035	0.001

Q – quartile; HG – healthy group; AXG – alloxan group; ATG – alloxan+taxifolin group; MDA – malondialdehyde; tGSH – total glutathione; TOS – total oxidant status; TAS – total antioxidant status; KW – Kruskal–Wallis test. As the post hoc test, *Tukey's honestly significant difference (HSD) test was performed after ANOVA (F (2,15)); **Kruskal–Wallis test was used and Dunn's test was performed as post hoc test.

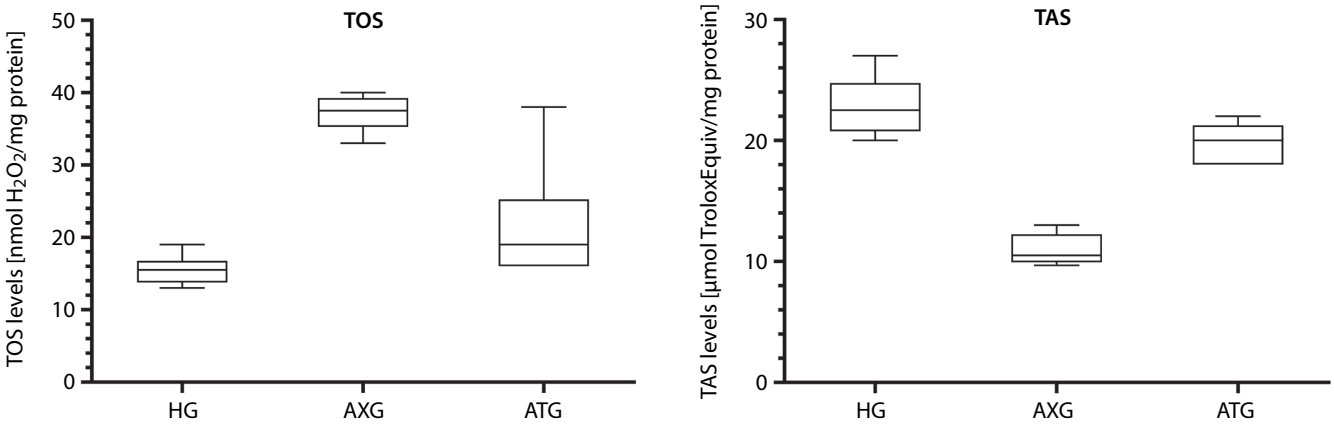

Fig. 3. TOS and TAS levels in the sciatic nerve tissue of the study groups

Q – quartile; TOS – total oxidant status; TAS – total antioxidant status; HG – healthy group; AXG – alloxan group; ATG – alloxan+taxifolin group; horizontal line – median; bottom line of the box – Q1 (25^{th}); topline of the box – Q3 (75^{th}); whiskers – minimum and maximum observation.

myelin sheath that surrounded axons lost its central position. Schwann cells showed hypertrophy and hyperplasia. Locally, myelin sheath degeneration, disorganization and loss were detected. Blood capillaries were dilated and congested (Fig. 4B). When the AXG was compared with the HG, there was a statistically significant difference in terms of myelinated axon degeneration, Schwann cell degeneration and congestion ($p < 0.001$). In rats treated with ATG, myelinated nerve fibers were generally normal in sight and axons were located centrally. Schwann cells were normal in shape, degeneration of myelin sheaths decreased and blood capillaries were also normal (Fig. 4C). When the ATG was compared with the AXG, there was a statistically significant difference in terms of myelinated axon degeneration, Schwann cell degeneration and congestion ($p < 0.001$). There was no significant difference between HG and ATG in terms of congestion ($p = 0.217$).

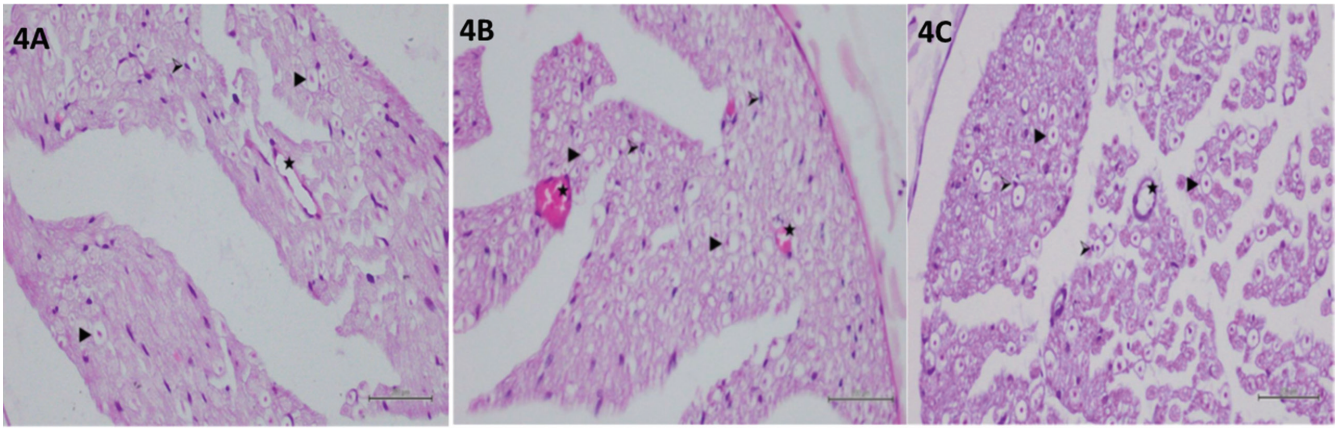

Fig. 4. Histopathological appearance of sciatic nerve tissue in the study groups. A. Hematoxylin and eosin (H&E) staining in sciatic nerve tissue in the healthy group; ▶ – myelinated axon; ➢ – Schwann cell nucleus; ★ – normal blood capillary; ×400 magnification; B. H&E staining in sciatic nerve tissue in the alloxan group; ▶ – swollen and pale degenerative myelinated axon; ➢ – hypertrophic and hyperplastic Schwann cell nucleus; ★ – dilated and congested blood capillary; ×400 magnification; C. H&E staining in sciatic nerve tissue in the alloxan+taxifolin group; ▶ – myelinated axon; ➢ – normal Schwann cell nucleus; ★ – normal blood capillary; ×400 magnification

Table 5. Kruskal–Wallis test results and post hoc p-values for group comparisons in histopathological evaluation

Histopathological change	Median (Q_1–Q_3)			KW results		Post hoc test p-values		
	HG	AXG	ATG	KW	p-value	HG vs AXG	HG vs ATG	AXG vs ATG
Myelinated axon degeneration*	0(0–0)	3(2–3)	1(0–1)	88.954	0.001	0.001	0.009	0.001
Schwann cell degeneration*	0(0–0)	3(2–3)	1(0–1)	90.129	0.001	0.001	0.010	0.001
Congestion*	0(0–0)	2(2–3)	0(0–1)	90.483	0.001	0.001	0.217	0.001

Q – quartile; HG – healthy group; AXG – alloxan group; ATG – alloxan+taxifolin group; KW – Kruskal–Wallis test; *Kruskal–Wallis test was used and Dunn's test was performed as post hoc test.

Discussion

The effect of taxifolin on alloxan-induced hyperglycemia-related neuropathy and neuropathic pain in rats was investigated in this study. Hyperglycemia in rats was performed by applying the method utilized before.[25] Pain is an important manifestation of hyperglycemia-associated neuropathy in animal models and patients with DM.[6] The paw pain threshold of the animals in the AXG, whose glucose concentration in plasma was above 250 mg/dL for 3 months, was observed to be significantly lower compared to the HG and ATG. The reason why we chose the paw of neuropathic pain in animals for the evaluation is because the first symptoms of neuropathy are observed in this area.[26] It was determined that neuropathy developing in diabetic rats caused a significant hyperalgesia in previous studies.[14] Najafi et al. demonstrated the role of LPO in the pathogenesis of diabetic neuropathy.[27] Moustafa et al. reported that the amount of MDA as the last product of LPO increased significantly in the sciatic nerve tissue of rats with DM.[11] In the study of Ince et al., it was reported that the increase in the amount of MDA is directly proportional to the decrease in the pain threshold.[28] In another study, it was shown that MDA has a role in the pathogenesis of nondiabetic neuropathic pain.[29] The literature supports the finding that the MDA value was higher in the AXG compared to the HG and ATG, and the pain threshold was lower.

The role of tGSH in the pathogenesis of neuropathic pain was also investigated in our study. Glutathione is an endogenous antioxidant molecule. It has very important roles in protecting cells from oxidative damage and maintaining redox homeostasis.[30] As it is commonly known, GSH is a tripeptide which contains glutamate, cysteine and glycine. Decreased GSH level triggers the development of neurodegenerative illnesses.[31] It has been reported that the content of GSH and other enzymatic antioxidants decreases significantly in alloxan-induced diabetic pain.[32] The tGSH amount and the paw pain threshold of the AXG was lower compared to the HG and ATG. The TOS and TAS levels were measured to evaluate the relationship between oxidative stress and neuropathic pain in the sciatic nerve tissue in more detail. The TOS and TAS reflect the total effects of all oxidants and antioxidants in tissues.[23,24] The low paw pain threshold in the AXG with high TOS levels and low TAS levels confirm the fact that our experimental results are compatible with the literature information.

Taxifolin significantly decreased the glucose concentration in plasma level increased by alloxan in our study. These findings are in line with the literature. Taxifolin has been shown to decrease carbohydrate absorption by inactivating some of the enzymes involved in carbohydrate metabolism.[33] Rehman et al. revealed that taxifolin inhibits α-amylase enzyme in diabetic animal models and prevents postprandial hyperglycemia.[34] Taxifolin, which suppresses the rise of glucose concentration in plasma caused by alloxan administration, also prevented the decrease of paw pain threshold of rats. No studies investigating the effect of taxifolin on diabetic neuropathy with pain were found in the literature. However, various flavonoids have been reported to alleviate the peripheral neuropathic pain state in different animal species.[35] As it is known, patients with diabetic neuropathy experience burning in their feet or hands in addition to various forms of pain.[35,36]

As stated above, the relation has been determined between diabetic neuropathic pain and oxidant–antioxidant levels.[13] The fact that taxifolin prevented the production of MDA, a product of LPO, from increasing with alloxan, and the decrease of GSH in the sciatic nerve tissue suggests that taxifolin provides a treatment for the pathogenesis of diabetic neuropathic pain. In the experiment, the results of which are in line with our study, an increase of the LPO as well as a decrease of the GSH and other nonenzymatic antioxidants in the diabetic neuropathic pain have been revealed.[18]

In our study, sciatic nerves were examined histopathologically for hyperglycemic neuropathy. The sciatic nerve is widely used in the evaluation of diabetic neuropathy.[32] In addition, the most common site of diabetic neuropathy is peripheral nerve tissues in the lower extremity.[3] As can be seen from our experimental results, taxifolin attenuated the development of myelinated nerve fibers damage (swelling, myelin sheath degeneration, disorganization and loss), hypertrophy and hyperplasia in Schwann cells, vasodilation and congestion. Recent studies have documented degeneration and the presence of demyelinating fibers in the sciatic nerves of diabetic animals.[37] Again, there are studies showing irregular myelin structure and sheath detachment in diabetic rats.[38] It has been reported that various histopathological symptoms such as atrophy of sciatic nerve axons, edema, myelin damage, and loss of myelin develop in diabetic neuropathy.[39] The change in the oxidant–antioxidant balance in the nervous tissue in favor of oxidants indicates that oxidative stress is an important factor in the pathogenesis of diabetic neuropathy.[37] This shows that all our experimental results obtained with taxifolin are in agreement with the literature.

Limitations

Our study has some limitations. In order to clarify the pathogenesis of the treatment of hyperglycemia-related neuropathy and neuropathic pain with taxifolin, proinflammatory cytokine levels, as well as enzymatic antioxidant activity levels such as catalase, superoxide dismutase, glutathione peroxidase, and glutathione reductase, should be investigated.

Conclusions

Alloxan-induced hyperglycemia significantly lowered the paw pain threshold of animals. Hyperglycemia caused oxidative stress in paw tissue. It has been shown

histopathologically that neuropathy develops in the sciatic nerve tissue. Taxifolin prevented the reduction of alloxan-induced hyperglycemia-related paw pain threshold, and the oxidant–antioxidant balance in the sciatic nerve tissue changed in favor of oxidants. Furthermore, taxifolin alleviated the morphological disorders developing in the sciatic nerve. Our experimental results indicate that taxifolin may be useful in the treatment of hyperglycemia-associated neuropathy and neuropathic pain. To clarify the mechanism of treatment with taxifolin, more detailed studies, such as investigations of the proinflammatory cytokines and enzymatic antioxidant activity levels (catalase, superoxide dismutase, glutathione peroxidase, and glutathione reductase), may be useful in providing a treatment for the etiopathogenesis of neuropathic pain in the future.

ORCID iDs

Murat Alay https://orcid.org/0000-0002-5318-9981
Miyase Gulcin Sonmez https://orcid.org/0000-0003-3536-5766
Aysegul Sakin https://orcid.org/0000-0002-8262-6570
Murat Atmaca https://orcid.org/0000-0003-4075-4686
Halis Suleyman https://orcid.org/0000-0002-9239-4099
Gulce Naz Yazici https://orcid.org/0000-0002-6989-997X
Abdulkadir Coban https://orcid.org/0000-0003-1711-5499
Bahadir Suleyman https://orcid.org/0000-0001-5795-3177
Seval Bulut https://orcid.org/0000-0003-4992-1241
Durdu Altuner https://orcid.org/0000-0002-5756-3459

References

1. Gugliandolo E, D'Amico R, Cordaro M, et al. Effect of PEA-OXA on neuropathic pain and functional recovery after sciatic nerve crush. *J Neuroinflammation*. 2018;15(1):264. doi:10.1186/s12974-018-1303-5
2. Nicodemus JM, Enriquez C, Marquez A, Anaya CJ, Jolivalt CG. Murine model and mechanisms of treatment-induced painful diabetic neuropathy. *Neuroscience*. 2017;354:136–145. doi:10.1016/j.neuroscience.2017.04.036
3. Marshall SM, Flyvbjerg A. Prevention and early detection of vascular complications of diabetes. *BMJ*. 2006;333(7566):475–480. doi:10.1136/bmj.38922.650521.80
4. Ward JD, Barnes CG, Fisher DJ, Jessop JD, Baker RW. Improvement in nerve conduction following treatment in newly diagnosed diabetics. *Lancet*. 1971;1(7696):428–430. doi:10.1016/s0140-6736(71)92415-9
5. Marfella R, Verrazzo G, Acampora R, et al. Glutathione reverses systemic hemodynamic changes induced by acute hyperglycemia in healthy subjects. *Am J Physiol*. 1995;268(6 Pt 1):E1167–E1173. doi:10.1152/ajpendo.1995.268.6.E1167
6. Thye-Rønn P, Sindrup SH, Arendt-Nielsen L, Brennum J, Hother-Nielsen O, Beck-Nielsen H. Effect of short-term hyperglycemia per se on nociceptive and non-nociceptive thresholds. *Pain*. 1994;56(1):43–49. doi:10.1016/0304-3959(94)90148-1
7. Wentholt IM, Kulik W, Michels RP, Hoekstra JB, DeVries JH. Glucose fluctuations and activation of oxidative stress in patients with type 1 diabetes. *Diabetologia*. 2008;51(1):183–190. doi:10.1007/s00125-007-0842-6
8. Gadjeva VG, Goycheva P, Nikolova G, Zheleva A. Influence of glycemic control on some real-time biomarkers of free radical formation in type 2 diabetic patients: An EPR study. *Adv Clin Exp Med*. 2017;26(8):1237–1243. doi:10.17219/acem/68988
9. Tosun M, Olmez H, Unver E, et al. Oxidative and pro-inflammatory lung injury induced by desflurane inhalation in rats and the protective effect of rutin. *Adv Clin Exp Med*. 2021;30(9):941–948. doi:10.17219/acem/136194
10. Johansen JS, Harris AK, Rychly DJ, Ergul A. Oxidative stress and the use of antioxidants in diabetes: Linking basic science to clinical practice. *Cardiovasc Diabetol*. 2005;4:5. doi:10.1186/1475-2840-4-5
11. Moustafa PE, Abdelkader NF, El Awdan SA, El-Shabrawy OA, Zaki HF. Liraglutide ameliorated peripheral neuropathy in diabetic rats: Involvement of oxidative stress, inflammation and extracellular matrix remodeling. *J Neurochem*. 2018;146(2):173–185. doi:10.1111/jnc.14336
12. Galeshkalami NS, Abdollahi M, Najafi R, et al. Alpha-lipoic acid and coenzyme Q10 combination ameliorates experimental diabetic neuropathy by modulating oxidative stress and apoptosis. *Life Sci*. 2019;216:101–110. doi:10.1016/j.lfs.2018.10.055
13. Solanki ND, Bhavsar SK. An evaluation of the protective role of *Ficus racemosa* Linn. in streptozotocin-induced diabetic neuropathy with neurodegeneration. *Indian J Pharmacol*. 2015;47(6):610–615. doi:10.4103/0253-7613.169579

Supplementary Table 1. Normality assumption evaluated using The Shapiro–Wilk test

Measurement	Group	Shapiro–Wilk		
		statistic	df	Sig.
Before alloxan	HG	0.874	6	0.245
	AXG	0.979	6	0.945
	ATG	0.899	6	0.368
3rd month after alloxan	HG	0.894	6	0.339
	AXG	0.944	6	0.692
	ATG	0.899	6	0.366
The difference	HG	0.915	6	0.473
	AXG	0.956	6	0.789
	ATG	0.970	6	0.890

The blood glucose measurements in the groups before alloxan, 3 months after alloxan and the difference values showed normal distribution. Analysis of variance (ANOVA) was performed. HG – healthy group; AXG – alloxan group; ATG – alloxan+taxifolin group; df – degrees of freedom.

Supplementary Table 2. Homogeneity of variances assumption

Measurement	Levene's statistic	df1	df2	Sig.
Before alloxan	0.423	2	15	0.662
3rd month after alloxan	0.239	2	15	0.790
The difference	2.215	2	15	0.144

Tukey's honestly significant difference (HSD) test was applied post hoc as the homogeneity of variances before alloxan and 3 months after alloxan, and the difference values were met.

Supplementary Table 3. Normality assumption evaluated using Shapiro–Wilk test

Measurement	Group	Shapiro–Wilk		
		statistic	df	Sig.
1st h	HG	0.890	6	0.317
	AXG	0.960	6	0.820
	ATG	0.892	6	0.331
2nd h	HG	0.963	6	0.841
	AXG	0.866	6	0.212
	ATG	0.920	6	0.503
3rd h	HG	0.958	6	0.804
	AXG	0.853	6	0.167
	ATG	0.898	6	0.362

The 1st, 2nd and 3rd h values were normally distributed in groups. Analysis of variance (ANOVA) was performed. HG – healthy group; AXG – alloxan group; ATG – alloxan+taxifolin group; df – degrees of freedom.

Supplementary Table 4. Homogeneity of variances assumption evaluated for 1st, 2nd and 3rd h values

Measurement	Levene's statistic	df1	df2	Sig.
1st h	1.947	2	15	0.177
2nd h	4.677	2	15	0.026
3rd h	4.643	2	15	0.027

Tukey's honestly significant difference (HSD) test was applied post hoc as the homogeneity of variances for 1st h values were met. For 2nd h and 3rd h values, homogeneity of variances assumption was not met; therefore, the Games–Howell test was applied as post hoc test.

Supplementary Table 5. Normality assumption evaluated using Shapiro–Wilk test

Parameter	Group	Shapiro–Wilk		
		statistic	df	Sig.
MDA	HG	0.859	6	0.186
	AXG	0.890	6	0.320
	ATG	0.879	6	0.265
tGSH	HG	0.976	6	0.931
	AXG	0.928	6	0.563
	ATG	0.972	6	0.907
TOS	HG	0.945	6	0700
	AXG	0.957	6	0.794
	ATG	0.700	6	0.006
TAS	HG	0.957	6	0.794
	AXG	0.885	6	0.295
	ATG	0.908	6	0.425

Malondialdehyde (MDA), total glutathione (tGSH) and total antioxidant status (TAS) were normally distributed in groups. Analysis of variance (ANOVA) was performed. Total oxidant status (TOS) did not met normality assumption; therefore, the Kruskal-Wallis test was chosen. HG – healthy group; AXG – alloxan group; ATG – alloxan+taxifolin group; df – degrees of freedom.

Supplementary Table 6. Homogeneity of variances assumption was evaluated for malondialdehyde (MDA), total glutathione (tGSH) and total antioxidant status (TAS)

Parameter	Levene's statistic	df1	df2	Sig.
MDA	0.877	2	15	0.436
tGSH	0.533	2	15	0.597
TAS	0.919	2	15	0.420

Tukey's honestly significant difference (HSD) test was applied post hoc as the homogeneity of variances for MDA, tGSH and TAS were met.

14. Kishore L, Kaur N, Singh R. Effect of kaempferol isolated from seeds of *Eruca sativa* on changes of pain sensitivity in streptozotocin-induced diabetic neuropathy. *Inflammopharmacology*. 2018;26(4):993–1003. doi:10.1007/s10787-017-0416-2
15. Peritore AF, Siracusa R, Fusco R, et al. Ultramicronized palmitoylethanolamide and paracetamol, a new association to relieve hyperalgesia and pain in a sciatic nerve injury model in rat. *Int J Mol Sci*. 2020;21(10):3509. doi:10.3390/ijms21103509
16. D'Amico R, Impellizzeri D, Cuzzocrea S, Di Paola R. ALIAmides Update: Palmitoylethanolamide and its formulations on management of peripheral neuropathic pain. *Int J Mol Sci*. 2020;21(15):5330. doi:10.3390/ijms21155330
17. Rice-Evans CA, Miller NJ, Paganga G. Structure-antioxidant activity relationships of flavonoids and phenolic acids. *Free Radic Biol Med*. 1996;20(7):933–956. doi:10.1016/0891-5849(95)02227-9
18. Cai C, Liu C, Zhao L, et al. Effects of taxifolin on osteoclastogenesis in vitro and in vivo. *Front Pharmacol*. 2018;9:1286. doi:10.3389/fphar.2018.01286
19. Jaouhari JT, Lazrek HB, Jana M. The hypoglycemic activity of *Zygophyllum gaetulum* extracts in alloxan-induced hyperglycemic rats. *J Ethnopharmacol*. 2000;69(1):17–20. doi:10.1016/s0378-8741(99)00064-1
20. Cadirci E, Suleyman H, Hacimuftuoglu A, Halici Z, Akcay F. Indirect role of beta2-adrenergic receptors in the mechanism of analgesic action of nonsteroidal antiinflammatory drugs. *Crit Care Med*. 2010;38(9):1860–1867. doi:10.1097/CCM.0b013e3181e8ae24
21. Ohkawa H, Ohishi N, Yagi K. Assay for lipid peroxides in animal tissues by thiobarbituric acid reaction. *Anal Biochem*. 1979;95(2):351–358. doi:10.1016/0003-2697(79)90738-3
22. Sedlak J, Lindsay RH. Estimation of total, protein-bound, and nonprotein sulfhydryl groups in tissue with Ellman's reagent. *Anal Biochem*. 1968;25(1):192–205. doi:10.1016/0003-2697(68)90092-4
23. Erel O. A new automated colorimetric method for measuring total oxidant status. *Clin Biochem*. 2005;38(12):1103–1111. doi:10.1016/j.clinbiochem.2005.08.008
24. Erel O. A novel automated method to measure total antioxidant response against potent free radical reactions. *Clin Biochem*. 2004;37(2):112–119. doi:10.1016/j.clinbiochem.2003.10.014
25. Icel E, Icel A, Uçak T, et al. The effects of lycopene on alloxan induced diabetic optic neuropathy. *Cutan Ocul Toxicol*. 2019;38(1):88–92. doi:10.1080/15569527.2018.1530258
26. Perry MC. *The Chemotherapy Source Book*. 4th ed. Philadelphia, USA: Lippincott Williams & Wilkins; 2008.
27. Najafi R, Hosseini A, Ghaznavi H, Mehrzadi S, Sharifi AM. Neuroprotective effect of cerium oxide nanoparticles in a rat model of experimental diabetic neuropathy. *Brain Res Bull*. 2017;131:117–122. doi:10.1016/j.brainresbull.2017.03.013
28. Ince I, Aksoy M, Ahiskalioglu A, et al. A comparative investigation of the analgesic effects of metamizole and paracetamol in rats. *J Invest Surg*. 2015;28(3):173–180. doi:10.3109/08941939.2014.998798
29. Kuyrukluyıldız U, Küpeli İ, Bedir Z, et al. The effect of anakinra on paclitaxel-induced peripheral neuropathic pain in rats. *Turk J Anaesthesiol Reanim*. 2016;44(6):287–294. doi:10.5152/tjar.2016.02212
30. Forman HJ, Zhang H, Rinna A. Glutathione: Overview of its protective roles, measurement, and biosynthesis. *Mol Aspects Med*. 2009;30(1–2):1–12. doi:10.1016/j.mam.2008.08.006
31. Matsumura N, Kinoshita C, Aoyama K. Mechanism of glutathione production in neurons. *Nihon Yakurigaku Zasshi*. 2021;156(1):26–30. doi:10.1254/fpj.20068
32. Yi Z, Shao-Long Y, Ai-Hong W, et al. Protective effect of ethanol extracts of *Hericium erinaceus* on alloxan-induced diabetic neuropathic pain in rats. *Evid Based Complement Alternat Med*. 2015;2015:595480. doi:10.1155/2015/595480
33. Yoon KD, Lee JY, Kim TY, et al. In vitro and in vivo anti-hyperglycemic activities of taxifolin and its derivatives isolated from pigmented rice (*Oryzae sativa* L. cv. Superhongmi). *J Agric Food Chem*. 2020;68(3):742–750. doi:10.1021/acs.jafc.9b04962
34. Rehman K, Chohan TA, Waheed I, Gilani Z, Akash MSH. Taxifolin prevents postprandial hyperglycemia by regulating the activity of α-amylase: Evidence from an in vivo and in silico studies. *J Cell Biochem*. 2019;120(1):425–438. doi:10.1002/jcb.27398
35. Basu P, Basu A. In vitro and in vivo effects of flavonoids on peripheral neuropathic pain. *Molecules*. 2020;25(5):1171. doi:10.3390/molecules25051171
36. Kaur S, Pandhi P, Dutta P. Painful diabetic neuropathy: An update. *Ann Neurosci*. 2011;18(4):168–175. doi:10.5214/ans.0972-7531.1118409
37. Ostovar M, Akbari A, Anbardar MH, et al. Effects of *Citrullus colocynthis* L. in a rat model of diabetic neuropathy. *J Integr Med*. 2020;18(1):59–67. doi:10.1016/j.joim.2019.12.002
38. Ling Q, Liu M, Wu MX, et al. Anti-allodynic and neuroprotective effects of koumine, a Benth alkaloid, in a rat model of diabetic neuropathy. *Biol Pharm Bull*. 2014;37(5):858–864. doi:10.1248/bpb.b13-00843
39. Huang Y, Hu B, Zhu J. Study on the use of quantitative ultrasound evaluation of diabetic neuropathy in the rat sciatic nerve. *Australas Phys Eng Sci Med*. 2016;39(4):997–1005. doi:10.1007/s13246-016-0448-8

Inhibition of miR-205 promotes proliferation, migration and fibrosis of tenocytes through targeting MECP2: Implications for rotator cuff injury

Xiuhua Mao[1,2,A–F], Zhenchun Yin[3,A–F]

[1] Hwa-Mei Hospital, University of Chinese Academy of Sciences, Ningbo, China
[2] Ningbo Institute of Life and Health Industry, University of Chinese Academy of Sciences, China
[3] Department of Plastic and Reconstructive Surgery, Ningbo First Hospital, China

A – research concept and design; B – collection and/or assembly of data; C – data analysis and interpretation; D – writing the article; E – critical revision of the article; F – final approval of the article

Advances in Clinical and Experimental Medicine, ISSN 1899–5276 (print), ISSN 2451–2680 (online) *Adv Clin Exp Med*. 2022;31(4):437–443

Address for correspondence
Zhenchun Yin
E-mail: yzc_05@sina.com

Funding sources
None declared

Conflict of interest
None declared

Received on June 8, 2020
Reviewed on August 19, 2020
Accepted on December 26, 2020

Published online on February 15, 2022

Abstract

Background. The production of inflammatory mediators is critical for tenocytes proliferation and migration, which play an important role in rotator cuff injury repair and regulation of collagen. MicroRNA (miRNA)-205 (miR-205) promotes the secretion of inflammatory factors. The mechanism of the tenocytes regulation by miR-205 remains unknown. In this paper, we showed that miR-205 can regulate the proliferation, migration and fibrosis of tenocytes.

Objectives. To investigate the function and mechanism of miR-205/MeCP2 pathway on the proliferation, migration and fibrosis of rotator cuff tenocytes, in order to provide a new perspective on the repair of rotator cuff tear injury.

Materials and methods. The tenocytes were collected under sterile conditions from the Achilles tendons of Sprague Dawley (SD) rats (weighing 150–200 g). The cells of passages 2–4 were used for the following experiments. All miRNA and vectors were transfected with Lipofectamine 2000. Reverse-transcription quantitative real-time polymerase chain reaction (RT-qPCR), Cell Counting Kit-8 (CCK-8) assay, luciferase reporter assay, and migration assay were performed. Then, immunoblotting analysis and statistical analysis were conducted.

Results. The CCK-8 and migration assay revealed that miR-205 inhibition resulted in increased tenocytes proliferation, migration and fibrosis. The miR-205 reduced the mRNA and protein expression levels of MECP2, which is involved in cell proliferation and migration of tenocytes. The miR-205 inhibited luciferase intensity under the control of the 3'UTRs of MECP2.

Conclusions. The inhibition of MECP2 reversed the effect of miR-205 inhibitor on tenocytes, including the proliferation and migration of tenocytes, indicating that miR-205 may be valuable in miRNA-based therapies for rotator cuff injury.

Key words: microRNA, fibrosis, miR-205, cell proliferation and migration, rotator cuff injury

Cite as
Mao X, Yin Z. Inhibition of miR-205 promotes proliferation, migration and fibrosis of tenocytes through targeting MECP2: Implications for rotator cuff injury. *Adv Clin Exp Med*. 2022;31(4):437–443. doi:10.17219/acem/131961

DOI
10.17219/acem/131961

Background

Rotator cuff injury often leads to pain, limited motion of shoulder and, in general, lowers the quality of life. As a common weighing of shoulder, rotator cuff injury includes several types like injury to tendinopathy, partial tears and complete tears.[1,2] Therefore, novel repair techniques are required. Biologic repair techniques have been considered to be the potential methods of restoring the histological structure. For example, the employment of cytokines and/or certain cells could possibly help in promoting the regeneration of rotator cuff tendons.[3,4]

A tendon is a fibrous cord of connective tissue at the end of a muscle, by which the muscle attaches to a bone or other structure.[5] Tenocytes are the basic functional units of tendons. They synthesize and secrete collagen and other extracellular matrix, and maintain the metabolism of tendon tissue. Tenocytes are essential for the production of the extracellular matrix during the tendon regeneration. Many factors contribute to this progression. For example, bone morphogenetic protein 2 (BMP2) can facilitate tendon repair by helping in the migration and proliferation of tenocytes.[6]

MicroRNAs (miRNAs) have been reported to regulate the expressions of various genes by targeting the 3'UTR of mRNA. This resulted in mRNA degradation or translational repression.[7,8] Increasing evidences demonstrated that miRNAs contribute to various biological processes.[9,10] Among them, miR-205 has been widely used in tumor immune regulation and inflammatory pathway regulation. It has been reported that miR-205 can promote the secretion of inflammatory factors.[11] At the same time, the downregulation of the miR-205 expression can promote the recovery of skin wound,[12] but its research on tendon cell function remains unexplored.

Methyl-CpG-binding protein 2 (MECP2) is a member of the methylated binding protein family and an epigenetic regulator associated with methylated DNA,[13] which was originally considered to repress transcription via its interactions with HDAC-Sin3 complex. Nowadays, with emerging studies, MECP2 has been widely reported to reduce inflammation, pain and injury. Moreover, it may play a role in tendon cell function. The evidence showed that MECP2 can promote myofibroblast differentiation and fibrosis, which are pivotal for wound healing.[14]

Objectives

In this study, we investigated the function and mechanism of miR-205/MECP2 pathway on the proliferation, migration and fibrosis of rotator cuff tenocytes, in order to provide a new perspective on the repair of rotator cuff tear injury.

Materials and methods

Tenocytes culture and transfection

All animal experiments were approved by the ethics committee of Hwa-Mei Hospital (University of Chinese Academy of Sciences, Ningbo, China). The tenocytes were collected under sterile conditions from the Achilles tendons of Sprague Dawley (SD) rats (weighing 150–200 g). The cells of passages 2–4 were used for the following experiments. All miRNA and vectors were transfected with Lipofectamine 2000 (Invitrogen, Waltham, USA).

Reverse transcription quantitative real-time polymerase chain reaction

Total RNA was extracted with TRIzol reagent (Qiagen, Hilden, Germany) and phenol/chloroform methods. An miR-205 RT primer was used for the cDNA synthesis of miR-205, and U6 small nuclear RNA was used as an internal control.

CCK-8 assay

Cell proliferation was measured using the Cell Counting Kit-8 (CCK-8) assay. Briefly, all transfected cells were incubated with CCK-8 for 2 h at 37°C, and the absorbance was assessed at 450 nm.

Migration assay

Tenocytes were incubated, collected and resuspended in Dulbecco's modified Eagle's medium (DMEM) containing 1% fetal bovine serum (FBS). Subsequently, 10^4 tenocytes were seeded onto the upper chamber. The migrated tenocytes were fixed and stained using crystal violet.

Immunoblotting analysis

Then, 50 μg of protein were loaded in 10% sodium dodecyl sulphate–polyacrylamide gel electrophoresis (SDS-PAGE). Rabbit polyclonal antibodies were used as primary antibodies. The bound antibodies were detected with conventional protocols.

Luciferase reporter assay

The DNA fragment corresponding to 3'UTR of MECP2 was cloned into the pmirGLO Vector (Promega, Beijing, China). The HEK-293T cells were seeded in 24-well plates and co-transfected with miR-205 and the wild-type or mutant 3'UTR, and were harvested for protein extraction. Luciferase intensity was examined with the Dual-Luciferase Reporter Gene Assay kit (Promega).

Statistical analyses

All data were presented as median (range, minimum–maximum). The GraphPad Prism v. 7.0 (GraphPad Software, San Diego, USA) and SPSS v. 18.0 software (SPSS Inc., Chicago, USA) were used for calculation. One-way analysis of variance (ANOVA) followed by Tukey's post hoc test were used for comparison among 3 groups. All experiments were repeated in triplicate for both duplicate detection and biological duplication. A value of $p < 0.05$ was considered statistically significant.

Results

Inhibition of mir-205 promotes proliferation, migration and fibrosis of tenocytes

To investigate the role of miR-205 in the tendon repair, the inhibition of miR-205 was achieved in tenocytes by transient transfection with miR-205 inhibitor. Cell proliferation was evaluated using CCK-8 assay (Fig. 1A). The results showed that the inhibition of miR-205 increased tenocytes proliferation, compared with control cells. Also, cell migration was enhanced by inhibition of miR-205 by transwell assay (Fig. 1B). In addition,

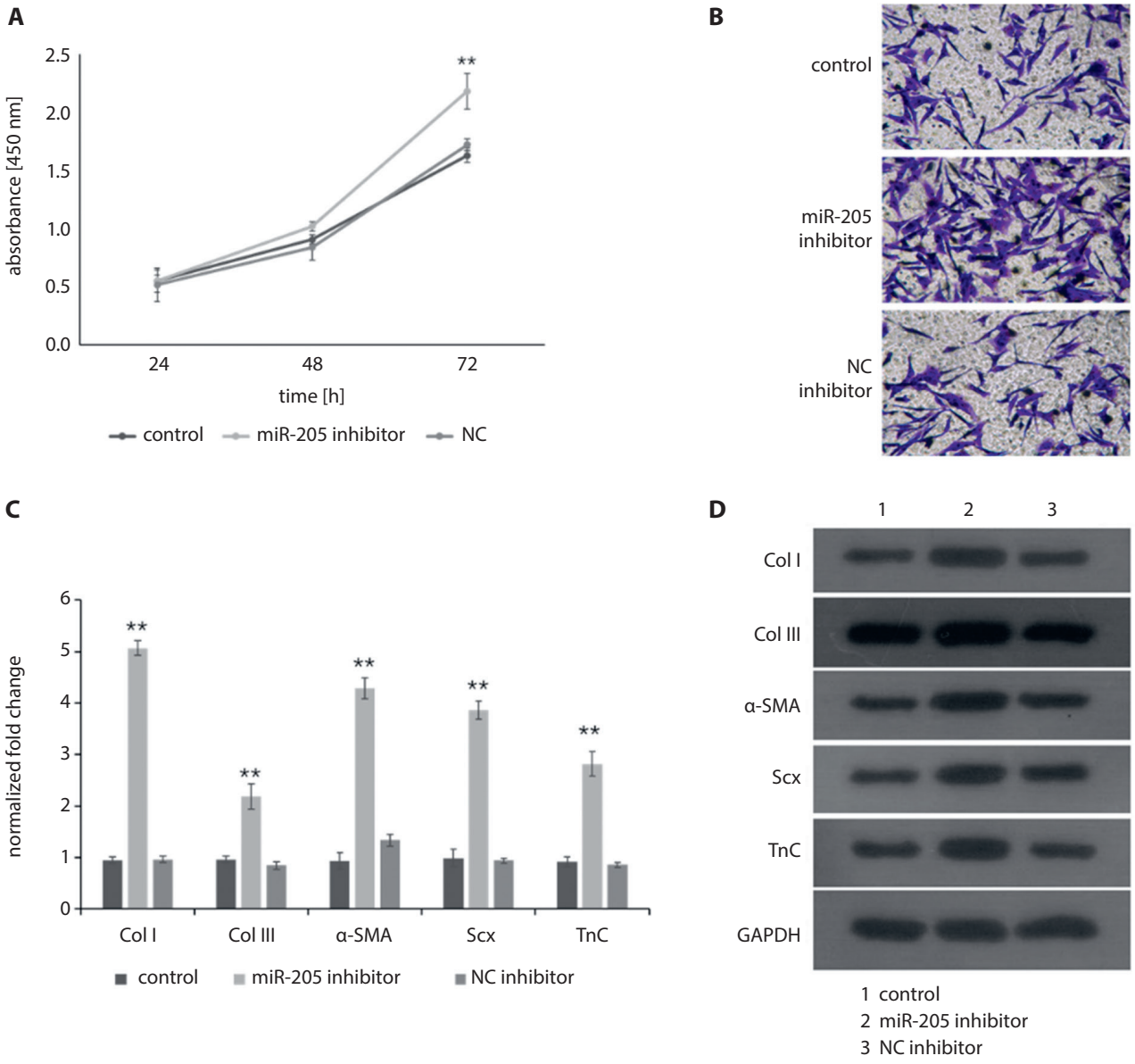

Fig. 1. Inhibition of miR-205 promotes proliferation, migration and fibrosis of tenocytes. Cells were transiently transfected with miR-205 inhibitor or control. A. Cell proliferation was measured with Cell Counting Kit-8 (CCK-8) assay at various timepoints following the transfection; B. Transfected cells were subjected to migration assay. The image displays the cells stained with crystal violet; C. Quantitative reverse-transcription polymerase chain reaction (qRT-PCR) for the mRNA expression levels of the fibrosis markers; D. Protein levels of the fibrosis markers. Data are from experiments repeated in triplicate for both duplicate detection and biological duplication; values are presented as the median (range, minimum–maximum). Boxplots show the minimum value, 1st quartile, median, 3rd quartile, and maximum value. *$p < 0.05$; **$p < 0.01$ compared to negative control (NC)

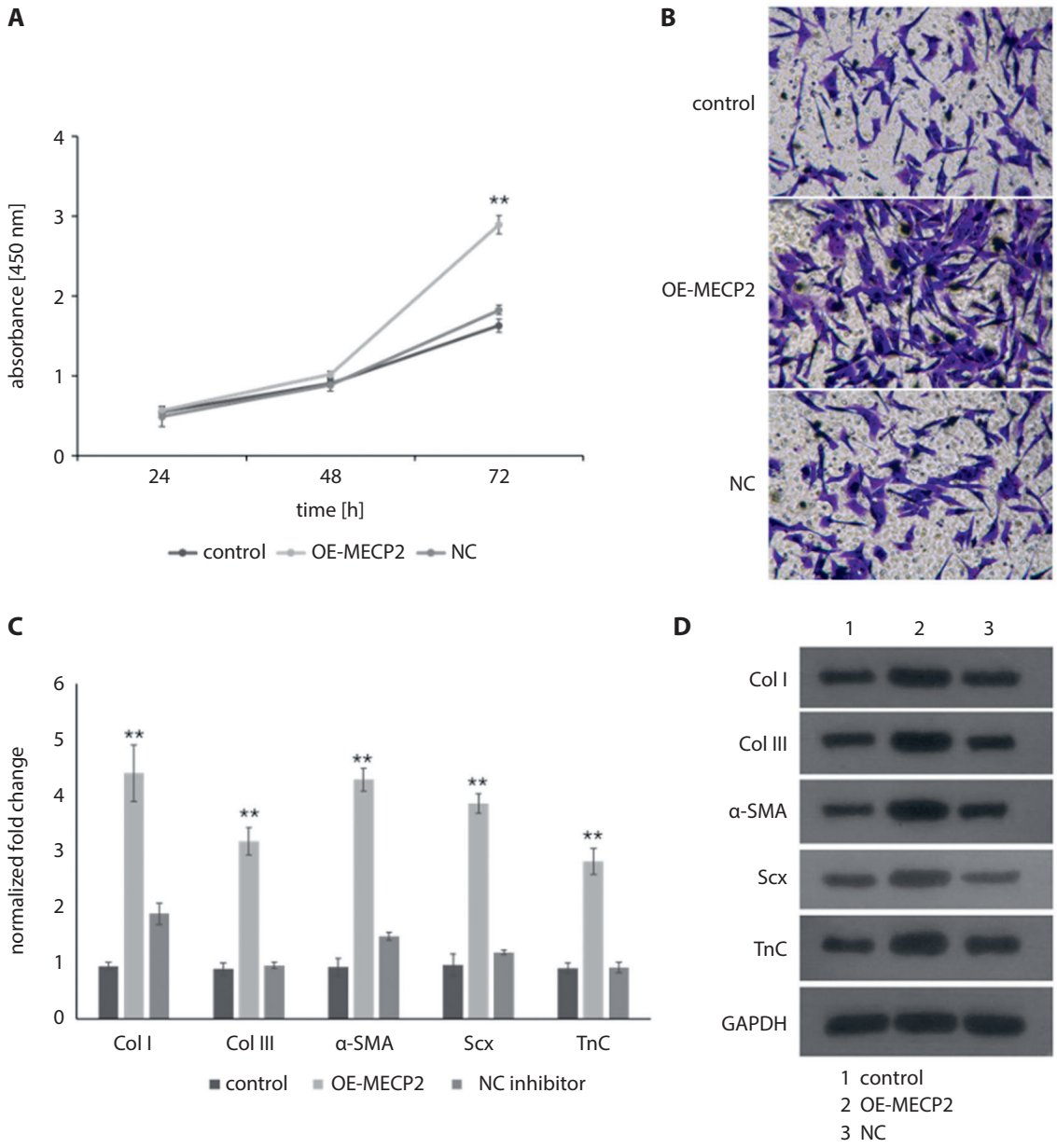

Fig. 2. The MECP2 promotes proliferation, migration and fibrosis of tenocytes. Cells were transiently transfected with MECP2 or control. A. Cell proliferation was measured with Cell Counting Kit-8 (CCK-8) assay at various timepoints following the transfection; B. Transfected cells were subjected to migration assay. The image displays the cells stained with crystal violet; C. Quantitative reverse-transcription polymerase chain reaction (qRT-PCR) for the mRNA expression levels of the fibrosis markers; D. Protein levels of the fibrosis markers. Data from experiments repeated in triplicate for both duplicate detection and biological duplication; values are presented as the median (range, minimum–maximum). Boxplots show the minimum value, 1st quartile, median, 3rd quartile, and maximum value. *p < 0.05; **p < 0.01 compared to negative control (NC)

the mRNA and protein levels of fibrosis maker of tenocytes were detected to be enhanced by inhibition of miR-205, including Col I, Col III, α-SMA, Scleraxis (Scx), and tenascin C (TnC) (Fig. 1C,D). Altogether, these findings demonstrated that the inhibition of miR-205 can promote proliferation, migration and fibrosis of tenocytes.

MECP2 promotes proliferation, migration and fibrosis of tenocytes

To gain more insight into the mechanisms underlying the biological function of MECP2 in the tendon repair progress, the ectopic expression of MECP2 was achieved in tenocytes by transient transfection. The CCK-8 assay was applied to determine cell proliferation, which showed that ectopic expression of MECP2 increased tenocytes proliferation compared with the control cells (Fig. 2A). Cell migration was enhanced by ectopic expression of MECP2 (Fig. 2B) and the levels of fibrosis makers of tenocytes, including Col I, Col III, α-SMA, Scx, and TnC, were also found to be enhanced (Fig. 2C,D). These results demonstrated that the overexpression of MECP2 can promote proliferation, migration and fibrosis of tenocytes.

miR-205 targets and negatively regulates MECP2

To confirm the direct regulation of miR-205 on MECP2, we cloned the 3'UTR-containing miR-205 binding sites (Fig. 3A) and this fragment was inserted into the 3' flank of the reporter gene. Dual luciferase reporter assay (Promega) was performed, and the result demonstrated that miR-205 significantly downregulated luciferase intensity of MECP2 (Fig. 3). To further validate this result, site mutations were introduced into the binding sites. As expected, miR-205 could not change the fluorescence intensity and mRNA level of MECP2 containing the mutant 3'UTR (Fig. 3B,C). Taken together, our studies proved that *MECP2* can be a direct target gene of miR-205.

Inhibition of MECP2 reverses the effect of miR-205 inhibitor on tenocytes

To further explore whether MECP2 participates in the miR-205-mediated proliferation, migration and fibrosis of tenocytes, cells were transfected with control, miR-205 inhibitor, inhibitor plus small interfering RNA against MECP2 (si-MECP2), and the inhibitor plus the negative control siRNA (si-NC). The inhibition of MECP2 reverses the effect of miR-205 inhibitor on tenocytes, including the proliferation and migration of tenocytes caused by miR-205 inhibitor (Fig. 4A,B). Quantitative reverse-transcription polymerase chain reaction (qRT-PCR) and western blot analysis showed that miR-205 inhibitor transfection promoted the protein expression of Col I, Col III, α-SMA, Scx, and TnC, which could be alleviated by downregulated MECP2 in tenocytes (Fig. 4). Together, these results suggested that the inhibition of miR-205 promotes proliferation, migration and fibrosis of tenocytes through targeting MECP2.

Discussion

With the aging of the population and the improvement in the general fitness of the population in China, the number of patients with rotator cuff tears caused by degeneration and sports injury has increased dramatically, and irreparable rotator cuff tear (IRCT) caused by various reasons has become more and more common.[15] Irreparable rotator cuff tear is different from huge rotator cuff tear, since not all huge rotator cuff tears are irreparable.[16] As the name suggests, the torn rotator cuff cannot be repaired in the original footprint area after conventional loosening. In addition, irreparable rotator cuff can affect the quality of tendon due to atrophy and steatosis. Even if its structure is directly repaired, it will fail to function due to its quality defects. The irreparability of rotator cuff is caused by many factors, and its incidence can be as high as 30%.

During the healing process of the tendon injury, double healing mechanisms are observed, which include the division and proliferation of tenocytes, the endogenous healing of repairing tendon rupture and defect, and the exogenous healing participated by the proliferation of tendon adventitia cells. The external healing process will cause

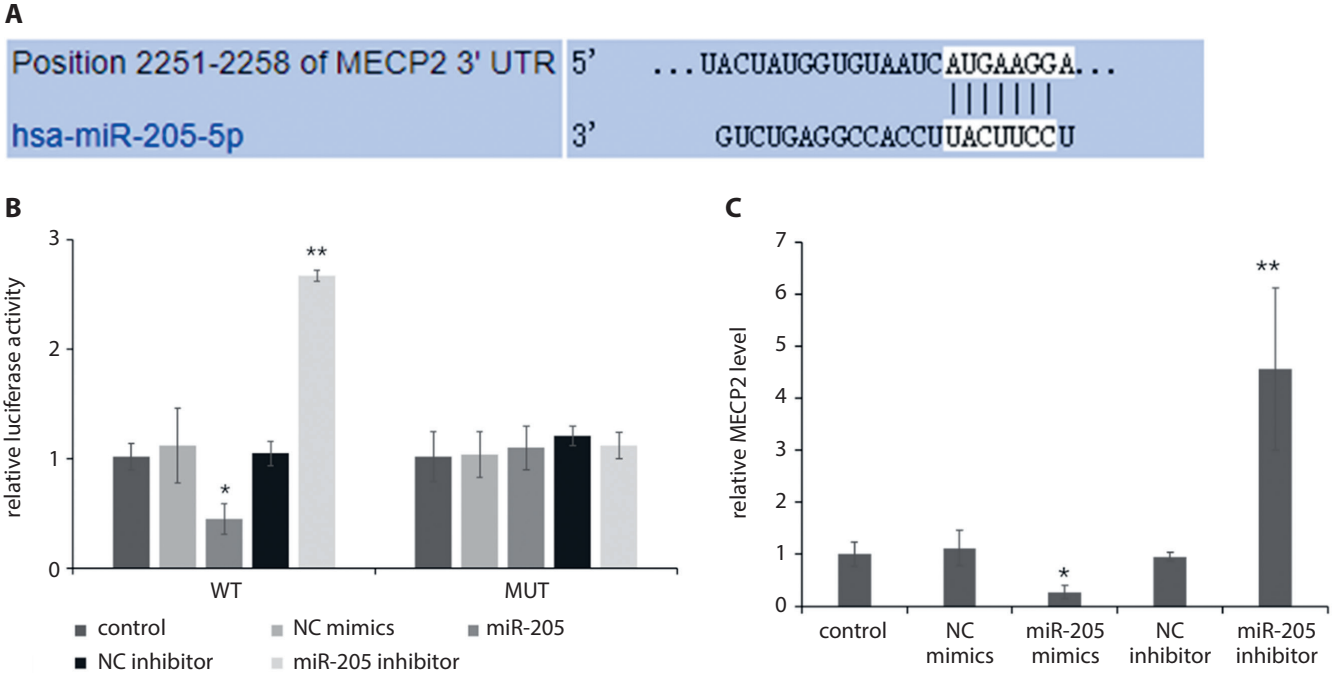

Fig. 3. The miR-205 targeting and negative regulation of MECP2. A. Alignments between miR-96 and the binding sites in the sequences at the 3'UTR of MECP2 mRNA; B. Cells were co-transfected with miR-96 and the WT or mutant 3'UTR of MECP2 mRNA, and subjected to luciferase reporter assay for the analysis of the effect of miR-96 on the intensity controlled by the 3'UTR; C. The mRNA expression level of MECP2 using quantitative reverse-transcription polymerase chain reaction (qRT-PCR). The β-actin was used as an internal control. Boxplots show the minimum value, 1st quartile, median, 3rd quartile, and maximum value. **p < 0.01 compared to mimics negative control (NC); ##p < 0.01 compared to inhibitor NC

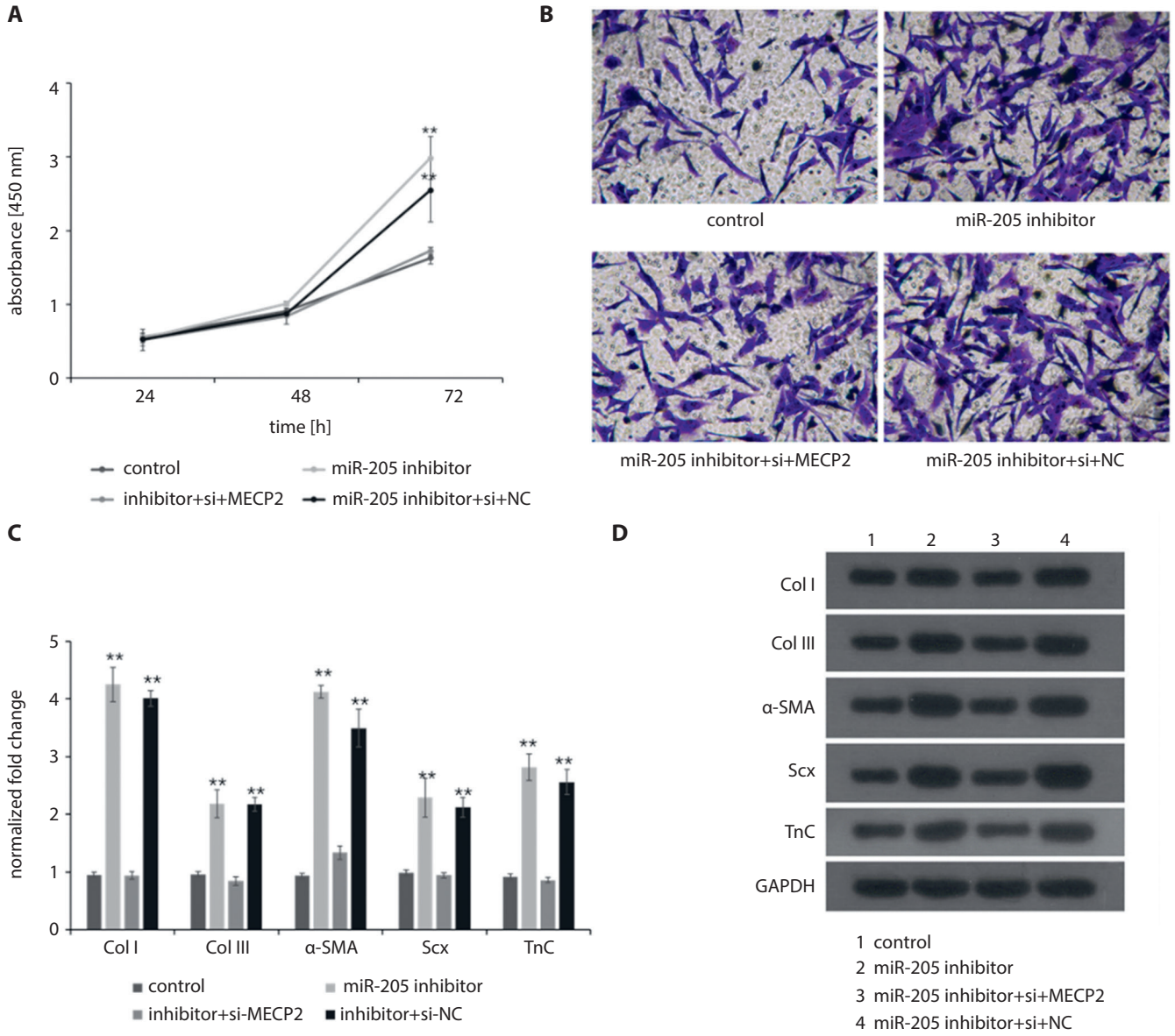

Fig. 4. The inhibition of MECP2 reverses the effect of miR-205 inhibitor on tenocytes. Cells were transiently transfected with miR-205 inhibitor, inhibitor plus small interfering RNA against MECP2 (si-MECP2), and the inhibitor plus the negative control siRNA (si-NC), or control. A. Cell proliferation was measured with Cell Counting Kit-8 (CCK-8) assay at various timepoints following the transfection; B. Transfected cells were subjected to migration assay. The image displays the cells stained with crystal violet; C. Quantitative reverse-transcription polymerase chain reaction (qRT-PCR) for the mRNA expression levels of the fibrosis markers; D. Protein levels of the fibrosis markers. Data from experiments repeated in triplicate for both duplicate detection and biological duplication; values are presented as the median (range, minimum–maximum). Boxplots show the minimum value, 1st quartile, median, 3rd quartile, and maximum value. **p < 0.01 compared to control, ##p < 0.01 compared to miR-205 inhibitor+si-NC

the adhesion between tendon and surrounding tissue, and restrict tendon sliding. It can regulate the proliferation of tenocytes and the internal healing mechanism of tendon dominant, promoting tendon healing and preventing postoperative adhesion of tendon.[17] Related growth factors play a key role in the repair of tendon and other soft tissue injuries.[18] Distinct molecular mechanism underlying the tendon injury, repair and regeneration will have a great influence on the treatment of tendon injury.

The miRNAs have been reported to function as key regulators of various biological processes. There is evidence that tendon injury repair is related to the differentially expressed miRNAs.[19–21] It has also been reported that exogenous miR-29a downregulated BMP2 and BMP12, while miR-26a and miR-30d did not have a significant effect on tenocyte gene expression, suggesting that miR-29a contributes to tendon homeostasis and can serve as a potential therapeutic target in treating tendinopathy.[22] In our study, we observed that the inhibition of miR-205 promoted tenocyte proliferation, migration and fibrosis, which indicated that miR-205 might negatively regulate the progress of tendon injury repair.

The MECP2 can inhibit the transcription of its downstream target genes and play a role in the transcriptional regulation through the specific binding with methylated DNA, thus, it is an important transcriptional inhibitor.[23]

The MECP2 cannot inhibit the corresponding downstream target gene efficiently when its expression is downregulated, which leads to the occurrence of various diseases.[24] It has been reported that MECP2 plays a pivotal role in Rett syndrome pathology and a novel double mutation that can affect the transcription repression domain of MECP2 and cause a severe phenotype of Rett syndrome.[25–27] The results of our study reported here show that MECP2, the target of miR-205 in tenocytes was identified as an important transcriptional inhibitor, which might be a novel critical factor in the proliferation, migration and fibrosis of tenocytes.

Limitations

Given that miR-205 is a 22-mer small RNA differentially expressed in various tissues, targets other than MECP2 should be present in tenocytes. Therefore, whether and how miR-205 regulates proliferation, migration or fibrosis of tenocytes through targeting other factors is still to be studied.

Conclusions

The inhibition of miR-205 could promote the proliferation, migration and fibrosis of tenocytes. In addition, MECP2 is the direct target of miR-205. The miR-205 acts on tenocytes through targeting MECP2. These data implicate a multifactorial effect of miRNA on tenocyte and gene expression. Our findings may provide important information on miRNAs in tenocytes. The results of this study may be valuable for further experimental investigation on the mechanism of the repair of rotator cuff tear injury.

ORCID iDs

Xiuhua Mao https://orcid.org/0000-0003-2726-6813
Zhenchun Yin https://orcid.org/0000-0002-5093-4560

References

1. Longo UG, Candela V, Berton A, et al. Genetic basis of rotator cuff injury: A systematic review. *BMC Med Genet*. 2019;20(1):149. doi:10.1186/s12881-019-0883-y
2. Sharma G, Bhandary S, Khandige G, Kabra U. MR imaging of rotator cuff tears: Correlation with arthroscopy. *J Clin Diagn Res*. 2017;11(5):TC24–TC27. doi:10.7860/JCDR/2017/27714.9911
3. Edwards SL, Lynch TS, Saltzman MD, Terry MA, Nuber GW. Biologic and pharmacologic augmentation of rotator cuff repairs. *J Am Acad Orthop Surg*. 2011;19(10):583–589. doi:10.5435/00124635-201110000-00002
4. Kovacevic D, Rodeo SA. Biological augmentation of rotator cuff tendon repair. *Clin Orthop Relat Res*. 2008;466(3):622–633. doi:10.1007/s11999-007-0112-4
5. Chen J, Xu J, Wang A, Zheng M. Scaffolds for tendon and ligament repair: Review of the efficacy of commercial products. *Expert Rev Med Devices*. 2009;6(1):61–73. doi:10.1586/17434440.6.1.61
6. Lee KW, Lee JS, Kim YS, Shim YB, Jang JW, Lee KI. Effective healing of chronic rotator cuff injury using recombinant bone morphogenetic protein-2 coated dermal patch in vivo. *J Biomed Mater Res B Appl Biomater*. 2017;105(7):1840–1846. doi:10.1002/jbm.b.33716
7. Bartel DP. MicroRNAs: Genomics, biogenesis, mechanism, and function. *Cell*. 2004;116:281–297. doi:10.1016/s0092-8674(04)00045-5
8. Brennecke J, Stark A, Russell RB, Cohen SM. Principles of microRNA-target recognition. *PLoS Biol*. 2005;3(3):e85. doi:10.1371/journal.pbio.0030085
9. Ambros V. The functions of animal microRNAs. *Nature*. 2004;431(7006):350–355. doi:10.1038/nature02871
10. Dubin JA, Greenberg DR, Iglinski-Benjamin KC, Abrams GD. Effect of micro-RNA on tenocytes and tendon-related gene expression: A systematic review. *J Orthop Res*. 2018;36(11):2823–2829. doi:10.1002/jor.24064
11. Yeh DW, Chen YS, Lai CY, et al. Downregulation of COMMD1 by miR-205 promotes a positive feedback loop for amplifying inflammatory- and stemness-associated properties of cancer cells. *Cell Death Differ*. 2016;23(5):841–852. doi:10.1038/cdd.2015.147
12. Wang T, Zhao N, Long S, et al. Downregulation of miR-205 in migrating epithelial tongue facilitates skin wound re-epithelialization by derepressing ITGA5. *Biochim Biophys Acta*. 2016;1862(8):1443–1452. doi:10.1016/j.bbadis.2016.05.004
13. He Y, Tsou PS, Khanna D, Sawalha AH. Methyl-CpG-binding protein 2 mediates antifibrotic effects in scleroderma fibroblasts. *Ann Rheum Dis*. 2018;77(8):1208–1218.
14. Mann J, Oakley F, Akiboye F, Elsharkawy A, Thorne AW, Mann DA. Regulation of myofibroblast transdifferentiation by DNA methylation and MeCP2: Implications for wound healing and fibrogenesis. *Cell Death Differ*. 2007;14(2):275–285. doi:10.1038/sj.cdd.4401979
15. Oh JH, Park MS, Rhee SM. Treatment strategy for irreparable rotator cuff tears. *Clin Orthop Surg*. 2018;10(2):119–134. doi:10.4055/cios.2018.10.2.119
16. Dines DM, Moynihan DP, Dines J, McCann P. Irreparable rotator cuff tears: What to do and when to do it: The surgeon's dilemma. *J Bone Joint Surg Am*. 2006;88(10):2294–2302. doi:10.2106/00004623-200610000-00025
17. Smietana MJ, Moncada-Larrotiz P, Arruda EM, Bedi A, Larkin LM. Tissue engineered tendon for enthesis regeneration in a rat rotator cuff model. *Biores Open Access*. 2017;6(1):47–57. doi:10.1089/biores.2016.0042
18. Randelli P, Randelli F, Ragone V, et al. Regenerative medicine in rotator cuff injuries. *Biomed Res Int*. 2014;2014:129515. doi:10.1155/2014/129515
19. Maurer B, Stanczyk J, Jüngel A, et al. MicroRNA-29, a key regulator of collagen expression in systemic sclerosis. *Arthritis Rheum*. 2010;62(6):1733–1743. doi:10.1002/art.27443
20. Zhang M, Gong W, Zuo B, et al. The microRNA miR-33a suppresses IL-6-induced tumor progression by binding Twist in gallbladder cancer. *Oncotarget*. 2016;7(48):78640–78652. doi:10.18632/oncotarget.12693
21. Dubin JA, Greenberg DR, Iglinski-Benjamin KC, Abrams GD. Effect of micro-RNA on tenocytes and tendon-related gene expression: A systematic review. *J Orthop Res*. 2018;36(11):2823–2829. doi:10.1002/jor.24064
22. Xiao M, Iglinski-Benjamin KC, Sharpe O, Robinson WH, Abrams GD. Exogenous micro-RNA and antagomir modulate osteogenic gene expression in tenocytes. *Exp Cell Res*. 2019;378(2):119–123. doi:10.1016/j.yexcr.2019.03.008
23. Nan X, Ng HH, Johnson CA, et al. Transcriptional repression by the methyl-CpG-binding protein MeCP2 involves a histone deacetylase complex. *Nature*. 1998;393(6683):386–389. doi:10.1038/30764
24. Lombardi LM, Baker SA, Zoghbi HY. MECP2 disorders: From the clinic to mice and back. *J Clin Invest*. 2015;125(8):2914–2923. doi:10.1172/JCI78167
25. Sharifi O, Yasui DH. The molecular functions of MeCP2 in Rett syndrome pathology. *Front Genet*. 2021;12:624290. doi:10.3389/fgene.2021.624290
26. Good KV, Vincent JB, Ausió J. MeCP2: The genetic driver of Rett syndrome epigenetics. *Front Genet*. 2021;12:620859. doi:10.3389/fgene.2021.620859
27. Ghorbel R, Ghorbel R, Rouissi A, et al. First report of an unusual novel double mutation affecting the transcription repression domain of MeCP2 and causing a severe phenotype of Rett syndrome: Molecular analyses and computational investigation. *Biochem Biophys Res Commun*. 2018;497(1):93–101. doi:10.1016/j.bbrc.2018.02.029

Cardiorenal syndrome: Decongestion in heart failure across wide spectrum of kidney pathophysiology

Aneta Kosiorek[1,B,D–F], Jan Biegus[1,B,E,F], Piotr Rozentryt[2,3,D–F], Magdalena Hurkacz[4,E,F], Robert Zymliński[1,A,D–F]

[1] Institute of Heart Diseases, Wroclaw Medical University, Poland
[2] Department of Toxicology and Health Protection, Faculty of Health Sciences in Bytom, Medical University of Silesia in Katowice, Bytom, Poland
[3] Department of Cardiology, Faculty of Medical Sciences in Zabrze, Silesian Centre for Heart Disease, Medical University of Silesia, Zabrze, Poland
[4] Department of Clinical Pharmacology, Wroclaw Medical University, Poland

A – research concept and design; B – collection and/or assembly of data; C – data analysis and interpretation;
D – writing the article; E – critical revision of the article; F – final approval of the article

Advances in Clinical and Experimental Medicine, ISSN 1899–5276 (print), ISSN 2451–2680 (online) *Adv Clin Exp Med*. 2022;31(4):445–455

Address for correspondence
Aneta Kosiorek
E-mail: anetakosiorek7@gmail.com

Funding sources
None declared

Conflict of interest
None declared

Received on September 22, 2021
Reviewed on October 19, 2021
Accepted on November 29, 2021

Published online on January 7, 2022

Abstract

Heart failure (HF) is a pathophysiologically complex disease that is exceptionally heterogeneous in terms of its etiology. It is associated with unsatisfactorily high mortality, both in-hospital and post-discharge, as well as with very frequent rehospitalizations. High phenotypic variability, coexistence of various hemodynamic disorders (such as changes in systemic and pulmonary vascular resistance, increased central venous pressure, impaired heart cardiac output, and fluid overload) and coexisting metabolic and neurohormonal disorders may eventually lead to impaired systemic perfusion. Congestion that impairs renal perfusion has a significant impact on both glomerular filtration and the renal tubular function. This review article discusses the importance of changes caused by HF in various nephron segments, phenotyping of cardiorenal syndromes, the role of effective natriuresis in decongestion, and the importance of known and new diagnostic biomarkers in predicting renal dysfunction. A better understanding of cardiac and renal interactions may help in selecting an effective, efficient and nephroprotective strategy of treatment for patients with HF.

Key words: heart failure, cardiorenal syndrome, worsening renal function, renal markers, natriuresis

Cite as
Kosiorek A, Biegus J, Rozentryt P, Hurkacz M, Zymliński R. Cardiorenal syndrome: Decongestion in heart failure across wide spectrum of kidney pathophysiology. *Adv Clin Exp Med*. 2022;31(4):445–455;31(4). doi:10.17219/acem/144327

DOI
10.17219/acem/144327

Introduction

Mutual hemodynamic and neurohormonal interaction of the heart and kidneys determines the exceptional dependence of both organs. Heart failure (HF) and kidney disease (KD) often coexist, which carries significant prognostic implications. Chronic kidney disease (CKD), defined as lowering of estimated glomerular filtration rate (eGFR) <60 mL/min/1.73 m^2 is present in 4.5% of general population and as many as 50% of patients with HF.[1,2] A large meta-analysis involving over 1,000,000 HF patients revealed that the presence of CKD doubles the risk of general mortality.[2]

Objectives

Modifications of diuretic treatment in patients with acute HF (AHF), associated with the use of both too high and too low doses of loop diuretics, result in excessive dehydration, risk of hypotension and worsening renal function. The aim of this review article was to evaluate and compare information about the important role of renal tubular function in the context of natriuresis and chloride metabolism associated with effective diuresis, including a comprehensive assessment of cardiorenal syndrome (CRS) and renal biomarkers. An optimal diuretic treatment, comprising different diuretic classes and their various activities, should be applied in patients with AHF.

Materials and methods

This review article provides an overview of current publications indexed in MEDLINE database (using PubMed and EBSCO), Scopus and Embase until July 2021. Taking into consideration the selected studies, the following keywords and Medical Subject Headings (MeSH) were used: "heart failure", "natriuresis", "spot urine sodium", "cardiorenal syndrome", "worsening renal function", and "acute kidney injury". The Boolean operators "AND" and "OR" were also used to narrow the search. The term "heart failure and worsening renal function" appeared in 1966 (Scopus), 1403 (PubMed) and 1223 (Embase) results, respectively. Additionally, a detailed search for articles was carried out using the keywords "heart failure AND cardiorenal syndrome AND acute kidney injury", which provided 297 results (51 in 2020 and 2021) in PubMed, 264 results (Scopus) and 328 results (Embase), respectively. Using the keywords "heart failure AND natriuresis" resulted in 1054 (Scopus), 969 (PubMed) and 1408 (Embase) articles found, respectively. In PubMed, the term "heart failure AND spot urine sodium" resulted in 33 articles (out of which 9 were published in 2020 and 2021), 50 articles in Scopus and 17 results in Embase. Due to the large number of articles related to the term "renal markers AND acute kidney injury", we had to narrow the search to selected renal biomarkers. In order to achieve a comprehensive pathophysiological approach, in addition to using selected keywords, we also performed a manual search.

Renal perfusion compared to oxygen use: differentiated distribution of energy expenditure

The kidneys are the most vascularized organ of the body. Renal blood flow (RBF) constitutes 20–25% of resting cardiac output (CO), and involves the renal cortex and medulla whose dynamics and metabolism differ.[3] In terms of anatomy, renal corpuscles (glomeruli surrounded by Bowman's capsule) and their vascularization are inside the cortex, while renal tubules, located outside the cortex, reach the medulla. Physiologically, the kidneys show a high demand for oxygen (O_2), but it is very different in the cortex and medulla. Perfusion of the cortex constitutes as much as 90% of blood flow and is autoregulated at low and normal oxygen consumption (VO2), which is first and foremost associated with the use of O_2 in renal tubules, necessary for the reabsorption of approx. 99.5% of filtered sodium. At the level of the medulla, blood flow is low and well-maintained even when systemic perfusion is significantly reduced.[4,5] In most tissues (e.g., in the brain), increased O_2 demand is followed by increased perfusion and O_2 supply. However, the load of reabsorbed sodium increases in the kidneys simultaneously with increased RBF and increased O_2 supply, which causes further increase in O_2 consumption and results in a high energy expenditure of the kidney. As a consequence, all of these processes may paradoxically cause hypoxia of intrarenal tissue and renal tubules (such a mechanism may occur in the case of hypertensive and diabetic nephropathy).[5] On the other hand, decreased CO, lowering of RBF in AHF and activation of the compensatory mechanisms (sympathetic nervous system (SNS) and renin–angiotensin–aldosterone system (RAAS)) result in poor renal perfusion, hypoxia of cells and renal tubules, as well as further damage thereto.[4]

The role of individual nephron segments in water and electrolyte balance

From the clinical perspective, renal metabolic function of the kidneys understood in the context of nephron activity should be analyzed in 3 anatomical and functional areas: glomeruli (filtration function), renal tubules (tubular function associated with reabsorption of tubular fluid with electrolytes with simultaneous secretion) and renal interstitium (absorption of water and electrolytes into peritubular capillaries).

Filtration function

The eGFR is the total result of the number of functional nephrons. Under physiological conditions, the pace of glomerular filtration of a single nephron is 40–70 nL/min with filtration fraction (FF) of 20–25%. With normal renal perfusion, hydrostatic pressure in glomerular capillaries slowly increases from the proximal to the distal end. As a result, the gradient of ultrafiltration pressure is equally maintained along the entire glomerular capillary.[5–7] The total volume of primary urine produced under normal conditions is approx. 180 L per day, containing approx. 1.5 L of NaCl, most of which is reabsorbed into renal interstitial fluid and systemic circulation. The primary filtrate contains electrolytes (sodium, chloride) and nitrogen metabolism products, urea, creatinine, uric acid, as well as mineral salts and amino acids.[1,8] Less than 1% of NaCl and only a small part of other dissolved substances are excreted with final urine. It is worth noting that glomerular filtration reflects only the filtration function of the nephron, which is very important in the production of primary urine. The formation of final urine and effective diuresis, understood as aquaresis and natriuresis as well as normal regulation of chloride concentration, stem from the efficiency of renal tubule function.[1,6]

Tubular function

Proximal tubule

Under normal conditions, the wall of the proximal tubule is freely permeable to water, which is accompanied by the reabsorption of sodium to maintain osmotic balance. Various transporters in the wall of the proximal tubule are responsible for such active transport (e.g., Na^+/K^+-ATPase of the basolateral membrane). This relatively stable sodium fraction (~75%) is reabsorbed in the proximal segment of the nephron and determined by Starling forces, regardless of neurohormonal activation. As a result of functional changes in the proximal renal tubule, as much as 85% of sodium can be reabsorbed in AHF (Fig. 1).[8]

Loop of Henle and distal tubule

Roughly 25% of sodium is then reabsorbed again in the site of action of the Na/K/Cl cotransporter in the thick ascending loop of Henle's limb. It is the site of action of loop diuretics (blocking of the cotransporter leads to an increase in the sodium load in the distal tubule and promotion of the excretion of sodium, chloride and – to a lesser extent – potassium). In the distal convoluted tubule, the sodium-chloride cotransporter is responsible for only about

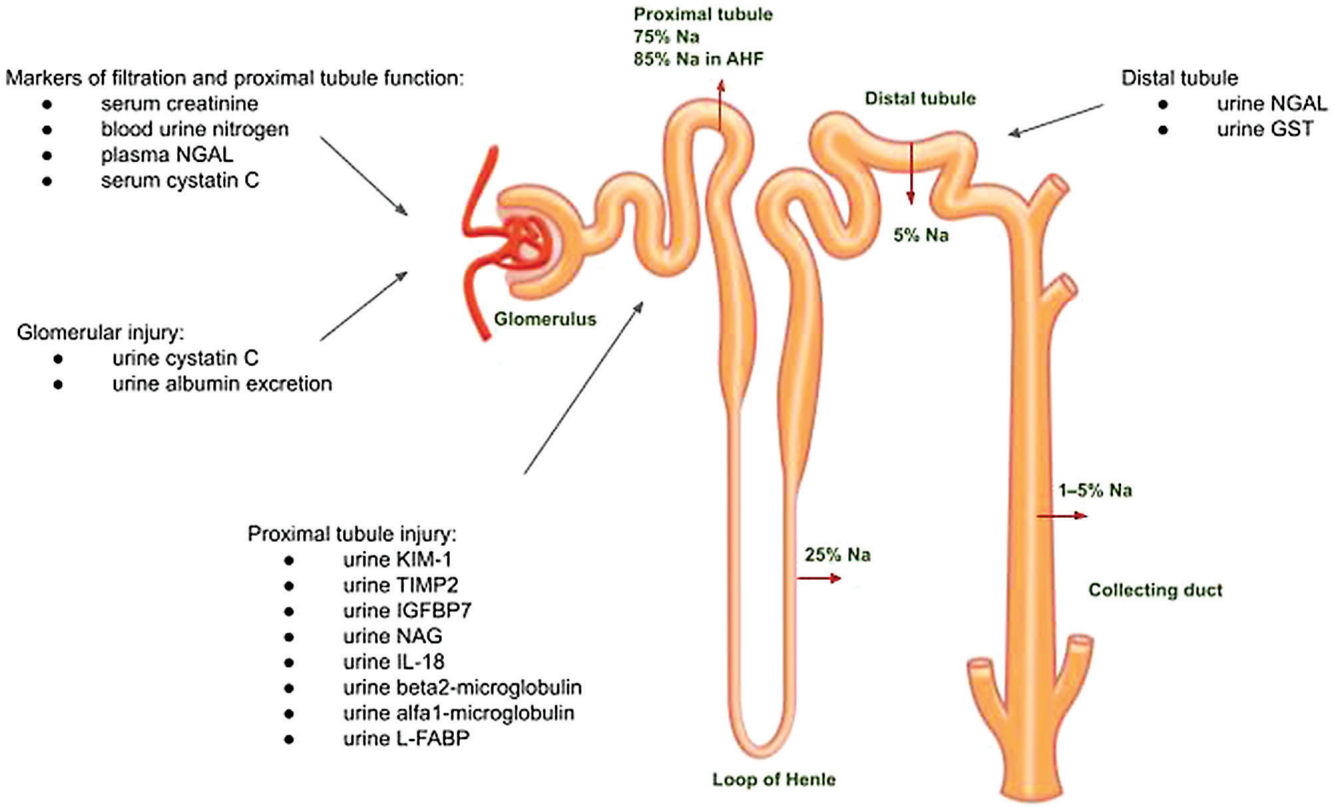

Fig. 1. Renal biomarkers and Na reabsorption: anatomic site along the nephron

NGAL – neutrophil gelatinase-associated lipocalin; KIM-1 – kidney injury molecule-1; IGFBP-7 – insulin growth factor-binding protein 7; NAG – N-acetyl-β-D-glucosaminidase; IL-18 – interleukin-18; L-FABP – urinary L-type fatty acid-binding protein; TIMP-2 – tissue inhibitor of metalloproteinases; GST – α-glutathione S-transferase; AHF – acute heart failure.

5% of sodium reabsorption. Since this is the site of action of thiazide diuretics, the diuretic effect of these medications is poorer than that of loop diuretics. In the collecting duct, an aldosterone-dependent cotransporter is active (and responsible for the absorption of 1–5% of sodium), which is inhibited by mineralocorticoid receptor antagonists.[6]

Chloride and tubuloglomerular feedback

Chloride is freely filtered by glomeruli. Approximately 60% of chloride is absorbed by the proximal renal tubule. Its concentration in urine depends proportionally on sodium concentration and is regulated by a number of transport processes.[9] Macula densa (MD), which is responsible for physiological tubuloglomerular feedback in the kidney and plays a role in sodium and chloride concentration regulation, is important for efficient function of the organ. It is located in the place where the distal tubule approaches the renal corpuscle and acts as an osmoreceptor of urine flowing through the distal convoluted tubule.[6] The MD reacts to changes in chloride concentration and the signal indicating changes in osmotic pressure are transmitted to the afferent glomerular arteriole. Describing the so-called "chloride theory", Kataoka draws attention to the essential role of chloride in the pathogenesis of congestion in AHF. Low chloride load (along with low sodium load) in the urine of patients with AHF, in whom there is an increased sodium resorption in the proximal tubule, stimulates the excretion of renin by juxtaglomerular cells. Renin causes the dilation of the glomerular afferent arteriole, the hyperfiltration of glomeruli and, as a result, the activation of the vicious circle of the RAA.[10,11] In turn, an increase in the influx of sodium and chloride into the distal tubule activates tubuloglomerular feedback by the breakdown of adenosine triphosphate (ATP) into adenosine, which leads to the constriction of the afferent glomerular arteriole and stops the activation of the RAA. Thanks to tubuloglomerular feedback, the nephron is also protected against hyperfiltration.[6,12]

Renal interstitium

In AHF, increased FF, which can be present even before the occurrence of a significant decrease in eGFR, causes significant changes in both hydrostatic and colloidal osmotic pressure in peritubular capillaries as well as in the interstitial portion of the kidney. Due to the fact that the kidneys are surrounded by a fibrous and fatty capsule and the renal fascia, hydrostatic pressure is evenly increased in the lumen of peritubular capillaries and renal interstitium (renal venous hypertension), while the oncotic pressure of the interstitial fluid decreases due to increased flow of lymph, which flushes out interstitial proteins. On the other hand, peritubular capillaries are impermeable to plasma proteins, which explains why intracapillary colloidal osmotic pressure remains high. These mechanisms facilitate passive resorption of sodium with resorption of water.[6,13]

Natriuresis and diuretic treatment strategy

Early measurement spot urine sodium (UNa) may be useful in identifying the patients who show poor response to diuretic treatment. In a prospective observational study, UNa was measured after the administration of the first dose of an intravenous diuretic medication. The risk of composite primary endpoint (death from any cause after 90 days, the use of a mechanical circulatory support system at hospital admission and inotropic agents at discharge) was twice as high in patients with UNa ≤ 60 mmol/L. Worsening renal function (WRF) occurred significantly more often in patients with UNa < 60 mmol/L.[1,14] In a Renal Optimization Strategies Evaluation (ROSE)-AHF study, a lower value of UNa ≤ 60 mmol/L within the first 24 h of diuresis was characteristic of patients in whom there was a risk of extended hospitalization.[15] In addition, the evaluation of renal function, understood as eGFR, does not provide reliable information on sodium balance.[16] Maintained eGFR profile (60 mL/min/1.73 m^2) in patients with HF and UNa ≤ 60 mmol/L is associated with high annual mortality rate.[16,17] Early monitoring, consisting in the recording of UNa 50–70 mmol/L after 2 h and/or diuresis 100–150 mL within the first 6 h of treatment, usually makes it possible to identify patients showing an inadequate response to diuretic therapy.[1,18,19] Therefore, it is necessary to interpret changes in renal function adequately early to identify patients in whom there is a risk of WRF and a lack of clinical improvement.[20,21] Furthermore, in AHF, sodium excretion is related to clinical status and has a different prognostic value between early phase of hospitalization and at discharge.[22] As a result, the physician will be able to make the decision of modifying the dose of the loop diuretic (double the dose) in order to obtain maximum plasma concentrations of the medication, or using sequential nephron blockade, i.e., combining the treatment with diuretics with a different mechanism of action.[1]

Phenotypes of CRS

In some HF patients, acute kidney injury (AKI) leads not only to transient but also permanent impairment of glomerular filtration. Apart from hemodynamic mechanisms (impaired organ perfusion due to decreased CO and high central venous pressure (CVP)), an important role is played by the dysfunction of SNS, activation of the RAAS, disruption of the hypothalamic–pituitary axis, and stimulation of inflammatory reactions, including changes in cytokine signalling.[23,24] It should be noted, however, that AKI may be iatrogenic and associated with suboptimal dosing of diuretics in patients with HF. Such treatment may increase the risk of excessive decongestion by decreasing intravascular volume, with secondary development of prerenal failure. From the clinical perspective, it is very important to identify this phenomenon quickly, for example by using

early biomarkers of renal tubular injury.[25] This strategy may play a key role in the appropriate modification of treatment and prevention of the development of CRS.

CRS type I

Sudden worsening of the CO (caused by myocardial ischemia, arrhythmia, severe valvular heart diseases, or myocarditis), that results in a cascade of hemodynamic and neurohormonal changes, leads to the arterial underfilling.[26] It causes RBF reduction, secondary activation of the compensatory mechanisms of RAAS and an increase in SNS tension. Angiotensin II activity results in the constriction of the efferent glomerular arteriole. In order to maintain optimal renal perfusion and constant FF, through an increase in the expression of vasodilators (prostaglandin, nitric oxide), the afferent glomerular arteriole is dilated.[6,26,27] An increase in FF initially masks the absolute decrease in eGFR, but after reaching the maximum FF at the value of ~60%, further RBF decrease causes a significant linear decrease in eGFR. Ultrafiltration pressure gradient cannot be maintained any longer at the entire length of the glomerular capillary, which partially loses its ultrafiltration efficiency (the "wasted capillary" phenomenon occurs). It leads to a decrease in the general number of functionally active nephrons, causing a decrease in glomerular filtration.[1] Reactively increased secretion of vasopressin results in reverse resorption of water from the collecting duct of the nephron.[3] Increased reflex adrenaline secretion causes a significant increase in renal vascular resistance, which leads to further impairment of renal perfusion. In addition, the expression of endothelin I (which is a substance with strong vasoconstrictive properties) leads to vasoconstriction, fostering remodeling processes and renal vascular fibrosis.[28] Also, abnormalities in the venous area of renal capillaries, stemming from increased CVP, lead to renal interstitial edema, hypoxia and dysfunction of renal tubules (resulting from increased hydrostatic pressure and impaired outflow of blood from the kidneys). In a similar mechanism, increased intra-abdominal pressure (IAP), occurring, for example, in the case of coexisting ascites, leads to an impaired renal perfusion due to compression. This is due to a decrease in abdominal perfusion pressure, which is the difference between mean arterial pressure and IAP.[29]

CRS type 2

Type 2 CRS is developed secondary to chronic HF, in the case of which we observe gradual, progressive activation of compensatory mechanisms (stimulation of RAAS, SNS and endothelin overproduction). These processes lead to worsening of renal perfusion through the development and perpetuation of structural changes in the renal parenchyma, renal vascular fibrosis as well as dysfunction of renal tubules. Apart from its vasoconstrictive effect, endothelin 1 production contributes to low urine sodium excretion, the occurrence of inflammation in the kidneys and increased expression of aldosterone. Moreover, the coexisting synthesis of fibronectin stimulates fibrotic processes that are frequently irreversible.[30] Aldosterone shows expression in preglomerular vessels, glomeruli and along distal tubules. Its increased production leads to vascular remodeling, glomerular sclerosis, generalized endothelial dysfunction, and increased oxidative stress.[31] The CRS has been divided into 5 subtypes (Fig. 2).[3]

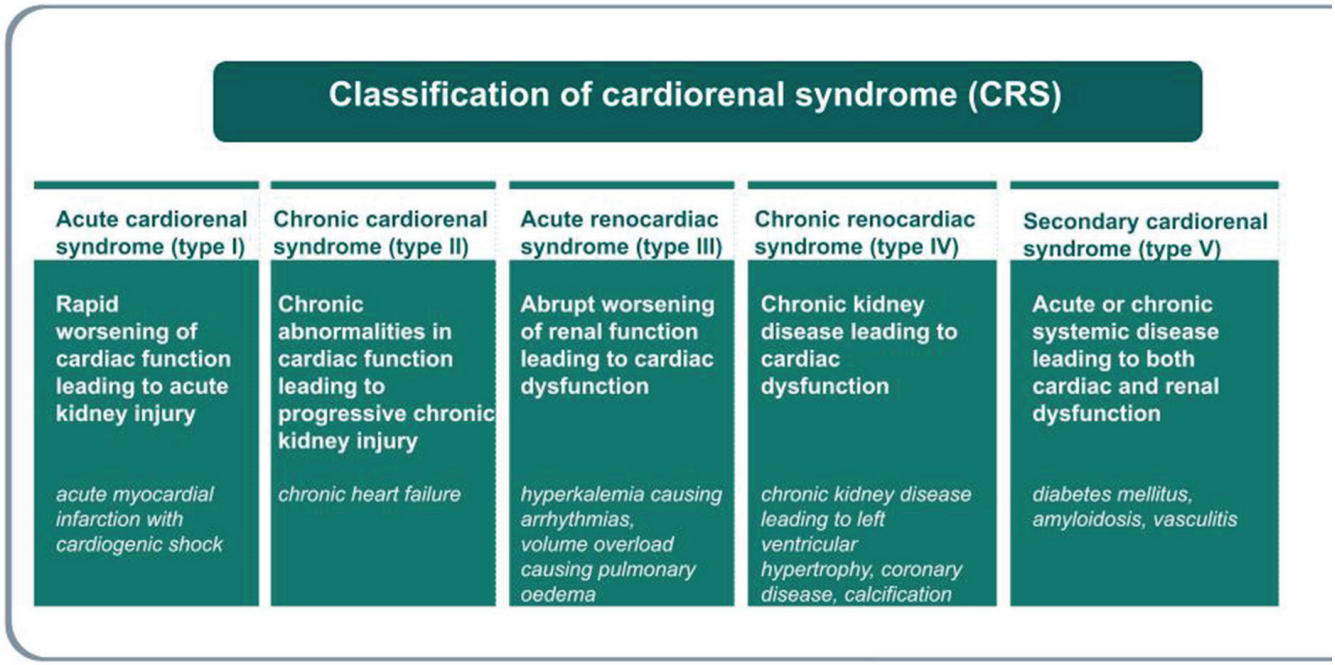

Fig. 2. Cardiorenal syndrome (CRS) subtypes

CRS: the updated concept

The AHF is a complex syndrome involving numerous organs, including kidneys.[32] The kidney is an important homeostatic organ and its activity is closely interrelated with the function of the cardiovascular system.[24] Although CRS subtypes systematize the knowledge that allows for research on the interaction between the cardiovascular system and the kidneys, it is only a simplification that ignores the interaction between the kidneys and other key organs and systems (lungs, liver, skeleton, gastrointestinal tract and its microbiome, SNS, adipose tissue, skeletal muscles).[33,34] It is crucial to notice the role of the kidneys in the metabolism of carbohydrates[35] as well as in the regulation of oxygenation of all tissues through their participation in the metabolism of iron and hemoglobin.[36] This homeostatically central role of the kidneys means that a dysfunction in any of these organs may have an impact on kidney function and such impact may be responsible for the differentiation of the renal response to various cardiovascular diseases.

Since the definition of CRS was developed, the understanding of the heterogeneity of HF, especially the role of other diseases and organs beyond the circulatory system, has increased significantly.[37] For this reason, the analysis of renal function within the conceptual paradigm of the CRS has exhausted all its options. There is a need for an interdisciplinary concept in which it will be possible, on the one hand, to understand the causes of high heterogeneity of renal function in HF and during its treatment, and on the other hand, to identify such functional renal responses and the circumstances of their emergence that are clinically unfavorable. Regardless of the phenotype of HF, the functional renal response to its presence and treatment may fall into one or a combination of the following clinically important categories:

– inadequate control of the extracellular fluid volume with different responses to the diuretics,
– decrease in glomerular filtration,
– decrease in diuresis,
– hyperkalemia/hypokalemia,
– hyponatremia,
– acidosis/alkalosis with hypochloremia.

The abovementioned dysregulation involving the kidneys occurs in everyday medical practice and it is difficult to relate it to the established concepts of KD, which includes its 2 types (acc. to KDIGO 2012):

1. CKD with eGFR below 60 mL/min/1.73 m^2 for 3 months or eGFR over 60 mL/min/m^2 with additional evidence of kidney injury:
   – albuminuria/proteinuria,
   – macroscopic or microscopic changes,
   – etiology (diabetes, hypertensive, interstitial disease, etc.).
2. AKI with an increase in serum creatinine concentration (SCr) by ≥0.3 mg/dL (26.5 μmol/L) within 48 h, or a ≥1.5-fold increase within the previous 7 days, or a decrease in diuresis by <0.5 mL/kg/h within 6 h.

These 2 types of KD can overlap, and this is very common in a significant percentage of patients with HF. However, these syndromes do not include abnormalities in fluid and electrolyte balance, fluid overload and resistance to diuretics. In clinical practice, we see patients with HF with preserved or reduced ejection fraction with concurrently impaired glomerular filtration, hyperkalemia or hypochloremic alkalosis due to the use of diuretics.

WRF in the course of HF

The AKI is associated with an increased risk of hospitalization and high in-hospital and post-discharge mortality.[38,39] It is important to note that the AKI is a clinical syndrome and is not synonymous to acute renal failure (ARF). The coexistence of a rapid, persistent worsening renal function, increased concentration of renal injury markers, accumulation of nitrogenous and non-nitrogenous metabolic products, as well as profound electrolyte disturbances leads to ARF. Based on, for example, the Risk, Injury, Failure, Loss, End-stage renal disease (RIFLE) criteria, we can calculate risk and damage and predict gradual progression of renal disease to end-stage renal failure. However, they only make it possible to characterize successive stages of renal failure development, without necessarily showing sensitivity in the detection of early intrarenal dysfunction.[3] Unfortunately, there are patients who remain at risk of developing progressive CKD, despite complete or nearly complete restoration of renal function after an AKI episode. The occurrence of AKI in patients previously diagnosed with CKD is associated with accelerated progression thereof as well as the occurrence of end-stage renal failure. The AKI occurs mainly in HF patients hospitalized due to AHF. The incidence of AKI in population is ~20%.[40–42] The significance of WRF among patients with AHF has been emphasized for years.[40,43] The presence of WRF, understood as an increase in SCr > 0.3 mg/dL in serum or a decrease in eGFR by >25% (expressed in mL/min/1.73 m^2, calculated according to the Modification of Diet in Renal Disease (MDRD) formula), together with worsening or lack of improvement in signs and symptoms of AHF, is known as the "true WRF". This condition requires intensification and optimization of pharmacological treatment (and, in some cases, the introduction of renal replacement therapy), especially when resistant fluid overload and metabolic disorders (hyperkalemia and acidosis) are also present, and is associated with worse prognosis. Authors of one study observed that general mortality increased in a 12-month follow-up of patients with true WRF (in a population of 266 patients with HF, 73 patients (27%) reached endpoint). In the group of patients with true WRF death occurred in 9 out of 11 (82%) patients, in the group with pseudo-WRF in 3 out of 27 (11%)

patients and in the group without WRF in 61 out of 228 patients (27%) ($p < 0.001$).[20,21] Importantly, in patients with simultaneously preserved diuresis, effective decongestion and improvement in clinical condition during the course of treatment, an increase in creatinine/decrease in eGFR does not imply worse prognosis ("pseudo WRF").[1,21] It is also worth noting that the administration of loop diuretics, angiotensin-converting enzyme (ACE) inhibitors or aldosterone antagonists before hospitalization due to HF does not have an impact on an increased risk of WRF. Pseudo-WRF may occur as a result of the implementation of a targeted therapy reflecting the neurohormonal blockade, understood as the inhibition of the RAA system, and it is not necessarily a sign of direct renal dysfunction. Only isolated changes in SCr occur in this group of patients.[1,2] Therefore, a consistent evaluation of renal function must be conducted in each patient suffering from HF, especially from AHF. Such strategy makes it possible to assess the effectiveness, efficacy and – thus – safety of the treatment. Therefore, researchers are still seeking markers that are sensitive, easy to determine and available that will be helpful in identifying patients with sub-clinical AKI who have an increased risk of adverse outcomes. There are some systems that prevent intravascular hypovolemia during decongestion, which may reduce the risk of WRF; however, this issue needs further investigation.[44] The safety of ultrafiltration also needs to be clarified in the future.[45]

Biomarkers of AKI

Monitoring of SCr, as a common endogenous marker of glomerular filtration function, is a standard in the evaluation of renal function. This method, however, has a number of limitations. Creatinine, a product of creatine metabolism, which is a reserve of high-energy phosphates in skeletal muscles, is freely filtered by renal glomeruli, without being resorbed or secreted in the kidney (except for 15% creatinine in urine which comes from tubular secretion in the proximal tubule through excretion of organic cations).[4] When eGFR is reduced, its half-life extends from 4 h to even 24–72 h. It is particularly important in the context of impaired metabolism in patients with end-stage renal disease (ESRD), in whom creatinine can be excreted or metabolized via extrarenal pathways (up to 66% of daily production), most likely by intestinal flora.[46,47] Therefore, SCr may increase only after 24–36 h despite early renal injury, which significantly delays the diagnosis of AKI.[1,7,47,48] There are also reports of delayed increases in SCr despite changes in eGFR occurring already at an early stage of AKI, which can only be visible after a 50% loss of renal functional capacity.[49] In addition, SCr depends not only on glomerular filtration function, but also on factors such as sex, age and body weight. In patients with low muscle mass, features of cachexia, liver diseases or sepsis, SCr is lower and, as a result, eGFR may be overestimated. A protein-rich diet – consuming large amounts of boiled meat – leads to an increase in SCr caused by increased intestinal resorption of creatinine from consumed meat.[1,7,46–48] Thus, an increase in its SCr is not specific for early renal tubule damage (but is rather an effect of the loss of glomerular filtration function) and requires consideration of prerenal and extrarenal causes.[47,49] Blood urea nitrogen (BUN) evaluation is also worth mentioning, which is also helpful in diagnostic evaluation of moderate and severe CKD, regardless of eGFR. It has also been shown that increased levels of BUN in AHF patients, even those in whom SCr levels are normal or slightly elevated, are correlated with increased mortality. The necessity to take into account SCr and the inertia of analysis resulting thereof, constitutes a limitation of the method.[50] General urinalysis is a widely available clinical parameter with diagnostic value in the evaluation of structural and functional causes of KD. The evaluation of urine sediment examination, based on the evaluation of active sediment, the number and type of epithelial cells or casts, is significant in diagnosis of KD. This interpretation, however, frequently does not indicate precisely whether the disease is acute or chronic.[3] Renal function should also be considered when evaluating the clinical significance of urine osmolality. Low urine osmolality is an independent risk factor for CKD progression, and its predictive ability is not superior to eGFR.[51]

Novel renal biomarkers

In the last decade, a very interesting diagnostic platform appeared among urinary markers that are of significance in early prediction of AKI. Such biomarkers can be divided into several groups according to their biological origin and time of release after renal injury (Table 1), or potentially reversible or irreversible effects on AKI (Fig. 3).[52]

Neutrophil gelatinase-associated lipocalin

The best known marker is the neutrophil gelatinase-associated lipocalin (NGAL), which is a sensitive and specific urine and serum biomarker for predicting AKI at an early stage. A 10-fold increase in NGAL serum concentration and over a 100-fold increase in its concentration in the urine of adults has been observed in AKI.[49,53] In a meta-analysis of 10 studies involving 2000 patients with CRS, an increase in serum and urine level of NGAL were predictive for renal replacement therapy and death.[3] What is more, an increase in serum NGAL indicates AKI progression after cardiac surgeries, secondary to post-contrast AKI, as well as septic shock in children.[49] Importantly, its high level is observed in the case of inflammation, as NGAL is an acute phase reactant and can be released from neutrophils and macrophages.[54] Therefore, in the context of diagnostic evaluation and intervention in early renal tubular injury, the dynamics of NGAL synthesis, both in the serum and

Table 1. Novel biomarkers of AKI

Renal biomarker	Anatomical and biological origin	Distribution after renal injury
NGAL	25 kDa glycoprotein produced by neutrophils and epithelial cells of kidney, trachea, lung, myocardium, stomach, and colon	– released from proximal and distal tubular cells – increased serum and urinary concentration within 2–4 h
KIM-1	transmembrane glycoprotein	– produced by proximal tubular cells – increased urinary concentration within 24–48 h
Cystatin C	13 kDa cysteine protease inhibitor produced by all nucleated cells; is freely filtered in glomeruli and reabsorbed by proximal tubular cells	– released from proximal tubular cells – increased urinary concentration within 12–24 h
IGFBP-7 TIMP-2	metalloproteinases involved in G1 cell cycle arrest at an early stage of renal tubular cell injury	– increased urinary concentration within 12 h
L-FABP	14 kDa intracellular lipid chaperone produced in proximal tubule and hepatocytes	– increased urinary concentration in 1 h
IL-18	pro-inflammatory cytokine	– released from proximal tubular cells within 6–24 h
NAG	lysosomal enzyme	– produced by proximal tubular cells within 12 h

NGAL – neutrophil gelatinase-associated lipocalin; KIM-1 – kidney injury molecule-1; IGFBP-7 – insulin growth factor-binding protein 7; NAG – N-acetyl-β-D-glucosaminidase; IL-18 – interleukin-18; L-FABP – urinary L-type fatty acid-binding protein; TIMP-2 – tissue inhibitor of metalloproteinases.

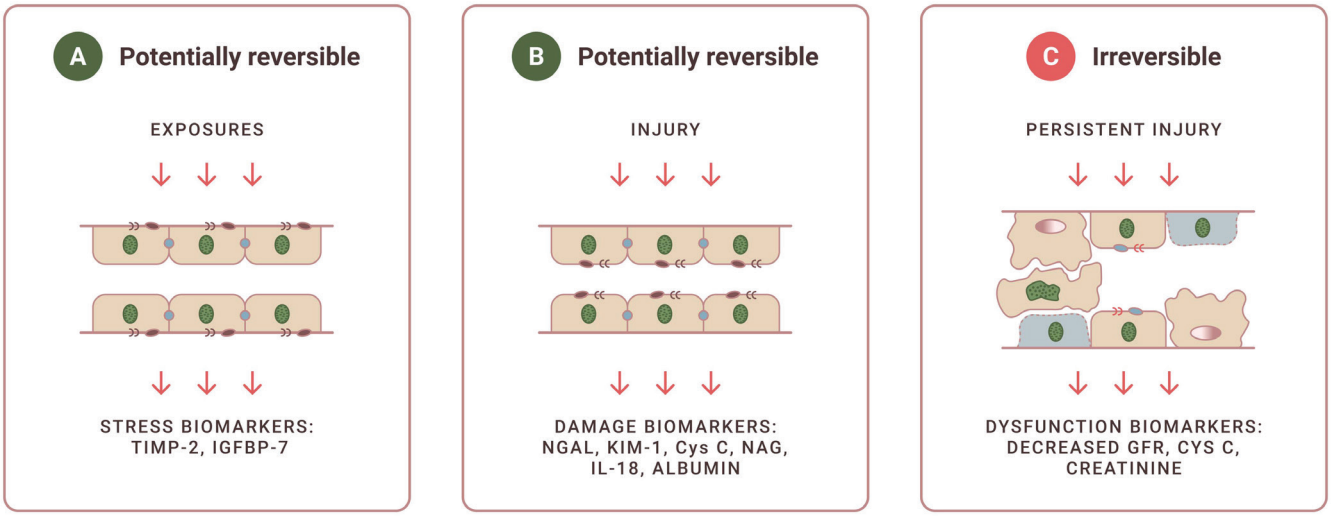

Fig. 3. Effect of reversible and irreversible renal injury on acute kidney injury (AKI)

NGAL – neutrophil gelatinase-associated lipocalin; KIM-1 – kidney injury molecule-1; IGFBP-7 – insulin growth factor-binding protein 7; NAG – N-acetyl-β-D-glucosaminidase; IL-18 – interleukin-18; L-FABP – urinary L-type fatty acid-binding protein; TIMP-2 – tissue inhibitor of metalloproteinases; GFR – glomerular filtration rate; Cys C – cystatin C.

urine, can be a useful tool for a noninvasive evaluation of AKI, even before the development of clinically evident form of the disease.[53]

Kidney injury molecule-1

In ischemic or nephrotoxic kidney injury, kidney injury molecule-1 (KIM-1) is produced and accumulated in very large amounts on the membrane of the renal proximal tubules. Studies have shown an increase in KIM-1 expression in kidney biopsy samples with confirmed acute tubular necrosis. An increase in the concentration of this biomarker in urine is crucial, especially in ischemic AKI, compared to other causes (e.g., in the case of post-contrast nephropathy or CKD, even despite concomitant urinary tract infection).[55] Studies also suggest that the urinary KIM-1 may constitute a predictive factor for the introduction of renal replacement therapy and causes a risk of death during hospitalization in patients with AKI. However, studies available to date are not sufficient to determine the cutoff value that is predictive for AKI in the setting of intensive medical care.[56]

Cystatin C

In a study involving 444 patients in an intensive care unit (ICU), cystatin C (Cys C) concentration in urine was significantly higher in patients with sepsis or AKI. However, results of studies investigating the use of Cys C serum concentration in the detection of AKI in patients in ICU were conflicting.[54,57,58] Therefore, Cys C (primarily due to its constant rate of secretion in the organism) is a good, early marker of GFR (without the impact of infection or liver diseases). Serum Cys C concentration also does not depend on age, sex, race, muscle mass, and

Table 2. Classifications of diuretics and their effect on the electrolyte balance (diuretic effect on serum chloride concentration)

Diuretic agent	Mechanism and site of action	Serum concentration			Urinary concentration			
		Na	Cl	K	Na	Cl	K	other
Loop diuretics	blocks Na/K/Cl cotransporter (loop of Henle)	↓	↓	↓	↑	↑	↑	–
Thiazide diuretics	blocks Na/Cl cotransporter (distal tubule)	↓	↓	↓	↑	↑	↑	–
MRA	blocks aldosterone receptor (collecting duct)	↓	→	↑	↑	?	↓	H↑ HCO3↑
Acetazolamide	blocks carbonic anhydrase (proximal tubule)	↑→	↑	↓	↑	↓	↓	HCO3↑ water↑
Aquaretic diuretics	blocks vasopressin V2 receptor (collecting duct)	↑	↑	↑	→	→	→	water↑↑↑
SGLT-2 inhibitors	blocks SGLT-2 (proximal tubule)	↑→	↑	→	↑→	↓	→	water↑ glucose↑

MRA – mineralocorticoid receptor antagonists, SGLT-2 – sodium-glucose cotransporter-2.

hydration. It is not, however, specific in diagnostic evaluation of AKI.[54]

Other biomarkers that are worth mentioning include tissue inhibitor of metalloproteinases (TIMP-2) and insulin-like growth factor-binding protein 7 (IGFBP7). They are available for clinical use in the USA. In 728 critically ill patients not showing any signs of AKI, the determination of urinary levels TIMP-2 and IGFBP7 constituted a predictive value for the development of AKI ($p < 0.002$).[3] The abovementioned renal markers in AKI have been summarized in Fig. 2.

Features of a perfect renal biomarker

Due to the limitations discussed above, researchers are constantly seeking an ideal diagnostic biomarker for predicting AKI. It should be characterized by, among other things, high specificity for the kidneys, the ability to distinguish types, duration and etiology of AKI (renal injury, including tubular and glomerular, prerenal and extrarenal AKI). It is recommended that its increase provide early information about kidney dysfunction and illustrate the scale of such damage (with an established threshold for the assessment of dysfunction progression and regression). It should also be widely available in everyday clinical practice and be easy, precise and quick in terms of determination, as well as inexpensive.[49] Despite intensive search, an ideal marker for early diagnosis of AKI has not been found yet, which seems understandable due to structural heterogeneity of the kidneys.

Classification of diuretics: clinical perspectives

Using the selected renal biomarkers may be helpful in predicting AKI, but there is no evidence on their effect on diuresis. The novel CRS-guided approach, which takes into account the importance of metabolism of both sodium and chloride, is important to regulate plasma volume, diuresis and natriuresis during decongestive treatment in AHF. The pathophysiological mechanisms in various nephron segments explain the crucial role of these electrolytes and highlight the need for proper choice of a combination of the different diuretic classes. Dyschloremia is postulated as one of the main causes of worsening HF during decongestive treatment.[59] A new classification of diuretics based on their effect on serum chloride concentration has been proposed in recent years. This concept is consistent with recent clinical observations that chloride-regaining diuretics preserve plasma volume, enhance vascular "tonicity" and avoid diuretic resistance (Table 2).[60]

Study limitations

The study lists selected renal biomarkers which are gaining increasing interest in research, but listing them all would exceed the scope of this publication. In addition, the review was limited to selected pathophysiological mechanisms related to the interdisciplinary complex issue involving cardionephrology.

Conclusions

These complex physiological interactions with anatomical and physiological division of the nephron determine the stability and water and electrolyte balance of the body. Not only aquaresis, but also natriuresis and chloride serum concentration may constitute a practical and useful idea for the evaluation of efficient decongestion in patients with HF. Complex assessment, involving such elements as permeability of the proximal tubule wall and tubuloglomerular feedback, in the context of sodium and chloride balance, with the use of biomarkers of renal function, may

play an important role in the evaluation of patients with HF at risk of AKI. Therefore, there is a need to update the concepts of CRS and strategies for their treatment in the context of renal function and its interaction with multiple organs.

ORCID iDs

Aneta Kosiorek https://orcid.org/0000-0002-7505-587X
Jan Biegus https://orcid.org/0000-0001-9977-7722
Piotr Rozentryt https://orcid.org/0000-0002-8979-2205
Magdalena Hurkacz https://orcid.org/0000-0003-0846-3168
Robert Zymliński https://orcid.org/0000-0003-1483-7381

References

1. Mullens W, Damman K, Testani JM, et al. Evaluation of kidney function throughout the heart failure trajectory: A position statement from the Heart Failure Association of the European Society of Cardiology. *Eur J Heart Fail*. 2020;22(4):584–603. doi:10.1002/ejhf.1697
2. Damman K, Valente MAE, Voors AA, O'Connor CM, Van Veldhuisen DJ, Hillege HL. Renal impairment, worsening renal function, and outcome in patients with heart failure: An updated meta-analysis. *Eur Heart J*. 2014;35(7):455–469. doi:10.1093/eurheartj/eht386
3. Rangaswami J, Bhalla V, Blair JEA, et al. Cardiorenal syndrome: Classification, pathophysiology, diagnosis, and treatment strategies. A scientific statement From the American Heart Association. *Circulation*. 2019;139(16):E840–E878. doi:10.1161/CIR.0000000000000664
4. Verma SK, Molitoris BA. Renal endothelial injury and microvascular dysfunction in acute kidney injury. *Semin Nephrol*. 2015;35(1):96–107. doi:10.1016/j.semnephrol.2015.01.010
5. Hansell P, Welch WJ, Blantz RC, Palm F. Determinants of kidney oxygen consumption and their relationship to tissue oxygen tension in diabetes and hypertension. *Clin Exp Pharmacol Physiol*. 2013;40(2):123–137. doi:10.1111/1440-1681.12034
6. Mullens W, Verbrugge FH, Nijst P, Tang WHW. Renal sodium avidity in heart failure: From pathophysiology to treatment strategies. *Eur Heart J*. 2017;38(24):1872–1882. doi:10.1093/eurheartj/ehx035
7. Denic A, Mathew J, Lerman LO, et al. Single-nephron glomerular filtration rate in healthy adults. *N Engl J Med*. 2017;376(24):2349–2357. doi:10.1056/nejmoa1614329
8. Verbrugge FH, Dupont M, Steels P, et al. The kidney in congestive heart failure: Are natriuresis, sodium, and diuretics really the good, the bad and the ugly? *Eur J Heart Fail*. 2014;16(2):133–142. doi:10.1002/ejhf.35
9. Nagami GT. Hipercloremia: por qué y cómo. *Nefrologia*. 2016;36(4):347–353. doi:10.1016/j.nefro.2016.04.001
10. Verbrugge F, Dupont M, Bertrand P, et al. Determinants and impact of the natriuretic response to diuretic therapy in heart failure with reduced ejection fraction and volume overload. *Acta Cardiol*. 2015;70(3):265–273. doi:10.1080/AC.70.3.3080630
11. Kataoka H. Proposal for heart failure progression based on the "chloride theory": Worsening heart failure with increased vs. non-increased serum chloride concentration. *ESC Heart Fail*. 2017;4(4):623–631. doi:10.1002/ehf2.12191
12. Schnermann J. Juxtaglomerular cell complex in the regulation of renal salt excretion. *Am J Physiol*. 1998;274(2):R263–R279. doi:10.1152/ajpregu.1998.274.2.r263
13. Lewy JE, Windhager EE. Peritubular control of proximal tubular fluid reabsorption in the rat kidney. *Am J Physiol*. 1968;214(5):943–954. doi:10.1152/ajplegacy.1968.214.5.943
14. Luk A, Groarke JD, Desai AS, et al. First spot urine sodium after initial diuretic identifies patients at high risk for adverse outcome after heart failure hospitalization. *Am Heart J*. 2018;203:95–100. doi:10.1016/j.ahj.2018.01.013
15. Cunningham JW, Sun JL, Mc Causland FR, et al. Lower urine sodium predicts longer length of stay in acute heart failure patients: Insights from the ROSE AHF trial. *Clin Cardiol*. 2020;43(1):43–49. doi:10.1002/clc.23286
16. Biegus J, Zymliński R, Testani J, et al. Renal profiling based on estimated glomerular filtration rate and spot urine sodium identifies high-risk acute heart failure patients. *Eur J Heart Fail*. 2021;23(5):729–739. doi:10.1002/ejhf.2053
17. Biegus J, Zymliński R, Sokolski M, et al. Serial assessment of spot urine sodium predicts effectiveness of decongestion and outcome in patients with acute heart failure. *Eur J Heart Fail*. 2019;21(5):624–633. doi:10.1002/ejhf.1428
18. Singh D, Shrestha K, Testani JM, et al. Insufficient natriuretic response to continuous intravenous furosemide is associated with poor long-term outcomes in acute decompensated heart failure. *J Card Fail*. 2014;20(6):392–399. doi:10.1016/j.cardfail.2014.03.006
19. Testani JM, Hanberg JS, Cheng S, et al. Rapid and highly accurate prediction of poor loop diuretic natriuretic response in patients with heart failure. *Circ Hear Fail*. 2016;9(1):e002370. doi:10.1161/CIRCHEARTFAILURE.115.002370
20. Sokolski M, Zymliński R, Biegus J, et al. Urinary levels of novel kidney biomarkers and risk of true worsening renal function and mortality in patients with acute heart failure. *Eur J Heart Fail*. 2017;19(6):760–767. doi:10.1002/ejhf.746
21. Sokolski M, Zymliński R, Sokolska JM, Biegus J, Banasiak W, Ponikowski P. True worsening renal function identifies patients with acute heart failure with an ominous outcome. *Polish Arch Intern Med*. 2019;129(5):357–360. doi:10.20452/pamw.4453
22. Biegus J, Zymliński R, Fudim M, et al. Spot urine sodium in acute heart failure: Differences in prognostic value on admission and discharge. *ESC Hear Fail*. 2021;8(4):2597–2602. doi:10.1002/ehf2.13372
23. Ronco C, McCullough P, Anker SD, et al. Cardiorenal syndromes: Report from the consensus conference of the Acute Dialysis Quality Initiative. *Eur Heart J*. 2010;31(6):703–711. doi:10.1093/EURHEARTJ/EHP507
24. Ronco C, Haapio M, House AA, Anavekar N, Bellomo R. Cardiorenal syndrome. *J Am Coll Cardiol*. 2008;52(19):1527–1539. doi:10.1016/j.jacc.2008.07.051
25. Van Veldhuisen DJ, Ruilope LM, Maisel AS, Damman K. Biomarkers of renal injury and function: Diagnostic, prognostic and therapeutic implications in heart failure. *Eur Heart J*. 2016;37(33):2577c–2585c. doi:10.1093/eurheartj/ehv588
26. Bongartz LG, Cramer MJ, Doevendans PA, Joles JA, Braam B. The severe cardiorenal syndrome: Guyton revisited. *Eur Heart J*. 2005;26(1):11–17. doi:10.1093/eurheartj/ehi020
27. Ronco C, Cicoira M, McCullough PA. Cardiorenal syndrome type 1: Pathophysiological crosstalk leading to combined heart and kidney dysfunction in the setting of acutely decompensated heart failure. *J Am Coll Cardiol*. 2012;60(12):1031–1042. doi:10.1016/j.jacc.2012.01.077
28. Neuhofer W, Pittrow D. Role of endothelin and endothelin receptor antagonists in renal disease. *Eur J Clin Invest*. 2006;36(Suppl 3):78–88. doi:10.1111/j.1365-2362.2006.01689.x
29. Damman K, van Deursen VM, Navis G, Voors AA, van Veldhuisen DJ, Hillege HL. Increased central venous pressure is associated with impaired renal function and mortality in a broad spectrum of patients with cardiovascular disease. *J Am Coll Cardiol*. 2009;53(7):582–588. doi:10.1016/j.jacc.2008.08.080
30. Zymliński R, Sierpiński R, Metra M, et al. Elevated plasma endothelin-1 is related to low natriuresis, clinical signs of congestion, and poor outcome in acute heart failure. *ESC Hear Fail*. 2020;7(6):3536–3544. doi:10.1002/ehf2.13064
31. Onozato ML, Tojo A, Kobayashi N, Goto A, Matsuoka H, Fujita T. Dual blockade of aldosterone and angiotensin II additively suppresses TGF-β and NADPH oxidase in the hypertensive kidney. *Nephrol Dial Transplant*. 2007;22(5):1314–1322. doi:10.1093/ndt/gfl780
32. Zymliński R, Sokolski M, Biegus J, et al. Multi-organ dysfunction/injury on admission identifies acute heart failure patients at high risk of poor outcome. *Eur J Heart Fail*. 2019;21(6):744–750. doi:10.1002/ejhf.1378
33. Evenepoel P, Opdebeeck B, David K, D'Haese PC. Bone–vascular axis in chronic kidney disease. *Adv Chronic Kidney Dis*. 2019;26(6):472–483. doi:10.1053/j.ackd.2019.09.006
34. Yang T, Richards EM, Pepine CJ, Raizada MK. The gut microbiota and the brain–gut–kidney axis in hypertension and chronic kidney disease. *Nat Rev Nephrol*. 2018;14(7):442–456. doi:10.1038/s41581-018-0018-2
35. Alsahli M, Gerich JE. Renal glucose metabolism in normal physiological conditions and in diabetes. *Diabetes Res Clin Pract*. 2017;133:1–9. doi:10.1016/j.diabres.2017.07.033
36. Eckardt KU. Iron and oxygen sensing: Discovering intricate links. *Kidney Int*. 2019;95(3):482–484. doi:10.1016/j.kint.2019.01.003

37. Ergatoudes C, Schaufelberger M, Andersson B, Pivodic A, Dahlström U, Fu M. Non-cardiac comorbidities and mortality in patients with heart failure with reduced vs. preserved ejection fraction: A study using the Swedish Heart Failure Registry. *Clin Res Cardiol*. 2019;108(9): 1025–1033. doi:10.1007/s00392-019-01430-0
38. Heywood JT, Fonarow GC, Costanzo MR, Mathur VS, Wigneswaran JR, Wynne J. High prevalence of renal dysfunction and its impact on outcome in 118,465 patients hospitalized with acute decompensated heart failure: A report from the ADHERE database. *J Card Fail*. 2007;13(6):422–430. doi:10.1016/j.cardfail.2007.03.011
39. Gansevoort RT, Correa-Rotter R, Hemmelgarn BR, et al. Chronic kidney disease and cardiovascular risk: Epidemiology, mechanisms, and prevention. *Lancet*. 2013;382(9889):339–352. doi:10.1016/S0140-6736(13)60595-4
40. Holgado JL, Lopez C, Fernandez A, et al. Acute kidney injury in heart failure: A population study. *ESC Hear Fail*. 2020;7(2):415–422. doi:10.1002/ehf2.12595
41. Go AS, Hsu CY, Yang J, et al. Acute kidney injury and risk of heart failure and atherosclerotic events. *Clin J Am Soc Nephrol*. 2018;13(6): 833–841. doi:10.2215/CJN.12591117
42. Pickering JW, Blunt IRH, Than MP. Acute kidney injury and mortality prognosis in acute coronary syndrome patients: A meta-analysis. *Nephrology*. 2018;23(3):237–246. doi:10.1111/nep.12984
43. Fortrie G, De Geus HRH, Betjes MGH. The aftermath of acute kidney injury: A narrative review of long-term mortality and renal function. *Crit Care*. 2019;23(1):24. doi:10.1186/s13054-019-2314-z
44. Biegus J, Zymlinski R, Siwolowski P, et al. Controlled decongestion by reprieve therapy in acute heart failure: Results of the TARGET-1 and TARGET-2 studies. *Eur J Heart Fail*. 2019;21(9):1079–1087. doi:10.1002/ejhf.1533
45. Urban S, Blaziak M, Biegus J, Zymlinski R. Ultrafiltration in acute heart failure: Current knowledge and fields for further research. *Adv Clin Exp Med*. 2021;30(7):1–10. doi:10.17219/ACEM/135347
46. Małyszko J. Przewlekła niewydolność nerek – problem tylko kardiologów? *Choroby Serca i Naczyń*. 2005;2(2):78–83. https://journals.viamedica.pl/choroby_serca_i_naczyn/article/view/12216. Accessed September 17, 2021.
47. Lamb EJ, Stevens PE. Estimating and measuring glomerular filtration rate: Methods of measurement and markers for estimation. *Curr Opin Nephrol Hypertens*. 2014;23(3):258–266. doi:10.1097/01.mnh.0000444813.72626.88
48. Ostermann M, Joannidis M. Acute kidney injury 2016: Diagnosis and diagnostic workup. *Crit Care*. 2016;20(1):299. doi:10.1186/s13054-016-1478-z
49. Lisowska-Myjak B. Laboratoryjne wskaźniki ostrego uszkodzenia nerek oznaczane w moczu i w surowicy. *Forum Nefrol*. 2010;3(2):71–81. https://journals.viamedica.pl/renal_disease_and_transplant/article/view/10386. Accessed September 16, 2021.
50. Khoury J, Bahouth F, Stabholz Y, et al. Blood urea nitrogen variation upon admission and at discharge in patients with heart failure. *ESC Hear Fail*. 2019;6(4):809–816. doi:10.1002/ehf2.12471
51. Lee MJ, Chang TI, Lee J, et al. Urine osmolality and renal outcome in patients with chronic kidney disease: Results from the KNOW-CKD. *Kidney Blood Press Res*. 2019;44(5):1089–1100. doi:10.1159/000502291
52. Ronco C, Bellomo R, Kellum JA. Acute kidney injury. *Lancet*. 2019; 394(10212):1949–1964. doi:10.1016/S0140-6736(19)32563-2
53. Makris K, Kafkas N. Neutrophil gelatinase-associated lipocalin in acute kidney injury. *Adv Clin Chem*. 2012;58:141–191. doi:10.1016/B978-0-12-394383-5.00012-6
54. Grigoryev DN, Liu M, Hassoun HT, Cheadle C, Barnes KC, Rabb H. The local and systemic inflammatory transcriptome after acute kidney injury. *J Am Soc Nephrol*. 2008;19(3):547–558. doi:10.1681/ASN.2007040469
55. Ichimura T, Bonventre JV, Bailly V, et al. Kidney injury molecule-1 (KIM-1), a putative epithelial cell adhesion molecule containing a novel immunoglobulin domain, is up-regulated in renal cells after injury. *J Biol Chem*. 1998;273(7):4135–4142. doi:10.1074/jbc.273.7.4135
56. Ichimura T, Hung CC, Yang SA, Stevens JL, Bonventre JV. Kidney injury molecule-1: A tissue and urinary biomarker for nephrotoxicant-induced renal injury. *Am J Physiol Renal Physiol*. 2004;286(3): F552–F563. doi:10.1152/ajprenal.00285.2002
57. Uchida K, Gotoh A. Measurement of cystatin-C and creatinine in urine. *Clin Chim Acta*. 2002;323(1–2):121–128. doi:10.1016/S0009-8981(02)00177-8
58. Conti M, Moutereau S, Zater M, et al. Urinary cystatin C as a specific marker of tubular dysfunction. *Clin Chem Lab Med*. 2006;44(3): 288–291. doi:10.1515/CCLM.2006.050
59. Kataoka H. Chloride in heart failure syndrome: Its pathophysiologic role and therapeutic implication. *Cardiol Ther*. 2021;10(2):407–428. doi:10.1007/S40119-021-00238-2
60. Kataoka H. Proposal for new classification and practical use of diuretics according to their effects on the serum chloride concentration: Rationale based on the "chloride theory." *Cardiol Ther*. 2020;9(2): 227–244. doi:10.1007/S40119-020-00172-9

Difference in the occurrence and intensification symptoms of stomatognathic system between women and men in medical staff working with patients infected with COVID-19

Zdzisław Artur Bogucki[1,A,B,D–F], Katarzyna Giniewicz[2,C]

[1] Department of Prosthetic Dentistry, Wroclaw Medical University, Poland
[2] Statistical Analysis Centre, Wroclaw Medical University, Poland

A – research concept and design; B – collection and/or assembly of data; C – data analysis and interpretation;
D – writing the article; E – critical revision of the article; F – final approval of the article

Advances in Clinical and Experimental Medicine, ISSN 1899–5276 (print), ISSN 2451–2680 (online) *Adv Clin Exp Med*. 2022;31(4):457–464

Address for correspondence
Zdzisław Artur Bogucki
E-mail: zdzislaw.bogucki@umed.wroc.pl

Funding sources
None declared

Conflict of interest
None declared

Received on November 2, 2021
Reviewed on December 15, 2021
Accepted on March 24, 2022

Published online on April 8, 2022

Abstract

Background. One of the groups most exposed to potentially harmful effects of the current pandemic on physical and mental health is medical personnel, in particular those working directly with patients infected with severe acute respiratory syndrome coronavirus 2 (SARS-CoV-2) or suffering from coronavirus disease 2019 (COVID-19).

Objectives. The response of the body to a persisting threat, constant contact with dying people and frequent deaths of patients is chronic stress syndrome. Its symptoms may take the form of psychosomatic or somatic reactions. The aim of the study was to determine the effect of stress on the severity of temporomandibular syndrome (TMD) in medical personnel.

Materials and methods. The study included a group of 160 people – 120 women and 40 men aged 35–60 years, working at the hospital wards as doctors, nurses and support staff, directly with patients infected with SARS-CoV-2 and suffering from COVID-19. The research was conducted in the form of a cross-sectional survey with the use of anonymous questionnaire. The final questionnaire was developed based on the tools commonly used for TMD, bruxism, anxiety, and depression assessment – 8Q/TMD and the Patient Health Questionnaire-8 (PHQ-8).

Results. After checking the significance of differences in responses to individual questions among men and women and applying the Bonferroni correction for multiple comparisons, Fisher's test and p-values for individual responses, an increase in pathological reactions was shown. The results showed that the COVID-19 pandemic has caused significant adverse effects on the psychoemotional status and causes or aggravates TMD symptoms.

Conclusions. The aggravation of the psychoemotional status caused by the COVID-19 pandemic can result in intensification of TMD symptoms and other symptoms in the stomatognathic system in medical staff working with patients infected with COVID-19.

Key words: psychosomatic disorders, temporomandibular disorders, orofacial pain, COVID-19, SARS-CoV-2

Cite as
Bogucki ZA, Giniewicz K. Difference in the occurrence and intensification symptoms of stomatognathic system between women and men in medical staff working with patients infected with COVID-19. *Adv Clin Exp Med*. 2022;31(4):457–464. doi:10.17219/acem/147672

DOI
10.17219/acem/147672

Background

For several months, the scientific world has been dominated by research on severe acute respiratory syndrome coronavirus 2 (SARS-CoV-2) infection. Many publications concern various aspects of the impact of this virus on the human body and its psychophysical impact on humans. The virulence and ease of SARS-CoV-2 transmission, the lack of specific treatment methods, insufficient availability of health services, and the lack of a vaccine or an effective drug for treatment pose a very high risk to the functioning of people and force radical changes in everyday life.[1–6] One of the groups most exposed to potentially harmful effects on physical and mental health is the medical personnel, in particular those working directly with patients infected with SARS-CoV-2 and suffering from coronavirus disease 2019 (COVID-19). This applies to doctors, nurses as well as auxiliary staff necessary for the proper functioning of a hospital.

The response of the body to a persistent threat, constant contact with dying people and frequent deaths of patients is chronic stress syndrome. Its symptoms may take a form of psychosomatic or somatic reactions. The typical psychological response is stress, anxiety, increased nervous tension, vegetative neurosis, or depression. All these reactions have a large impact on the stomatognathic system and may manifest as the onset or intensification of dysfunction. Pain associated with temporomandibular disorders (TMD) can affect the daily activities, physical and psychosocial functioning, and quality of life of those affected.[7–15]

Objectives

The aim of the study was to determine the effect of chronic stress in medical staff working directly with patients infected with COVID-19, and to determine the difference in the occurrence and severity of symptoms in the stomatognathic system in women and men from the medical staff working with patients infected with COVID-19 and the occurrence or severity of TMD.

Materials and methods

The study was conducted before an effective COVID-19 vaccine was developed. The study included a group of 160 people – 120 women and 40 men aged 35–60 years, working at the hospital wards as doctors, nurses and support staff, directly with patients infected with SARS-CoV-2 and suffering from COVID-19. The research was conducted in the form of a cross-sectional survey with the use of anonymous questionnaire. The final questionnaire was developed based on the tools commonly used for TMD, bruxism, anxiety, and depression assessment – 8Q/TMD, and the Patient Health Questionnaire-8 (PHQ-8). People qualified for the study declared in a separate statement that in the period before the pandemic they had no symptoms related to TMD.

Anxiety and depression

The PHQ-8 is a screening tool used for assessing anxiety and depression. The severity of symptoms is rated on a scale from 0 to 3, where 0 means no symptoms and 3 means maximum severity. The score is the sum of the 8 items. The total score for this questionnaire ranges from 0 to 24 points and condition of the patient is typically rated using the following cutoff points (according to the standard of this questionnaire): a PHQ-8 cutoff point ≥10. The cutoff point for this survey is 10 points. It is a scale that determines the appearance of pathological changes and is a parametric measure for this questionnaire for all studies with its use (and therefore independent of the researcher). A score of 10 or greater is considered major depression and 20 or more – severe major depression.

The questions included in the PHQ-8 survey concerned the feeling of constant stress related to working with SARS-CoV-2-infected and COVID-19 patients, and the resulting possible psychological reactions: depression, helplessness, trouble sleeping, constant fatigue, eating disorders, trouble concentrating, and attention deficit hyperactivity disorder (ADHD).

The initial question in the questionnaire used in this study concerned gender. Then, the respondents answered whether in the last 2 weeks, in connection with work in the infectious diseases ward and work with patients infected with COVID-19, they:

1. felt little interest or pleasure in the activities;
2. felt depressed, helpless;
3. had trouble sleeping, drowsiness, the need to sleep longer;
4. felt constant fatigue, less energy;
5. experienced lack of appetite or increased appetite;
6. felt fear for themselves or their families;
7. had trouble concentrating on the things they were doing;
8. experienced slowness or hyperactivity in speaking or performing activities.

The following question was also asked: How often in the last 2 weeks did you experience stress related to working with patients infected with COVID-19: a) not at all; b) for a few days; c) throughout the entire period.

TMD screening

The 8Q/TMD questionnaire was used to collect the data, which is a reliable and acceptable tool for screening TMD status. The questionnaire has excellent negative predictive value and is considered an important screening tool. The questions in the 8Q/TMD questionnaire related to possible reactions to the psyche of the respondents

under extreme working conditions, the occurrence of ailments from the temporomandibular joints, tooth clenching and increased tension of the facial muscles, as well as general health. The severity of individual symptoms is assessed on a 4-point scale from 0 to 3, where 0 means no symptoms and and 3 means maximum severity. The respondents answered the following questions regarding the working conditions during the last 2 weeks, in connection with work in the infectious diseases ward and work with patients infected with COVID-19:

1. Have the working conditions influenced the feeling of stress?
2. Have the working conditions had an impact on overall health?
3. Did the working conditions affect the psyche?
4. Have the working conditions influenced relations with the environment, family and friends?
5. Have the working conditions influenced the sense of risk?
6. Have you experienced pain or increased tension in your facial muscles, temporomandibular joint discomfort or clenching of your teeth in the past?
7. Do the current working conditions affect the occurrence of these ailments?
8. Do the current working conditions affect the severity of these ailments?

The surveys were conducted 2 months after the commencement of work in closed wards with infected patients. Questionnaires assessed the last 2 weeks prior to receiving PHQ-8 and TMD-8, and were delivered in writing. The participants replied anonymously and voluntarily. Informed consent was obtained from all subjects as necessary, after presenting the study objectives.

The research was conducted in full compliance with the Declaration of Helsinki.

Statistical analyses

The analysis consisted in checking by means of the Fisher's test whether there was a statistically significant difference in the responses of men and women to individual questions. For this purpose, 2 × 4 tables were plotted, in which the lines contain information about gender, and the columns contain answers to individual questions: 0, 1, 2, and 3 for each of the questionnaires. Then, the tables were created for each answer separately to check if any of the genders answered 0, 1, 2, or 3 more often than the other.

There were 4 such 2 × 2 tables for each question, so when checking the significance of differences with the Fisher's test, the Bonferroni correction was applied by multiplying the p-values by 4. All tests were performed at the significance level of 0.05. Due to the fact that there were many more women who filled in the questionnaire, it was decided to present the data as percentage values. The proportion of people with specific symptoms was analyzed using Wald 95% confidence interval (Wald 95% CI).

Results

The obtained test results are given in Table 1,2. The analysis focused on the differences between women and men in the study. For each of the questions, it was checked whether there were statistically significant differences between men and women.

Analysis – PHQ-8

Question 1

There was a statistically significant difference between the studied women and men (Fisher's test, $p = 0.002$). The significance of differences in answers to particular questions among men and women was checked, and the Bonferroni correction was applied for multiple comparisons. Significantly more men answered "1" to the question about feeling little interest or pleasure in performing activities (Fisher's test, p-values for each answer: 1, 0.002, 1, and 0.290 for 0, 1, 2, and 3, respectively).

Question 2

There was a statistically significant difference between the studied women and men (Fisher's test, $p = 0.002$). Significantly more men answered "1" to the question about feeling depressed and helpless (Fisher's test, p-values for individual answers: 0.422, 0.007, 0.137, and 1 for 0, 1, 2, and 3, respectively).

Question 3

There was a statistically significant difference between the studied women and men (Fisher's test, $p < 0.001$). Significantly more men answered "0" and "1" to the question about perceived sleep problems, drowsiness and the need to sleep longer, significantly more women answered "3" to the same question (Fisher's test, p-values for individual answers: 0.014, <0.001, 0.914, and 0.010 for 0, 1, 2, and 3, respectively).

Question 4

There was a statistically significant difference between the studied women and men (Fisher's test, $p < 0.001$). Significantly more men answered "0" and "1" to the question about feeling constant fatigue and less energy, significantly more women answered "3" to the same question (Fisher's test, p-values for individual answers: 0.014, <0.001, 0.119, and <0.001 for 0, 1, 2, and 3, respectively).

Question 5

There was a statistically significant difference between the studied women and men (Fisher's test, $p < 0.001$).

Table 1. Statement of temporomandibular disorders (TMD) questionnaire (8Q/TMD questionnaire)

Statement of TMD questionnaire	Answer	Percentage of females [%]	Percentage of males [%]	p-value (Fisher's test)
1	0	0	0	1
	1	3.33	20	0.007
	2	13.33	20	1
	3	83.33	60	0.015
2	0	0	20	<0.001
	1	16.67	20	1
	2	20	20	1
	3	63.33	40	0.063
3	0	0	0	1
	1	0	10	0.014
	2	33.33	20	0.649
	3	66.67	70	1
4	0	0	0	1
	1	0	10	0.013
	2	33.33	40	1
	3	66.67	50	0.355
5	0	0	10	0.014
	1	3.33	30	<0.001
	2	16.67	0	0.016
	3	80	60	0.077
6	0	33.33	40	1
	1	20	30	0.786
	2	26.67	20	1
	3	20	10	0.914
7	0	20	40	0.077
	1	20	20	1
	2	20	10	0.914
	3	40	30	1
8	0	23.33	40	0.257
	1	23.33	10	0.290
	2	10	10	1
	3	43.33	40	1

Significantly more men answered "0" and "1" to the question about feeling lack of appetite or increased appetite, significantly more women answered "3" to the same question (Fisher's test, p-values for individual answers: <0.001, 0.002, 1, and <0.001 for 0, 1, 2, and 3, respectively).

Question 6

There was a statistically significant difference between the studied women and men (Fisher's test, p-value = 0.001). Significantly more men answered "2" to the question about feeling fear for themselves or their family, significantly more women answered "3" to the same question (Fisher's test, p-values for individual answers: 1, 0.433, 0.017, and 0.002 for 0, 1, 2, and 3, respectively).

Question 7

There was a statistically significant difference between the studied women and men (Fisher's test, $p < 0.001$). Significantly more men answered "1" to the question about experiencing problems with concentrating on the things performed, significantly more women answered "2" and "3" to the same question (Fisher's test, p-values for individual answers: 1, <0.001, <0.001, and 0.009 for 0, 1, 2, and 3, respectively).

Question 8

There was a statistically significant difference between the studied women and men (Fisher's test, $p < 0.001$).

Table 2. Statement of Patient Health Questionnaire-8 (PHQ-8) questionnaire

Statement of PHQ-8 questionnaire	Answer	Percentage of females [%]	Percentage of males [%]	p-value (Fisher's test)
1	0	10	10	1
	1	6.67	30	0.002
	2	60	50	1
	3	23.33	10	0.290
2	0	10	20	0.422
	1	3.33	20	0.007
	2	70	50	0.137
	3	16.67	10	1
3	0	0	10	0.014
	1	3.33	30	<0.001
	2	20	10	0.914
	3	76.67	50	0.010
4	0	0	10	0.014
	1	10	60	<0.001
	2	26.67	10	0.120
	3	63.33	20	<0.001
5	0	0	20	<0.001
	1	13.33	40	0.002
	2	30	30	1
	3	56.67	10	<0.001
6	0	0	0	1
	1	3.33	10	0.433
	2	10	30	0.017
	3	86.67	60	0.002
7	0	0	0	1
	1	10	70	<0.001
	2	55	20	0.001
	3	35	10	0.009
8	0	10	0	0.154
	1	13.33	70	<0.001
	2	48.33	30	0.182
	3	28.33	0	<0.001

Significantly more men answered "1" to the question about feeling slowed down or hyperactive in speaking or performing activities. Significantly more women answered "3" to the same question (Fisher's test, p-values for individual answers: 0.154, <0.001, 0.182, and <0.001 for 1, 2, and 3, respectively).

Analysis – TMD

How often have you experienced stress related to working with patients infected with COVID-19 over the last 2 weeks?

There was a statistically significant difference between the studied women and men (Fisher's test, $p < 0.001$). Significantly more men answered "1" to the question whether working conditions influenced the feeling of stress, significantly more women answered "3" to the same question (Fisher's test, p-values for individual answers: 1, 0.007, 1, and 0.016 for 0, 1, 2, and 3, respectively).

Whether working conditions had an impact on overall health

There was a statistically significant difference between the studied women and men (Fisher's test, $p < 0.001$). Significantly more men answered "0" when asked if working conditions had an impact on general health (Fisher's test, p-values for individual answers: <0.001, 1, 1, and 0.063 for 0, 1, 2, and 3, respectively).

Whether the working conditions had an influence on the psyche

There was a statistically significant difference between the studied women and men (Fisher's test, p = 0.003). Significantly more men answered "1" to the question whether the working conditions had an impact on their psyche (Fisher's test, p-values for individual answers: 1, 0.014, 0.649, and 1 for 0, 1, 2, and 3, respectively).

Whether the working conditions had an impact on relations with the environment, family and friends

There was a statistically significant difference between the studied women and men (Fisher's test, p = 0.003). Significantly more men answered "1" to the question whether working conditions had an impact on relations with the environment, family and friends (Fisher's test, p-values for individual answers: 1, 0.014, 1, and 0.355 for 0, 1, 2, and 3, respectively).

Whether working conditions had an influence on the sense of risk

There was a statistically significant difference between the studied women and men (Fisher's test, p < 0.001). Significantly more men answered "0" and "1" to the question whether working conditions influenced the sense of risk, significantly more women answered "2" (Fisher's test, p-values for individual answers: 0.014, <0.001, 0.016, and 0.077 for 0, 1, 2, and 3, respectively).

Have you had pain or excessive tension in your facial muscles, temporomandibular joint discomfort or clenching of your teeth in the past?

No statistically significant difference between the studied women and men was observed (Fisher's test, p = 0.275). The value of 0, i.e., no symptoms, was compared with values greater than 0, which meant the occurrence of symptoms of varying severity. Sixty-five percent of respondents indicated that in the past, they had experienced pain or increased tension in the facial muscles, with the Wald 95% CI: [57.6%; 72.4%] for complaints of the temporomandibular joints or clenching of the teeth. It is more than 50%, so we can say with 95% certainty that most people have suffered from the abovementioned ailments in the past.

Do the current working conditions influence the occurrence of these ailments?

No statistically significant difference between the studied women and men was detected (Fisher's test, p = 0.074). The value of 0, i.e., no symptoms, was compared with values greater than 0, which meant the occurrence of symptoms of varying severity. Seventy-five percent of respondents indicated that the current working conditions had an influence on the occurrence of the ailments (Wald 95% CI: [68.3%; 81.7%]). This is more than 50%, so we can say with 95% certainty that most people believe that the current working conditions have an influence on the occurrence of ailments.

Do the current working conditions exacerbate these ailments?

No statistically significant difference between the studied women and men was observed (Fisher's test, p = 0.122). The value of 0, i.e., no symptoms, was compared with values greater than 0, which meant the occurrence of symptoms of varying severity. Answering this question, 72.5% of people indicated that the current working conditions had an impact on the severity of the ailments (Wald 95% CI: [65.6%; 79.4%]). This is more than 50%, so we can say with 95% certainty that most people believe that the current working conditions have an influence on the severity of ailments.

Discussion

The genetic material of SARS-CoV-2 indicates that it belongs to a very large group of coronaviruses, most of which attack animals. However, some of them can cross the interspecies barrier. Today we know 7 coronaviruses attacking the human body. Three of them are very dangerous to humans: Middle East respiratory syndrome (MERS), SARS-CoV and its very close relative SARS-CoV-2; the remaining 4 only cause mild cold in humans. The SARS-CoV-2 has most likely crossed the bat–human barrier. It is not clear whether it needed an intermediate host – there are many indications that armored pangolins played this role.[16–18]

Relatively quickly, it was possible to elucidate the exact structure of SARS-CoV-2, and thanks to this, to learn, among other things, that it attacks human cells using its characteristic spikes (S proteins), by means of which it attaches to receptor proteins (ACE2) found in the membrane of human cells. Using these spikes, the virus penetrates ACE2, where it releases its genetic material, reproducing copies of SARS-CoV-2. The proteins to which the virus attaches are found in large amounts in the cells of the respiratory tract and lungs, hence the name responsible for the current SARS coronavirus pandemic (severe acute respiratory syndrome).

The SARS-CoV-2 spreads by droplets, thus when an infected person coughs, sneezes or talks, an aerosol with secretions from their upper respiratory tract and the virus present in it rises in the air. Due to the high virulence of SARS-CoV-2, even a small amount can lead to infection of the surrounding environment (e.g., workspace). An approach to spreading SARS infection that takes into account the phenomenon of clustering of problems during

a pandemic and the formation of feedbacks that multiply the stress to which healthcare workers are subjected is needed. It is a type of syndemic where there is aggregation and interaction of the SARS pandemic, comorbidities (often chronic), mental and behavioral problems, or health and environmental conditions. Overlapping each other, each of these factors strengthens.[19]

Medical personnel working with infected patients is aware of this persistent danger. Additionally, the lack of specific methods of treatment, insufficient availability of health services, the lack of a vaccine or an effective drug, constant contact with dying people, and frequent deaths of patients do not remain indifferent to the psychophysical state. A prolonged exposure to chronic stress disorder can exacerbate the symptoms of TMD or be a trigger of them. This, in turn, may additionally adversely affect the psychoemotional state of patients. Since both depression and TMD can be induced and aggravated by psychological factors, the differences in their incidence may result from psychological differences between the subjects. These factors can potentially modulate the psychoemotional state of participants, influence their coping strategies, and thus increase the incidence of both depression and TMD.

The influence of these factors is visible in the studied group of patients and reflected in the obtained results. There are no reports in the literature referring directly to such group of respondents. The obtained results correlate with the data provided in studies on people not directly related to the treatment of those infected with COVID-19. However, it is clearly visible that the intensification of TMD symptoms and depression is more frequent in healthcare workers. This is due to their greater awareness of the consequences of possible COVID-19 infection, overwork, and the direct and frequent sight of people dying from the infection.[3–7]

Apparently, anxiety and personal worries caused by the pandemic increased the incidence of TMD and depression. This is consistent with the results presented in the literature stating that anxiety, stress, coping strategies, and life catastrophes (i.e., events causing stress) can accelerate or prolong the symptoms of TMD and that psychosocial factors are associated with the occurrence of depression.[15–18] When the pandemic situation changed rapidly from one day to the next, uncertainty and fears about the present and the future were common, and in the study group, they were particularly intense and persistent. Under such conditions, the significant increase in the likelihood of TMD and depression is not surprising, even though medical personnel is used to dealing with extreme and stressful situations.

Limitations

The main problem encountered in this study is that no one has ever done this type of research in relation to COVID-19 SARS-CoV-2, based on the surveys we have selected. Obviously, these surveys have been widely used for many years, but there has been no research focused on the issues we raise. For this reason, there are no references to literature and no possibility of discussion. Thereby, the Limitations subsection was introduced into the text of the work, where the methodological difficulties resulting from this type of research are explained.

At the conceptual/theoretical level, correlational studies must at least try to examine the nomological network of stress-related symptoms by examining associations with antecedents, outcomes, mediators, or moderators. The current study mostly focused on describing the mean level and/or prevalence of symptoms in the sample. This type of analysis is too descriptive. The correlations between items from a questionnaire like the PHQ-8 are presumed to be explained by a common cause. Therefore, most studies in psychology regroup similar items into factors. Items are useful to make inferences about a concept and, ideally, should not be interpreted in isolation from one another. Exceptions are possible, but running multiple tests (based on highly correlated single-item scores) typically increase the likelihood of rejecting null hypothesis.

Conclusions

The results showed that the COVID-19 pandemic has caused significant adverse effects on the psychoemotional status and causes or aggravates TMD symptoms in medical staff working with patients infected with COVID-19, resulting in the intensification of TMD symptoms and thus leading to increased orofacial pain.

References

1. LeResche L. Epidemiology of temporomandibular disorders: Implications for the investigation of etiologic factors. *Crit Rev Oral Biol Med*. 1997;8(3):291–305. doi:10.1177%2F10454411970080030401
2. Macfarlane TV, Glenny AM, Worthington HV. Systematic review of population-based epidemiological studies of orofacial pain. *J Dent*. 2001;29(7):451–467. doi:10.1016/s0300-5712(01)00041-0
3. Nilsson IM, List T, Drangsholt M. Prevalence of temporomandibular pain and subsequent dental treatment in Swedish adolescents. *J Oral Facial Pain*. 2005;19(2):144–150. PMID:15895837.
4. Berger M, Oleszek-Listopad J, Marczak M, et al. Psychological aspects of temporomandibular disorders: Literature review. *Curr Issues Pharm Med Sci*. 2015;28:55–59. doi:10.1515/cipms-2015-0044
5. de Leeuw R, Klasser GD. Differential diagnosis and management of TMDs. In: de Leeuw R, Klasser GD, eds. *Orofacial Pain: Guidelines for Assessment, Diagnosis, and Management/American Academy of Orofacial Pain*. 6th ed. Hannover, Germany: Quintessence Publishing Co. Inc.; 2018:143–207. ISBN: 978-0-86715-768-0.
6. Manfredini D, Lobbezoo F. Role of psychosocial factors in the etiology of bruxism. *J Oral Facial Pain*. 2009;23(2):153–166. PMID:19492540.
7. Winocur E, Uziel N, Lisha T, Goldsmith C, Eli I. Self-reported bruxism: Associations with perceived stress, motivation for control, dental anxiety and gagging. *J Oral Rehabil*. 2010;38(1):3–11. doi:10.1111/j.1365-2842.2010.02118.x
8. Wang C, Pan R, Wan X, et al. Immediate psychological responses and associated factors during the initial stage of the 2019 coronavirus disease (COVID-19) epidemic among the general population in China. *Int J Environ Res Public Health*. 2020;17(5):1729. doi:10.3390/ijerph17051729

9. Almeida-Leite CM, Barbosa JS, Conti PCR. How psychosocial and economic impacts of COVID-19 pandemic can interfere on bruxism and temporomandibular disorders? *J Appl Oral Sci*. 2020;28:20200263. doi:10.1590/1678-7757-2020-0263
10. Lövgren A, Parvaneh H, Lobbezoo F, Häggman-Henrikson B, Wänman A, Visscher CM. Diagnostic accuracy of three screening questions (3Q/TMD) in relation to the DC/TMD in a specialized orofacial pain clinic. *Acta Odontol Scand*. 2018;76(6):380–386. doi:10.1080/00016357.2018.1439528
11. Lövgren A, Marklund S, Visscher CM, Lobbezoo F, Häggman-Henrikson B, Wänman A. Outcome of three screening questions for temporomandibular disorders (3Q/TMD) on clinical decision-making. *J Oral Rehabil*. 2017;44(8):573–579. doi:10.1111/joor.12518
12. Manfredini D, Winocur E, Guarda-Nardini L, Paesani D, Lobbezoo F. Epidemiology of bruxism in adults: A systematic review of the literature. *J Oral Facial Pain*. 2013;27(2):99–110. doi:10.11607/jop.921
13. Stanhope J. Patient Health Questionnaire-4. *Occup Med. (Lond)*. 2016;66(9):760–761. doi:10.1093/occmed/kqw165
14. Manfredini D, Serra-Negra J, Carboncini F, Lobbezoo F. Current concepts of bruxism. *Int J Prosthodont*. 2017;30(5):437–438. doi:10.11607/ijp.5210
15. Wright EF. *Manual of Temporomandibular Disorders*. 3rd ed. Ames, USA: Wiley-Blackwell; 2014:1–15. ISBN: 978-1-118-50269-3.
16. Maciaszek J, Ciulkowicz M, Misiak B, et al. Mental health of medical and non-medical professionals during the peak of the COVID-19 pandemic: A cross-sectional nationwide study. *J Clin Med*. 2020;9(8):2527. PMID:32764509.
17. Wang C, Pan R, Wan X, et al. A longitudinal study on the mental health of general population during the COVID-19 epidemic in China. *Brain Behav Immun*. 2020;87:40–48. doi:10.1016/j.bbi.2020.04.028
18. Song K, Xu R, Stratton TD, et al. Sex differences and psychological stress: Responses to the COVID-19 epidemic in China. *MedRxiv*. 2020:2020;1–23. doi:10.1186/S12889-020-10085-W
19. Varshney M, Parel JT, Raizada N, Sarin SK. Initial psychological impact of COVID-19 and its correlates in Indian community: An online (FEEL-COVID) survey. *PLoS ONE*. 2020;15(5):e0233874. doi:10.1371/journal.pone.0233874